APPLICATION OF FUZZY CONTROL IN VEHICLE HANDLING SIMULATION AND PATH PLANNING

E. UZUNSOY

PH. D. 2003

UNIVERSITY OF BIRMINGHAM

APPLICATION OF FUZZY CONTROL IN VEHICLE HANDLING SIMULATION AND PATH PLANNING

by

ERDEM UZUNSOY

A thesis submitted to the School of Engineering
of the University of Birmingham
for the degree of
DOCTOR OF PHILOSOPHY

Vehicle Technology Research Centre
School of Engineering
Department of Mechanical and Manufacturing Engineering
The University of Birmingham
August 2003

To my wife 'Deniz' & my daughter 'Defne'

SYNOPSIS

This thesis describes the development and implementation of a control routine for vehicle handling dynamics simulation studies. A new vehicle handling simulation tool which is called HANDSIM (HANDling SIMulation) has been developed in the Matlab/ Simulink® environment for the purpose and it is benchmarked by the well known vehicle dynamics simulation tool CarSimEd®. The control code has been implemented into the tool in the same environment.

The main objective of this work is to develop a vehicle driver model which imitates a human driver by using an intelligent control theory, fuzzy logic. The control routine includes direction, speed and yaw rate control of the vehicle. The speed and direction control are the main elements in the driver model as yaw rate control is provided by the corrective braking and tractive inputs. The fuzzy controller for path planning is designed to fit any type of ground vehicle, as long as the tyre and vehicular parameters are supplied. Using the fuzzy controller, paths of varying complexity were generated through specified target points placed at varying distances and the simulation results showed that these paths could be traversed with reasonable accuracy at a wide range of speeds. The use of fuzzy logic as a controller eliminates the need for complex mathematical functions in describing vehicle paths, a particularly important requirement in realistic simulation of the handling responses of a vehicle.

The developed simulation tool HANDSIM and the fuzzy path planning controller are assessed by the modelling and simulation of a University of Birmingham Formula Student race car with a novel rear suspension load transfer system. According to the simulation results, some design changes are suggested to improve the load transfer of the suspension with a view to improve the car's handling characteristics. As a result, while the abilities of HANDSIM are proved as a vehicle handling dynamics simulation tool, a sophisticated approach to vehicle path planning is also introduced, both of which may be useful in the studies of future automated highways.

ACKNOWLEDGEMENTS

I would like to thank my supervisor ***Dr. O. A. Olatunbosun*** for his kind supervision, constant direction and enthusiasm throughout this work, even in his busiest times.

Sincere thanks are due to the *Turkish Higher Education Council, Yildiz Technical University-Istanbul/TURKEY* and *the Department of Mechanical & Manufacturing Engineering – The University of Birmingham* for the provision of the scholarship and payment of the University fees. Special thanks to *Prof. Irfan Yavasliol* who has always been on my side from the beginning and sparked the idea of studying on vehicle dynamics.

I would also like to thank my friends *Dr. G. H. Kang* and *Mr. L. Bolarinwa* for our technical discussions, *Mr. Carl Hingley* for his kind support in experimental studies.

Sincere thanks to my parents *Guner Uzunsoy* and *Mustafa Uzunsoy* for all their support from the beginning and being with us during the birth of our daughter in the UK.

Finally, I would like to thank to my family: My wife *Deniz* who has always been a great support to me in my life and during my research effort and our little baby girl *Defne* who has brought joy to our life.

TABLE OF CONTENTS

LIST OF FIGURES

LIST OF TABLES

Page No.

LIST OF SYMBOLS

F_y	: Tyre lateral force
α	: Tyre slip angle
B	: Stiffness factor
C	: Shape factor
D	: Peak value
E	: Curvature factor
S_h	: Horizontal shift
S_v	: Vertical shift
$\dot{V}$	: Lateral acceleration of the vehicle
V	: Lateral velocity of the vehicle
$\dot{U}$	: Longitudinal acceleration of the vehicle
U	: Longitudinal velocity of the vehicle
$\dot{r}$	: Yaw acceleration of the vehicle
r	: Yaw rate of the vehicle
ψ	: Yaw angle
$\dot{p}$	: Roll acceleration of the vehicle
p	: Roll rate of the vehicle
ϕ	: Roll angle
a	: Front wheelbase
b	: Rear wheelbase

P_b : Braking pressure

r : Effective tyre radius

T_b : Braking torque

T_d : Driving torque

F_b : Braking force

F_x : Tractive force

bgain : Braking gain

dgain : Driveline gain

thr : The percentage of the throttle being open

F_x : Tractive force

F_y : Lateral force

F_b : Braking force

L : Left

R : Right

x', y' : *Calculated coordinates for x , y point in the body centred axis system (m)*

x, y : *Any defined x ,y point in the Earth fixed coordinate system (m)*

r : *Vehicle yaw angle (deg)*

X, Y : *Instantaneous position of the vehicle on the x and y coordinates. (m)*

m : *Vehicle mass (kg)*

g : *Gravitational acceleration (9.81 m/s²)*

h_u : *Height of unsprung mass (m)*

K_{ϕ} *:Roll stiffness*

C_{ϕ} *:Roll damping*

$\phi, \dot{\phi}$ *:Roll angle, velocity*

K_{ϕ} :Roll stiffness of the suspension

K_s :Vertical rate of each of the left and right springs

s :Lateral separation of the springs

CHAPTER 1

INTRODUCTION

In recent years many research efforts on developing road vehicles have focused especially on the dynamic characteristics of the vehicle. Manufacturers have tried to attract people's attention to their cars using visible and easily discernible features like design, engine and transmission system performance. However, increasing intensity of road traffic and many drivers, who have different reaction and reaction time necessitate improved vehicle-handling properties as much as possible.

A road vehicle is a very complex machine, which includes thousands of different parts. However, an ordinary driver considers just some characteristics like ease of use, reliability and an attractive inner and outer design in choosing which car to buy. Meanwhile, each vehicle must be designed to be driven safely by even the most inexperienced driver under most road conditions. Therefore, road vehicle and driver interactions have now assumed great importance in vehicle design studies. Researches are directed to improve the vehicle handling properties, which can give the average driver self-confidence and safe handling, especially on sharp cornering and lane change manoeuvres.

Nowadays, improvements in vehicle handling properties are realised in computer models with the support of experimental testing. The main reason for this is financial. It costs much less to try an idea on a computer than out on a test track. It is cheaper and much faster to digitally prototype. There are also a number of situations, which are very difficult and costly to test experimentally like roll over limits of trucks. However, very complicated mathematical models are needed to represent real vehicle handling situations correctly but consideration of cost and accuracy limit the ability of most models to reproduce real life behaviour. Some of the early simulations used special hardware and were capable of real time simulation. Whether the simulations were performed with analogue, digital, or hybrid computers, model equations were formulated as a set of non-linear ordinary differential equations (ODEs). Although vehicle simulation was shown to be technically feasible, the software was so difficult to use that simulation remained an exotic technology limited to researchers and few specialists. However, in the mid-1980’s two new types of software became available that helped make simulation a more popular engineering tool. One is the interactive graphical simulation environment, such as Simulink/MATLAB®. The other is the mechanical multibody simulation program such as ADAMS® [1].

In fact Simulink® and similar simulation environments are not ideal for vehicle dynamics since they do not support 3D mechanical multibody systems. Thus, the user must provide their own ODEs to simulate vehicle dynamics models. On the other hand, the need to create their own ODEs gives the researchers more flexibility to develop their own ideas and modelling skills.

In vehicle handling research, as in many other studies, accuracy of the simulation is improved by the use of more complex models. It is, however, possible to use simplified models in order to reduce simulation time as well as to improve ease of use and understanding of the simulation. For this reason, a compromise between accuracy and simplicity is required.

To design or improve a vehicle's handling properties is a complicated exercise. Vehicle handling dynamics strongly depends on the tyre characteristics. Therefore, before a handling analysis, a tyre modelling theory must be established which is complex enough to provide the level of accuracy required in the simulation. Depending on the tyre model, which will be chosen, the complexity of the whole study, may either be increased or decreased. The study of physical tyre models is already a subject area by itself and highly complicated studies can be done just for physical tyre modelling by using some specific methods like finite element analysis. Therefore, for the purpose of vehicle handling dynamics analysis, a proper method should be chosen to consider both the accuracy and simplicity of the study. From this point of view, extracted experimental tyre data is implemented as a tyre model by using interpolation methods, in this thesis. Therefore, the need for detailed tyre construction analysis, many possible coefficients and data are eliminated. As a result, an easy to use handling model has been obtained by implementing this tyre model into the dynamics modelling of the vehicle.

Vehicle handling characteristics are the responses of the vehicle to steering commands and to environmental effects such as road disturbance and wind that affect the direction of motion. There are two basic issues in vehicle handling: One is the control of the direction of motion and the other is the stability of the direction of motion against external disturbances. General vehicle handling dynamics tests to reveal the vehicle responses simply take constant radius steer and/or lane change manoeuvre at constant vehicle forward speed into account. However, vehicle behaviours can not be limited just to the constant parameters such as radius of steer and vehicle speed. These are idealised tests, which have little bearing on normal driving. In fact, a vehicle runs generally under variable effects of the forces and moments. From the computer simulation point of view, having a general path generator can present the researcher with great flexibility in defining vehicle handling dynamics tests. Therefore, there is a necessity for having a driver model, which is capable of dealing with the external forces to keep the vehicle on the path. From this point of view, a fuzzy driver model namely Fuzzy Pilot has been developed to imitate the human driver giving flexibility in planning any type of path and this model has been implemented into the vehicle model. As this first part of the project is concluded by the development of a new vehicle handling dynamics simulation tool namely HANDSIM combined with the Fuzzy Pilot, the second part of the project investigates the control issue of vehicle handling dynamics. Two different control ideas have been developed and implemented into HANDSIM. The first one is a novel rear suspension design which can be referred to as a passive control system. Not only a suspension system provides the passenger comfort presenting a good ride but also it provides road holding, which is the subject area of vehicle handling dynamics as well. The system includes a pair of damper units mounted diagonally across the rear rockers without anti-roll bars unlike the front suspension system. This system had been realised on the University of Birmingham’s Formula racing car. The analysis of the system has been done using the developed simulation tool and at the same time, a second control scheme which controls the yaw rate of the vehicle by applied braking and tractive forces using fuzzy logic theory has been applied to improve the vehicle’s handling characteristics forcing the vehicle to stay on the proposed path. Results have been discussed for the suspension system itself, yaw control scheme and for combination of the both systems together.

CHAPTER 2

LITERATURE REVIEW

2.1. Introduction

Tyre forces and moments -provided by the friction between tyres and ground- are of primary importance in vehicle handling. Unfortunately, the dynamic behaviour of the rolling pneumatic tyre is still very difficult to characterise. The non-linear shape of the tyre characteristics may cause considerable changes in handling properties at different levels of lateral accelerations (cornering). Therefore in vehicle modelling an appropriate tyre representation is very important for model reliability. Various methods are available for describing the tyre force system.

The effectiveness of the tyre model usually plays one of the most important roles in vehicle dynamics studies. In many cases a good steady state tyre model is enough for generation of lateral and longitudinal force in handling and braking simulations. However, as Guo et al [2] pointed out, in many drastic handling and control scenarios, transient tyre properties are not negligible, especially at relatively low vehicle speeds.

After a detailed review of tyre models, the basics and the improvements on the vehicle ride, handling dynamics and control, which are the focus of this study, are discussed. There are two basic issues on vehicle handling dynamics: One is the ability of the vehicle to stabilise its direction of motion against external disturbances; the other is the control of the direction of motion of the vehicle [3]. The second one generally needs the application of control theory that could be seen in modern vehicles such as anti-lock brake system (ABS), active and semi-active suspension systems, traction control systems (TCS), direct yaw control and roll control systems. Although vehicle ride is studied as a different subject area, in many studies it is studied in conjunction with vehicle handling as they are both affected by the vehicle suspension system. A vehicle suspension system needs not only to provide for a good ride but also for good handling as well. However, the requirements for good handling are often in conflict with the requirements for good ride, therefore, there is a need to get a compromise between good ride and handling characteristics. In this chapter, first tyre modelling studies and then vehicle handling and ride researches including some of the control strategies like direct yaw control and four wheel steering are reviewed.

2.2. Pneumatic Tyre

The pneumatic tyre is a vital component of a road vehicle as it interacts with the road in order to produce the forces necessary for the support and movement of the vehicle. A thorough understanding of the behaviour of the pneumatic tyre is an essential aspect of analysing the dynamics of vehicles. All forces and moments generated in the tyre are as a result of tyre deflections due to the interaction between road and tyre. Tyre vibrations increase because of road irregularities, tyre non-uniformities and tyre axle movements. While the tyre can isolate some of the vibrations in certain frequency ranges, it also causes an increase in some frequency ranges. A good estimation of these forces and moments under various steady and transient vehicle manoeuvres is essential for a vehicle handling analysis.

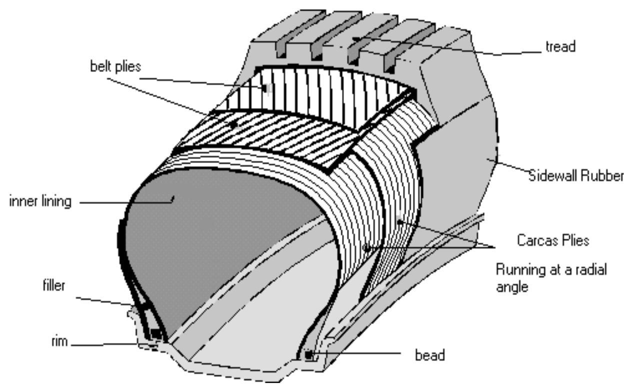

Figure 2.1 Construction of a pneumatic tyre [4].

The behaviour of a pneumatic tyre is governed by its complex construction. Figure 2.1 shows the construction of a radial ply tyre, which is an example of the modern automobile tyre. Directional stability of the tyre is provided by the enclosed pressurised air acting on the sidewalls of carcass plies. While softness of the carcass affects the ride comfort, increased stiffness of the belt affects the quality of cornering properties.

2.3. Cornering Stiffness

The vehicle lateral dynamics depends on the cornering stiffness ($C\alpha$), which is related to the characteristics of the tyre-road interaction, the load and longitudinal velocity. The value of $C\alpha$ is affected by many factors such as tyre pressure, load, velocity, etc. A tyre generates a lateral force during cornering that is related to the slip angle. The slip angle is the angular difference between the heading direction of the tyre and the direction of the travel of the tyre. The lateral force due to the slip angle is characterised by the initial slope of the force versus slip angle curve. The initial slope is called the cornering stiffness of the tyre and is defined as in equation (1.1) [5], below:

$$C_\alpha = \left(\partial F_y / \partial \alpha\right)|_{\alpha=0} \tag{1.1}$$

where:

F_y = the lateral tyre force

α = The slip angle

The cornering stiffness is the parameter, which is most susceptible to change, and in fact it is a direct function of the manoeuvring condition. Its dependence on tyre load is often ignored. Classical tyre modelling calculates the tyre lateral force as a function of slip angle and cornering stiffness and this relationship is linear under moderate manoeuvring conditions. According to Alter [4], two major deficiencies exist in this approach. First, it cannot simulate the tyre saturation. Instead, it assumes the lateral force will increase indefinitely with sideslip angle. Second, tyre-cornering stiffness is primarily a function of tyre normal loading, but camber, braking, acceleration and even the slip angle itself also affect it. However, especially in the last decade, there have been many researches which take variations in cornering stiffness into consideration. [6], [7], [8], [9], [10], [11]. Some of them are discussed in the section 2.4. In some studies, for simplicity and also for sufficient accuracy, the cornering stiffness can be expressed as a function of the tyre vertical load using empirical relations. J.C. Huston [5] and A.Y. Lee's [12] studies can be shown as examples of this type.

2.4. Tyre Representation

A basic vehicle handling model takes into account three fundamental components: Lateral force and self-aligning moment depending on sideslip and, longitudinal force depending on longitudinal slip. In particular, lateral force is the key component for the road holding behaviour for both steady state and transient response simulations. Self-aligning moment is quite useful to determine steering effort and driving feel and consequently, the interaction between driver and the vehicle. On the other hand, an effective representation of longitudinal force components is fundamental to a complete dynamic model. As a matter of fact the components are all dependent on vertical load and camber angle as well, which are usually provided as inputs to the vehicle model. Because of the complex structure of the pneumatic tyre, rolling road tests are the most effective way to determine its properties. Then, various methods can be used to describe the tyre force system.

Tyre models for vehicle-handling dynamics studies may be classified in two main categories: those employing basic physical equations to create a model by considering tyre structure and material properties – referred to as physical tyre model, or those using measured data in a graphical or tabulated format or using empirically obtained formulae – referred to as empirical tyre models. Physical tyre models are also referred to as analytical tyre model in the literature. However, because there is some confusion in the use of this term in the literature, just physical tyre model is used in this thesis. The most well-known tyre model for the physical tyre model is attributed to Fiala and for the empirical tyre model is the Magic Formula Tyre Model. Some models may be extensions or further development of existing models. For instance, Best [13] adapted the magic tyre formula to present the lateral tyre force in his model and showed the non-linear relationship between the lateral force and slip angle. However, a tyre lag is also included, by implementation of a unit gain first order lag to the result of lateral tyre force function.

A Semi-physical tyre model may also be added to this basic classification. In the semi-physical tyre model, tyre experimental data is used with the basic physical equations [14].

In real road conditions, the variation of lateral force against slip angle is not linear, depending on the vertical load and relaxation length (σ). Relaxation length depends on the distance needed by the tyre to reach a certain percentage of the steady state situation after a stepwise change of the slip angle. According to Maurice et al [15], the relaxation length variation closely resembles the variation of the local cornering stiffness $\partial F_y/\partial\alpha$. Furthermore it appears that the shape of relaxation length as a function of the load changes with increasing average slip angle.

The vertical load deflection behaviour is one of the important properties of a pneumatic tyre. As Wang et al [16] reported, it influences essentially the vehicle vertical motions and the time variations of the vertical tyre load. If the distance between tyre centre and road surface is kept constant, such as a tyre on a drum test stand, the vertical load of the tyre will be reduced with the increase of the lateral force acting on the tyre.

The cornering characteristic curves of the tyre are obtained under two possible conditions: constant vertical force (F_v) or constant distance from tyre centre to road surface. The former implies that the distance of the tyre centre is variable according to the change of the slip angle to keep the vertical load constant.

2.4.1. Physical Tyre Models

A physical modelling study of tyre is subject to multi-layered, non-uniform, anisotropic; cord rubber structure of the tyre. Therefore, physical analysis of the tyre structure is highly complex. The behaviour of this structure can be simulated using some methods such as finite element analysis. There is a pressing need for simplification to understand tyre behaviour. There are three principal models for understanding tyre forces and deflections in cornering and giving some insight into footprint behaviour: the elastic foundation model, the string model and the beam model. In the elastic foundation model (Figure 2.2), each small element of the contact patch surface is considered to act independently; if forced by the ground it can be displaced from its null position relative to the foundation and resist with a given stiffness.

In the string model, lateral displacement of each element is also resisted by tension between the elements because of changes in the displacement slope. In the beam model each element exerts bending moments on its neighbour [17]. Figure 2.3 shows the string and beam models on elastic foundation model.

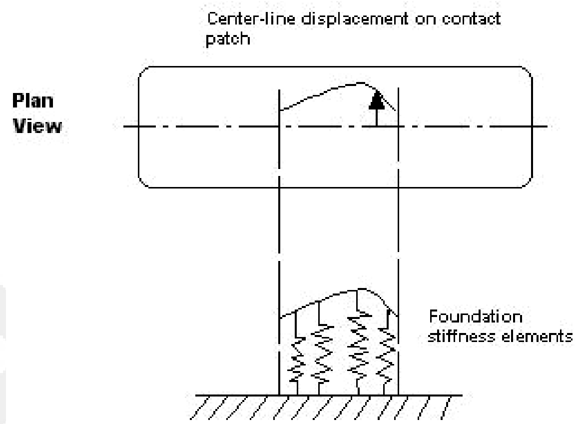

Figure 2.2 Elastic foundation tyre model

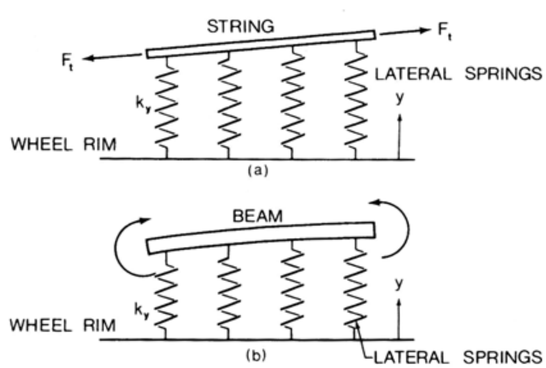

Figure 2.3 (a) String model. (b) Beam on elastic foundation model [18]

The foundation stiffness model allows a discontinuous distribution of displacement and slope of the centreline. The string model allows discontinuous changes of slope, but not of deflection. The beam model does not allow discontinuities of either [17]. The string and beam models can be used together. However, none of these models can reflect the true complexity of a real tyre. Therefore, various stiffness values are selected empirically to obtain realistic results. Contact friction is one of the fundamental properties in modelling tyre behaviour. All physical models need to deal with contact friction, at least because of the non-linear characteristics of tyre forces with respect to the kinematics inputs [19].

2.4.2. Empirical Tyre Models

Empirical models employ experimental data and/or special functions and they can give more accurate results for certain conditions. Empirical models can also cover the full range of data, which a vehicle handling analysis requires, by using both extrapolation and interpolation. One of the empirical methods to represent tyre behaviour is polynomial curve fitting, which can give good results especially in steady state conditions. The curve fitting quality can be quite good but it also depends on the number and distribution of experimental data. Real time interpolations are also demanding of CPU effort and hence time consuming. Therefore, they can be very hard to use, especially if they need a lot of experimental data to determine a large number of the equation coefficients to derive new equations. Furthermore, extrapolation method, which is used in these types of models, can give large deviations from the actual conditions.

2.4.3. Semi-physical Tyre Model

There are other possible ways to present a tyre model - those referred to as semi-physical tyre models like the "brush" model, which are designed to operate in the same way as a real tyre.

The model will contain parameters, which represent physically identifiable parts or properties of the real tyre, like the carcass and tread structural stiffness and the friction coefficient. Smaller amounts of experimental results are needed for accurate representation since extrapolation out of their domain is usually feasible. On the other hand it is somehow difficult to comply with the need for simplicity, computational effectiveness and good accuracy at the same time [14].

2.5. Some Major Tyre Models

2.5.1. Magic Formula Tyre Model

In 1987, an empirical description, which is based on physical insight in tyre force generating properties, was presented [9]. Improvements in this formula were published later. In the same literature, it is reported that, in a co-operative effort TU-Delft and Volvo developed several versions. Today, the most common approach to computer based tyre representation is the Magic Formula Tyre model. The magic formula described only the steady state tyre behaviour in its early versions. In 1997, Pacejka [6] improved and published the model by adding the transient properties, although some transient tyre modelling studies had already been done with some additions to the core of the model by different researchers such as Kusaka et al. [11]. Therefore, the relations, which are presented below are the fundamentals of the model. The model provides a set of mathematical formulae from which the forces and moments acting from the road under longitudinal, lateral and camber slip conditions, which may occur simultaneously, can be described. The basic formula is presented below [11].

$$F_y = D.\sin(C.\tan^{-1}.(B.x - E.(B.x - \tan^{-1}(B.x)))) + S_{vy} \quad (1.2)$$

$$x = \alpha + S_{hy} \quad (1.3)$$

where,

B: stiffness factor

C: shape factor

D: peak value

E: curvature factor

S_h: horizontal shift

S_v: vertical shift

α: slip angle

Figure 2.4 illustrates the meaning of the coefficients. By selecting values for the parameters the general curve can serve as the description for the lateral force or brake force or even the aligning torque. The basic formula produces anti-symmetric curves with respect to axes shifted over the offsets S_h and S_v [11]. The offsets S_h and S_v appear to occur when ply-steer and conicity effects and possibly the rolling resistance cause the F_y and F_x curves not to pass through the origin. Also, wheel camber will give rise to a considerable offset of the F_y vs. α curves. Such a shift may be accompanied by a significant deviation from the pure anti-symmetric shape of the curve. To accommodate such an asymmetry, the curvature factor E is made dependant on the sign of the abscissa (x). 'B' stretches the horizontal axis and influences the slope at $\alpha = 0$ (Cα, BCD). BCD corresponds to the slope at the origin $(x = y = 0)$. The shape of the curve is defined by 'C'. 'D' represents peak value and contains the friction coefficient. ‘E’ influences the curvature at the peak without influencing the cornering stiffness. Pacejka [13] [14] [15] [16] advises that the values of these parameters should lie within certain ranges. For instance, C parameter should be C > 1 and typically C = 1.3 for the side force and C = 2.4 for the aligning moment. E parameter should be – (1 + 0.5C^2) < E < 1.

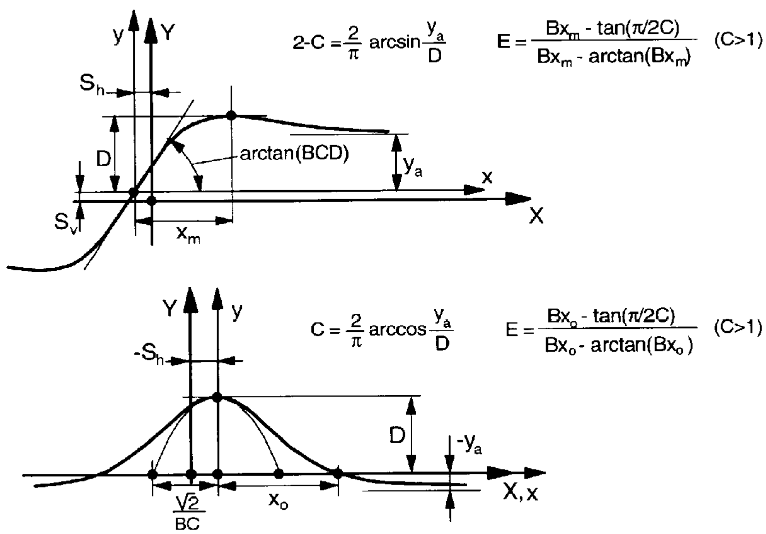

Figure 2.4 Coefficients of Pacejka's formula [11]

The Magic Formula requires a considerable amount of experimental data to define 40 coefficients. Once those have been found the formula is quite efficient from the computational point of view.

A large number of researchers have used the magic formula as a main tyre model. However, as an empirical model, magic formula may not fit every size of tyre, exactly as it was pointed out by Jang [10]. Jang criticised the two coefficients of the magic formula by claiming that the parameters had not been well represented in Pajecka’s original study. Jang’s study was to evaluate a power steering system model for possible use in the National Advanced Driving Simulator (NADS). He used the magic formula as a tyre model and discussed the results. For this reason, a step steering input of the hand wheel resulting in a J-turn manoeuvre was used. In that test, the step steer angle was 33.3° and the vehicle speed was 22.4 m/sec. The lateral acceleration, A_y, yaw rate, r, and hand wheel torque were compared with the experimental results.

From Pajecka's basic equation, the parameters B, C, D, and E respectively consist of some equations with several coefficients. Comparing the experimental results with the simulation results, the simulation prediction for the lateral acceleration had some steady state error, but the hand wheel torque prediction was even worse [10].

Assuming the real tyre for Jang's Ford Taurus is different from the tyre that Pacejka studied experimentally, Jang changed two coefficients, which had the most effect on the lateral force and aligning moment. Those coefficients are the A3 values, which are for lateral force and aligning moment in Pacejka's research [9]. After the proposed adjustment, the simulation responses have been improved. Also from the results of this research, it is already clear that the magic formula and similar models give generic representation of tyre behaviour and the data for specific tyres have to be obtained from experimental measurement.

2.5.2. First-Order Lag Tyre Model

For the transient and non-linear tyre forces, some researchers have used a modified 'Magic Formula' for instance, by using a first order lag tyre model. One example of this study belongs to Kusaka [11]. It is normally assumed that tyre lateral force changes instantaneously with slip angle, but, lateral force actually observed, behaves as shown in the Figure 2.5. It varies considerably at different forward speeds. This result is an evidence of the lag characteristic of lateral forces.

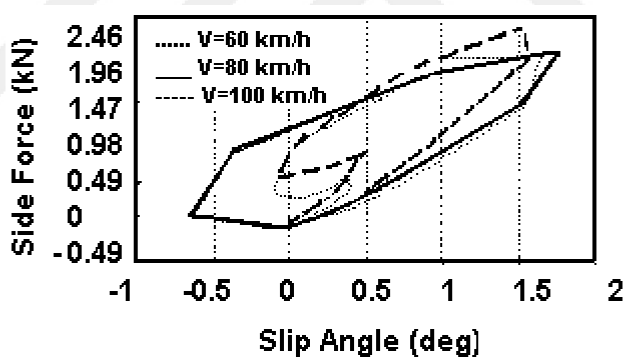

Figure 2.5 Tyre side force response with varying speeds [11].

This dynamic characteristic is known generally as relaxation characteristic of the tyre and it may be modelled as a first order lag system. The model can be derived by using first-order lag system transfer function, which is derived from the equilibrium of lateral force and reaction force of lateral stiffness and the relationship between slip angle and lateral force. Although some researchers, like Kuppers [20], have used second-order system as a transient part of the tyre model, even the first order lag model shows a fairly similar pattern with the measured data. [18] The self-aligning moment appears to behave rather differently and its responses cannot be represented by a relaxation length system only. The first-order lag tyre model gives a rather good representation of the lateral force response, also at shorter wavelengths.

2.5.3. Pragmatic Tyre Model

In this case, Maurice et al [21] has developed a new pragmatic approach, based on the analytical frequency response functions of the pneumatic trail of the brush type tyre model. These models may be referred to as pragmatic models as they represent tyre behaviour by means of relatively simple differential equations, rather than physical models.

For very low frequencies and large wavelengths, the tyre approaches the steady state. When the wavelength becomes shorter, the flexibility of the tyre sidewalls, including the effects of internal air pressure, becomes especially important as this causes a delayed response to a change of an input motion quantity. In many studies transient tyre behaviour is modelled using the relaxation length. This tyre parameter corresponds to the travelled distance, which is needed for the tyre to reach a certain percentage (63%) of the ultimate steady state situation after a change of the input. The relaxation length is strongly dependent on the vertical force and on the average slip level and is used in a first order differential equation to model the transient force response [21].

2.5.4. Fiala Tyre Model

Fiala presented his theories and modelling of cornering characteristics in 1954 [22]. After that, there were theoretical elaboration concerning the properties of braking dynamics and a theoretical account of the dynamics of braking while cornering. The Fiala model is easy to work with and runs fast. It is suitable for simplicity but not for accuracy. This model is also a part of ADAMS/Tire package for the reason of its ease of use.

According to Gim [23], Fiala's tyre model has an important lack of parameter. Fiala ignored pneumatic trail by not considering the self-aligning moment effect and simply applying a concentrated force to the centre of the contact patch. Since the pneumatic trail has significant values during both free rolling and cornering manoeuvres, however, it should not be ignored.

Assumptions in the model:

a) Rectangular contact patch or footprint
b) Pressure distribution uniform across contact patch
c) Tyre modelled as a beam on an elastic foundation.

Uniform distribution of the pressure is not in conflict with the idea of concentrated force at the centre of the contact patch. The centre of the beam is located at the centre of the contact patch, and therefore there is no pneumatic trail.

2.5.5. Use of Neural Networks as a Tyre Model

With the recent developments of Neural networks theory, some researchers have created alternative tyre models, which are test based but do not imply the use of any fitting formula [24]. In the last few years the wish to emulate some of the human capabilities has led to intensive studies about the principles governing human brain neuro-cognitive performances and the learning phenomena. From these efforts, several kinds of neuro algorithms have been introduced to reproduce some of the neuro computation abilities in artificial systems (either software-simulated or implemented in electronic devices). Generically speaking an artificial neural network (ANN) is a system constituted by many simple processors (the neurones) operating in parallel, which are able to perform a non-linear calculation (the so called activation function) on the input signals to yield an output. The neurones are linked together by means of synaptic connections according to different possible architectures; the strength of the connections (weights) represents the information stored in the system while the learning procedure corresponds with the setting operation of the weight value. If the network input variable vector is referred to as X=(x1, x2,..., xn) and U=(u1,u1,...,um) as the output variable vector, an ANN is able to learn the generic associative law between U and X by adapting its weights during a training phase in which some of these associations (training samples) are shown to the network. Neurocomputation is particularly useful where:

a) It is not possible to find a mathematical model representing the relationship U=U (X);

b) The problem is multi-dimensional (large number of input variables X to be taken into account);

c) The amount of samples is redundant compared to information complexity (large amount of experimental samples)

ANN properties make them suitable to model real life systems on the basis of experimental measurements. This is why Huston [5] decided to test them as an alternative to the traditional Pacejka’s approach in the tyre-modelling problem.

2.5.6. Interpolation Method

Although, sometimes the interpolation method is mentioned as a tyre model, actually it is only a method, which is employed in the provided tyre models. It is possible to simulate a vehicle’s handling characteristics by using interpolation of experimental data. An interpolation tyre model takes measured data for many operating points and calculates conditions for some new operating point by interpolating between the measured data. For example, under the values of 2000 N at 2 degrees slip angle and 4000 N at 4 degrees slip angle at some given vertical load; if it is also demanded to get result at 3 degrees it is possible that a lot worse might be done than to interpolate and guess at 3000 N. The sensitivity of the resultant forces or moments is related to the chosen method of the interpolation. An Example of the application of this method is in the work of Blundell [25].

The simulation is limited to the provided tyre and similar types. One of the disadvantages of this method is the increased simulation time due to the interpolation of large quantities of data at every integration time step. However, while this was an important problem in the last decade, nowadays, high-speed personal computers have partly overcome this problem. The second disadvantage is related to effects of tyre design changes on the vehicle handling dynamics. These effects can not be simulated by simply using an interpolated tyre data. In this case, a tyre model which depends on the tyre force and moment characteristics should be chosen.

2.6. A Tyre Modelling Package:

ADAMS / Tyre

ADAMS/Tyre is not a Tyre modelling method. It is a 'Comprehensive package of tyre models for simulating tyre-surface interaction' by its own definition [24]. Not only can it be used for Handling Analysis but also Durability Analysis and Comprehensive Slip. Six different tyre models are in the package. The major features of the package are shown in the Table 2.1 [22].

According to the table, the package includes six main tyre models. While the Magic formula and Smithers models need Coefficients from fitted test tyre data, University of Arizona, Fiala and Simple Equation models need basic tyre parameters. Among all these tyre models, only 'Interpolation and Point follower model' needs the Measured Tyre data. Apart from the simple equation model, all models can be applied to the handling analysis.

However, durability analysis can be done only with the simple equation model. All models except the interpolation and the simple equation models use 3D discrete triangular surfaces and General data method (1) for the road representation. For this representation, while the interpolation method has 2D continuous flat or sine and point follower, the simple equations model has 2D continuous flat or sine and equivalent plane method.

Table 2.1. The major features of the ADAMS/Tire [22]

	TIRE MODELS					
DATA REQUIRED	**Delft (Pacejka Magic Formula)**	**Smithers**	**University of Arizona**	**Fiala**	**Interpolation & Point Follower**	**Simple Equation & Equivalent Plane**
Basic Tyre Properties			●	●		●
Measured Test Data					●	
Coefficients from Fitted Test Tyre Data	●	●				
APPLICABILITY						
Handling Analysis	●	●	●	●	●	
Durability Analysis						●
Comprehensive Slip	●		●		●	
ROAD REPRESENTATION						
2D Continuous Flat or Sine or Discrete Linear Surfaces					●	●
3D Discrete Triangular Surfaces	●	●	●	●		
General Data Method(1)	●	●	●	●		
Point Follower Method (2)					●	
Equivalent Plane Method (3)						●

(1) This method computes vertical force using the tyre penetration and penetration rate on a 3D discrete triangular surface.
(2) This method computes vertical force using the tyre penetration and penetration rate on a 2D surface.
(3) This method estimates an area equivalent to the area of deformation and uses the estimated area to compute the vertical force.

2.7. Vehicle Ride & Handling Dynamics

In the broadest terms, handling is the performance of the system consisting of the driver and vehicle combination during driving. Choosing the axis system is the first step in the modelling of this system. There are two major vehicle axis systems, which are mainly seen in the literature: SAE (Society of Automotive Engineers) vehicle axis system and ISO (International Organisation for Standardisation) axis system. Even though there is no difference at the end of the analysis, sometimes these two different systems may cause some confusion in understanding the literature. It is expected that SAE will also accept to use the International standards in the near future and there will be an accord. Therefore, the ISO axis system is preferred for use in the next chapters of this thesis.

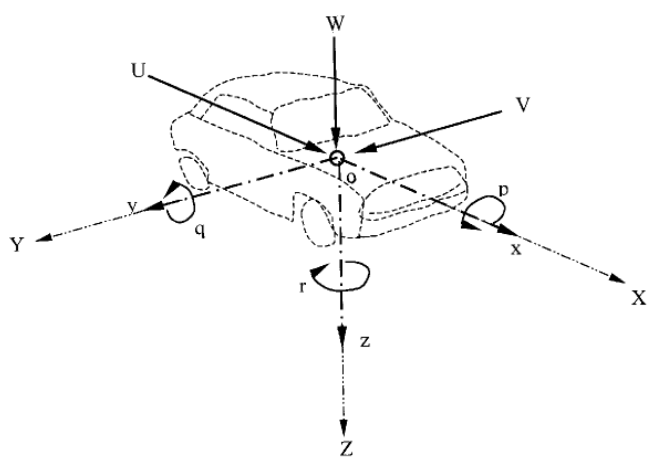

Figure 2.6 Body and earth fixed coordinates and the SAE axis system [26].

When analysing the motion of the body, it is more convenient to state its equations of motion in terms of a co-ordinate system that is attached to the moving body rather than in terms of a fixed inertial co-ordinate system. These moving co-ordinates will therefore translate and rotate with the body and are referred to as “Body fixed Axes”. Such a co-ordinate system x-y-z is shown in Figure 2.6. In this figure, axes depend on the SAE system.

The ISO axis system is depicted in Figure 2.7 It is coincident with a fixed inertial co-ordinate system X-Y-Z. However, the origin ‘O’ of the moving system has three translational velocities U, V and W while at the same time the system rotates about the three axes with angular velocities p, q and r. Therefore, the system x-y-z will no longer be coincident with the system X-Y-Z.

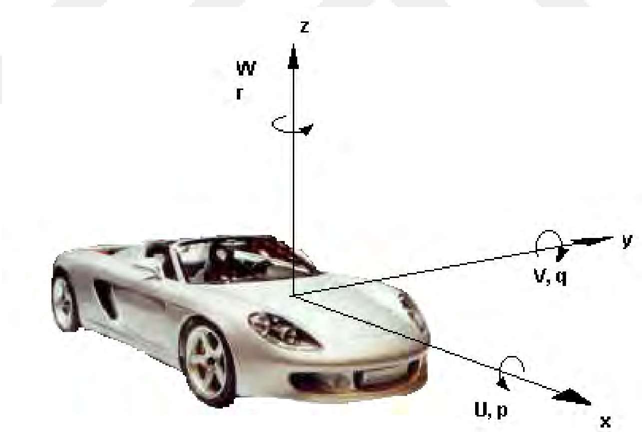

Figure 2.7 The ISO body fixed vehicle dynamics axis system.

In a road vehicle, the driver operates the steering wheel causing the steered wheels to work with a sideslip and to generate lateral forces. These forces cause a change of attitude of the vehicle and then a sideslip of all wheels: The resulting forces bend the trajectory. However the linearity of the behaviour of the tyre and the very high value of cornering stiffness give the driver the impression of safe handling. The wheels seem to be in pure rolling and the trajectory seems to be determined by the directions of the midplanes of the wheels. This impression has influenced the study of the handling of motor vehicles for a long time.

For all the linear part of the behaviour of the tyre, the driver's impression is in accordance with the kinematic behaviour. When high values of slip angles are reached, however, the average driver has the impression of losing control of the vehicle. If radial tyres are used, this impression occurs when approaching the limit of lateral forces.

Vehicle ride and handling analysis has received the most attention and represents the largest growth area in the application of multi-body dynamics [27]. Since the initial non-linear vehicle handling analysis by McHenry [28], an enormous amount of study on vehicle multi-body dynamics has been done under steady state and transient vehicle motions. Sources of non-linearity exist in suspension kinematics, steering characteristics, tyre properties and vehicle body articulation as influenced by roll and pitching moments, as well as by significant longitudinal lateral and vertical forces. Other sources of non-linearity include stiffness and damping behaviour of suspension bump and rebound stops and shock absorbers.

2.7.1. Steady State Handling Models

Steady state is taken to mean the absence of ground or wind disturbances, and fixed controls [17]. This expression includes constant turning radius, constant longitudinal speed, constant angular speed and constant magnitude of lateral acceleration, although the velocity and acceleration are not constant in direction relative to the ground. The parameters representing the motion state of the vehicle in steady conditions are its constant longitudinal speed and the turning radius. The speed and turning radius are the basic dependent variables, which result from the driver control inputs to the system. These input variables are the steer angle, the accelerator position and the gear-lever position.

2.7.2. Transient or Non-Steady State Handling Models

The steady state responses show the final condition of a car due to the application of steering, which moves to a given angle and is then held constant. The steady state does not depend upon the way in which the steering is applied. On the other hand, the transient behaviour is affected by the steering pattern, which controls the time history of the responses before a steady state is reached [29]. Generally, depending on the simulation conditions, steady state response conditions are reached in less than 1 second. Therefore, in some handling and control test procedures it is reasonable to use about 90 percent of the steady state value to define the general response time.

2.7.3. Complexity of vehicle models

From the handling point of view vehicle design has been based on the experience and expertise of test drivers. However, greater contribution from the analysis of theoretical models will be a necessity to obtain higher performance levels and decrease design costs. Vehicle handling dynamics can be studied using different types of mathematical models with different levels of approximation. The approximation level determines the physical parameters of the vehicle, which are assigned in a design study or measured for existing vehicles. As it is also pointed out by Russo et al [30], the more complete a mathematical model is the realistic will be the simulated vehicle behaviour. According to You et al [29] the two degrees of freedom model (2DOF) is the simplest one in understanding vehicle handling. However, it is difficult to express complex vehicle motions accurately with a 2DOF model. For example, You [29] examined the four-wheel steering cars (4WS) by using a 3DOF model including steering and roll motion. Nevertheless, for simplicity, he disregarded the longitudinal and pitch dynamics in the model. In most suspension modelling studies the quarter car model (2DOF) is chosen for its simplicity. However, without considering the suspension kinematics the simple model may not be as effective as might be expected [31]. Handling and ride characteristics of a vehicle are largely affected by the front and rear suspension geometries. A convenient point to start to analyse a chosen suspension system is a quarter car model, through half vehicle models (front suspension and steering system or rear suspension system) to an ultimate non-linear full vehicle-handling model [27].

On the other hand, Horiuchi et al [32] used a more complex seven-degree of freedom model including longitudinal, lateral and yaw motion. The model does not include the pitch and roll motions. In fact, the longitudinal acceleration affects the normal loading through the pitch motion while the lateral acceleration affects the normal loading through the vehicle roll motion. However, while the pitching and rolling of the vehicle are ignored by the basic equations of motions, Horiuchi takes the pitch and roll motions effects into consideration on each wheel's vertical load equations. This is another way of introducing complexity into a simple model.

2.7.4. Vehicle Ride and Suspension Characteristics

The lateral force exerted by the road on a tyre depends on the slip angle, the camber angle, the vertical tyre deflection and the longitudinal slip. The angular positions and the vertical force depend on the suspension system, which locates the wheel relative to the vehicle body. Therefore, suspension system design plays an important role in the cornering and handling characteristics and requires detailed consideration [17]. Bump and Heave, Roll, the roll centre, load transfer, pitch, steering and ride height can be counted as suspension characteristics.

Vehicle suspension systems are rated by their ability to improve vehicle handling and passenger comfort. Current vehicle suspension systems using passive components can only offer a compromise between good handling and comfort by providing fixed spring and damping coefficients. While sport cars use stiff suspension systems for improved handling characteristics, softer systems are used on a classic passenger car with relatively weaker handling capabilities but improved comfort. Especially in the last decade active suspension systems have been promoted as a solution to this conflict. The system isolates the car body from wheel vibrations induced by uneven terrain. Without an active suspension system, performance of a passive suspension system can be improved by hanging extra sprung masses off the wheels, or the complete redesign of the mechanical suspension system may be necessary [33].

2.7.4.1. Sprung and Unsprung Weight and Weight Distribution

Unsprung weight includes the mass of the tyres, brakes, suspension linkages and other components that move in accordance with the wheels. These components are on the roadway side of the springs and therefore react to roadway irregularities with no damping, except the pneumatic resilience of the tires. The rest of the mass is on the vehicle side of the springs and therefore comprises the sprung weight. Disturbances from the road are filtered by the suspension system and as a result are not fully experienced by the sprung weight. The ratio between sprung and unsprung weight is one of the most important factors influencing vehicle handling and ride characteristics.

Unsprung weight represents a significant portion of the total weight of the vehicle. In today's standard-size automobile, the weight of unsprung components is normally in the range of 13 to 15 percent of the vehicle kerb weight. In the case of a 1400 kilograms vehicle, unsprung weight may be as high as 200 kilograms. A 200 kilograms mass reacting directly to roadway irregularities at motorway speeds can generate significant vertical acceleration forces. These forces degrade the ride, and they also have a detrimental effect on handling. The Early researchers believed that the primary job of the suspension system was to absorb the bumps and smooth out the ride. Nowadays, it is clear that to keep the tyre in contact with the road is also an equally important function of a suspension system. Bumps must be overcome by the springs to keep the tyre in contact with the road. As a result, the lighter the vehicle, the less compressive force is available and the easier it is for the vertical motion of the wheels to overcome the inertia of the sprung mass.

The weight distribution is also an important factor in vehicle handling. The weight bias of the vehicle determines its oversteer - understeer character. The terms oversteer and understeer were originated by Maurice Olley and refer to the steady state path of a vehicle when acted upon by a lateral force at the centre of gravity [34]. Neutral steer corresponds to zero yawing velocity in the steady state, oversteer to a negative yawing response and understeer to a positive yawing response under an applied lateral force at ISO axis system. An understeering vehicle, when tested on a constant radius turn, requires the steering angle to be increased as speed is increased. On the contrary, an oversteering vehicle, when tested on a constant radius turn, requires the steering angle to be reduced as speed is increased. Although these characteristics are determined by the vehicle weight distribution in the design, they also depend on the design of the suspension system and can be enhanced or moderated by changing the tyre and wheel size. During severe oversteer; the steering angle may reach full lock in the opposite direction while the vehicle continues on into the turn. The vehicle is then said to "spin out." A vehicle that understeers is considered safer in the hands of the average driver. Neutral steer is the ideal situation. However, vehicle dynamics is highly complex and its behaviour cannot be predicted precisely and a neutral steer vehicle can easily turn into one with oversteer vehicle characteristic. Because of this, generally, manufacturers produce slightly understeering vehicles in order to avoid oversteer. Therefore, load and inertial effects on vehicle handling characteristics has been an important subject for vehicle dynamics researchers. The reason why manufacturers tend to produce understeering vehicles also leads researchers to examine the change of inertial properties of vehicles in cornering, lane change and uneven manoeuvres in terms of loading and load transfer. Heydinger [35] is one of the researchers who have studied the effects of loading on different vehicles using supplied vehicle data. He used a detailed computer vehicle dynamics simulation, which is called the Vehicle Dynamics Analysis Non-Linear (VDANL), to compare the effects. According to Heydinger, loading has a relative effect on vehicle mass moment of inertia. Increasing a vehicle's load will increase its mass moments of inertia, however, as a result of the compression of the vehicle springs the roll moment of the vehicle will decrease.

2.7.4.2. Steering

Vehicle stability characterisation clearly depends on steering manoeuvring conditions as well as vehicle parameters. Directional control is normally achieved by steering the front wheels, by rotating them about roughly vertical axes. This is mainly the result of steering movement by the driver, but partly the result of suspension characteristics. Rear wheel steering is inherently unstable at high speeds, but because of its convenience, it is sometimes preferred on low speed vehicles such as dumper trucks.

Since late 1986, there have also been four-wheel steer (4WS) vehicles on the market. 4WS was first introduced in passenger cars by Honda [4]. Four wheel steer turns both the front and rear wheels of a vehicle during a steering input. Two different steer types are applicable for front and rear wheels in the system - counter steer and same steer. In the counter steer type, front wheels and rear wheels turn in opposite directions and this method is preferred for low speeds. In the same steer type, as its name implies, front and rear wheels turn in the same direction at certain ratios to each other. However, after over ten years of its introduction, researchers could not report any considerable advantage of 4WS system against two-wheel steer (2WS). A serious problem with 4WS vehicles is excessive rear overhang swing [12]. For a comparison of the two systems both Alter [4] and Lee [12] practised the lane change manoeuvre and skid pad test simulation on both 2WS and 4WS passenger cars. According to both researchers, performance benefit achievable with a 4WS vehicle was not significant relative to that achievable with a 2WS vehicle. However, Alter [4] suggested that the performance benefits of 4WS exist only in rear heavy vehicles, which themselves make up only a small minority of the production vehicles marketed today.

In recent years, there has been a steady decline in the number of reported studies on four wheel steering. Although some researches have tried to explain the system's ineffectiveness, other researches have claimed its benefits. For instance, ‘You’ and Jeong [29] claimed that the 4WS system's efficiency is superior to that of the 2WS system on the basis of variable control at different speeds. They examined the challenging application of a robust control scheme for the steering autopilot design of a 4WS vehicle. The vehicle control system is formulated using a mixed H_2 /H_∞ approach with pole constraint via linear matrix inequality (LMI). Both the wheel angles and wheel torque are actively controlled to improve manoeuvrability and directional stability. As a result they obtained greater manoeuvrability and improved directional stability for the 4WS system.

However, according to Abe et al [36], there has been no general consensus on what type of control law is suitable for the 4WS yet. After extensive research and reviewing the studies which had been done, Furukawa and Abe [37] concluded that regardless of how much the advanced control theories were used, there is a wall of vehicle dynamics and control which is difficult to make a break through in terms of four wheel steering systems.

2.8. Control systems in vehicle handling dynamics

Traditionally, the control of vehicle handling dynamics has been the responsibility of the driver alone, using the accelerator, brakes and steering wheel. Recently, automated control systems have assumed a more significant role in areas such as active suspension, four-wheel steer and Direct Yaw Control [36]. The reason for this significant role is directly related to the idea of safe handling for the average driver during cornering, and lane change manoeuvres in even on uneven road conditions, as mentioned in the introduction in Chapter 1.

2.8.1 Vehicle Chassis control systems

The vehicle chassis control system is in general used to control vehicle lateral, vertical and longitudinal motions in order to improve handling performance, ride comfort and traction / braking performance. These control systems basically depend on steering, suspension and traction / braking control [37]. The most common chassis control systems for the improvement of handling performance are four-wheel steering and the yaw control, which were mentioned in section (2.7.3).

Figure 2.8 indicates that any chassis control aiming at improving vehicle handling performance must rely on the tyre lateral force and that the tyre longitudinal force can also be used for the chassis control. These two forces depend on the vertical load and have an interdependency relationship. This relationship makes the vehicle dynamics characteristics very complex and a deeper observation and study is required for more effective chassis control [37].

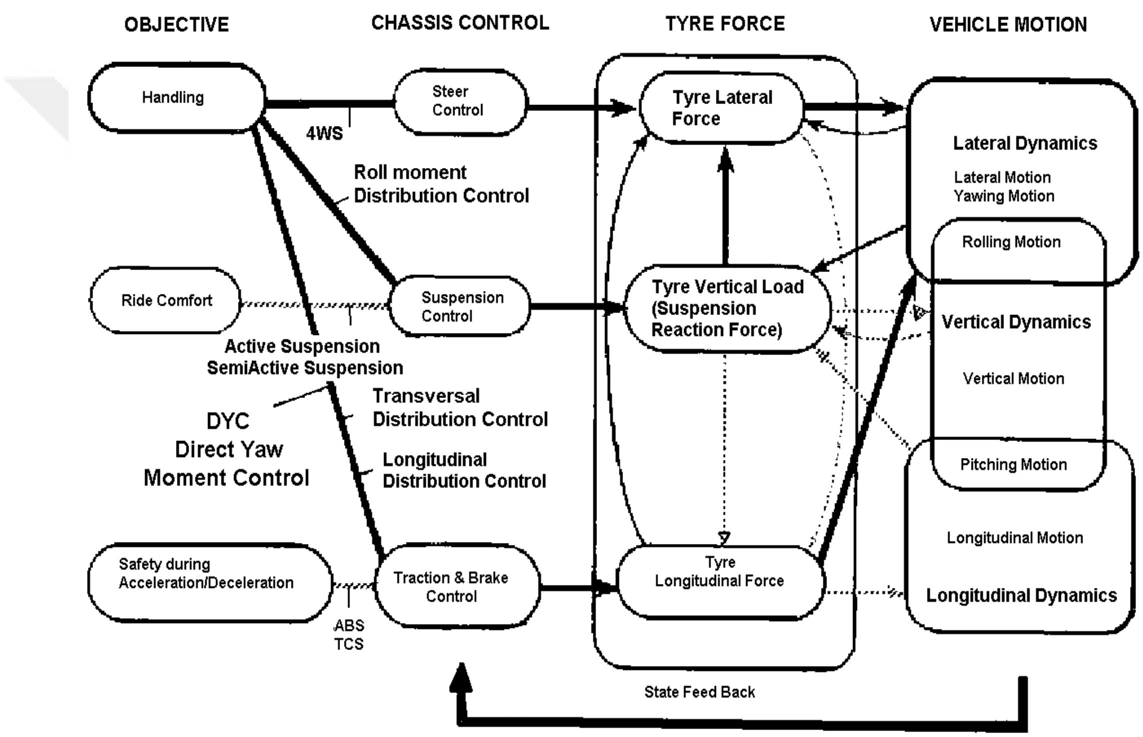

Figure 2.8 Outline of vehicle chassis control [37].

There is a non-linear relationship between tyre lateral force and vertical load. By considering this phenomenon, vehicle lateral motion can be controlled by controlling the distribution of active roll moment between front and rear active suspensions. Since the total sum of left and right lateral forces becomes smaller as the transverse load transfer by the roll moment becomes greater due to the non-linearity of tyre lateral force against its vertical load, the balance of lateral forces between the front and rear wheels during vehicle cornering manoeuvre can be controlled by controlling the longitudinal distribution of the roll moment [37]. This situation might be referred to as on-line tuning of roll stiffness of the front and rear suspensions.

Active (controlled) suspension systems are now more commonly available on production passenger vehicles, and most of the recent suspension modelling studies has been carried out using commercial simulation packages specifically tailored for the purpose such as ADAMS. Blundell studied the compliance of the suspension systems due to the bushes [25]. He suggested that the bush stiffness should be taken into account in a kinematic analysis because of its considerable effect on vehicle handling and he performed the modelling and handling analysis in ADAMS. Kim [31] showed the importance of kinematic analysis. Comparing two active suspension systems with equivalent parameters but different control laws (sky-hook and sliding mode control) and structures, he showed that they produced different responses. In terms of the lateral dynamics of vehicle, there are main two methods to control the vehicle lateral motion by using the tyre longitudinal force - the indirect method and the direct method. In the indirect method, since the longitudinal force acting on the tyre reduces the lateral force, the balance between the lateral forces of front and rear wheels can be varied by distributing the longitudinal force acting on the rear and front wheels. This method aims to control the vehicle lateral motion as much as possible and points out mainly controlled four-wheel drive (4WD) vehicles.

The other approach is the direct method. If the traction force and braking force are properly distributed to the right and left wheels, a yaw moment will be obtained in accordance with the forces distributed and thus the vehicle lateral motion can be accurately controlled. A yaw moment control (DYC) system controls the vehicle motions by a yaw moment, which is actively generated by the intentional distribution of the tyre longitudinal forces. One of the important advantages of this method is that the tyre longitudinal force has no feed back from the vehicle motion as long as it is within the limit of the tyre capacity due to the vertical load. DYC systems using tractive / braking forces have been researched and developed also to improve handling and stability. One such system uses active traction control system of each wheel through the feedback of state variables, such as yaw rate and/or vehicle body slip angle. These active control systems can generate yaw moment directly to compensate for vehicle yaw motion not only in linear ranges but also in non-linear ranges. Therefore, the direct yaw moment control systems are expected to suppress the deterioration of the steering control effects in non-linear or large lateral acceleration ranges as they occur in 4WS systems.

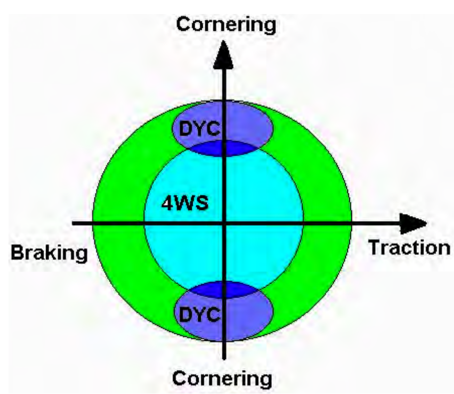

Figure 2.9 Effective areas of 4WS and DYC [38]

Nowadays, several control systems can be used in a vehicle at the same time. As Harada [39] mentioned, integrated control systems with both active suspension and rear wheel steering systems contributes to active safety more effectively under steady state conditions. Although each system has its own specific function, under certain conditions, their working range may go into a conflict. In this case, the control system law, which will be implemented, needs to get a compromise between working range and timing. Therefore, in a research study it would be better to examine the proposed systems together. For example, Nagai et al [40] studied an integrated control system design for active rear wheel steering and Direct Yaw Moment Control. He used a control system, which forces the vehicle to follow the desired path, based on the 2DOF steering model by using the state feedback of both yaw rate and side slip angle. He used Simulink® as a simulation tool and the results showed an improved handling and stability even in strong non-linear ranges of the tyres. According to Nagai et al the effective areas of 4WS and DYC systems are given in Figure 2.9.

Most of the controlled vehicle handling researches include the feedback control as a control scheme. A few of them also include the feedforward control scheme [13], [41], generally, for the estimation of slip angle. Lyapunov, the sliding mode control and LQR are the most common control logics used. However, there is a lack of experience in the intelligent control schemes such as fuzzy logic and neural networks. In the last decade, intelligent control schemes have been increasingly applied in various fields. Lauffenburger et al. [42] applied polar polynomial curves to represent the desired path of a vehicle, and fuzzy logic control was used to determine the constraints of the maximum points of the polynomial, with the driver's profile, in terms of experience, being used as an additional parameter. An inexperienced driver negotiating a bend increases the steering angle smoothly during the first half of the turn and decreases it during the second half. This technique is guided by maximum comfort and safety.

The trajectory in the same turn is completely different for an experienced driver whose objective is to minimise the time taken to traverse the turn. Mouri [43] and Furusho [44] proposed a path tracking system to regulate the lateral position of the centre of gravity of the vehicle by minimising a cost function based on the lateral displacement of the centre of gravity and the front wheel steering angle. A virtual point regulator which also takes the yaw angle into consideration in addition to this basic approach has been proposed by Marumo et al. [45]. The virtual point is at a point on the driver's line of sight and is a function of the vehicle yaw angle, the lateral displacement at the vehicle centre of gravity and the distance between the virtual point and the centre of gravity. The cost function is, therefore, now based on the lateral displacement of the virtual point and the front wheel steering angle. This increases the robustness and the performance of the control system. Due to the nature of processes like using a virtual point to represent, simply, the human driver's line of sight, intelligent control system models which can mimic the driver's experience, such as fuzzy logic control or neural networks, are the most preferable control schemes in these studies. These control models are intended basically to command the steer angle. Additionally, yaw angle error and yaw rate may also be used as inputs to the intelligent control system. This kind of process, based on fuzzy logic, was referred to as 'fuzzy pilot' by Piancastelli & Sarubbi [46].

2.9. Sensory systems in vehicle control

The measurement system consists of devices, which can obtain a quantitative comparison between a predefined standard and a measured parameter. Transducers, sensors and detectors are some of the names used to describe a measurement system [47].

Transducers are devices capable of converting one form of energy or physical quantity to another. Often this energy or stimulus determines the quantity of the signal obtainable. Sensors are devices used for the purpose of detecting, measuring or recording physical phenomena and subsequently responding by transmitting information, initiating changes or effecting systems control [42].

From these definitions it is apparent that the difference between these devices is difficult to distinguish. Therefore, for the purpose of automotive applications, these devices can be classified as sensory systems. Chassis control and management systems need a suitable sensory system and the majority of the sensors used in chassis control systems assist the vehicle ride, which is subsequently affected by the vehicle suspension system. Sensors required by chassis control systems are shown in the below table 2.2.

Table 2.2 Sensors required by chassis control systems [47]

ABS	4WS	4WD	AS
Wheel Speed	Steering wheel angle	Brake on-off	Actuator stroke
Longitudinal acceleration	Rear steering angle	Wheel speed	Yaw rate
Lateral acceleration	Yaw rate	Throttle angle	Vehicle speed
-	Lateral acceleration	Steering wheel angle	Longitudinal acceleration
	Vehicle speed	-	Hub-vertical acceleration

The primary function of the suspension system is to control the attitude of the vehicle body with respect to the road surface. This includes the monitoring and control of parameters such as pitch, roll, bounce and yaw motions. There are several types of suspension systems used such as passive, active and semi-active suspension systems. For a typical controlled suspension system, there are sensors for monitoring the vertical displacement (bounce) of the road wheels relative to the vehicle body. This type of sensor can range from a simple potentiometer to more complex sensors such as linear variable-inductance position sensors and optical sensors. Accelerometer sensors can also be used for advanced braking systems incorporating antilock braking (ABS) /traction control, steering systems and safety systems. For the suspension control, the combination of these sensors is used to monitor and control the bounce, roll and pitch motions of the vehicle, but yaw motion can be monitored by the use of a yaw rate sensor (e.g. optical fibre gyroscope, solid state piezo-electric devices). An integrated control strategy will include steering wheel rotation sensor, vehicle velocity sensor and throttle position sensors [47].

2.10. Vehicle Handling Test Standards and Methods

The tests consist of one steady state and a number of transient procedures. Steady State cornering test is the most frequently used procedure to supply data on the steering tendency of vehicles. This test is designed to measure the steer angle as a function of steady state lateral acceleration and to describe the understeer or oversteer for the right and left turns. Figure 2.10 shows the simple constant radius steer manoeuvre.

Sinusoidal Steering Wheel Input is used to evaluate the frequency response properties of a vehicle as the intensity of periodic steering wheel input to vehicle reaction. The procedure assumes that the response characteristics of a vehicle can be examined in a linear way with good approximation. The frequency response function describes the amplitude ratio of output to input value and phase lag between both values in the steady state condition and dependence on the frequency [48]

The single lane change manoeuvre is applied to analyse the amount of required steering to be performed by the driver to keep the vehicle on the desired track and to stabilise the vehicle. It may also be called single sinusoid steer test. Figure 2.11 shows the single lane change manoeuvre.

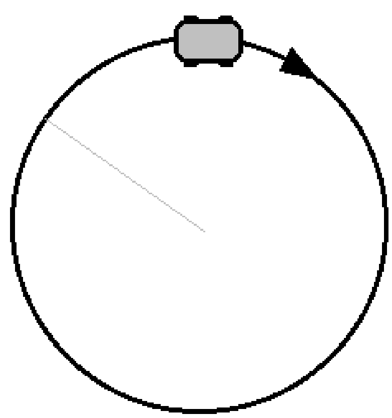

Figure 2.10 Constant Radius steer test.

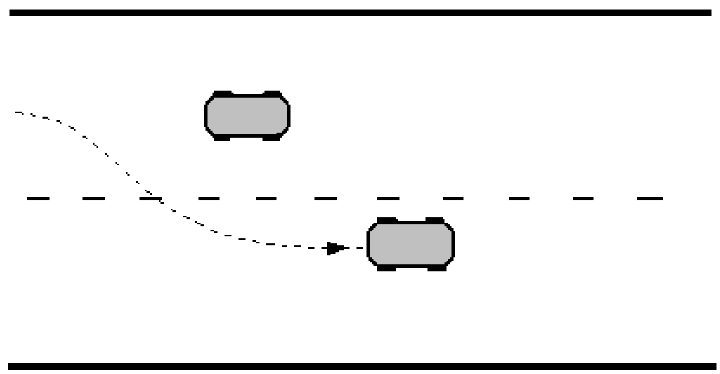

Figure 2.11 Single lane change manoeuvre.

2.11. Conclusions

This review shows that the selection of the tyre model is the initial and the most important step in a vehicle handling analysis. The convenience, accuracy and ease of the analysis are firstly related to the chosen tyre model. As a result of the review, the Interpolation method is seen as the most convenient method to use in this study. There are two main reasons for the selection. Firstly, crucial tyre data for a vehicle handling dynamics study can simply be extracted from the results of the experiments on a tyre test rig which simulates the dynamics behaviour of a tyre. Secondly, avoiding the complexity of a physical tyre model and an empirical model, like the Magic Formula Tyre Model will enable the aim of ease of simulation to be achieved while maintaining accuracy. Vehicle ride and handling dynamics modelling with the control systems have also been reviewed after the tyre models. It is clear that computer simulations have become an inevitable part of the vehicle research for decades. More sophisticated simulation tools are on the market than ever before and even it is quite possible that zero-prototype vehicle development may be realised by in the next 10-20 years. However, this trend is also increasing the cost of the research for individual researchers, who need to use those sophisticated software. The wide-perspective of this thesis is devoted to a full vehicle model handling dynamics analysis. Specifically, this thesis intends to first develop a vehicle handling simulation tool which provides ease of use and adequate sophistication. This tool is then to be applied using a new approach to driver modelling and path planning. In the literature there is an important lack of the application of modern intelligent control logic to vehicle dynamics. These classes of logic have been considerably improved in the last decade, yet traditional control schemes are still dominant. There is therefore a need to research and apply intelligent control schemes, which best mimic the human decision making, in certain situations, with increasing intensity. From this point of view, computer simulation of vehicle handling dynamics with integrated fuzzy logic control will be the objective of this study.

CHAPTER 3

VEHICLE HANDLING DYNAMICS MODELLING

3.1. Introduction

The axis systems have been discussed in the previous chapter. Therefore, on the basis of chosen ISO body fixed axis system, it is now necessary to state the Newtonian equations of a rigid body. In this chapter, the general dynamic equations of the vehicle and the implemented tyre modelling are presented and depending on these equations, more complex vehicle dynamics model equations are derived starting from the simplest two-degree of freedom model on the base of the assumptions, which are subject to the general of the thesis.

3.2. Tyre Modelling

As it is discussed in the chapter 1, tyre modelling can be a very complex study as itself. However, for the purpose of vehicle handling dynamics analysis, a proper method should be chosen to consider both the accuracy and simplicity of the study. From this point of view, interpolated tyre data method is used to extract the modelling parameters. Tyre data is obtained both from the experiments which were held on the tyre test rig in the Automotive Research Laboratory/University of Birmingham, and the literature [25] (Figure 3.1). Experiments have been held on an AVON 20.0x6.0-13 specifically produced for racing type tyre. The tyre tests for AVON 20.0x6.0-13 was carried out at a speed of 20 kph vehicle equivalent speed on a drum and with an internal pressure of 14 psi. The characteristic data of the tyre is represented on the Figure 3.3.

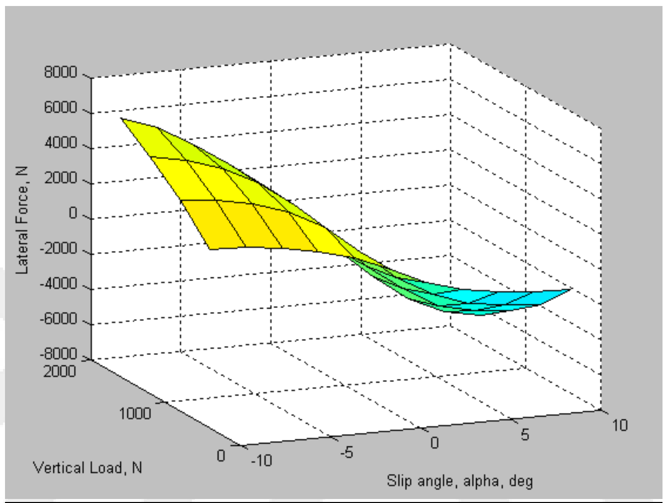

Figure 3.1 Tyre characteristics for DUNLOP D8 195/65 R15 [25]

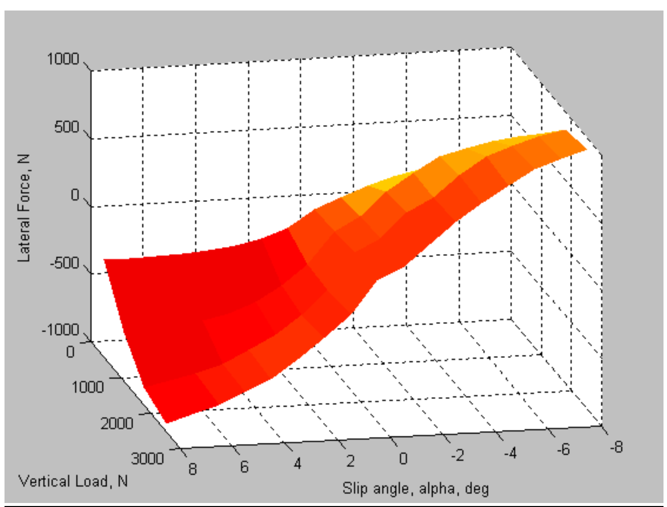

Figure 3.2 Tyre characteristics for Goodyear Formula SAE 20.0x6.5-13 [49]

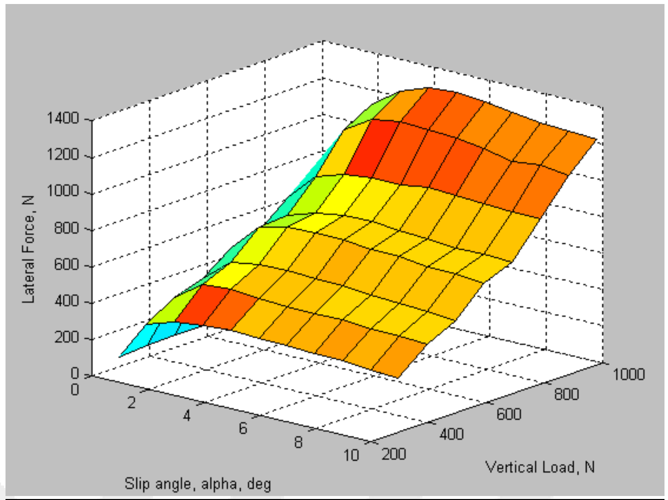

Figure 3.3.Tyre characteristics for the AVON 20.0x6.0-13 Tyre

Varying the load from 300 N to 1000 N with 100 N increments, lateral forces and aligning moment values were taken from -10 to 10 degrees of slip angle with 1 degree increment at zero camber angles. Detailed tyre construction analysis, many possible coefficients and data are eliminated by using this method. As a result, an easy to use handling model has been obtained implementing this tyre model into the dynamics modelling of the vehicle. Any tyre data provided in a matrix form can be implemented to the vehicle model. Interpolation tyre data table for GOODYEAR, AVON and DUNLOP tyre can be found in Appendix A.

<u>3.2.1. Interpolation methodology</u>

Lateral force and aligning moment values of the tyre are obtained at certain slip angles and vertical loads, experimentally (see Appendix A). The most important parameter for the interpolation is the cornering stiffness of the tyre which is provided by the below equation [3.1]:

$$C_{\alpha} = \frac{F_y}{\alpha} \tag{3.1}$$

Using this equation, a look up table is formed for the cornering stiffness of the tyre. Tyre slip angle is a function of lateral force and the cornering stiffness and it is also represented in terms of the velocities of the vehicle in the equations (3.2) and (3.3) both for the front and rear axle, respectively [26].

$$\alpha_f = \left(\frac{V + a \cdot r}{U} \right) - \delta \tag{3.2}$$

$$\alpha_r = \left(\frac{V - b \cdot r}{U} \right) \tag{3.3}$$

where,

V	: Lateral velocity of the vehicle
U	: Longitudinal velocity of the vehicle
r	: Yaw velocity of the vehicle
a	: Front wheelbase
b	: Rear wheelbase

Providing the load transfer between the tyres, which is a subject of the Chapter 5, the data is interpolated to find the cornering stiffness and then the lateral force of the tyre using the '*interp2*' function of Matlab® and the equation (3.1). The *interp2* command interpolates between data points. It finds values of a two-dimensional function f(x, y) underlying the data at intermediate points [50]. The methodology of this function is given below expression and Figure 3.4.

“Cornering stiffness = interp2(‘SlipAngleData’,‘LoadData’,‘CorneringStiffData’,‘SlipCalculated’,‘LoadCalculated’);”

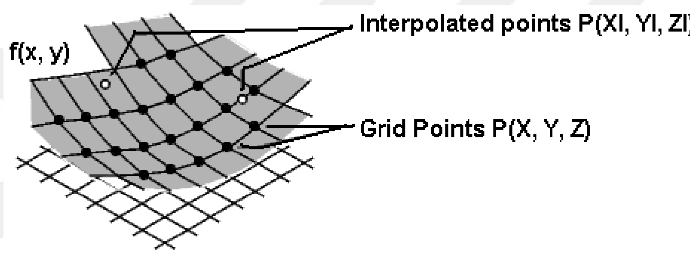

Figure 3.4 The coverage of *interp2* interpolation function in Matlab [50]

3.3. Modelling the tractive and braking characteristics

A simple approach is used to represent the braking and traction forces and the resultant moments by avoiding the complexity of the brake and engine/driveline dynamics. The forces and moments applied on a tyre are shown in Figure 3.5. The proposed method will provide a more general representation of the forces and moments which are going to be needed as inputs in the Simulation tool, which will be discussed in Chapter 4. For this reason, a gain factor is introduced both for the braking and the driveline. The derivation of the braking and the tractive force equations are shown from the Equation [3.4] to [3.7] below.

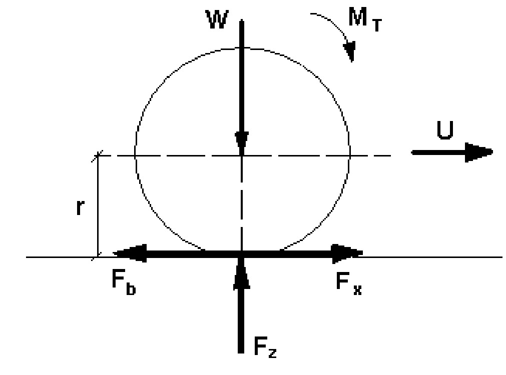

Figure 3.5 Forces acting on a tyre from the side view.

$$T_b = bgain \cdot P_b \tag{3.4}$$

$$F_b = \frac{T_b}{r} \tag{3.5}$$

$$T_d = dgain \cdot thr \tag{3.6}$$

$$F_x = \frac{T_d}{r} \tag{3.7}$$

where,

P_b : Braking pressure

r : Effective tyre radius

T_b : Braking torque

T_d : Driving torque

F_b : Braking force

F_x : Tractive force

$bgain$: Braking gain

$dgain$: Driveline gain

thr : The percentage of the throttle being open

3.4. Formulating the equations of motion (vehicle model)

The dynamic equations can be obtained using Lagrange Equations or Newton-Euler basic dynamic equations. Since Lagrange equations require partial differentiation, the Newton-Euler method, which simply requires matrix operations, is applied in this thesis. Based on the Newton Euler approach, three equations can be written for the x, y, and z-axes for both forces and moments applied. Therefore, these six equations describe the motion of vehicle body with six degrees of freedom [48].

$$\sum F_x = m(\dot{U} - rV + qW) \tag{3.8}$$

$$\sum F_y = m(\dot{V} - pW + rU) \tag{3.9}$$

$$\sum F_z = m(\dot{W} - qU + pW) \tag{3.10}$$

$$\sum M_x = I_{xx}\dot{p} - (I_{yy} - I_{zz})qr + I_{yz}(r^2 - q^2) - I_{zx}(qp + \dot{r}) + I_{xy}(pr - \dot{q}) \tag{3.11}$$

$$\sum M_y = I_{yy}\dot{q} - (I_{zz} - I_{zz})rp + I_{zx}(p^2 - r^2) - I_{xy}(rq + \dot{p}) + I_{yz}(qp - \dot{r}) \tag{3.12}$$

$$\sum M_z = I_{zz}\dot{r} - (I_{xx} - I_{yy})pq + I_{xy}(q^2 - p^2) - I_{yz}(pr + \dot{q}) + I_{zx}(rq - \dot{p}) \tag{3.13}$$

where $\sum F_x$, $\sum F_y$ and $\sum F_z$ are the applied forces and $\sum M_x, \sum M_y$ and $\sum M_z$ are the resultant external moments that are applied to the body about the axes x, y and z. Because of the complexity of the moment equations, the coordinate system is attached to the body. Therefore the product moments of inertias each become zero and the moment equations are reduced to the equations given from (3.14) to (3.16).

$$\sum M_x = I_{xx}\dot{p} - (I_{yy} - I_{zz})qr \tag{3.14}$$

$$\sum M_y = I_{yy}\dot{q} - (I_{zz} - I_{zz})rp \tag{3.15}$$

$$\sum M_z = I_{zz}\dot{r} - (I_{xx} - I_{yy})pq \tag{3.16}$$

3.5. Vehicle Dynamics Models

There are two types of vehicle dynamics models, steady state and transient motion models. Steady state exists when periodic (or constant) vehicle responses to periodic (or constant) control and / or disturbance inputs do not change over an arbitrarily long time. The motion responses in steady-state are referred to as steady-state responses [51]. Transient state exists when the motion responses, the external forces relative to the vehicle, or the control positions are changing with time [51].

The behaviour of a road vehicle can mostly be expressed as non-linear. The sources of non-linearities are mainly three: The presence of products of the variables of motion in the equation, the presence of trigonometric functions and the non-linear nature of the forces due to the tyres. These non-linearities can be neglected if the side slip angles of the wheels and of the vehicle; the steering angles are very small. These conditions generally apply for the vehicle, which is driven far from the limit performances. When a vehicle goes to its limit of performance like in race driving and, even more, when uncontrolled motion occurs during an accident a fully non-linear model must be used [52].

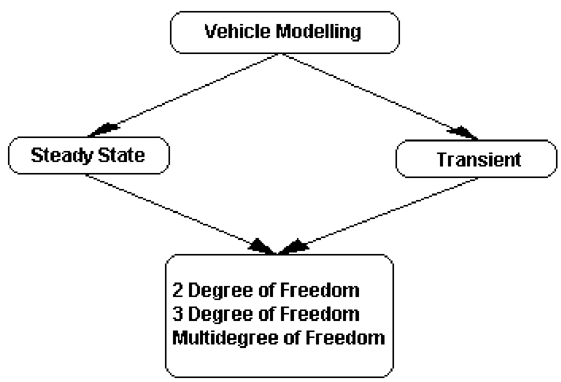

Figure 3.6 A classification of vehicle modelling

<u>3.5.1. Two Degree of Freedom (The Quarter Car) Model</u>

The dynamics of a vehicle can be represented by various models of varying complexity characterised by the number of degrees of freedom. Two degrees of freedom- Bicycle Model is the simplest one. It represents the lateral and yaw motion of the vehicle. Figure 3.7 shows the two-degree of freedom model.

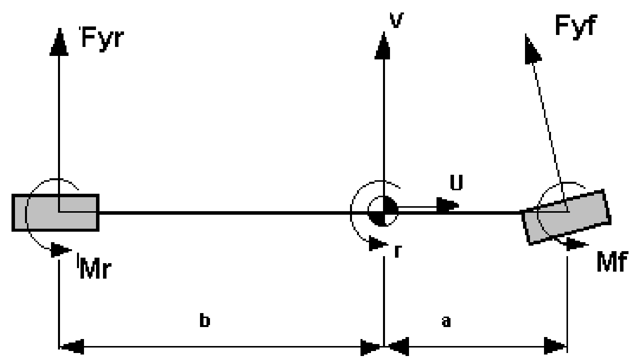

Figure 3.7 Two Degree of Freedom model.

This model includes several assumptions:

- **Vehicle does not roll:** However, the general expression of "there will be no load transfer between the outer and the inner set of wheels if vehicle does not roll" is not exactly true. In a zero-roll model, total load transfer depends on the lateral force, the centre of the vehicle mass height and the track. The effect of the roll at maximum lateral acceleration is about 5% of the total weight compared with a load transfer of about 35% of the weight from the other factors [51]. The derivation of load transfer equations will be discussed in suspension system modelling in Chapter 6.

- **Vehicle travel on a smooth plane:** Pitch and bounce effects are ignored.

- **Symmetrical vehicle**: Vehicle is assumed to be physically symmetrical in the *x-z* plane and the principal axes of inertia are assumed to be located at the centre of the mass of the vehicle, therefore, the products of inertia $I_{xz} = I_{yz} = I_{xy} = 0$

By considering these assumptions, the following simplified equations can be extracted:

$$\sum F_y = m(\dot{V} + rU) \tag{3.17}$$

$$\sum M_z = I_{zz}\dot{r} \tag{3.18}$$

$$m(\dot{V} + rU) = \left[F_{yr} + F_{yf} \cdot \cos(\delta) + \left(F_{xf} - F_{bf}\right) \cdot \sin\delta\right] \tag{3.19}$$

$$I_{zz}\dot{r} = a \cdot F_{yf} - b \cdot F_{yr} \tag{3.20}$$

The two-degree of freedom model cannot represent motions such as pitch and roll, and so, more complex models are required for analysing these motions.

3.5.2. Three & Multi Degree of Freedom Models

The first step in creating the model is to expand the bicycle model to a four-wheeled system. A Three-degree of freedom model simply adds roll to the bicycle model and usually denoted by ϕ for the roll angle and p for the roll angular speed. Therefore, this model takes into account yaw, sideslip and roll. It was first systematically investigated by Segel [3].

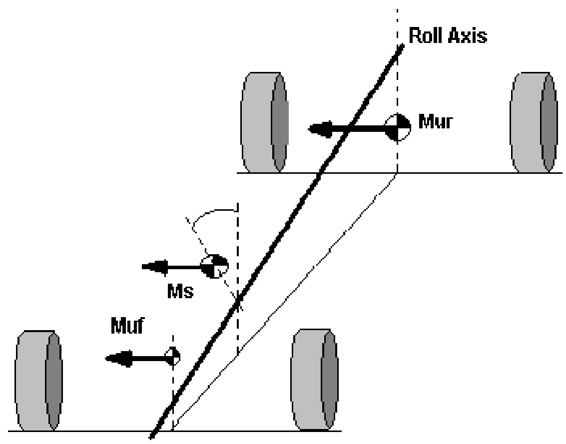

Figure 3.7 Roll axis of the three degree of freedom model

The six degree of freedom model equations are reduced to three fundamental equations of motion in the three degree of freedom model, which are shown below:

$$\sum F_y = m(\dot{V} + rU) \tag{3.21}$$

$$\sum M_z = I_{zz}\dot{r} \tag{3.22}$$

$$\sum M_x = I_{xx}\dot{p} \tag{3.23}$$

Adding force equations on the longitudinal plane (Equation [3.24]), this model can simply be transformed into Four degrees of freedom model enabling the inclusion of traction and braking forces on handling manoeuvres. Using increased degrees of freedom can increase the accuracy of the model. However, increased freedom also increases the input parameters and calculation time. Therefore, pitching effects of the braking and tactive forces and the longitudinal load transfer are ignored.

$$\sum F_x = m(\dot{U} - rV) \tag{3.24}$$

The following equations are derived according to the below forces shown in Figure 3.8, where:

F_x : Tractive force

F_y : Lateral force

F_b : Braking force

L : Left, R : Right

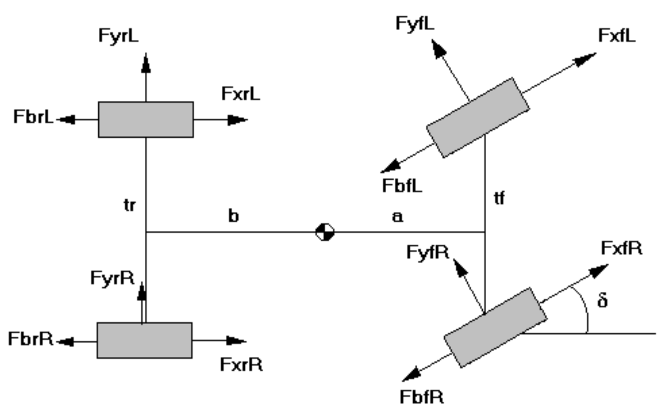

Figure 3.8 Acting forces on a vehicle from top view

$$m(\dot{U} - rV) = \begin{bmatrix} F_{xrL} + F_{xrR} + (F_{xfL} + F_{xfR}) \cdot \cos\delta - F_{brL} - F_{brR} - \ldots \\ \ldots - (F_{bfL} + F_{bfR}) \cdot \cos\delta - (F_{yfL} + F_{yfR}) \cdot \sin(\delta) \end{bmatrix} \tag{3.25}$$

$$m(\dot{V}+rU)=\begin{bmatrix} F_{yrL}+F_{yrR}+\left(F_{yfL}+F_{yfR}\right)\cdot\cos(\delta)+\left(F_{xfL}+F_{xfR}\right)\cdot\sin\delta-\ldots \\ \ldots-\left(F_{bfL}+F_{bfR}\right)\cdot\sin\delta \end{bmatrix} \tag{3.26}$$

$$I_{xx}\dot{p}=\left[m_s\cdot\left(\dot{V}+r\cdot U\right)\cdot d+m_s\cdot g\cdot d\cdot\phi-C_\phi\cdot\phi'-K_\phi\cdot\phi\right] \tag{3.27}$$

$$I_{zz}\dot{r}=\begin{bmatrix} a\cdot\left(F_{yfL}+F_{yfR}\right)\cdot\cos\delta+\left(t_f/2\right)\cdot\left(F_{yfL}-F_{yfR}\right)\cdot\sin\delta+\ldots \\ \ldots+a\cdot\left(F_{xfL}+F_{xfR}\right)\cdot\sin\delta+\left(t_r/2\right)\cdot\left(F_{brL}-F_{brR}-F_{xrL}+F_{xrR}\right)-\ldots \\ \ldots-b\cdot\left(F_{yrL}+F_{yrR}\right)-\left(t_f/2\right)\cdot\left(F_{xfL}+F_{bfR}-F_{xfR}-F_{bfL}\right)\cdot\cos\delta-\ldots \\ \ldots-a\cdot\left(F_{bfR}+F_{bfL}\right)\cdot\sin\delta \end{bmatrix} \tag{3.28}$$

From the equations 3.25, 3.26, 3.27 and 3.28 the following equations of motion are obtained.

$$\dot{U}=\left[\left(\frac{\begin{matrix}\left(F_{xfR}-F_{bfR}-F_{bfL}\right)\cdot\cos\delta+F_{yfL}\cdot(\delta)+F_{xrL}+F_{xrR}-F_{brL}-\ldots \\ \ldots-F_{brR}-\left(F_{yfL}+F_{yfR}\right)\cdot\sin(\delta)\end{matrix}}{m}\right)+r\cdot V\right] \tag{3.29}$$

$$\dot{V}=\left(\frac{\left(F_{yfL}+F_{yfR}\right)\cdot\cos(\delta)+\left(F_{xfL}+F_{xfR}-F_{bfL}-F_{bfR}\right)\cdot\sin\delta+F_{yrL}+F_{yrR}}{m}\right)-r\cdot U \tag{3.30}$$

$$\dot{p}=\left(\frac{m_s\cdot\left(\dot{V}+r\cdot U\right)\cdot d+m_s\cdot g\cdot d\cdot\phi-C_\phi\cdot\phi'-K_\phi\cdot\phi}{I_{xx}}\right) \tag{3.31}$$

$$\dot{r} = \begin{bmatrix} a \cdot \left(F_{yfL} + F_{yfR}\right) \cdot \cos(\delta) + \left(t_f / 2\right) \cdot \left(F_{yfL} + F_{xfR}\right) \cdot \sin(\delta) + \ldots \\ \ldots + a \cdot \left(F_{xfL} + F_{xfR}\right) \cdot \sin\delta + b \cdot F_{xrR} + \left(t_r / 2\right) \cdot \left(F_{brL} - F_{brR} + F_{xrL}\right) - \ldots \\ \ldots - b \cdot \left(F_{yrL} + F_{yrR}\right) - \left(t_f / 2\right) \cdot \left(F_{xfL} + F_{bfR}\right) \cdot \cos\delta - \ldots \\ \ldots - a \cdot \left(F_{bfR} + F_{bfL}\right) \cdot \sin\delta - \left(t_f / 2\right) \cdot F_{yfR} \cdot \sin(\delta) \end{bmatrix} \cdot \left(\frac{1}{I_{zz}}\right) \quad (3.32)$$

As it will be discussed in the next Chapter, the equations of motions are solved using ode45 function of Matlab. Ode45 is based on an explicit Runge-Kutta (4, 5) formula, the Dormand-Prince pair [50]. It is a one-step solver - in computing of a time dependant function y (tn), it needs only the solution at the immediately preceding time point, y (tn-1). In general, ode45 is the best function to apply as a "first try" for most problems and the results are in good accuracy [50].

3.6 Conclusions

Mathematical modelling of the vehicle has been studied in this chapter. The model equations cover two, three and the four degrees of freedom systems. While two-degree of freedom system simply includes lateral and yaw motions of the vehicle, three-degree of freedom model includes also roll motion and four degrees of freedom model adds the total forces applied on the longitudinal plane. The model complexity and accuracy can be increased by increasing the degree of freedom. However, one of the purposes of this study is to obtain both simplicity and the accuracy together. By considering the tractive and braking forces will be applied as minor corrective control inputs for the yaw control of the vehicle, pitching effect of these forces, and as a result the pitch degree of freedom, are simply ignored. Therefore, avoiding the unnecessary complexities, simulation time and cost can be decreased. The development of the vehicle handling simulation tool and the suspension dynamics are discussed in Chapters 4 and 6, respectively.

CHAPTER 4

PROGRAMMING AND VEHICLE HANDLING SIMULATION

4.1. Introduction

Road vehicle dynamics simulation tools to predict the vehicle behaviours have been in use for decades. Computerised simulation of a vehicle system by using a validated tool may save lots of money in development of vehicle technologies as well as the whole vehicle itself. In some cases, there may not be an alternative to predict the vehicle responses without the computerised simulation. Such response may be the rollover situations of heavy trucks. Vehicle manufacturers have spent enormous amount of money to develop a new model vehicle using the prototypes. This process was not only money matter, it was also time consuming. After 1990s, with the new technologies, high-speed computers have come to a point which many vehicle dynamics responses and long term behaviours of the vehicle parts such as durability can be simulated. Especially in the last few years, bringing the separate vehicle system simulation ideas together, a new target is defined as zero-prototype that aims a new vehicle to come to the production line just by using the computer simulation tools. There are many vehicle dynamics simulation tools either for general or specific purpose. These tools are used both for the academic research and commercial reasons. Although the numerous advantages of these tools, they may not be the solution for some of the extreme research studies due to the universal fitting approach to the defined problems and their increasing costs to the individual researchers. From this point of view, Handsim which is a vehicle handling dynamics simulation tool including some control ideas on its own database, has been developed. The tools which will be discussed in the next sections are well known in the vehicle dynamics field. In this chapter, first, some of the vehicle dynamics simulation tools are reviewed. Because one of them which is called CarSimEd is used for benchmarking, it has a dominant place in the review. Then, the newly designed vehicle handling dynamics simulation tool, which is called HANDSIM is introduced.

4.2. Vehicle simulation tools

Vehicle simulation tools may be classified as for special purposes and for general purposes. Special purpose simulators mean that the tools have been developed for specific purposes by the developers and may not have general application needed by other researchers. However, general-purpose vehicle dynamics simulation tools may be used by most researchers to solve a wide variety of problems. Although, general purpose tools present the features required by most researchers for simulating their own applications, these tools are not exactly perfect for the particular applications and may need further improvement or additional code to take advantage of improved computer technology and vehicle dynamics science. In the section 4.2.1, 4.2.2 and 4.2.3 some of the well known simulation tools are reviewed.

4.2.1. ACSL - Advanced Continuous Simulation Language

ACSL (Advanced Continuous Simulation Language) is the time-proven standard for continuous simulation [53]. It is a language based on FORTRAN and designed to help to mathematically model and analyse the behaviour of a continuous system described by time dependent non-linear differential equations or transfer functions. Flexibility, reliability, and sophisticated design, incorporated in a compact and efficient package, have made ACSL the standard in simulation software. It is used in diverse fields such as Automotive, Chemical Processing, Aerospace, Power Generation, and Agriculture [53].

4.2.2. ADAMS/Car

ADAMS simulation software packages ranges from land vehicles to air vehicles and control. ADAMS/Tire was mentioned in Chapter 2. It is a package that is used to develop a vehicle tyre model. There is another software package to simulate vehicle dynamics and vehicle handling characteristics in ADAMS. It is ADAMS/Car [54]. Using ADAMS/Car, automotive engineers build computer models of entire vehicles, complete with suspensions, powertrains, engines, steering mechanisms, anti-lock braking systems, and other complex assemblies. Models are then exercised under various road conditions in the computer, performing every manoeuvre normally run on a test track to predict handling characteristics such as body roll, ride quality including vibration and bumps, vehicle safety, and performance parameters. Simulations can also include traction control, anti-lock braking, and other control systems. This capability not only gives automotive engineers greater flexibility in performing "what-if" simulations, but also gives them control over parameters such as weather, driver expertise, and road conditions which can vary widely on physical test tracks [54].

4.2.3. CarSimEd®

CarSimEd® is an easy to use software package simulating and analysing the braking and handling behaviours of vehicles with four-wheel independent suspension. It has several separate simulation programs. Each solves equations of motion numerically for a mathematical model designed to predict vehicle behaviour. Run time changes depend on the features of the computer.

The main simulation program in CarSimEd® is a handling model with 31 state variables covering 18 Degrees of freedom system (ten for the five rigid bodies-six for the main body and one for the each wheel- and eight for the auxiliary state variables) [55]. The simulation uses a non-linear tyre model and includes the major kinematics and compliance effects in the suspensions and steering systems in passenger vehicles.

For control inputs, CarSimEd® accepts time histories of brake input, throttle input, and steering wheel angle (open loop control). It also has a closed loop controller to maintain constant speed in the absence of braking inputs [55]

As a result:

- The handling model does not support closed loop steering control to follow a prescribed path, nor does it support closed loop speed control for variable speed.

- The handling model assumes constant steer ratios. (No Ackerman effect).

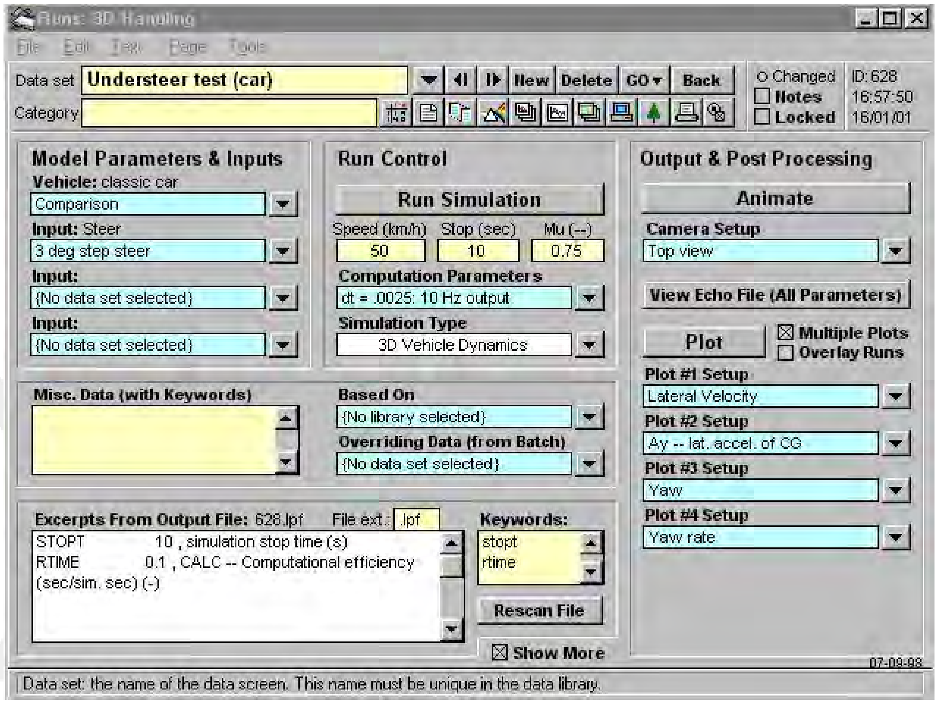

Figure 4.1 The main interface of the CarSimEd®

- The standard tyre model does not allow specification of forces and moments for large slip angles. Large slip is handled using built in functions but they cannot be adjusted by the user.

- The vehicle model does not have aerodynamics effects.

- The road surface is smooth and level with a constant friction coefficient [55].

The most important advantage of CarSimEd is the free of charge availability and having the most general vehicle handling analysis features. These features make the CarSimEd the preferred benchmark tool for the development of Handsim.

4.3. Development of the Vehicle Handling Simulator: HANDSIM

One of the main goals of this thesis, which is mentioned in the first chapter, is to develop a mathematical model of vehicle handling and implement it as an easy to use computerised simulation tool. The model should satisfy the simplicity and accuracy at the same time and it should be suitable to develop control algorithms for studying vehicle handling dynamics. For this reason, a technical computing language MATLAB, which stands for Matrix Laboratory, has been chosen to develop the simulator tool. In this section, before presenting the simulator, the structure of the MATLAB environment will be discussed, briefly.

4.3.1. A Language for Technical Computing: MATLAB

MATLAB, which is a high performance-technical computing language, integrates computation, visualisation and programming in an easy to use environment, where problems and solutions are expressed in a familiar mathematical notation. Typical uses include [50]:

- Math and computation
- Algorithm development
- Modelling, Simulation and prototyping

- Data analysis, exploration and visualisation
- Scientific and engineering graphics
- Application development, including graphical user interface building

The name MATLAB stands for MATrix LABoratory. Complex problems can be solved without using any programming languages like FORTRAN and C. The system consists of five main parts [50]:

1. **The MATLAB Language:** This is a high-level matrix/array language with control flow statements, functions, data structure, input-output and object-oriented programming feature. It allows both small and large and complex application programming.

2. **The MATLAB working environment:** This is the set of tools and facilities for managing the variables in a workspace and importing and exporting data. It also includes tools for developing, managing, debugging and profiling M-files, MATLAB’s applications.

3. **Handle Graphics:** This is the MATLAB's graphic system. It includes command for two and three-dimensional data visualisation, image processing, animation and presentation graphics. It also includes low-level commands that allow creating graphics with fully customised appearance as well as complete Graphical User Interfaces (GUI).

4. **Mathematical function library:** This is a collection of computational algorithms ranging from elementary functions to more sophisticated functions like Bessel functions and fast Fourier transforms.

5. **Application program interface:** This is a library that allows writing C and FORTRAN programs that interact with MATLAB.

4.3.2. SIMULINK

Simulink is a companion program to MATLAB. It is an interactive system for simulating non-linear dynamic systems. It is a graphical mouse-driven program that allows modelling a system by drawing a block diagram on the screen and manipulating it dynamically. It can work with linear, non-linear, continuous time, discrete time, and multivariable and multirate systems.

4.3.3. Implementation of the equations of motions in MATLAB

Derivation of the equations of motions has been realised by using the system of Ordinary Differential Equations (ODEs). There are several methods to solve differential equations such as Laplace transformation, Cramer's rule, etc. However, because the simulation is done in a computer, numerical iteration method is the preferred one.

MATLAB has three main non-stiff solvers for the ODEs [50]:

1. **Ode45:** ode45 is based on an explicit Runge-Kutta (4, 5) formula, the Dormand-Prince pair. [Mathworks] It is a one step solver in computing y (t_n), It needs only the solution at the immediately preceding time point, y (t_{n-1}). In general, ode45 is the best method for the 'first try' for most problems.

2. **Ode23:** Ode23 also depends on an explicit Runge-Kutta (2, 3) pair of Bogacki and Shampine. It may be more efficient than ode45 at crude tolerances and in the presence of mild stiffness. Ode23 is also a one step solver like ode45.

3. **Ode113:** Ode113 is a variable order Adams-Bashforth-Moulton PECE solver. It may be more efficient than ode45 at stringent tolerances and when the ode function is expensive to evaluate. It is a multi-step solver so that it needs the solutions at several preceding time points to calculate the current solution.

Because of the advantages like shorter calculation time and the accuracy, ode45 is used in this thesis as a solver. The general syntax for ode45 is presented below:

$$[T,Y,TE,YE,IE] = solver(odefun,tspan,y0,options)$$

The arguments of the syntax are subjected to the below table 4.1.

Table 4.1 Some of the odefile solver arguments [50]

odefun	A function that evaluates the right-hand side of the differential equations. All solvers solve systems of equations in the form or problems that involve a mass matrix, M (t, y) ý = f (t, y). The `ode23s` solver can solve only equations with constant mass matrices. `ode15s` and `ode23t` can solve problems with a mass matrix that is singular, i.e., differential-algebraic equations (DAEs).
`tspan`	A vector specifying the interval of integration, `[t0 tf]`. To obtain solutions at specific times (all increasing or all decreasing), use `tspan = [t0, t1... tf]`.
`y0`	A vector of initial conditions.
`options`	Optional integration argument created using the `odeset` function.

Calculation of the lateral velocity, yaw rate, lateral displacement, yaw angle for both 2 DOF and 3DOF systems; and roll rate and roll angle for 3 DOF system, by using the acceleration equations are presented below. The acceleration equations are first integrated into the velocity, then into the displacement or angles by the chosen odefile solver which is ode45. The function ode45 addresses another Matlab function file to solve the equations. Therefore, ode45 function including the defined options for the integration and the equations should be in different Matlab m.files, especially the functions which has complicated equations and external inputs. The general flow diagram of the simulation is given in Figure 4.2. Main control file includes the codes which manages every major steps of the simulation from the start to the finish. It also contains the vital codes to make the necessary connections between the graphical user interfaces and the equation files for the data processing. Graphical user interfaces make the simulation user friendly and the type of the simulation and complexity can be managed by these interfaces using the buttons.

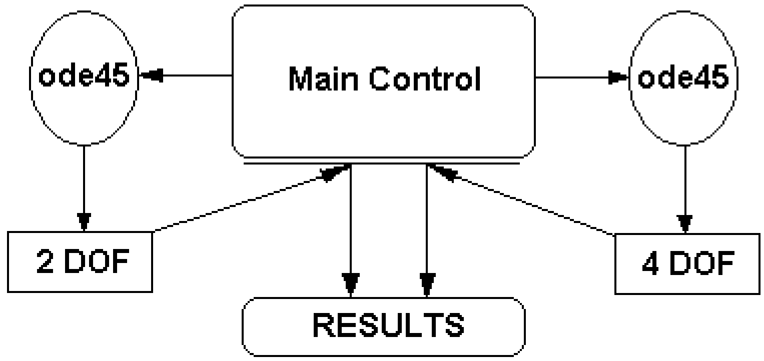

Figure 4.2 Basic flow diagram of the simulation

As it is explained before, the Matlab m.file including the function ode45 calls back the function file which includes the model equations. This file is given below. The equations are the Matlab codes of the model equations which were discussed in the Chapter 3.

```
[t,result,o3] = ode45('equation2',[0 time],[0 0 0 0 0 0],options,mail);
```

```
function [udot,alpha1,alpha2,Fyf,Fyr] = equation2(t,u,init,mail);

%Definitions of the Terms to the function file:
%==========================================================================================
tita = mail(1);mass = mail(2);vel_U = mail(3);Iz = mail(4);Ix = mail(5);cor_stiff =  mail(6);cor_stifr = mail(7);algnmof = mail(8);
algnmor=mail(9);fwheelbase = mail(10);rwheelbase = mail(11);notsine=mail(12);period=mail(13);
%==========================================================================================
switch notsine                                                  % Switch for Sine steer
   case 0
      if t <= period
         tita1 = tita*sin(2*pi*period^-1*t);
      else
         tita1 = 0;
      end
   case 1
      tita1 =tita;
end

alpha1 = -(((u(1) + fwheelbase*u(2))/ (vel_U) ) - (tita));      % Front axle Slip angle (rad)

alpha2 = -(((u(1) - rwheelbase*u(2))/ (vel_U)) );               % Rear axle slip angle (rad)

Fyf = cor_stiff*alpha1;                                         % Lateral force (front)
Fyr = cor_stifr*alpha2;                                         % Lateral Force (rear)

v1 = ( ((Fyf*cos(tita)) + Fyr)/mass) - (u(2)*vel_U) );          % Lateral velocity

r1 = ( ((fwheelbase*Fyf)*cos(tita)) - (rwheelbase*Fyr) -algnmof) /Iz;     % Yaw velocity
```

```
v2 = u(1);                                              % Lateral displacement

r2 = u(2);                                              % Yaw angle

X  = ((vel_U)*cos(u(4)) - u(1)*sin(u(4)));             % Longitudinal displacement in Earth fixed Coord.
Y  = ((vel_U)*sin(u(4)) + u(1)*cos(u(4)));             % Lateral displacement in Earth fixed Coord.

udot = [v1;r1;v2;r2;X;Y];
```

'udot' is a column vector, which presents the resultant parameters of the simulation namely 'result', all together. Demanded data can be extracted from the vector to examine the simulation results in figures. For instance, result (:, 1) provides the data for the lateral velocity.

The same process is valid for the four-degree of freedom systems modelling files. The model also includes the roll degree of freedom and some suspension system characteristics as it is discussed in Chapter 3.

```
[t,result,o3] = ode45('equation3',[0 time],[vel_U 0 0 0 0 0 0 0 0],options,mail);
```

```
function u = equation3(t,u,init,mail,alpha,Fv1,co_stif,algnmo);

%Definitions of the Terms to the function file:
%==========================================================================================================
tita=mail(1);mass=mail(2);vel_U=mail(3);Iz=mail(4);Ix=mail(5);period=mail(6);sine=mail(7);d=mail(8);g=mail(9);ms=mail(10);fwheelbase
=mail(11);rwheelbase=mail(12);mf=mail(13);mr=mail(14);Hcg=mail(15);horcf=mail(16);Hu=mail(17);Hs=mail(18);trackf=mail(19);x=mail(
20);msf=mail(21);muf=mail(22);horcr=mail(23);Ix=mail(24);msr=mail(25);mur=mail(26);algnmor=mail(27);tita1=mail(28);Ksf=mail(29);K
sr=mail(30);cf=mail(31);cr=mail(32);algnmof=mail(33);crd=mail(34);trackr=mail(35);krd=mail(36);Fxf=mail(37);Fxr=mail(38);Fxor=mail(3
9);Fxof=mail(40);Fxir=mail(41);Fxif=mail(42);Fbof=mail(43);Fbor=mail(44);Fbif=mail(45);Fbir=mail(46);steptime=mail(47);wthouttyre=m
ail(48);page1b=mail(49);
%==========================================================================================================

switch sine                                             % Steer Angle selection for 'Sine Steer' or Constant Radius:
   case 0
      if t <= period
         tita2 = tita*sin(2*pi*(period^-1)*t);
      elseif period < t <= 1.5*period
         tita2 = 0;end
      if t > 1.5*period
         tita2 = tita*sin(2*pi*(period^-1)*t);
         % Single lane change because of zero steer angle.
      end
   case 1
      tita2 =tita;
end
```

```
%>[ Suspension Stiffness & Damping parameters & Lateral Load transfer ]<
%===============================================
Cfif = (cf * trackf^2 / 2);%( 2* cr * ( u(5)/(1.6158*u(5)^2 + 0.387) )^2);
Cfir = (( 2* cr * ( u(5)/(1.6158*u(5)^2 + 0.387) )^2) + (2 * crd * ( u(5)/(3.8788*u(5)^2 + 0.2574) )^2 ) );

Kfif = (Ksf * trackf^2 / 2);%(2 * Ksf * (u(5)^2 / (1.6158*u(5)^2+0.387 ) )^2);
Kfir = (2 * Ksr * (u(5)^2 / (1.6158*u(5)^2+0.387 ) )^2);

alpha1 = -(((u(2) + fwheelbase*u(3))/ (u(1)) ) - (tita2));                     % Front axle Slip angle (rad)
alpha2 = -(((u(2) - rwheelbase*u(3))/ (u(1))) );                               % Rear axle Slip angle (rad)

Fvof = (0.5*mf*9.807) +  (1/trackf) * ( (msf*(u(2)+u(3)*(u(1))) * horcf + Kfif*u(5) + Cfif*u(4)) );   % Load Transfer - outer front
Fvif = (0.5*mf*9.807) -  (1/trackf) * ( (msf*(u(2)+u(3)*(u(1))) * horcf + Kfif*u(5) + Cfif*u(4)) );   % Load Transfer - inner front
Fvor = (0.5*mr*9.807) +  (1/trackr) * ( (msr*(u(2)+u(3)*(u(1))) * horcr + Kfir*u(5) + Cfir*u(4)) );   % Load Transfer - outer rear
Fvir = (0.5*mr*9.807) -  (1/trackr) * ( (msr*(u(2)+u(3)*(u(1))) * horcr + Kfir*u(5) + Cfir*u(4)) );   % Load Transfer - inner rear

%> [ IF Condition for Tyre Data Choice % Corn.Stiffness/Lateral Force Calc. ] <
%============================================================================

if wthouttyre == 1
   corstiff = findobj(page1b,'tag','dat1');
   corr_stiff = get(corstiff,'string');
   corstifr = findobj(page1b,'tag','dat2');
   corr_stifr = get(corstifr,'string');
   cof = eval(corr_stiff);
   cor = eval(corr_stifr);

   cor_stiff = cof;
   cor_stifr = cor;
   cor_stifof = cof/2;
   cor_stifor = cor/2;
   cor_stifif = cof/2;
   cor_stifir = cor/2;
else

   cor_stifof = interp2(alpha,Fv1,co_stif,alpha1,Fvof);                    % (N/rad)
   cor_stifor = interp2(alpha,Fv1,co_stif,alpha2,Fvor);                    % (N/rad)
   cor_stifif = interp2(alpha,Fv1,co_stif,alpha1,Fvif);                    % (N/rad)
   cor_stifir = interp2(alpha,Fv1,co_stif,alpha2,Fvir);                    % (N/rad)

   cor_stiff  = (cor_stifof + cor_stifif);                                 % [N/rad]
   cor_stifr  = (cor_stifor + cor_stifir);

   %algnmofo = interp2(alpha,Fv1,algnmo,alpha1,Fvof);
   %algnmofi = interp2(alpha,Fv1,algnmo,alpha1,Fvif);

   %algnmoro = interp2(alpha,Fv1,algnmo,alpha2,Fvor);

   %algnmori = interp2(alpha,Fv1,algnmo,alpha2,Fvir);

   %algnmof = (algnmofo + algnmofi);

   %algnmor = (algnmoro + algnmori);
   algnmof=0;algnmor=0;
end

Fyof = cor_stifof.*alpha1;
Fyor = cor_stifor.*alpha2;
Fyif = cor_stifif.*alpha1;
Fyir = cor_stifir.*alpha2;

Fyf = (Fyof + Fyif);
Fyr = (Fyir + Fyor);

%===>[ GENERAL EQUATIONS OF MOTION ]<===:
%========================================

u2 = (((Fxif+Fxof-Fbof-Fbif)*cos(tita2) + Fxir + Fxor - Fbir - Fbor -(Fyif+Fyof)*sin(tita2) )/ mass) + (u(3)*u(2));
```

```
v2 = ( (( ((Fyif+Fyof)*cos(tita2)) + ((Fxif+Fxof-Fbif-Fbof)*sin(tita2)) + (Fyir+Fyor))/mass) - (u(3)*(u(1))) );

r2 = ( (fwheelbase*(Fyif+Fyof)*cos(tita2)) + ((trackf/2)*(Fyif-Fyof)*sin(tita2)) + (fwheelbase*(Fxif-Fbif+Fxof-Fbof)*sin(tita2))+...
   ((trackf/2)*(Fxof-Fbof-Fxif+Fbif)*cos(tita2)) - (rwheelbase*(Fyir+Fyor)) - ((trackr/2)*(Fxir-Fbir-Fxor+Fbor)))/Iz;%-algnmof

p2 = ( ms*(v2+u(3)*(u(1)))*d + ms*g*d*u(5) - (Cfif + Cfir)*u(4) - (Kfif + Kfir)*u(5) )/Ix;

fi = u(4);

v1 = u(2);                                          % Lateral displacement

r1 = u(3);                                          %  Yaw Angle

X = ((u(1))*cos(u(7)) - u(2)*sin(u(7)));            %  Longitudinal DISPLACEMENT Earth fixed

Y = ((u(1))*sin(u(7)) + u(2)*cos(u(7)));            %  Lateral DISPLACEMENT

u = [u2;v2;r2;p2;fi;v1;r1;X;Y];
```

4.4. Graphical user interfaces of the HANDSIM

The objective of creating an interface for a simulator program is mostly because of consideration of the end-user. The end-user may be regarded as a number of users and / or experts, who are not interested in the details of the mathematical model or processing but the results.

Handling simulator interfaces are constructed in MATLAB / Simulink by using the GUI (Graphical User Interfaces) menu. These interfaces, which are easy to use and have some functions like radiobuttons, popup menus, frames, etc., give the developer an opportunity to present the simulator to the end-user in a simple and functional form. In Figure 4.3 the starting interface of the HANDSIM is shown. By clicking on the "About Simulator" button, the user can get brief information about the simulation tool. This information interface is presented in the Figure 4.4.

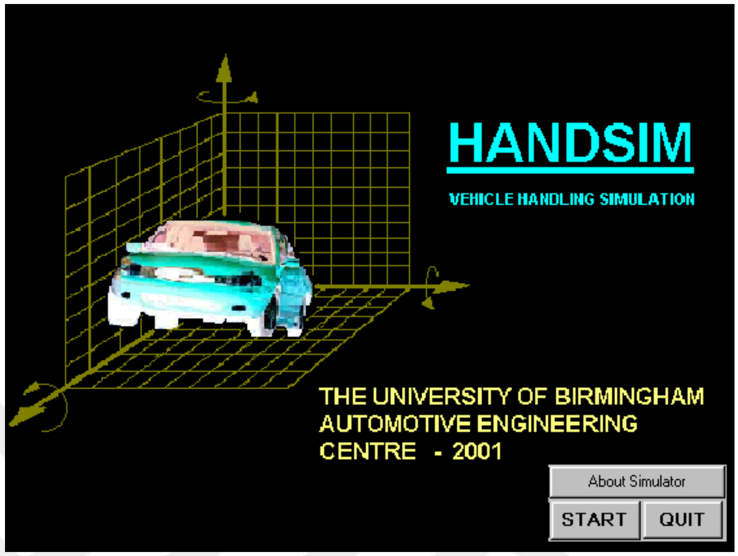

Figure 4.3. Starting interface of the HANDSIM.

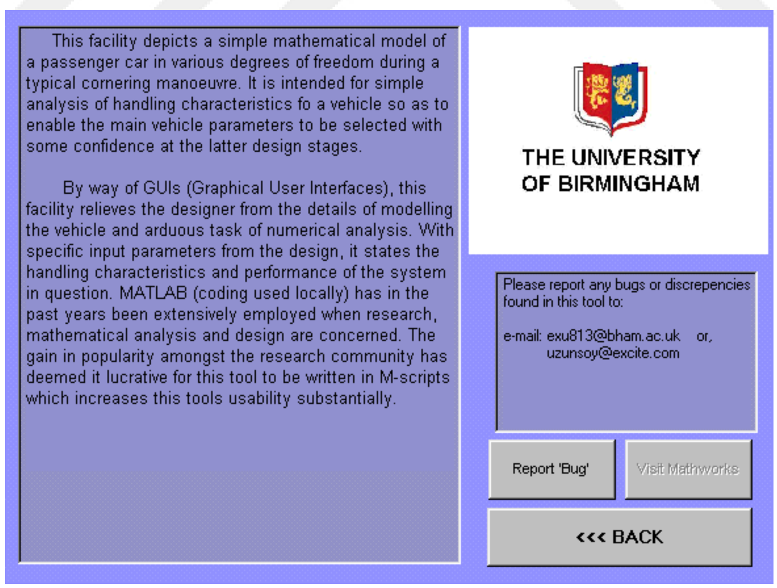

Figure 4.4. Information interface of the HANDSIM.

The third and the main control interface of the tool is opened by the 'Start' button. This interface consists of three columns, which are 'Model parameters and inputs', 'Run control' and

'Output and post processing'. It is shown in figure 4.5. The terms and choices of the columns of the main interface are explained in Table 4.2, 4.3 and the 4.4 for each column. Handsim gives the user a limited opportunity to analyse braking and tractive effects on the vehicle by differing the forces applied on to each tyres. However, rather than a control action – because the forces applied are just once and for a limited period – this could be used as another analysis to get the vehicle responses at braking and/or traction conditions.

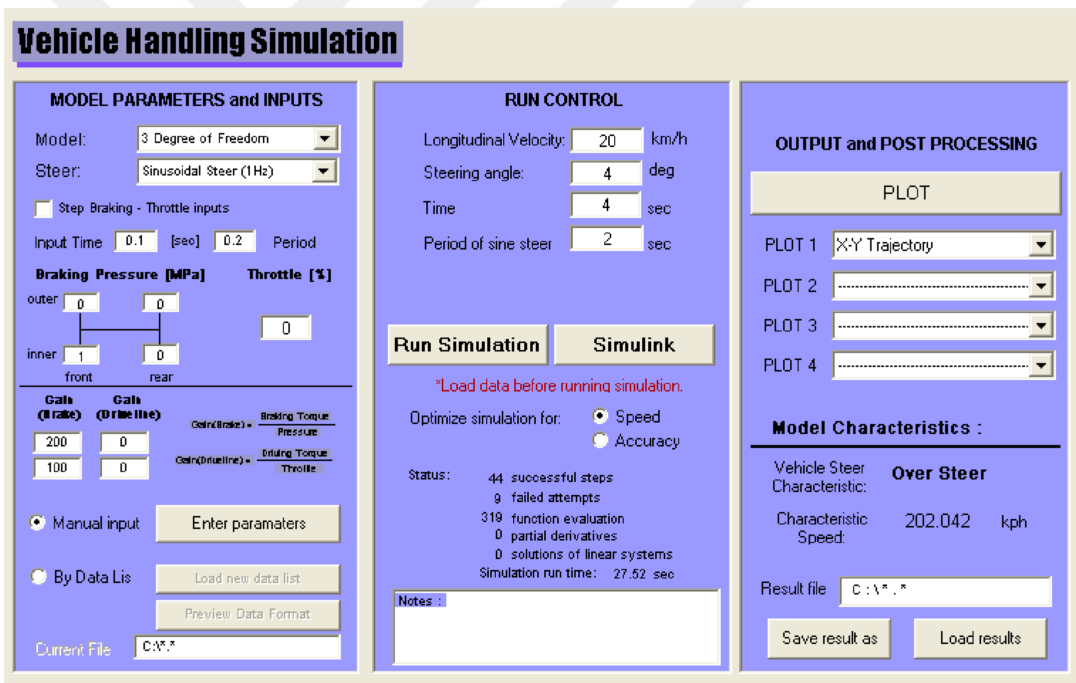

Figure 4.5. The main interface of the HANDSIM.

After loading the input data, simulation can be activated by using the 'Run Simulation' button. The simulation run time will be shown on the 'Status' window, and then preferred figures of the simulation results, which are mentioned after the table explanations, can be plotted by using the *plot* pushbutton.

Another important interface, which can be switched from the main interface, is referred to as 'Data Entry'. This screen is presented in the Figure 4.6. All the necessary vehicular data including tyre and suspension system is entered in this interface.

Table 4.2 Model Parameters and inputs in the main interface

COLUMN 1	Function	Description
MODEL PARAMETERS & INPUTS	Model	A choice of the degree of freedom of the analysis
	Steer	A selection of the vehicle handling test method for constant turning radius steer , sine steer or vehicle path planning.
	Manual Input	A radio button, which gives a choice to specify the vehicle parameters by using the 'Enter Parameters' pushbutton.
	By Data List	A radio button, which gives an opportunity to use a certain vehicle data, which was saved before as m.file.
	Preview Data Format	It represents the data format, which will be saved as a m.file.

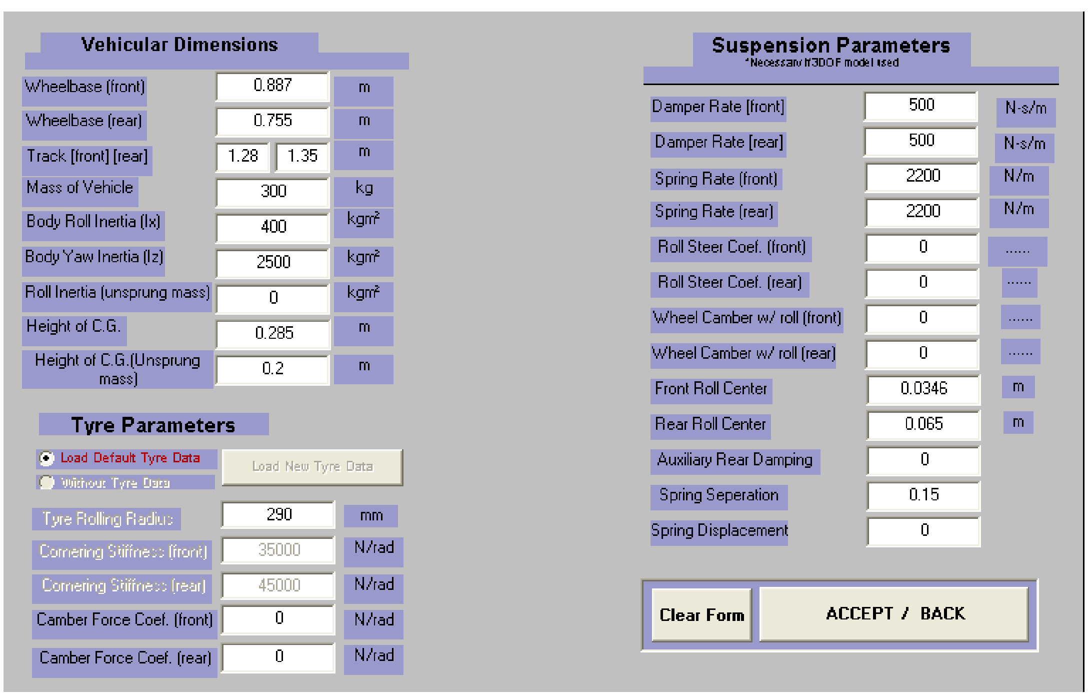

Figure 4.6 Data entry interface of the HANDSIM.

The HANDSIM has two different size and purpose tyre data, which are for passenger (DUNLOP D8 195/65 R15) and racing cars, in its own data base. As far as a tyre data, which includes the vertical load, slip angle and lateral force values, is provided it is not necessary to know the tyre cornering stiffness value (Cα) for the tyre. By using the vehicle mass, wheelbase and given steering angle parameters, tyre-cornering stiffness will be computed for both front and rear axles. Nevertheless, there is a choice to enter a constant cornering stiffness value for different tyre types and this function can be activated by clicking the radiobutton: 'Load Different Tyre Data'. (Figure 4.6). However, tyre camber angle is assumed to be zero in the existing tyre data. The program also has an entry, camber force coefficient for both front and rear axles. The same radiobutton activates this function. Choosing the 'Load Different Tyre Data' radiobutton eliminates the usage of camber effect and the constant cornering stiffness and switches the new editable tyre data entry interface. If the rows of the cornering stiffness are kept empty or zero, the program will automatically use its own tyre data to calculate the cornering stiffness.

Table 4.3. Run control column of the main interface

COLUMN 2	Function	Description
RUN CONTROL	Longitudinal Velocity	Constant vehicle forward speed in kilometre per hour
	Steering Angle	Tyre steer angle in degree.
	Time	Simulation run time in second.
	Period of Sine Steer	If the steer type is chosen as Sine Steer in column 1
	Optimise Simulation For	Speed: for the initial and quick simulation Accuracy: for more accurate simulation results are obtained by producing more time steps.
	Status	Gives statistical results about the simulation

Table 4.4 Output and Post processing column of the main interface

Column 3	Function	Description
OUTPUT AND POST PROCESSING	Plot 1, 2, 3, and 4	They present opportunity to plot multiple result figures for maximum 4-chosen analyses at the same time.
	Vehicle Steer Characteristic	It defines the handling tendency of the vehicle: Oversteer, Neutralsteer or Understeer.
	Result File	This section gives an opportunity to save the simulation results as .mat file.

A maximum of four figure windows are released at the same time when it is clicked on the 'Plot' button. A series of MATLAB m. files connect the chosen figures to the command of 'Plot' pushbutton and vehicle handling analysis results can be seen in those figure windows in detail. There are 12 figures available for the analysis, automatically:

- Vehicle lateral velocity vs. time (m/s)
- Vehicle lateral acceleration vs. time (m/s^2)
- Vehicle yaw angle vs. time (deg)
- Vehicle yaw rate vs. time (deg/s)
- Vehicle yaw acceleration vs. time(deg/s^2)
- Vehicle roll angle vs. time (deg)
- Vehicle roll rate vs. time (deg/s)
- Vehicle roll acceleration vs. time (deg/s^2)
- Side slip gain vs. time
- Yaw gain vs. time (1/ s)
- Roll gain vs. time

- Fz vs. time (Tyre load distribution vs. time) (N)
- X - Y Trajectory vs. time (m)
- Handling Characteristics
- Slip angles
- Cornering stiffness of the tyres

4.5. Benchmarking and the validation of Handsim

The CarSimEd is used as a benchmark simulation tool and the Handsim is validated by the provided results for a given vehicle data in the CarSimEd. As emphasised before, the HANDSIM can be run in both two and four-degree of freedom model analysis. Because of the difference between the complexities of the two models, there are some amounts of expected numerical difference between the results. However, regardless of the model used, the first important output of the simulation is the steering characteristic of the vehicle. The simulation has been run for the comparison using data for an understeering vehicle. This characteristic can be defined by the Yaw Gain vs. Speed curve of the vehicle. According to Gillespie [56], while this graph shows a linear proportional trend for a neutral steer vehicle, it also shows increasing convex and concave trends for oversteer and understeer conditions, respectively. In figure 4.7, the yaw gains vs. time graph of the HANDSIM shows understeer characteristic, clearly. However, in this figure, for exact definition of the characteristic, the simulation was run in a higher speed than is used for the comparison.

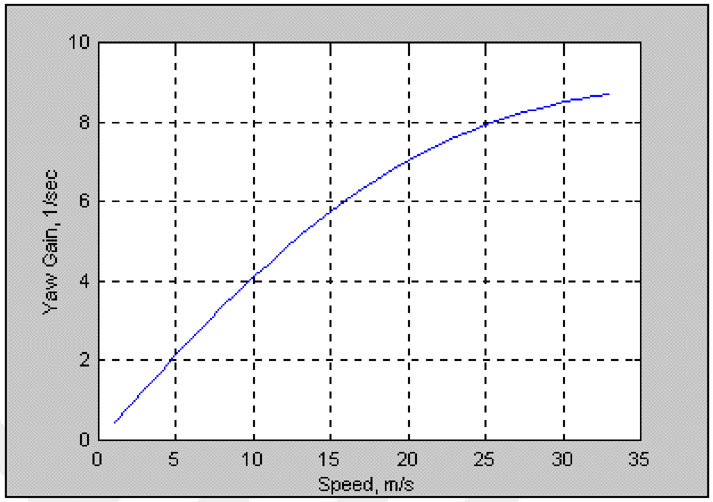

Figure 4.7 Steering characteristic of the simulated vehicle

Handling analysis can be performed in three different ways in the HANDSIM: Constant radius turn, Sinusoidal Steer or path planning. Path planning is developed using the basics of fuzzy logic control theory in the Simulink environment and implemented into the Handsim. This is a method that mimics a human driver and as a result any type of vehicle path can be realised by defining the coordinate points. Because the path planning is a subject to Chapter 6, the rest of the methods are discussed in this chapter. The results of the Constant radius test method can be seen in the validation procedure with CarSimEd®. Single Sinusoidal Steer test gives an opportunity to examine the vehicle's handling behaviour during a lane change manoeuvre. As an example, some handling responses of the single sinusoidal steer are shown in the following figures for the same conditions with the validation procedure but in 3-second period.

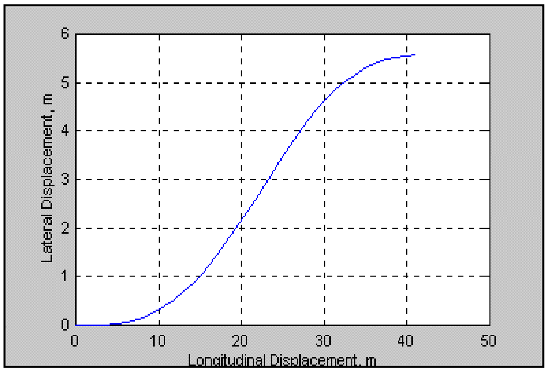

Figure 4.8 X-Y Trajectory of the vehicle

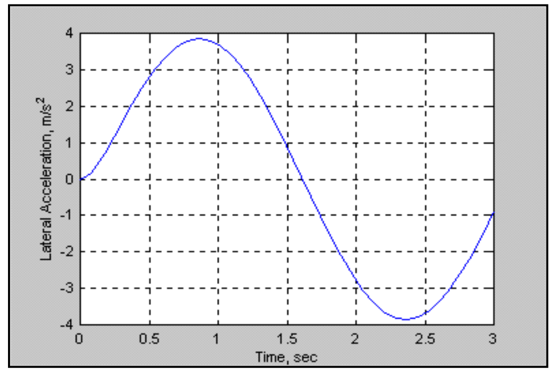

Figure 4.9 Lateral Acceleration vs. time

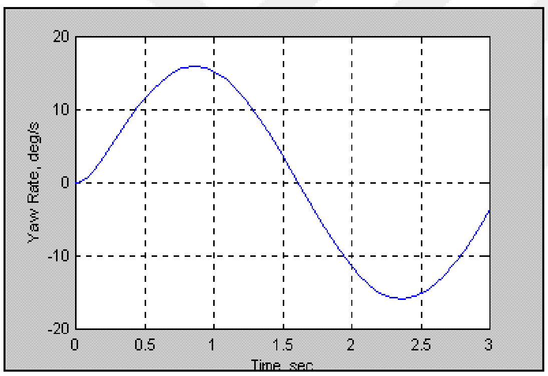

Figure 4.10 Vehicle yaw rate vs. time

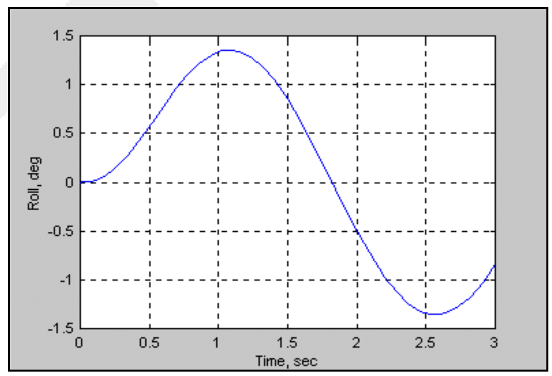

Figure 4.11 Vehicle roll angle vs. time

The HANDSIM has two different handling models in complexity: Two degree of freedom and Four-degree of freedom models. The features of these two models explained in chapter 3. In this section some distinctions are shown from the Figure 4.12 to 4.14. Because the four degrees of freedom model takes into account the suspension characteristics and the lateral load transfer of the vehicle, the numerical values of like lateral acceleration, yaw rate and yaw angle are less than the results of two degrees of freedom system.

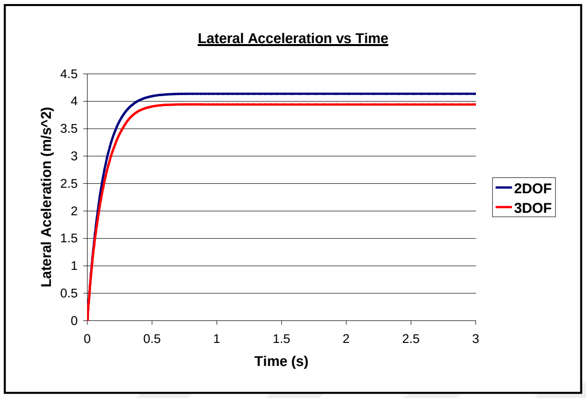

Figure 4.12 Lateral acceleration vs. time

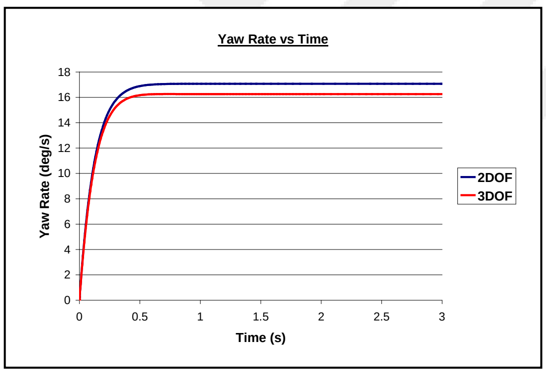

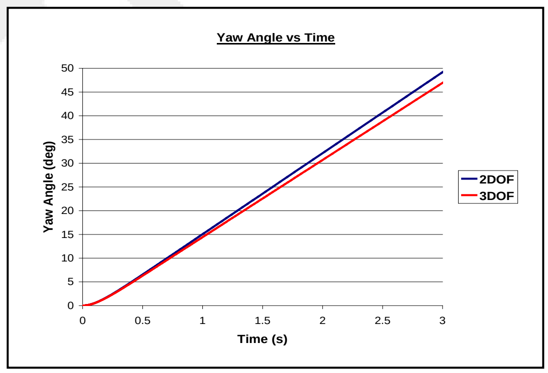

Figure 4.13 Yaw rates in both models

Figure 4.14 Yaw Angles in both models

Simulation control parameters and some of the vehicle parameters used for both tools are presented below in Table 4.5 and 4.6. The comparison shown here is based on Handsim's 4DOF vehicle handling model, in constant longitudinal velocity, with understeer vehicle characteristics. Simulation run time also has an important place in analysis. However, it also strictly depends on the computer speed.

Table 4.5 Control parameters used during the simulation

Control Parameters	Value
Longitudinal Velocity	40 kph
Steering Angle	3°
Simulation Time	4 sec

Table 4.6 Some of the vehicle parameters used during the simulation

VEHICLE PARAMETERS	VALUE
Roll Inertia Ixx (kgm^2)	400
Yaw Inertia Izz (kgm^2)	3136
Height of C.G. (m)	0.55
Wheelbase (m)	2.7
Vehicle Mass (Front) (kg)	999.86
Vehicle Mass (Front) (kg)	700.14
Total Vehicle Mass (kg)	1700
Height of C.G. Unsprung Mass	0.3
Track Width (m)	1.5

The resultant graphs of both simulation tools are depicted from the figures 4.15 to 4.20 below. Although all figures indicate the comparison between the CarSimEd® and HANDSIM, figures 4.15 and 4.16 are also presented for a reason which basically aims to show the similarities between two simulation tool's results at different vehicle speeds. These figures indicate X-Y trajectory of the vehicle for each simulation tools at 40 km/h and 50 km/h longitudinal vehicle speeds, respectively. The other parameters used in the following figures belong to the normal procedure. X-Y trajectory figures present an essential comparison for the two simulation tools. The simulation results from the figures 4.15 and 4.16 show almost the same tendency in each tool.

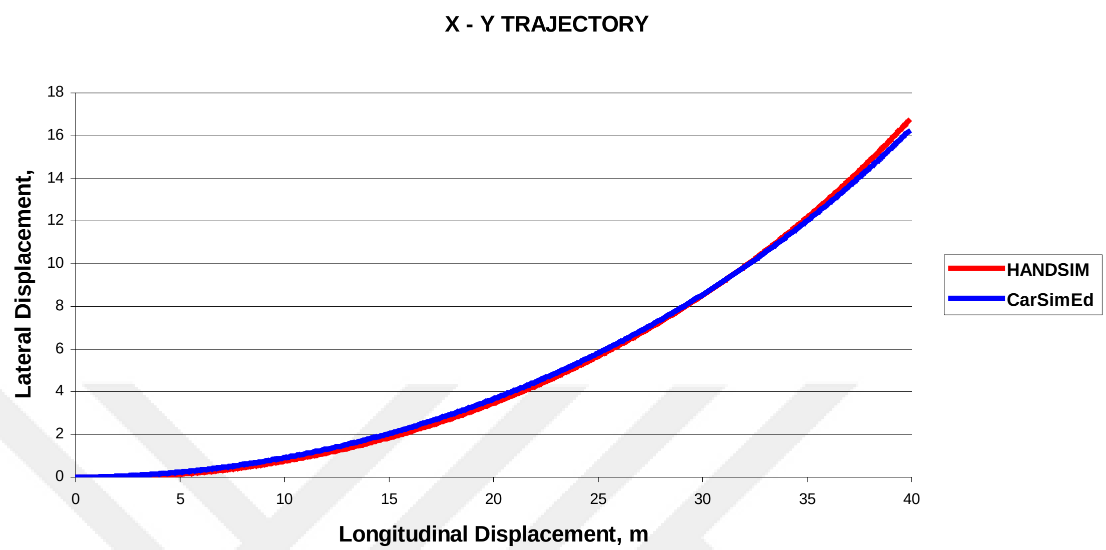

Figure 4.15 X-Y trajectory of the vehicle at 40 km/h longitudinal velocity

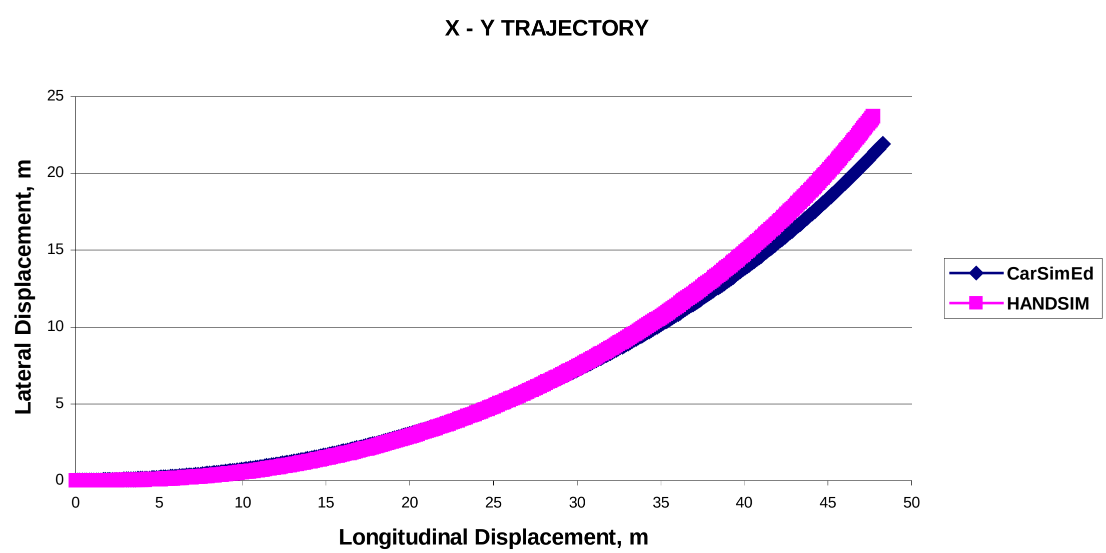

Figure 4.16 X-Y trajectory of the vehicle at 50 km/h longitudinal velocity

In the general of the analysis, there is close agreement between the results obtained from the two different simulation tools. As it can be seen from the Figure 4.15, X-Y trajectory of the vehicle during the given simulation time period, almost the same as in each simulation tools. In like manner, the results of acceleration, velocity and load transfer show close agreement. The slight difference in Figure 16 can be explained by slightly higher yaw rate and lateral acceleration, which are shown in Figures 18 and 19, in HANDSIM. However, it should be point out that there are some differences in CarSimEd which can not be edited beyond some points. For instance, as the cornering stiffness is updated continuously in HANDSIM, CarSimEd uses constant cornering stiffness value.

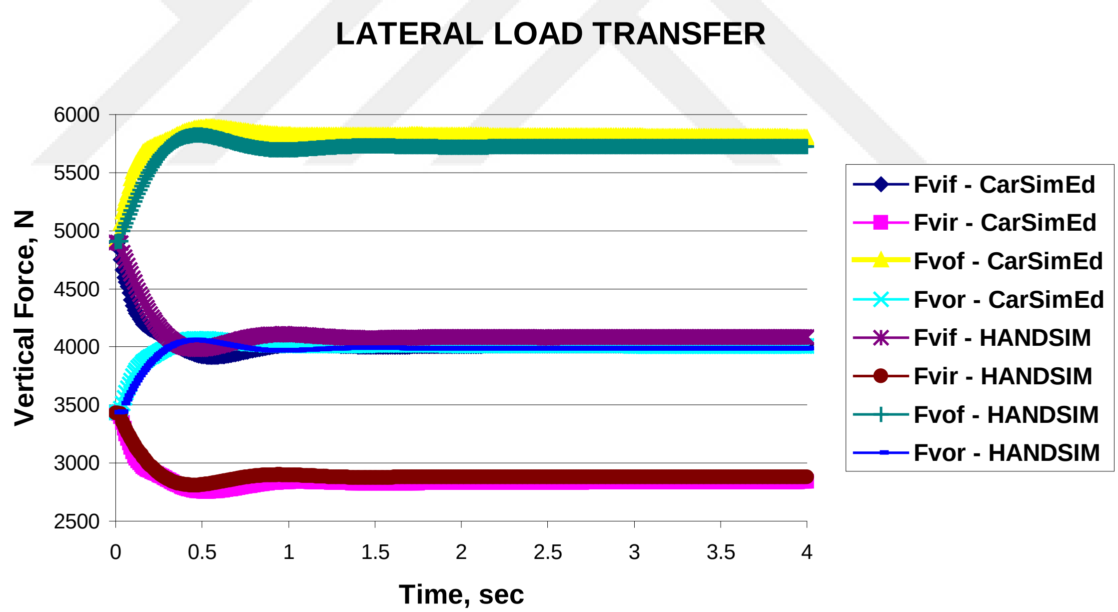

Figure 4.17 Vertical forces on each tyre both from CarsimEd and Handsim

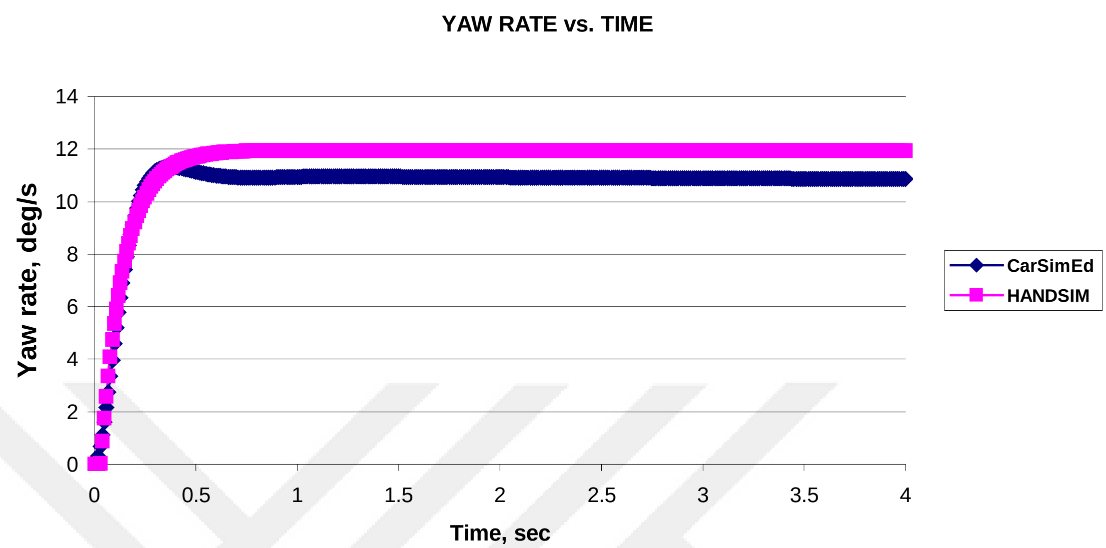

Figure 4.18 Vehicle yaw rate vs. time

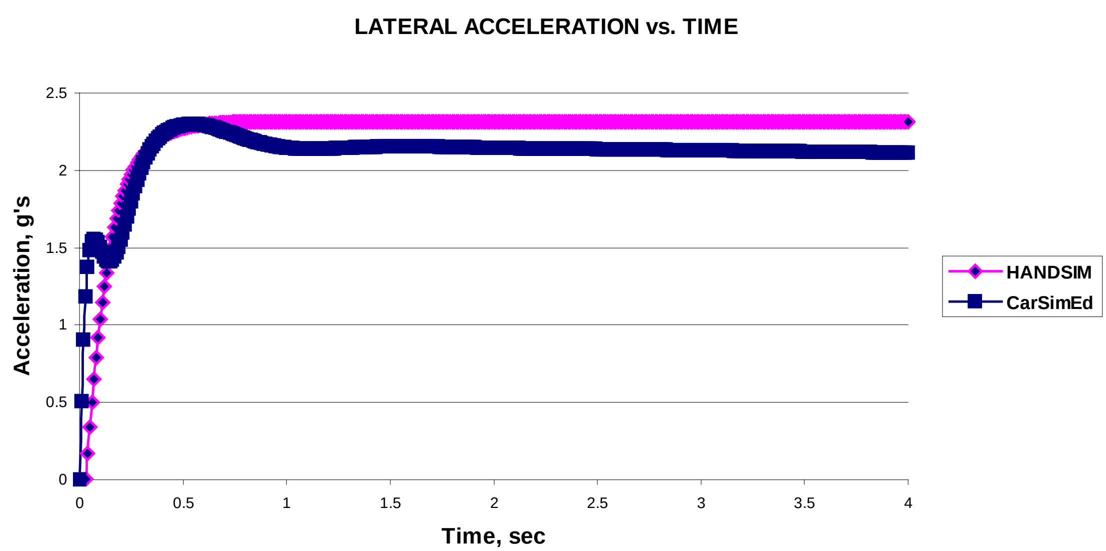

Figure 4.19 Vehicle lateral acceleration vs. time

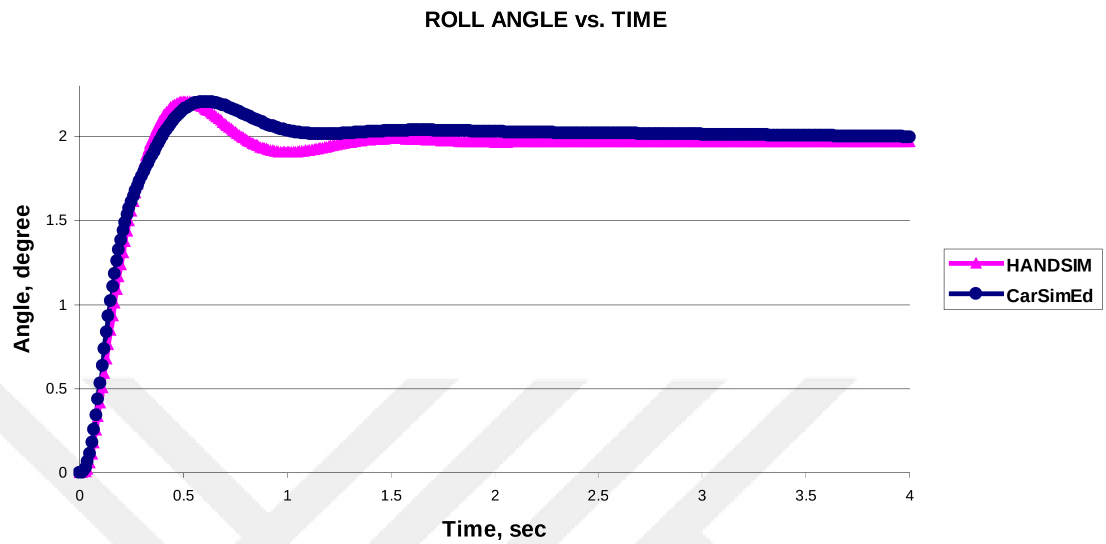

Figure 4.20 Vehicle roll angle vs. time

4.6 Conclusions

The vehicle handling simulation tool presented here has been developed in the MATLAB and SIMULINK environment. These tools present the researcher a flexible and easy development environment. The knowledge of any other computer programming language like FORTRAN or C++ is not necessary. Most commercial simulation tools or packages are general purpose tools and are often not easy to use or difficult to adapt for a research study so it has been a necessity to consider a special simulation tool for this study. Therefore, the HANDSIM has been tailored specifically to the needs of research in vehicle handling dynamics in an uncomplicated manner such that it can be modified or further developed in the future. As a result, Handsim has been validated as a reliable tool by a version of the well known vehicle dynamics simulation tool CarSimEd.

CHAPTER 5

VEHICLE PATH PLANNING

5.1. Introduction

Computer simulation has been used in vehicle dynamics studies for decades. Advances in the science of vehicle dynamics and far more improved computer technology now enable automobile manufacturers to get closer to zero-prototype production than ever before. From the computer simulation point of view, having a general path generator can present researchers with great flexibility in defining vehicle handling dynamics tests. The process used for generating the vehicle's path in this study is referred to as 'path planning' because of some distinctive approaches used. A vehicle model is used in conjunction with the fuzzy pilot model to generate the vehicle's path through a number of specified points through which the vehicle must pass. The simulation is carried out in the Matlab© programming environment using a Simulink© vehicle model under Fuzzy logic control intended to imitate how a real driver would steer the vehicle to create a path through the specified points. The complexity of the path is defined by the specified points and their spacing, which can be used to describe road features such as corners, chicanes etc. The ability of a vehicle to negotiate the defined road features can therefore be simulated by testing how accurately the vehicle model/fuzzy pilot combination can create a path through the specified points.

The three types of generalised tests normally used for vehicle handling dynamics are lane change, constant radius steer and constant steer. These are idealised tests, which have little bearing on normal driving. From the computer simulation point of view, having a general path generator can present the researcher with great flexibility in defining vehicle handling dynamics tests. For example, in the simulation studies, a lane change manoeuvre can simply be represented by sinusoidal steer, with the frequency and amplitude of the sine function being used to define the vehicle position. However, the steering input required for a lane change manoeuvre by a driver driving a real vehicle is not sinusoidal and the vehicle path cannot be represented by a simple mathematical function. Therefore, complex mathematical functions, especially higher order polynomials are generally used to define the vehicle path.

Lauffenburger et al. [42] applied polar polynomial curves to represent the desired path of a vehicle and fuzzy logic control was used to determine the constraints of the maximum points of the polynomial, with the driver's profile, in terms of experience, being used as an additional parameter. An inexperienced driver negotiating a bend increases the steering angle smoothly during the first half of the turn and decreases it during the second half. This technique is guided by maximum comfort and safety. The trajectory in the same turn is completely different for an experienced driver whose objective is to minimise the time taken to traverse the turn. A number of vehicle path tracking researches [57], [58] are mainly aimed at the future automated highway systems and a number of different approaches have been used in these studies. Mouri [43] and Furusho [44] proposed a path tracking system to regulate the lateral position at the centre of gravity of the vehicle by minimising a cost function based on the lateral displacement at the centre of gravity and the front wheel steering angle. A virtual point regulator, which also takes the yaw angle into consideration in addition to this basic approach, has been proposed by Marumo et al. [45]. The virtual point is at a point on the driver’s line of sight and is a function of the vehicle yaw angle, the lateral displacement at the vehicle centre of gravity and the distance between the virtual point and the centre of gravity. The cost function is, therefore, now based on the lateral displacement at the virtual point and the front wheel steering angle. This increases the robustness and the performance of the control system. Due to the nature of processes like using a virtual point to represent, simply, the human driver’s line of sight, intelligent control system models which can mimic the driver’s experience, such as fuzzy logic control or neural networks, are the most preferable control schemes in these studies. These control models are intended basically to command the steer angle. Additionally, yaw angle error and yaw rate may also be used as inputs to the intelligent control system. This kind of process, based on fuzzy logic, was referred to as ‘fuzzy pilot’ by Piancastelli & Sarubbi [46].

The simulation model is implemented for a generalised vehicle model and although the specific vehicle models used in this study are fairly simple, vehicle models of any complexity can be used. The vehicle model is simply included as a Simulink block in the overall simulation model.

5.2. Fuzzy Logic

Information accepted by methods based on conventional mathematics must be precise, for example, the speed of a car v = 100 kph. Such information can be represented graphically by means of the so called singleton [59]. Exact information can only be delivered by precision engineered measuring devices, whereas a man can directly estimate the speed of a car by applying such terms as low, medium and high. The functions ‘low’, ‘medium’ and ‘high’, called membership functions determine if the precise speed value is respectively low, medium or high. Such information can be defined as a ‘**granule of information**’ [59]. The numbers of granules defined depend on the demand of the precision. If the number is increased adding ‘very low’ and ‘very high’ the precision is also increased. The granularity of information is defined by the width of a granule (membership function). Therefore, the granule ‘low’ can have various widths, according to the total number of granules of information used by a man.

A granule of an infinitely small width is called the singleton, which represents the precise information, i.e. such information which is employed by conventional mathematics. The information represented by the granule of a finite (greater than zero) width has been called by Prof. Lotfi A. Zadeh, the developer of the concept of granularity, **fuzzy information**. The mathematics field using such information has been called **fuzzy set theory** [59]. The most important element of this theory is **fuzzy logic**, applied for fuzzy modelling and control. Fuzzy set theory has opened new exploratory possibilities such as creating artificial intelligence similar to human intelligence, the creation of computers programmed with words, the application of information of any granularity for modelling, control, optimisation and diagnostics of the systems and the possibility of adapting granularity of information according to the required accuracy of modelling, control, optimisation, diagnostics, etc. Such adaptation is applied by man.

5.2.1. Modelling basics in Fuzzy Logic:

Assuming that someone controls a plant by realising the input / output mapping shown in Figure 5.1, the basic fuzzy approach for modelling the plant is discussed in this section. The developer of the model should first remember the extreme states of the plant for its outset. For this particular example, a model with two rules is given in Figure 5.2, by the developer's own mind.

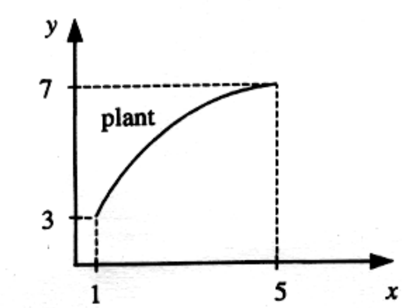

Figure 5.1 Input-output characteristic of the plant to be controlled [59]

If the model represented in Figure 5.2 is exact but insufficient, the developer will try to increase its accuracy, bearing in mind the essential, medium state (Figure 5.3), thereby creating a new rule determining the operation of the plant and progressively introducing new, smaller granules of information. Moreover, if the model represented in Figure 5.3 proves insufficient, the developer can examine the next essential state of the plant, decrease the granularity of the information and increase the number of verbal rules characterising the operation of the plant and subsequently obtain a higher accuracy of modelling.

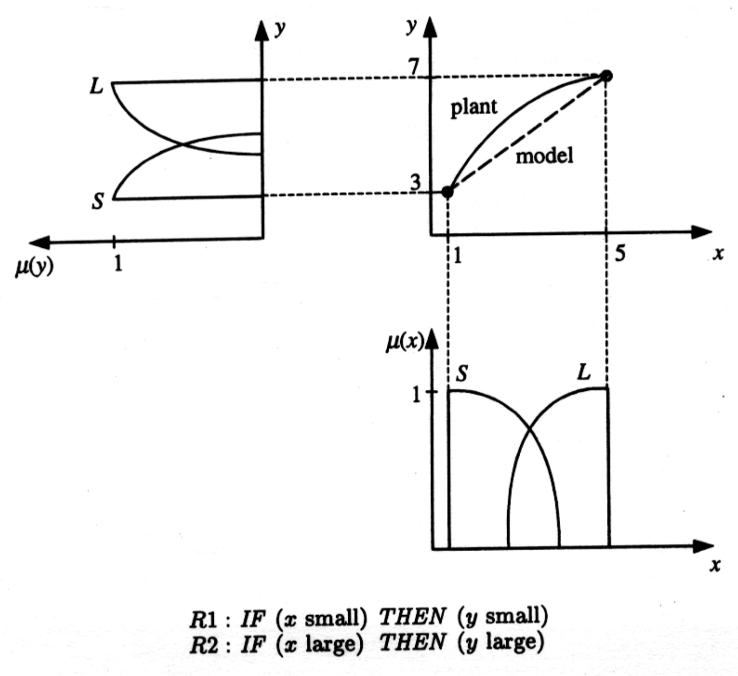

Figure 5.2 Model of the plant based on two granules [59]

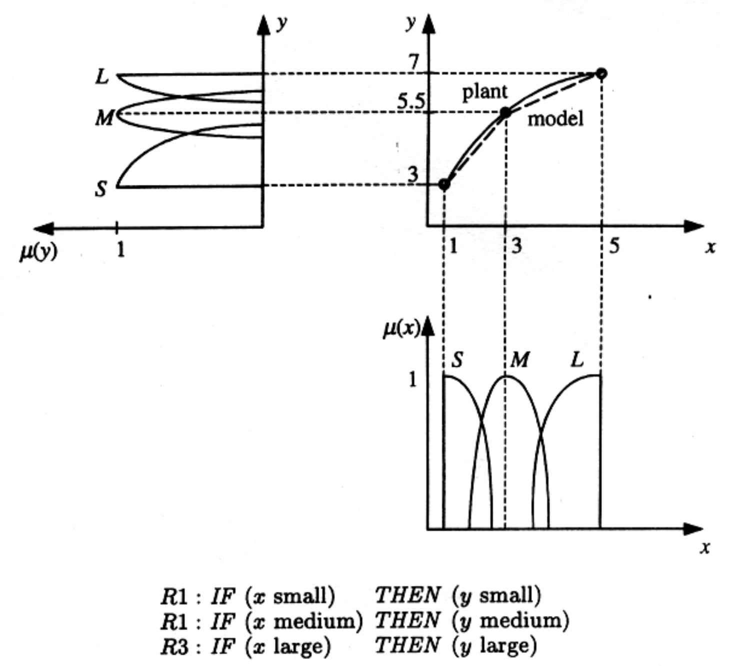

Figure 5.3 Model of the plant based on three granules [59].

Psychological studies [59] show that an average capable man can remember only 5 to 9 characteristic states of a plant. Therefore, for each variable, maximum 5 to 9 granules of information are applied. This kind of granularity is totally sufficient for controlling vehicles, aircraft and many other different objects and solving everyday problems. While computer technology makes it possible to apply any granularity of information, however, there is a need to limit the complexity due to the reasons that are described below:

1. Within the kernel of the systems, there may be some active disturbances which cannot be measured or even may not be known by the developer. Their influences are dependent on magnitude and can cause unforeseen, variable responses of the system that can be attributed to chaotic events.
2. To create a model, only the most essential causal factors should be detected and involved. In a complicated system the number of reasons which could cause the observed operation of the system, increases steeply with the level of its complexity
3. Sometimes the precise measurement of some signals in a system is impossible. This means that even though the model is accurate, it can create inaccurate results which do not correspond to a known behaviour of the real system.

Consequently, exact modelling using a very small granule of information is possible in the case of simple systems with a small number of inputs. In non-trivial systems, especially those having a greater number of inputs, the developer is forced to apply information of a larger granule (fuzzy information).

5.2.2. Membership functions used in fuzzy sets

Many different membership functions are applied in practice. Some of them varying from simple to complex are discussed in this section. The most often applied membership functions are the functions consisting of straight segments as represented in Figure 5.4.

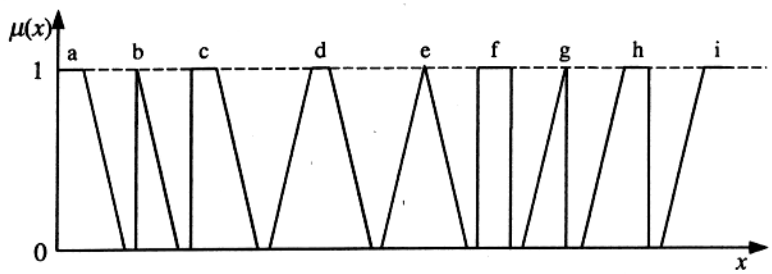

a – the left outside membership function
b,g – triangular asymmetrical membership function
c – trapezoidal asymmetrical membership function
d – trapezoidal symmetrical membership function
e – triangular symmetrical membership function
f – rectangular membership function
h – trapezoidal asymmetrical membership function
i – the right outside membership function

Figure 5.4 Most commonly used membership functions [59].

The advantage of the polygonal functions is that they can be defined using a minimal amount of information in comparison with other membership functions. Data relating to the corner points are sufficient. This is especially important in the modelling of systems for which the developer does not have much data. Another advantage is the ease of modification of parameters in the membership functions. However, polygonal functions are not continuously differentiable. In the opinion of some scientists non-continuously differentiable membership functions make the process of adapting fuzzy models difficult [59].

The membership functions used by a human can be termed intuitive membership functions. The intuitive membership functions such as rectangular in shape are continuous in the whole range of numerical universe of discourse. Any little variation of variable x in the defined range causes no step variation of its qualitative evaluation made by a human. In the case of a triangular membership function, for a minimal variation of a variable x in the neighbourhood of the point b a sudden jump occurs both in the value and the sign of the derivative. Therefore, a triangular membership function represents a very rough approximation of the human manner of evaluation. Nevertheless, this does not mean that a model with triangular membership functions cannot be satisfactorily exact.

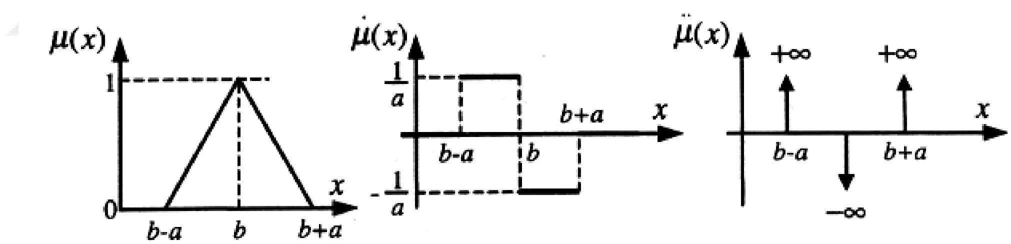

Figure 5.5 Triangular membership functions and their derivatives [59]

In the case of the triangular function, the curvatures at the points (b-a), b, (b+a) are so large that the second derivative tends to infinitely large values (Figure 5.5). A more suitable function for the human manner of qualitative evaluation of variables is shown in Figure 5.6. Because it has little curvatures and a continuous first and second derivative.

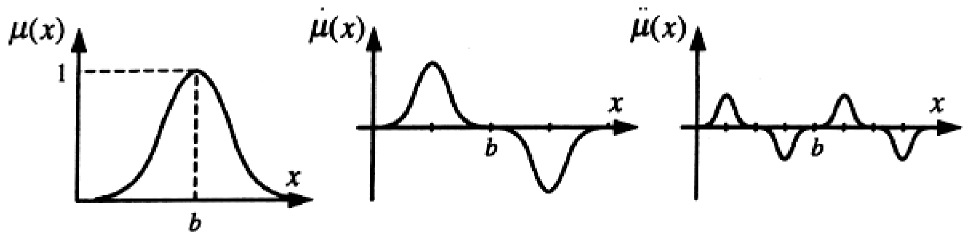

Figure 5.6 Example of continuous membership function with little curvatures

The Gaussian function is expressed by the Equation (5.1).

$$\mu(x) = \exp\left[-\left(\frac{x-b}{a}\right)^2\right] \tag{5.1}$$

The shape of the Gaussian function sometimes referred to as the Gauss bell [59], is determined by 2 parameters *a* and *b*, where b is the modal value of the function, while the width of the function is determined by the parameter *a*. The Gaussian function has the width of 2*a* at the level of $\mu(x) = e^{-1} \cong 0.36788$. In order to determine the parameter *a* using the expert method one can employ the concept of the critical point k of a membership function. This is the point of a membership function at which the grade of membership amounts to 0.5. Each Gaussian curve has two critical points as shown in Figure 5.7. If it is assumed that the adjoining membership functions intersect each other at around the height of $\mu(x_k) = 0.5$, then the critical point k can be defined as the point having a coordinate *x* such that the developer is not able to decide if it belongs more to the right or left fuzzy set. Knowing the modal value of the Gauss curve *b*, the second parameter can be calculated [59]:

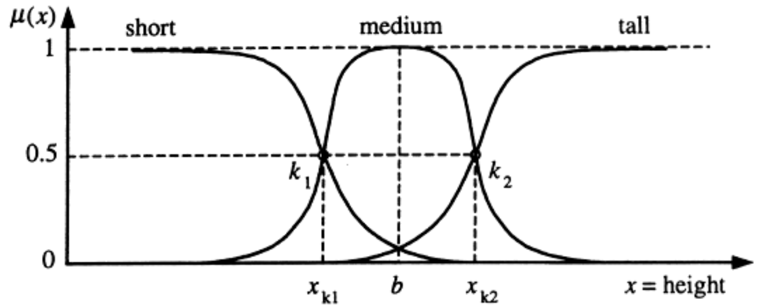

Figure 5.7 Gaussian function as membership function for the fuzzy set “medium height”

$$\mu(x_k) = \exp\left[-\left(\frac{x_k - b}{a}\right)^2\right] = 0.5, \tag{5.2}$$

$$a = \frac{|x_k - b|}{\sqrt{\ln 2}} \tag{5.3}$$

While the use of Gaussian functions provide smooth, continuously differentiable hyper surfaces of a fuzzy model, symmetry of these functions cause a dissatisfied partition of unity condition. A satisfied partition of unity is the sum of memberships of each element *x* from the universe of discourse is equal to 1:

$$\sum_h \mu_{A_h}(x) \equiv 1, \qquad \forall x \in X$$

where:

h is the number of the fuzzy set.

Satisfying the condition of a partition of unity usually gives the model a smoother surface in comparison with models employing sets of the type represented in Figure 5.8.

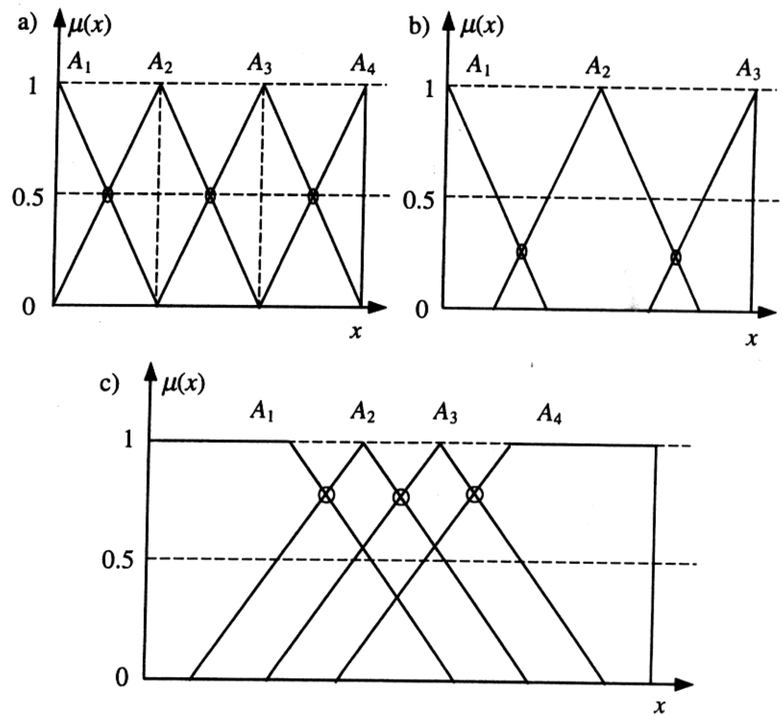

Figure 5.8 Examples of the fuzzy sets satisfying (a) and not satisfying (b,c) the condition of a partition of unity [59]

In the use of the Gaussian function it becomes necessary to identify a greater number of parameters than in the case of triangular membership functions and this makes the adjustment of models difficult. Another disadvantage is the infinitely large support of the function. These mean that each element *x* of the universe of discourse X belongs to each fuzzy set represented by this function. This is not the purpose in modelling even if the effect is negligibly small, provided that the width of this function is not too large. As a result of these disadvantages of the Gaussian functions, asymmetrical Gaussian functions are introduced. Asymmetrical functions better enable the realisation of the partition of unity condition.

5.3. Vehicle path planning

For the purpose of vehicle path planning by using fuzzy logic, a Simulink vehicle model is developed on the basis of the derived dynamic equations in Chapter 3. The equations developed give the option of representing a vehicle with either a two degrees of freedom (2 DOF) model or a four degrees of freedom (4 DOF) model. Therefore, this vehicle path planning method is taken into account both for 2 DOF and 4 DOF vehicle models. Due to the nature of the dynamic equations, the simulation of the 2 DOF model is always at constant speed. However, some action must be taken to maintain the same condition in the analysis of the 4 DOF model. Therefore, fuzzy control logic is applied to keep the velocity constant during the simulation, but the relevant logic is not covered here because it is considered to be more related to Yaw Control of the vehicle which is the subject of the Chapter 7. Simulink model blocks to represent the two degrees of freedom model in lateral motion and yaw motion are shown in Figures 5.9 and 5.10 respectively. Simulink model blocks for the four degrees of freedom model in lateral motion, yaw motion, roll motion and longitudinal motion are presented in Figures 5.11, 5.12, 5.13 and 5.14, respectively. Simulink representations of the basic equations of motions are presented with their algebraic equations which were discussed in Chapter 3.

(Figure5.9): $m(\dot{V}+rU)=\left[F_{yr}+F_{yf}\cdot\cos(\delta)+\left(F_{xf}-F_{bf}\right)\cdot\sin\delta\right]$

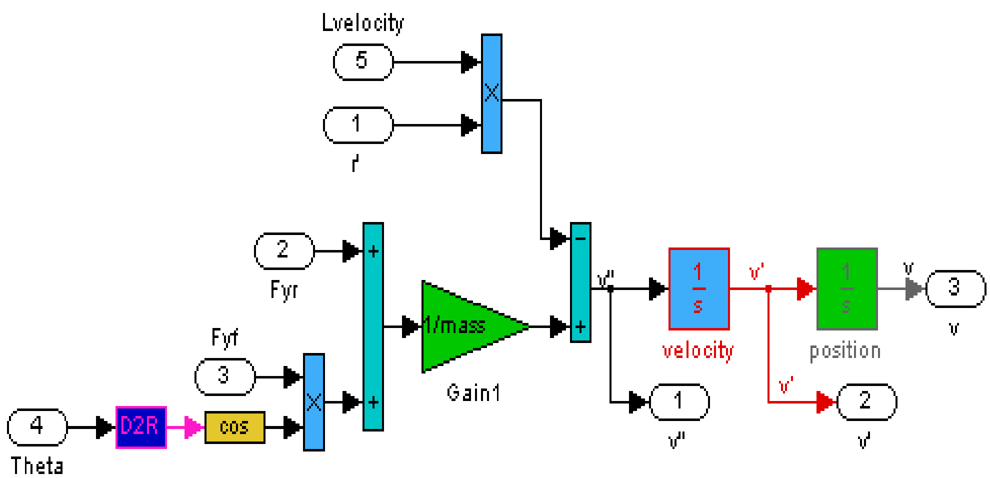

Figure 5.9 Vehicle lateral motion equations in 2 DOF

(Figure 5.10): $I_{zz}\dot{r}=a\cdot F_{yf}-b\cdot F_{yr}$

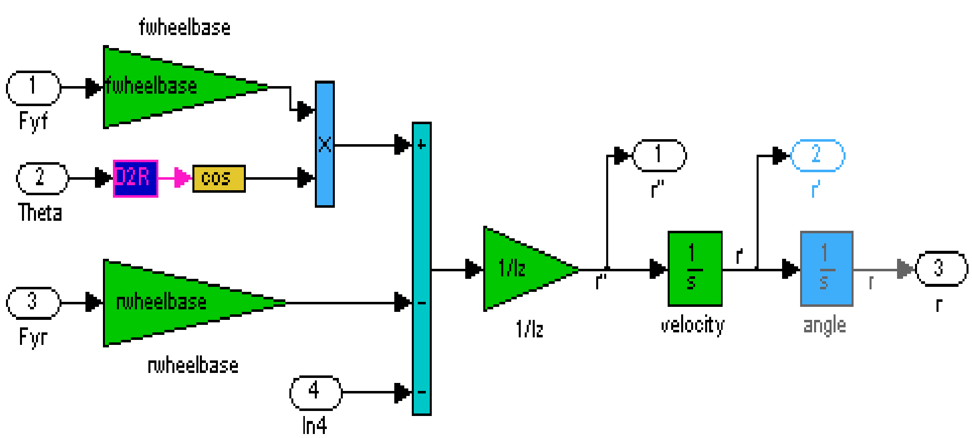

Figure 5.10 Vehicle yaw motion equations in 2 DOF

(For-Figure 5.11): $$m(\dot{V}+rU)=\begin{bmatrix} F_{yrL}+F_{yrR}+\left(F_{yfL}+F_{yfR}\right)\cdot\cos(\delta)+\left(F_{xfL}+F_{xfR}\right)\cdot\sin\delta-\ldots \\ \ldots-\left(F_{bfL}+F_{bfR}\right)\cdot\sin\delta \end{bmatrix}$$

(For-Figure 5.12): $$I_{zz}\dot{r}=\begin{bmatrix} a\cdot\left(F_{yfL}+F_{yfR}\right)\cdot\cos\delta+\left(t_f/2\right)\cdot\left(F_{yfL}-F_{yfR}\right)\cdot\sin\delta+\ldots \\ \ldots+a\cdot\left(F_{xfL}+F_{xfR}\right)\cdot\sin\delta+\left(t_r/2\right)\cdot\left(F_{brL}-F_{brR}-F_{xrL}+F_{xrR}\right)-\ldots \\ \ldots-b\cdot\left(F_{yrL}+F_{yrR}\right)-\left(t_f/2\right)\cdot\left(F_{xfL}+F_{bfR}-F_{xfR}-F_{bfL}\right)\cdot\cos\delta-\ldots \\ \ldots-a\cdot\left(F_{bfR}+F_{bfL}\right)\cdot\sin\delta \end{bmatrix}$$

(For-Figure 5.13): $$I_{xx}\dot{p}=\left[m_s\cdot\left(\dot{V}+r\cdot U\right)\cdot d+m_s\cdot g\cdot d\cdot\phi-C_\phi\cdot\phi'-K_\phi\cdot\phi\right]$$

(For-Figure 5.14): $$m(\dot{U}-rV)=\begin{bmatrix} F_{xrL}+F_{xrR}+\left(F_{xfL}+F_{xfR}\right)\cdot\cos\delta-F_{brL}-F_{brR}-\ldots \\ \ldots-\left(F_{bfL}+F_{bfR}\right)\cdot\cos\delta-\left(F_{yfL}+F_{yfR}\right)\cdot\sin(\delta) \end{bmatrix}$$

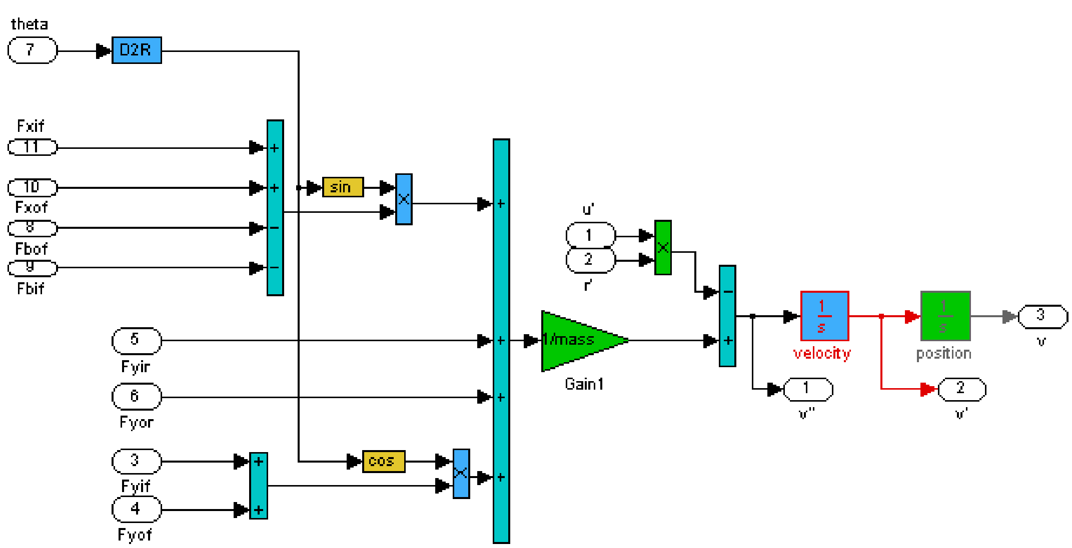

Figure 5.11 Vehicle lateral motion equations in 4 DOF

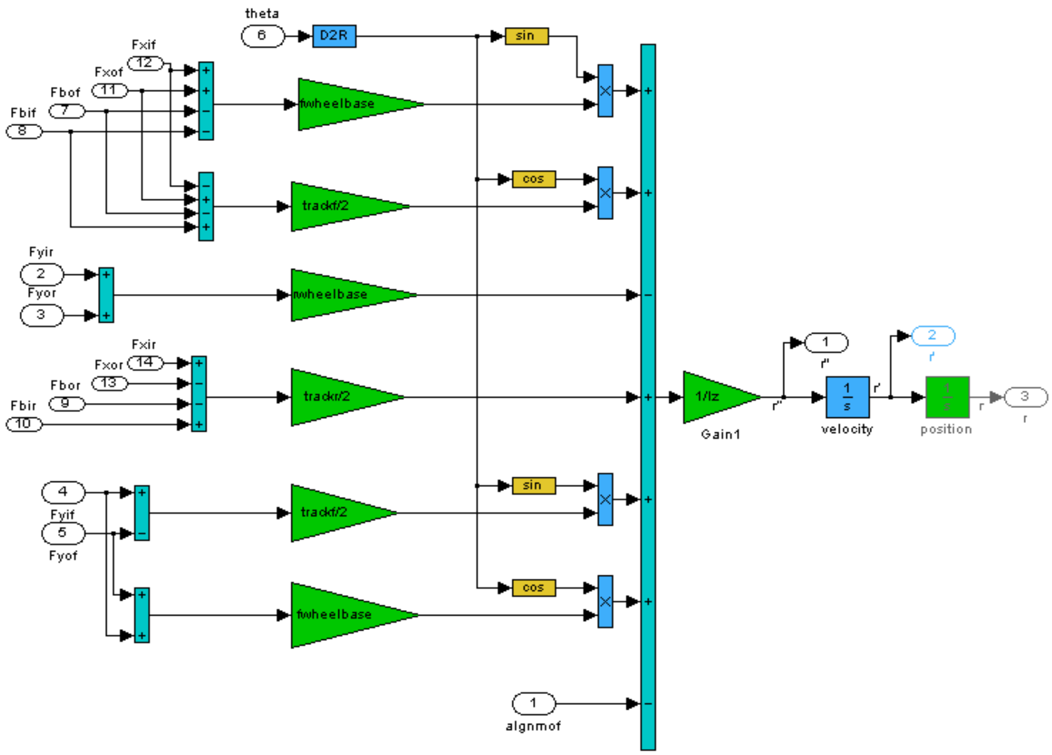

Figure 5.12 Vehicle yaw motion equations in 4 DOF

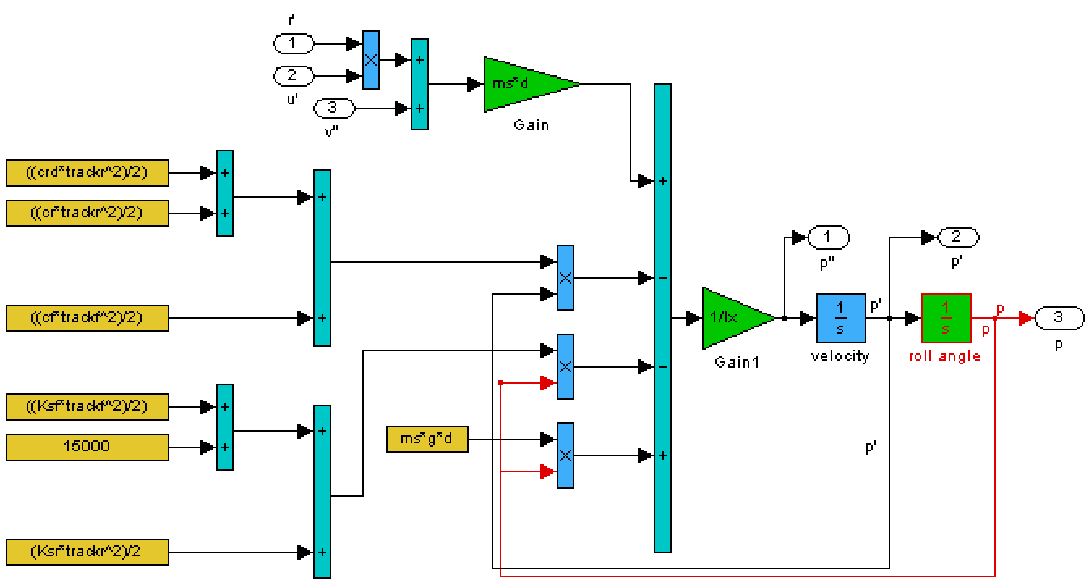

Figure 5.13 Vehicle roll motion equations in 4 DOF

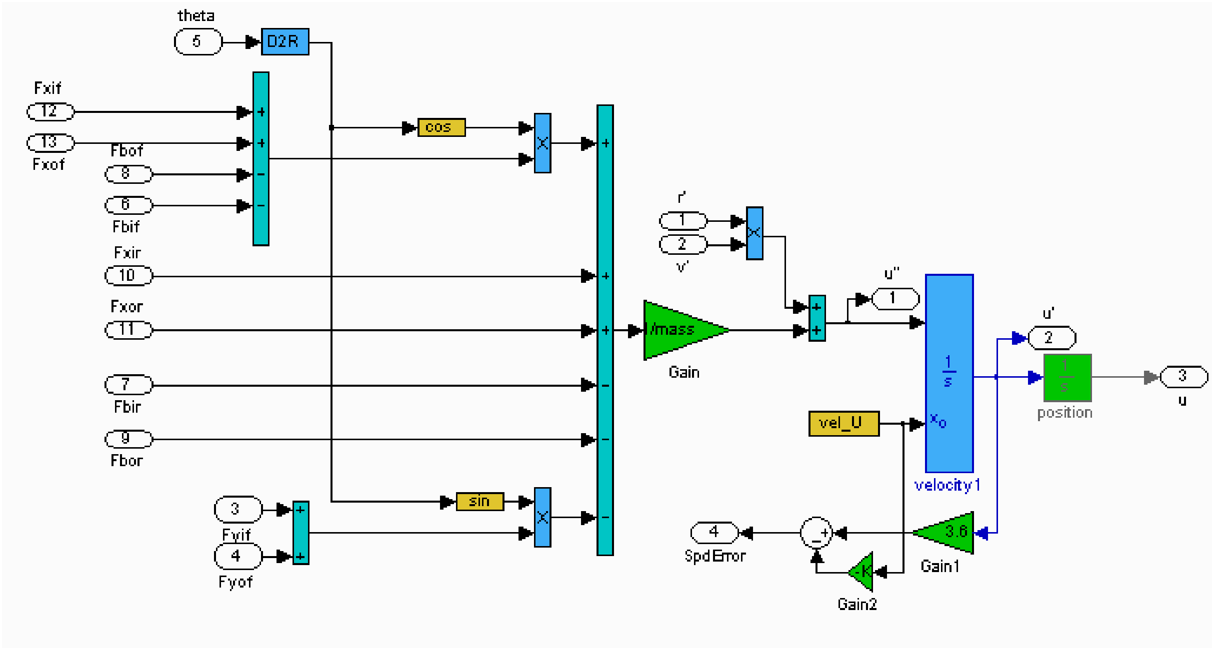

Figure 5.14 Vehicle longitudinal motion equations in 4 DOF

5.3.1. Definition of target points for the path planning and inputs for the fuzzy controller

A Matlab m-file [Appendix B] has been written to identify the next two target points in the vehicle path at each time step of the simulation. This is to take into account that a real driver will steer the vehicle not simply to reach the next target point but also to orient it in a suitable direction to approach the subsequent target point. This situation affects the direction of approach to the first target with a view to a good approach to the next target point. These two target points do not change until the first target point has been reached. However, if the first target point has been passed (i.e. x' is negative – the target point is behind the current position) because of a loss of control, the original second target becomes the first target and the next point becomes the new second target. The results provided by the Vehicle Model block are processed in the Fuzzy Inputs block and then sent to the fuzzy logic controller block which is called 'Fuzzy

Pilot'. The Fuzzy Pilot is intended to react as a real driver, so it determines the direction in which to turn the steering wheel, and by how much, by considering the membership functions of the relevant inputs. A very general flow diagram of the vehicle model and fuzzy pilot interaction is shown in Figure 5.15. The vehicle model block is replaceable by any vehicle model regardless of its complexity. The path which vehicle is supposed to follow is mapped on the Earth fixed coordinates before a simulation study. Any number of pairs of X and Y coordinate points can be used. This mapped data is then converted into the vehicle body centred coordinate system. The new x and y points in the body fixed coordinates are defined by the equations 5.4 and 5.5 and corresponding Simulink blocks shown in Figures 16 and 17 and dependant Figures 18, 19, 20 and 21. Figure 16 shows the selection process of the next two target points in the Earth fixed coordinate system.

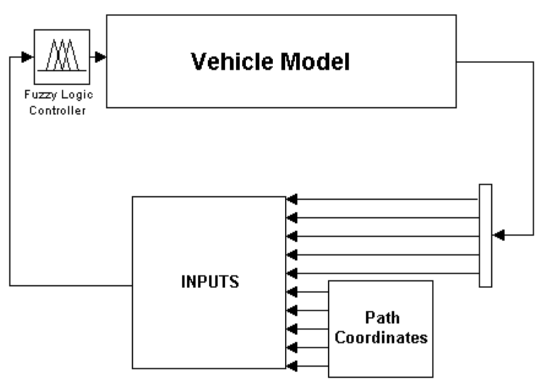

Figure 5.15 General flow diagram of the vehicle path planning in Simulink.

$$x' = (x - X) \cdot \cos(r) + (y - Y) \cdot \sin(r) \tag{5.4}$$

$$y' = (y - Y) \cdot \cos(r) - (x - X) \cdot \sin(r) \tag{5.5}$$

where,

x', y': Calculated coordinates for x , y point in the body centred axis system (m)

x, y: Any defined x ,y point in the Earth fixed coordinate system (m)

r: Vehicle yaw angle (deg)

X, Y: Instantaneous position of the vehicle on the x and y coordinates. (m)

In the figures representing the Simulink blocks for axis conversion, x1dat, y1dat, x2dat and y2dat refer to Earth fixed coordinate pairs while the symbol: (') refers to the coordinate pairs on body fixed axis system (BFA). In the Figure 17 this conversion can be seen in general blocks. Figures 5.18, 5.19, 5.20 and 5.21 show the conversions of x1dat, x2dat, y1dat, and y2dat to body fixed coordinates based on equations (5.4) and (5.5), respectively.

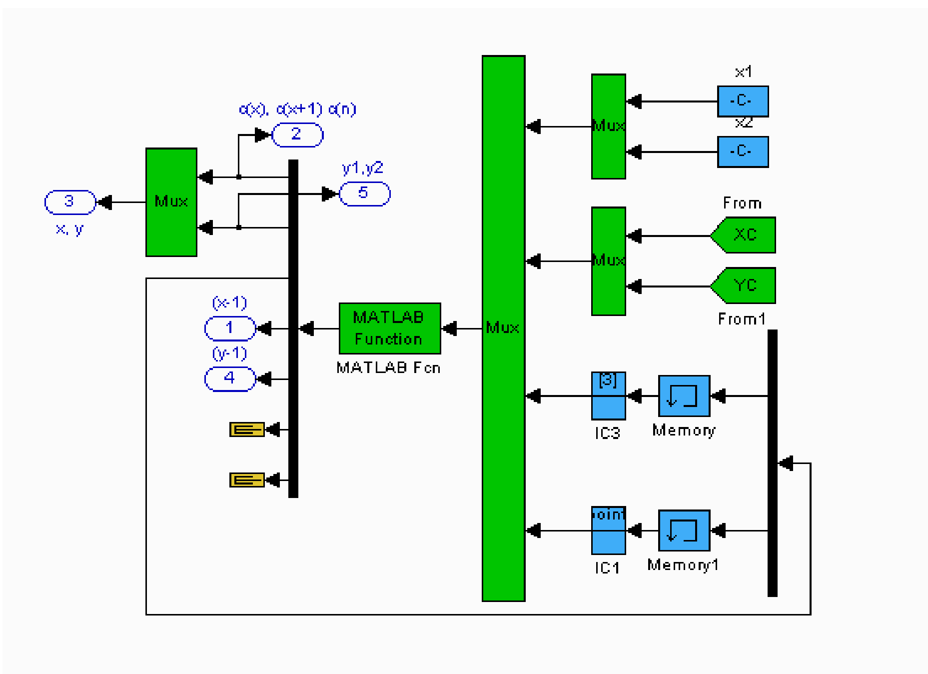

Figure 5.16 Simulink blocks for the selection of next two target points.

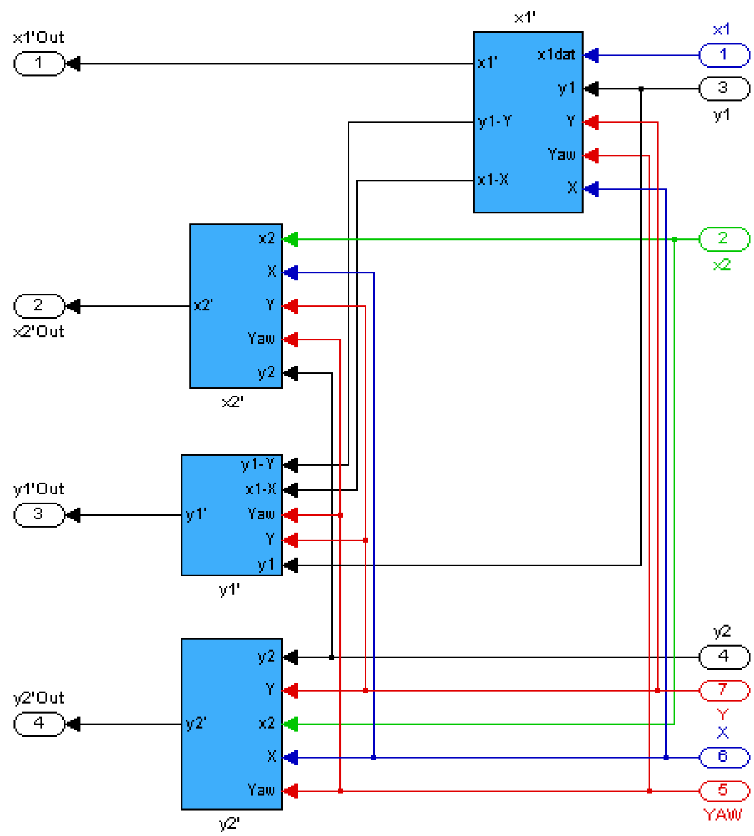

Figure 5.17 Axis conversion from earth fixed to body fixed

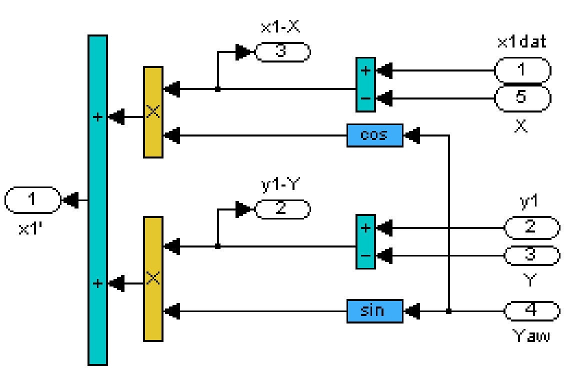

Figure 5.18 The first 'x' target on BFA

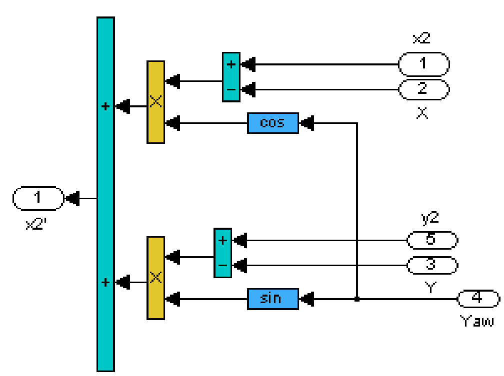

Figure 5.19 The second 'x' target on BFA

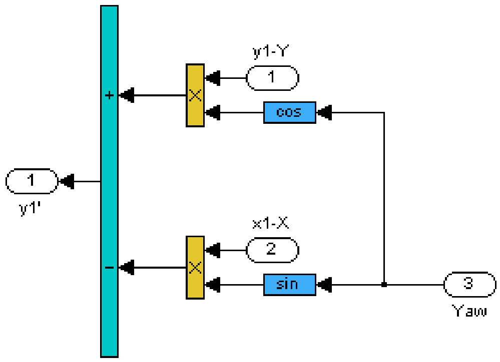

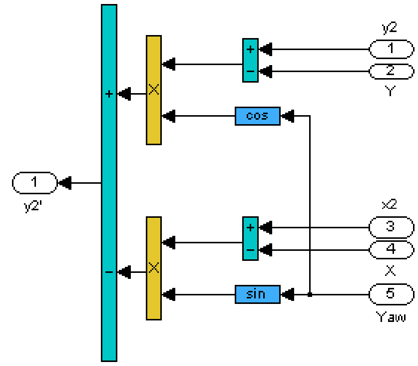

Figure 5.20 The first 'y' target on BFA Figure 5.21 The second 'y' target on BFA

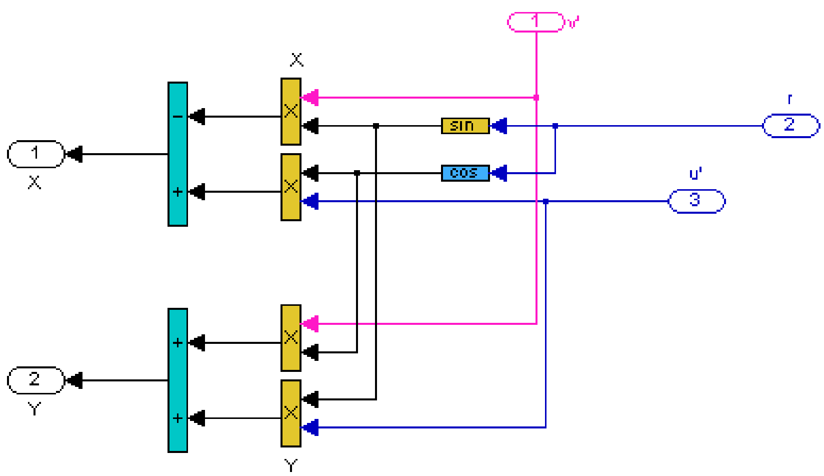

Figure 5.22 Instantaneous X and Y points during the travel

5.3.2. Fuzzy inputs for vehicle path planning provided in Simulink

Two angles and one distance inputs are derived for the fuzzy logic controller by the position of the vehicle to the coordinate pair which are shown in Figure 5.23. In Figure 5.23, *Error1* is the angle between the axis of last heading of vehicle and the first target point A, which vehicle must be directed to. The angle *Error2* shows the severity of the turning after reaching the point A. The equations of *Error1* and *Error2* are shown in the Equation 6 and 7. Both *Error1* and *Error2* are variable angles which are sent as feedback inputs to the fuzzy controller at every time step of the travel. The third input of the controller is '*distance*'. '*Distance*' is the linear distance from the point 'O' to the point 'A', in Figure 5.23.

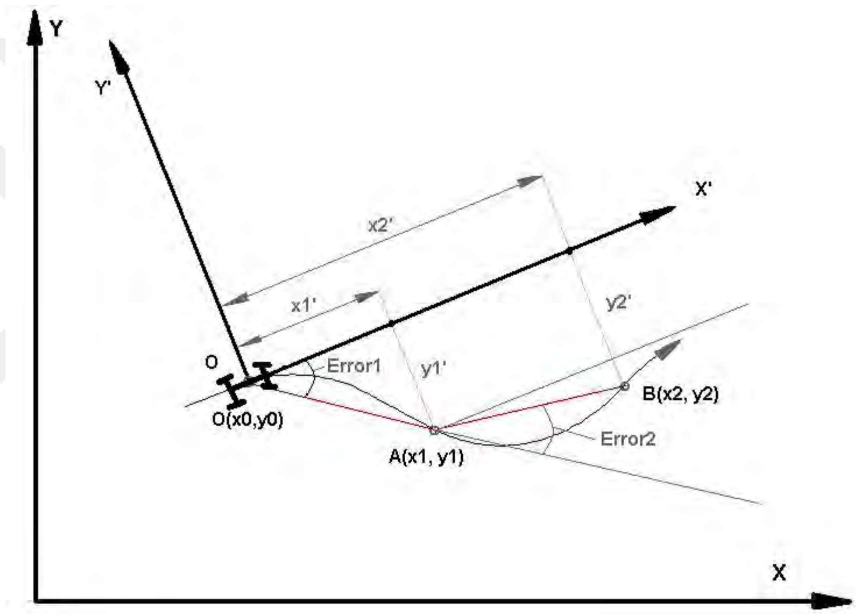

Figure 5.23 Moving axis system and error formation for the fuzzy path planning

$$Error1 = \tan^{-1}\left(\frac{y_1'}{x_1'}\right) \quad (5.6)$$

$$Error2 = Error1 - \tan^{-1}\left(\frac{y_2' - y_1'}{x_2' - x_1'}\right) \quad (5.7)$$

The direction of the vehicle is determined in the Angles block of the vehicle Simulink model in Figure 5.24, which actually represents the Equations (5.6) and (5.7).

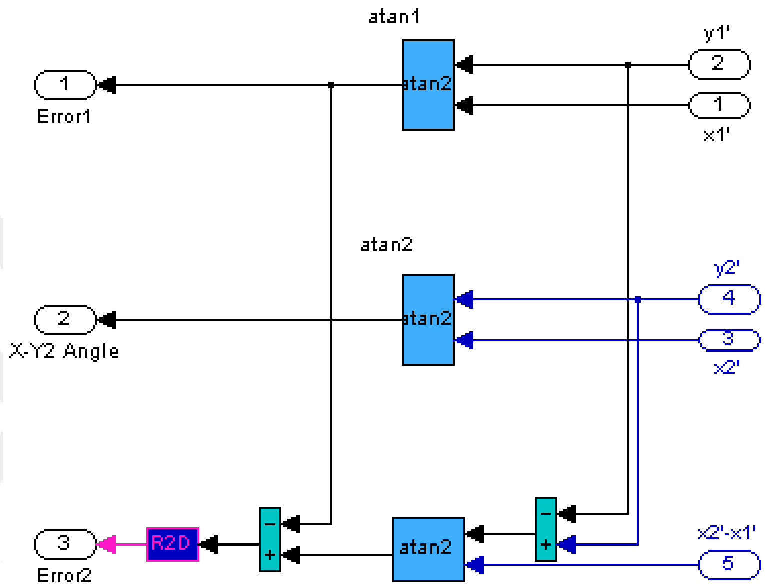

Figure 5.24 The Simulink block of Error1 and Error2

Obviously, the outputs of the vehicle Simulink model; *Error1*, *Error2*, and *Distance* become the inputs of the Fuzzy Inference System namely Fuzzy Pilot in this study.

5.3.3. Fuzzy Inference System in Development of 'Fuzzy Pilot'

Fuzzy pilot is a term that is used to define a driver model for the vehicle handling dynamics simulation studies. The objective of developing the model using Fuzzy Logic is to provide a smart control tool, which implements the human intelligence at a fairly simple level, in computerised vehicle path formation. Fuzzy logic controller is developed by using Fuzzy

Logic Toolbox in Matlab R13 / Simulink environment. The controller is implemented into the vehicle Simulink model in conjunction with the developed vehicle handling simulation tool, Handsim. The flow diagram of the Fuzzy Inference System (FIS) with regard to vehicle path planning is shown in Figure 5.25.

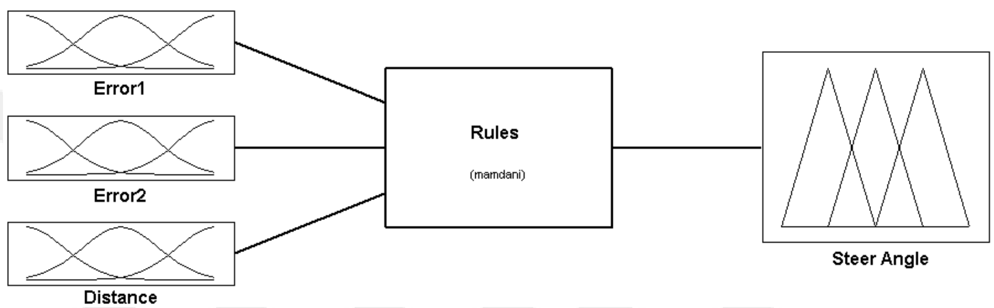

Figure 5.25 Fuzzy Inference System (FIS)

Error 1 and Error 2 have the same membership functions as represented in Figure 5.26. There are seven membership functions defined to represent Negative High (High-), Negative Medium (M-), Negative Low (L-), Zero (Z), Positive Low (L+), Positive Medium (M+) and Positive High (High+) angles.

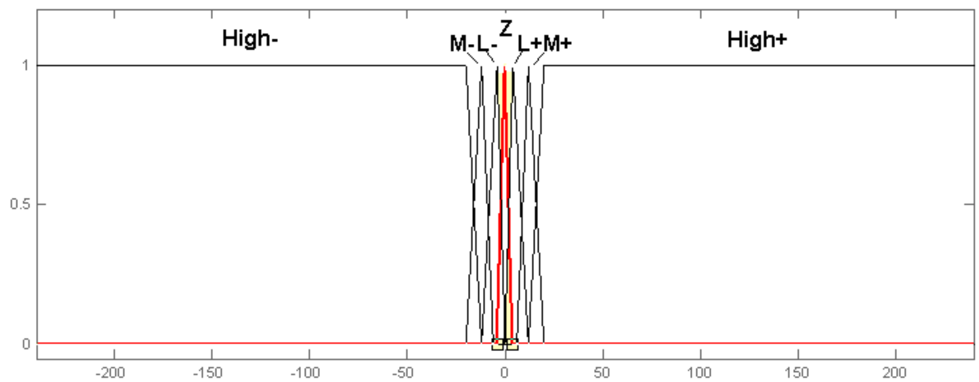

Figure 5.26 Membership functions for both Error1 and Error2

The range of the angle error is kept wide although the range of low and medium error is adjusted into relatively narrow angles. By covering this high angle area, even if a vehicle goes out of control, up to the given limits, the possibility exists to try to escape from that condition and head for the missed point or the following point as an ordinary human driver will behave. Figure 5.27 shows the distance input of the FIS. This input includes 3 membership functions namely *All*, *Very Low* and *Low*. Both *Low* and *Very Low* have membership relations from the distance zero to 15th meter which is roughly determined by just over the average turning radius of passenger cars.

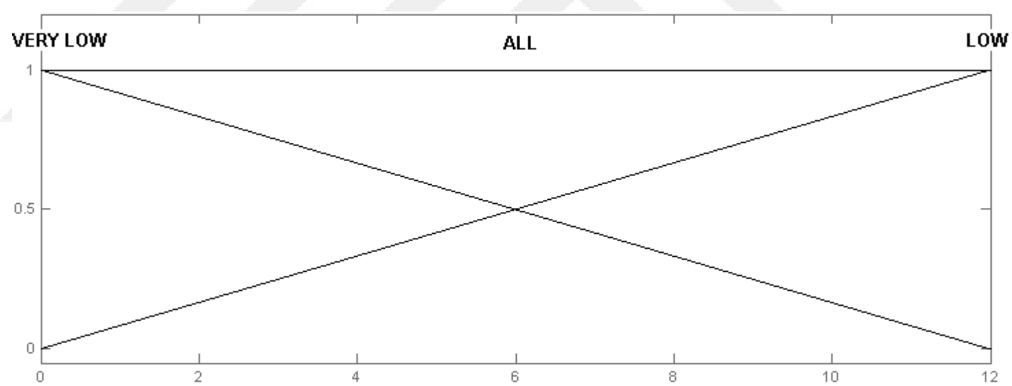

Figure 5.27 Membership functions for the input: '*Distance'(m)*

The Fuzzy output is the Steering Wheel angle defined as between -80 and +80 degrees steering wheel angle (Figure 5.28). Even though the Steering Wheel turning range is limited in the Fuzzy Inference system, a Simulink block which introduces a steering gear ratio is added just after the fuzzy controller (Figure 5.29). For example for the given values a gear ratio of 16 gives a maximum of 5 degrees at the steered road wheel. This allows for flexibility in defining the steer angle at the steered wheel for different vehicles.

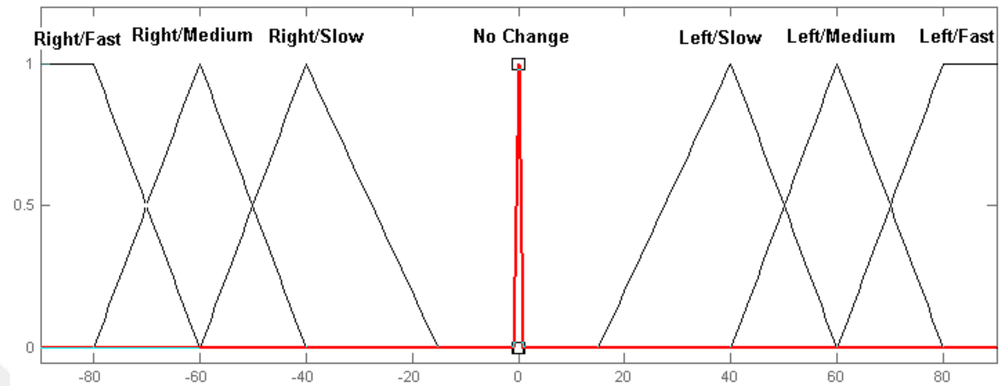

Figure 5.28 Membership functions for output: Steering Wheel Angle (degree)

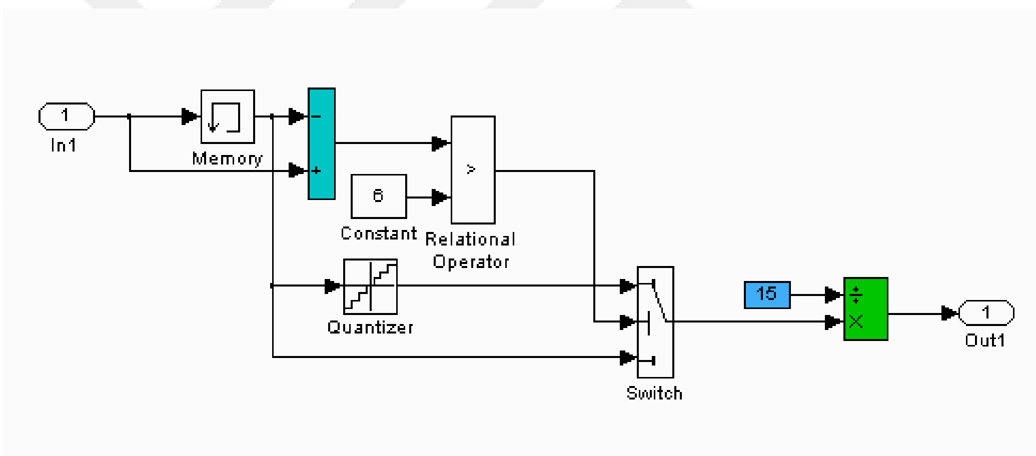

Figure 5.29 Simulink block of gear ratio

Membership functions of each input and the output are connected and processed by defined rules.

<u>5.3.4. Fuzzy Rules</u>

Fuzzy rules are written in normal human language using IF-THEN reasoning. The rules below from 1 to 16 are taken as a sample group from the whole range of rules which are 130 in total.

The complete rule structure is presented in numerical form in Appendix C. The first 14 are, in fact, very similar but the 15th and 16th rules represent an additional approach.

1. **If *Error1* is *Low+* and *Error2* is *Low+* and *Distance* is not All then *SteerWAngle* is *Left/Slow***
2. **If *Error1* is *Low+* and *Error2* is *Medium+* and *Distance* is not All then *SteerWAngle* is *Left/Medium***
3. **If *Error1* is *Low+* and *Error2* is *High+* and *Distance* is not All then *SteerWAngle* is *Left/Slow***
4. **If *Error1* is *Low+* and *Error2* is *Low-* and *Distance* is not All then *SteerWAngle* is *Left/Medium***
5. **If *Error1* is *Low+* and *Error2* is *Medium-* and *Distance* is not All then *SteerWAngle* is *Left/Fast***
6. **If *Error1* is *Low+* and *Error2* is *High-* and *Distance* is not All then *SteerWAngle* is *Left/Fast***
7. **If *Error1* is *Low-* and *Error2* is *Low-* and *Distance* is not All then *SteerWAngle* is *Right/Slow***
8. **If *Error1* is *Low-* and *Error2* is *Medium-* and *Distance* is not All then *SteerWAngle* is *Right/Medium***
9. **If *Error1* is *Medium+* and *Error2* is *Low+* and *Distance* is not All then *SteerWAngle* is *Left/Medium***
10. **If *Error1* is *Medium+* and *Error2* is *Medium+* and *Distance* is not All then *SteerWAngle* is *Left/Medium***
11. **If *Error1* is *Medium+* and *Error2* is *High+* and *Distance* is not All then *SteerWAngle* is *Left/Slow***
12. **If *Error1* is *Medium-* and *Error2* is *Low-* and *Distance* is not All then *SteerWAngle* is *Right/Medium***
13. **If *Error1* is *Medium-* and *Error2* is *Medium-* and *Distance* is not All then *SteerWAngle* is *Right/Medium***
14. **If *Error1* is *Medium-* and *Error2* is *High-* and *Distance* is not All then *SteerWAngle* is *Right/Slow***
15. **If *Error1* is *Low+* and *Error2* is *High+* and *Distance* is *Low* then *SteerWAngle* is *Right/Slow***
16. **If *Error1* is *Low+* and *Error2* is *High+* and *Distance* is VeryLow then *SteerWAngle* is *Left/Fast***

From the rule-1, it is obvious that for the low level angle Error feedbacks, low increments in terms of Steering Wheel angle will be enough to satisfy the right direction. In rules 2 and 3, this approach differs slightly. Because the second target requires a sharper angle of turn, the driver can take care of the second target by using higher steering angle increments, however, if the second target requires a very acute turn for that particular condition, then the driver might aim for a wider angle of approach to the first point for the purpose of ‘seeing’ the second target more easily. Likewise, rule 4 aims to use the same logic by increasing the steering wheel angle more than necessary for the first target. Differently, rules 15 and 16 take into account the distance to the target. These rules are closely related to the rule 3. However, as rule 3 follows the first target, strictly, rule 15 turns the left going vehicle to the right. Therefore, the vehicle gains a wider angle to the second target in the low distance area. Finally, rule 16 provides a sharper left turn to hit the first target as this manoeuvre also targets the second point in the very low distance area. The complete form of the fuzzy rules are given in Appendix C including the rules for speed and yaw control of the vehicle.

5.4. Simulation and Results

A Formula SAE- Student Racing Car is the subject of a study reported in this section. Some of its specifications and simulation parameters are presented in the Table 1, below.

Table 5.1 Vehicle control and simulation parameters

Path Coordinates	(m)	X(0, 30, 60, 90, 120, 105, 70, 40) Y(0, 12, 0, 8, 25, 70, 50, 80)
Wheelbase[front, rear]	(m)	[0.821, 0.821]
Track [front, rear]	(m)	[1.35, 1.25]
Mass of vehicle + driver	(kg)	300
Roll, Yaw inertias	(kgm^2)	50, 200
Damper Rate [front, rear]	(Ns/m)	750, 750
Spring Rate [front, rear]	(N/m)	22000, 22000
Anti Roll Bar Rate (front)	(Nm/rad)	3000
Height of C.G	(m)	0.285
Roll Centre [front, rear]	(m)	0.016, 0.055

Simulations were run at different vehicle speeds from 10 to 60 Kph to test the efficiency of the fuzzy pilot both for 2 DOF and 4 DOF vehicle models. The simulation results are shown in Figures 5.30 and 5.31, respectively. From the Figures 5.30 and 5.31 it is very obvious that the vehicle follows the path very well without any distinction until the speed of 45 Kph. Starting from this speed, the driver finds it difficult to keep the vehicle on the path traversed at the low speeds. This is especially obvious in the more realistic 4 DOF model analyses (Figure 5.31). Differences in the path responses of the 2 DOF and 4 DOF models are illustrated in Figures 5.32 to 5.36. In Table 5.2, the time to complete the path and the distance travelled is also compared for different speeds above 40 Kph.

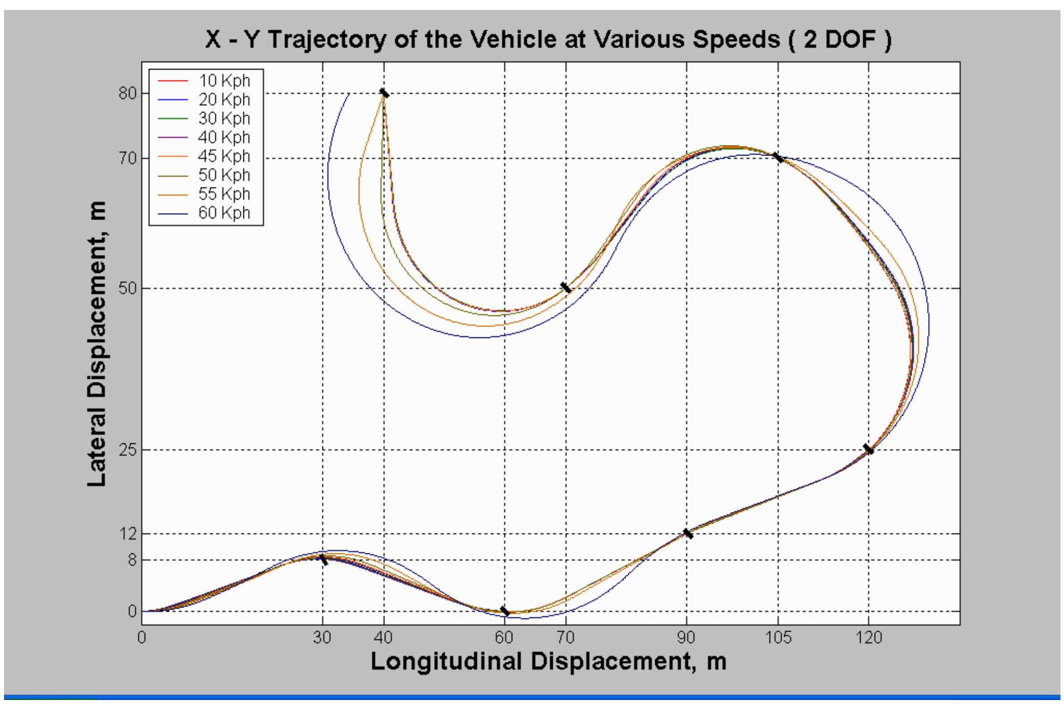

Figure 5.30 Resultant paths at different vehicle speeds with 2 DOF model

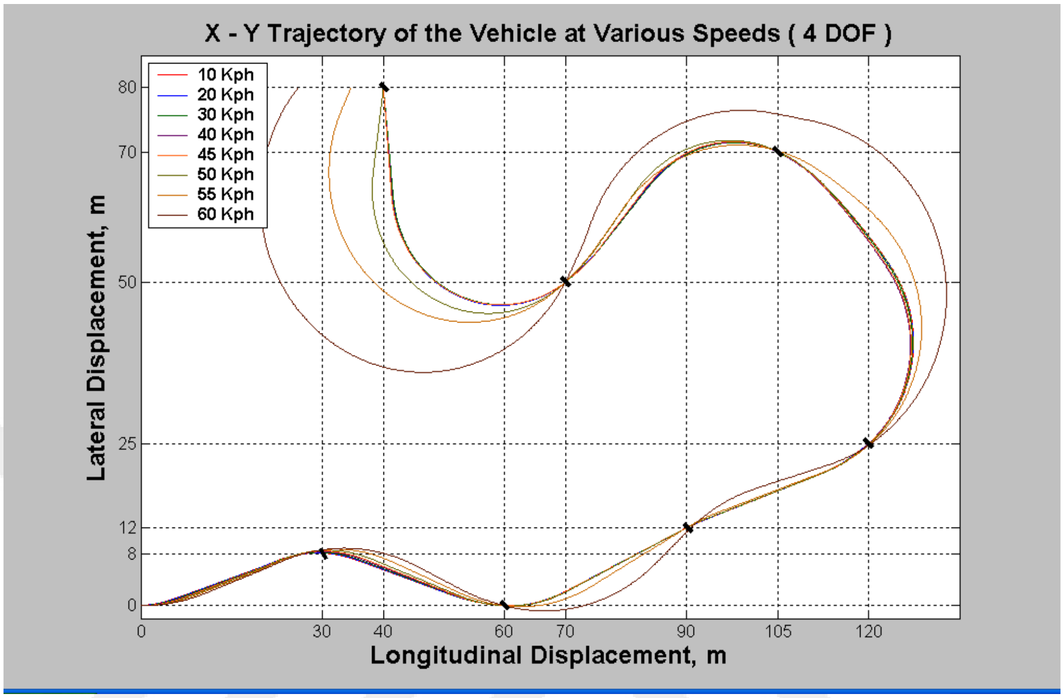

Figure 5.31 Provided path at different vehicle speeds with 4 DOF model

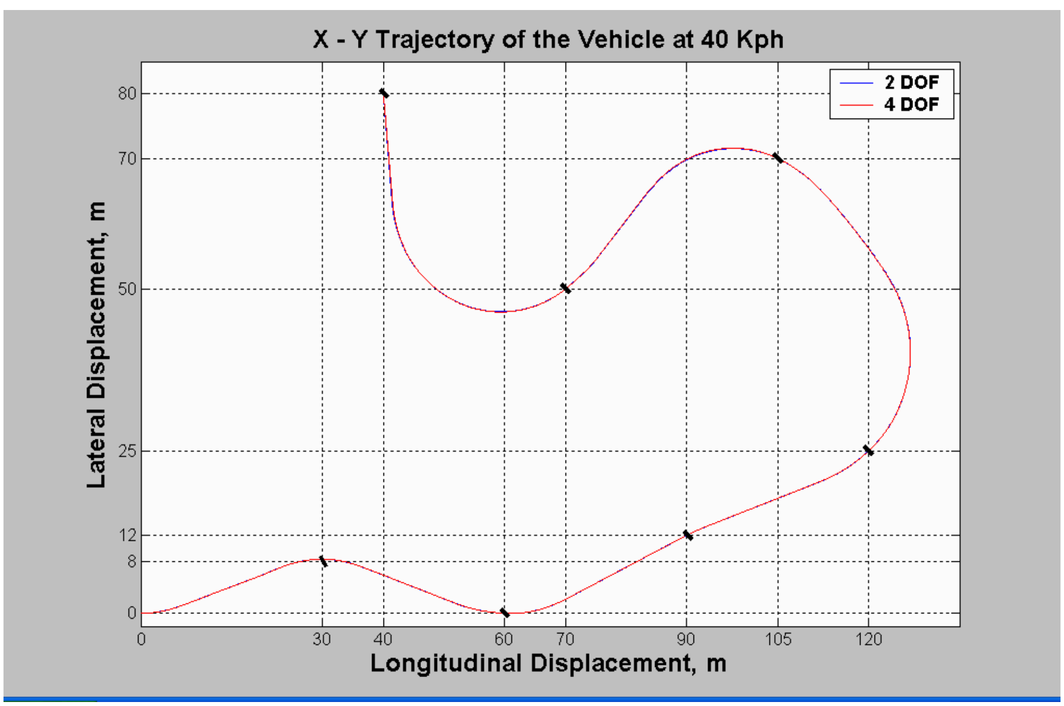

Figure 5.32 Provided path at 40 Kph vehicle speeds with 2 DOF and 4 DOF models

Table 5.2 Displacement against time in 2 DOF and 4 DOF models

	2 DOF		4 DOF	
	Displacement (m)	**Time (sec)**	**Displacement (m)**	**Time (sec)**
45 Kph	**283.25**	**22.66**	**283.31**	**22.66**
47.5 Kph	**283.285**	**21.47**	**284.518**	**21.56**
50 Kph	**286.667**	**20.64**	**289.056**	**20.81**
55 Kph	**295.167**	**19.32**	**299.303**	**19.59**
60 Kph	**305.167**	**18.31**	**339.162**	**20.35**

Table 5.2 and Figures 5.33 to 5.36 show that above a certain speed, the 2 DOF vehicle model simulations give better results than the 4 DOF model simulations, which is as expected. Especially above 50 kph vehicle speed the path completion time is also affected by the part loss of control of the vehicle. It is clear from the figures that the more realistic 4 DOF vehicle model cannot pass through the last point. Therefore, at high speeds, the difference in the two models is shown by either the path completion time, or the distance travelled. Some of the steering wheel angle responses of the vehicle are shown from Figures 5.37 to 5.40. Figures 5.38 and 5.40 show the first 60 meters of the path at different speeds in detail, on Earth fixed coordinates system.

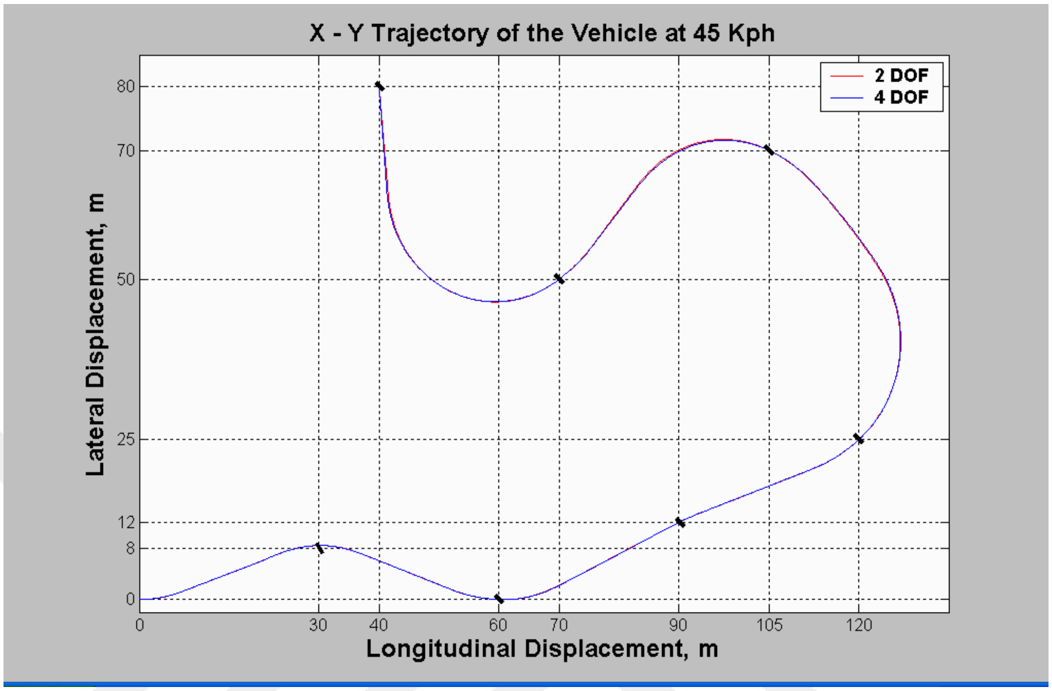

Figure 5.33 Resultant paths at 45 Kph vehicle speeds with 2 DOF and 4 DOF models

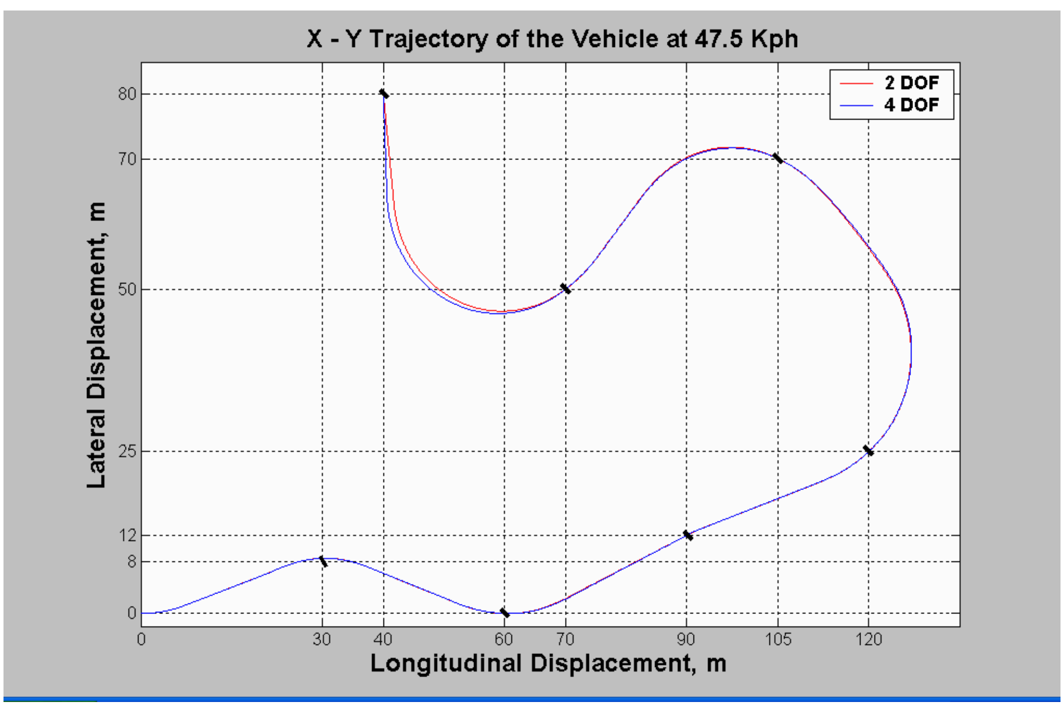

Figure 5.34 Provided paths at 47.5 Kph vehicle speeds with 2 DOF and 4 DOF models

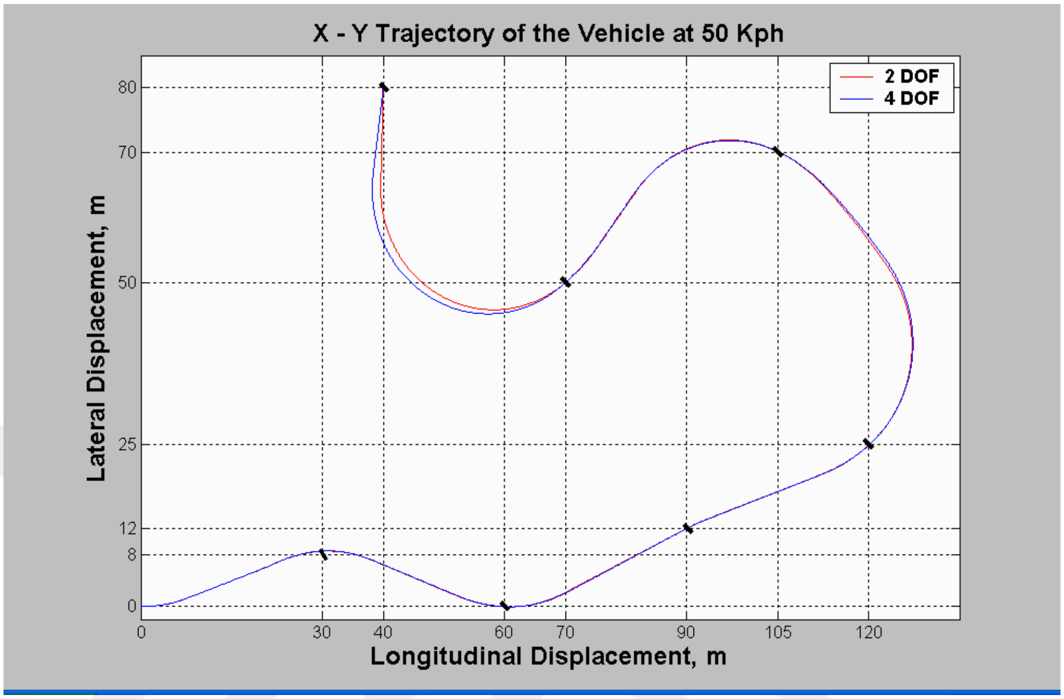

Figure 5.35 Resultant paths at 50 Kph vehicle speed with 2 DOF and 4 DOF models.

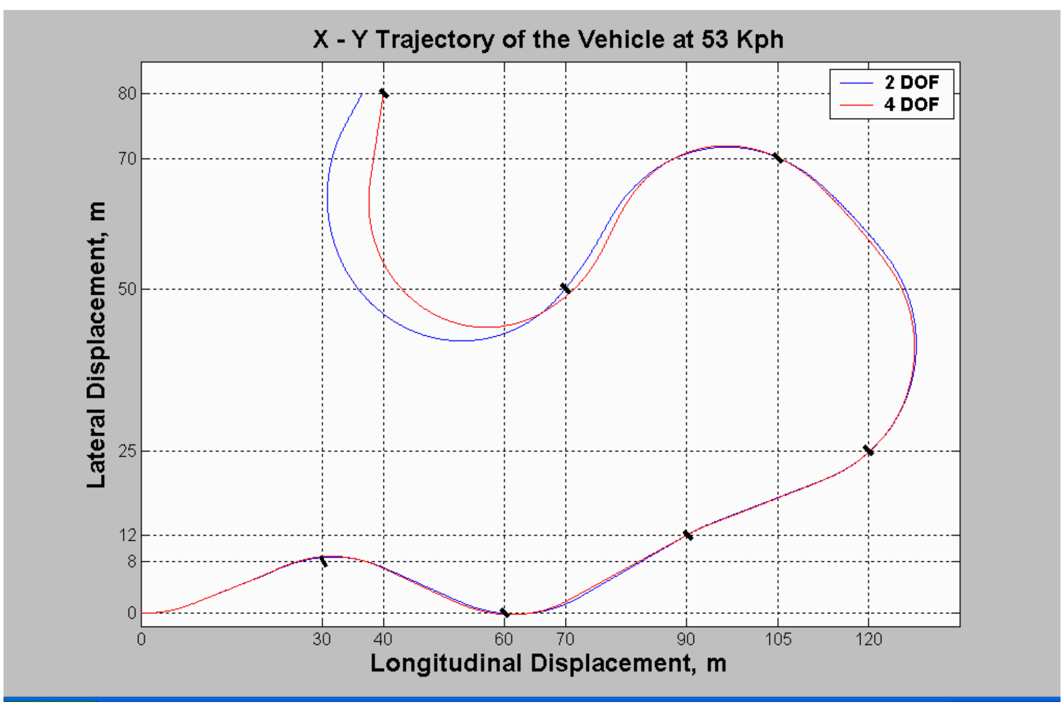

Figure 5.36 Resultant paths at 53 Kph vehicle speeds with 2 DOF and 4 DOF models

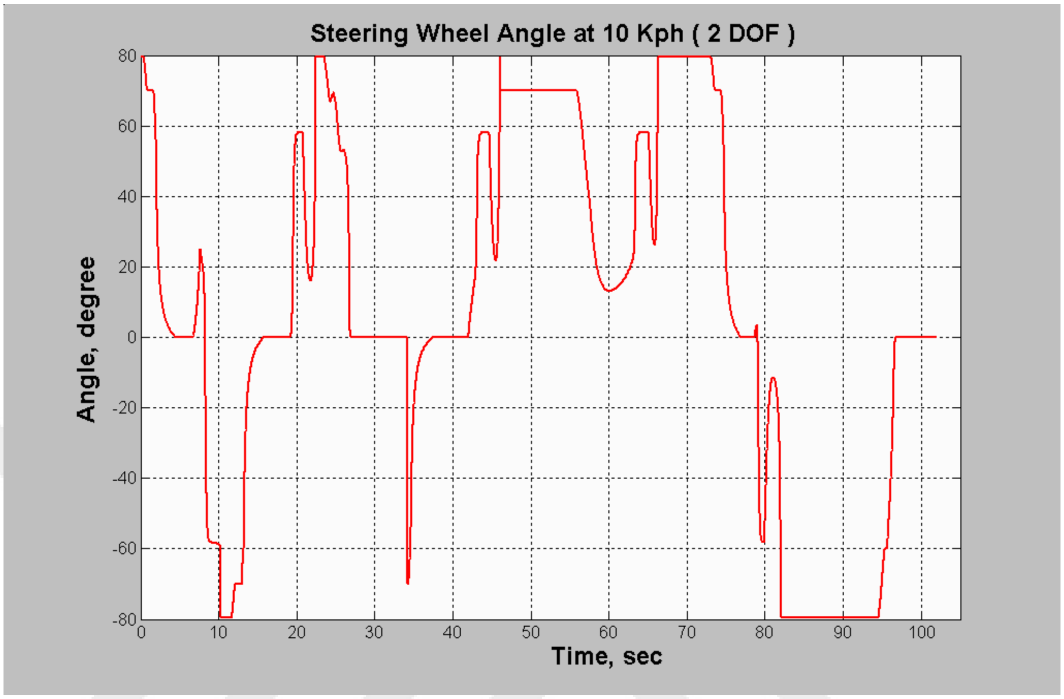

Figure 5.37 Resultant Steering Wheel Angle response at 10 Kph vehicle speed

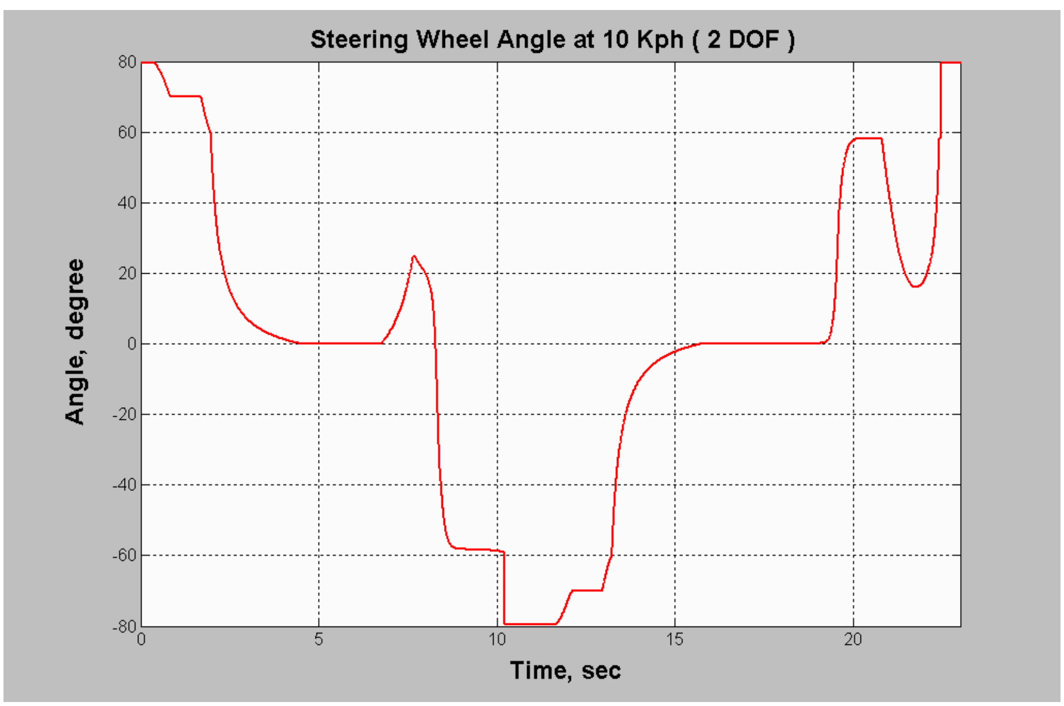

Figure 5.38 Detailed view of the Steering Wheel response up to 25th second at 10 Kph

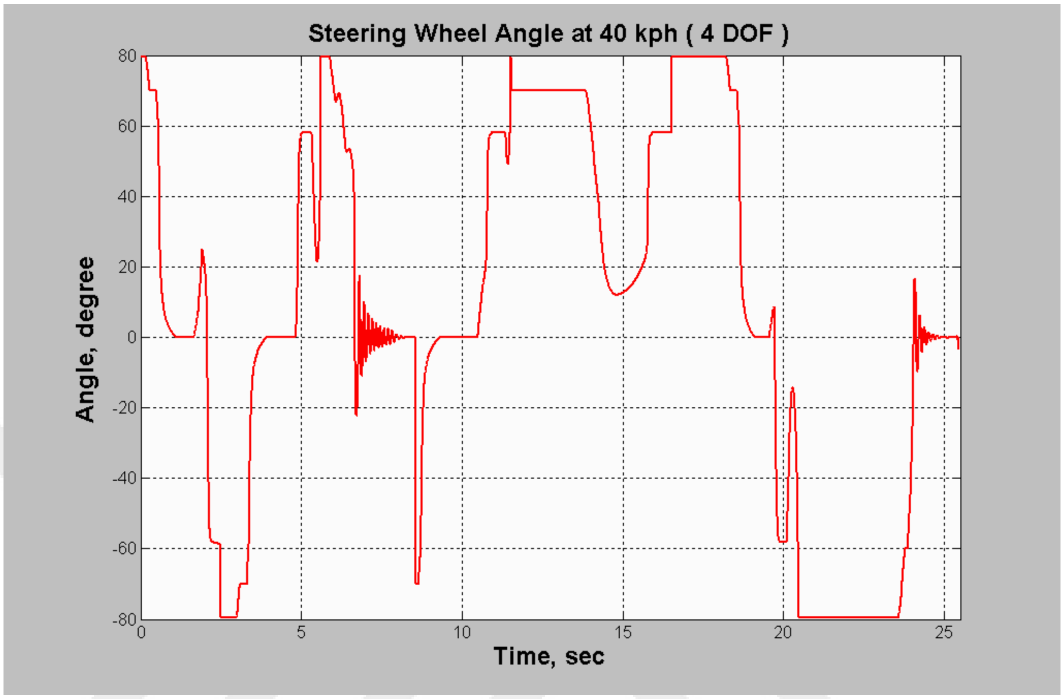

Figure 5.39 Provided Steering Wheel Angle response at 40 Kph vehicle speed

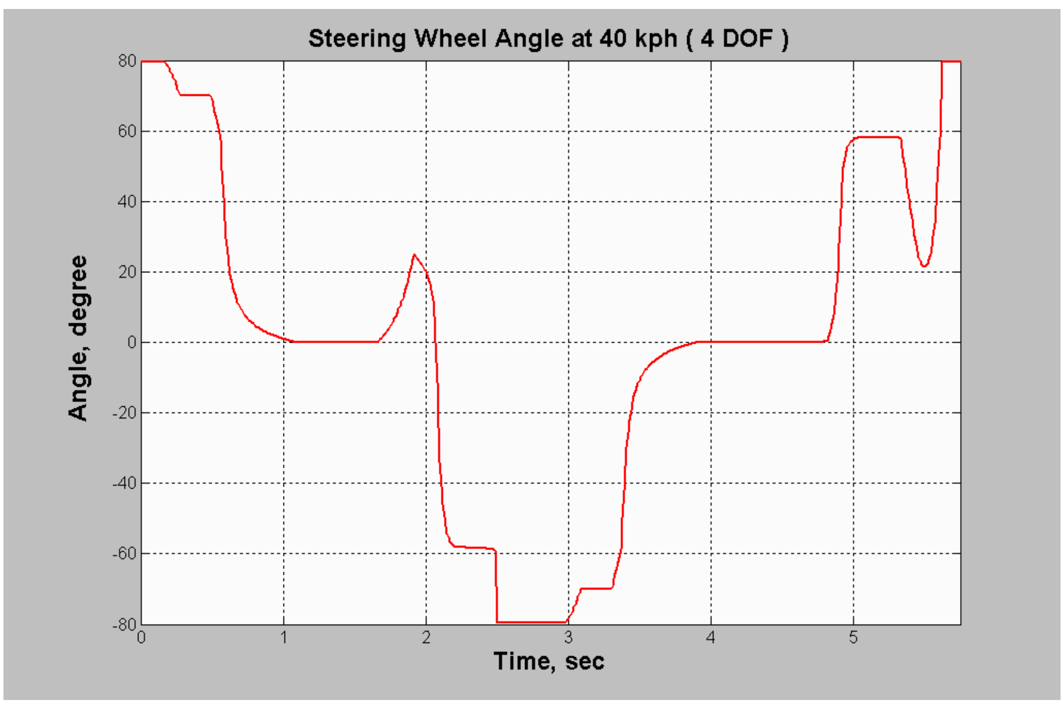

Figure 5.40 Detailed view of the Steering wheel response up to 5.8 seconds

Figure 5.41 shows the resultant vehicle path for the given coordinates X (0, 30, 60, 80, 120, 170, 200, 300) and Y (0, 8, 4, 4, 4, 20, 0, 50) at 25 Kph vehicle speed. This figure is to present how accurate the vehicle can hit the targets with different distances and presents a series of vehicle manoeuvre including a lane change.

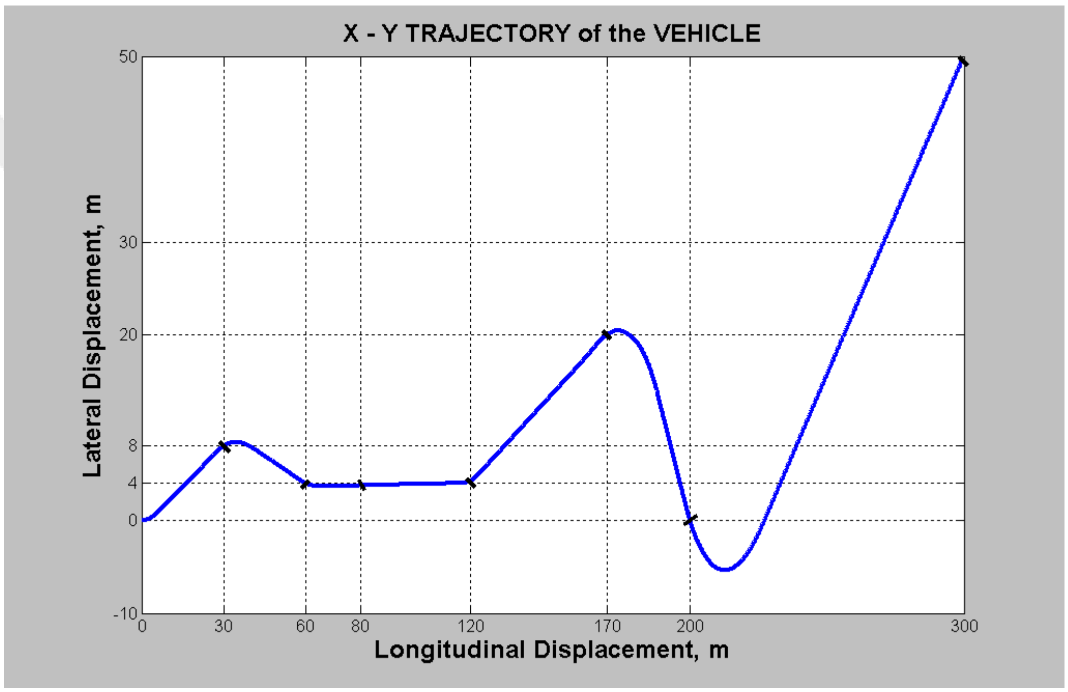

Figure 5.41 Resultant path at 25 Kph vehicle speed with 4 DOF model

5.5 Conclusions

A driver model has been developed by using Fuzzy Logic Theory to imitate a human driver. The method used in this study is aimed at producing a driver model which can be used or easily modified for any vehicle. The distance between the defined target points are varied to test the consistency of the model. According to the results, at any given distance the path has been planned well and for the given conditions up to certain velocity (45 Kph) all the targeted points were hit almost without any error.

CHAPTER 6

SUSPENSION SYSTEM MODELLING & ANALYSIS

6.1. Introduction

In this chapter, the effect of suspension design on vehicle handling performance is studied. A novel rear suspension system, implemented in a University of Birmingham Racing (UBR) Formula Student car, is modelled using the developed simulation tool, Handsim, and the effect of the system on the vehicle's handling performance is discussed by considering the results obtained from the simulation. The aim of implementing this suspension system is to improve the handling characteristics of the vehicle in severe cornering manoeuvres. The improvement is assessed in terms of the handling performance of the car with the modified suspension system (including rear suspension auxiliary dampers) compared to the normal suspension system (i.e. without the auxiliary dampers). Both the front and rear suspension systems are modelled to determine the complete effect of the suspension system on the vehicle handling dynamics. While the front suspension system is an application of the double wishbone design, the rear suspension is a combination of a conventional double wishbone and two diagonally mounted additional damper units, referred to as the rear load transfer mechanism. The kinematics of both systems are analysed using the velocity diagram approach. Then, a four-degree of freedom vehicle model, including the roll motion, is used to analyse the effects of the suspension system in terms of handling dynamics. The results are discussed from the design point of view.

6.2. Formula SAE Student Car Suspension System

Double wishbone suspension is the most commonly used design in race cars, including a toe or steering link at the front [60]. The Formula Student car (Car-201) suspension system, which is the subject of this study, is of a double wishbone design both at the front and rear. While the front suspension system also includes the anti roll bar, the rear design, which is the main subject of this study, includes two diagonally mounted dampers aimed at improving the handling properties of the vehicle. The main objective for modifying the rear suspension system is first to instantaneously produce high roll stiffness at the rear of the vehicle by the action of the diagonal dampers at the beginning of a turn. This instantaneously results in oversteer characteristics which enables the car to turn into the corner quickly. As the extra roll stiffness due to the diagonal dampers is removed, the handling characteristics revert to understeer, giving the driver the confidence to accelerate out of the corner.

The amount that the roll centre moves during suspension travel is determined by the lengths, angles and placement of the suspension links. It is generally assumed that the use of independent suspensions at the rear wheels results in better ride comfort because there is greater design freedom for geometry modifications and also because both suspension units move separately. However, an analysis shows that this is not always true [61].

For example, for a double wishbone suspension that has shorter lower links to reduce the amount of installation space needed for the rear suspension, when the body sinks down low, the roll centre tends to drop significantly from its original design position. The distance between the vehicle's centre of gravity and the roll centre increases considerably when the latter moves downward under a fully loaded condition. As a result, when lateral force acts on the centre of gravity to produce roll, a large moment may occur to initiate roll damping. The result will be a reduction in vehicle stability during high speed cornering, and it will also have a marked effect on all handling properties in general [61].

In the Formula racing cars there are few differences from one car to the next in terms of the wishbone design. However, the mounting of the shock absorbers and the actuation system may vary considerably. This is a result of the different chassis designs. The CAD design of the double wishbone which is used in the Car-201 is shown in Figure 6.1. In both chassis and wishbone design, necessary space for the other elements like springs and shock absorbers, brake pedals, differential, and even the legs of the driver must be provided.

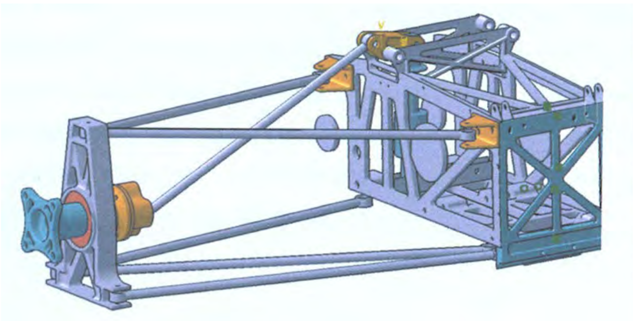

Figure 6.1 Rear suspension system wishbone design (Car-2001) [60]

A significant difference in Car 201's rear suspension system from previous models is the mounting of the struts (combined spring and shock absorber) in the relatively narrow differential box. The struts are mounted to the bottom plate keeping in-plane suspension design. The struts are actuated by rockers attached to the top plate and the rockers are moved by the push rod mounted to the lower end of the wishbone. In the design process of the overall suspension system, the use of CarSimEd™ was attempted by the design team. However, the results proved unreliable and the package was deemed not suitable and very complicated to use [60] different cars of the UBR (University of Birmingham Racing Team) are shown in Figure 6.2 to Figure 6.5. A general view of the Car-201 and its rear suspension links and rear suspension unit are shown in Figures 6.2 and 6.3. Similar views are presented for the Car-12 in Figure 6.4 and Figure 6.5, respectively. The shock absorbers used are custom-built Risse Racing's type-Jupiter-5®, which is shown in Figure 6.6, with adjustable compression and rebound damping [60]. These shock absorbers have different damping circuits for rebound and compression to be able to achieve the adjustability in both directions. Due to the coil over spring design there is the possibility of applying a preload to be able to fine tune the shock absorbers [62].

Figure 6.2 UBR Car-201

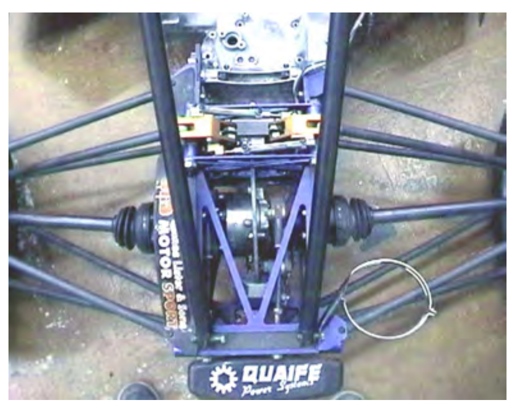

Figure 6.3 UBR Car-201 –Rear Suspension

Figure 6.4 UBR Car 12 **Figure 6.5 UBR Car 12 –Rear Suspension**

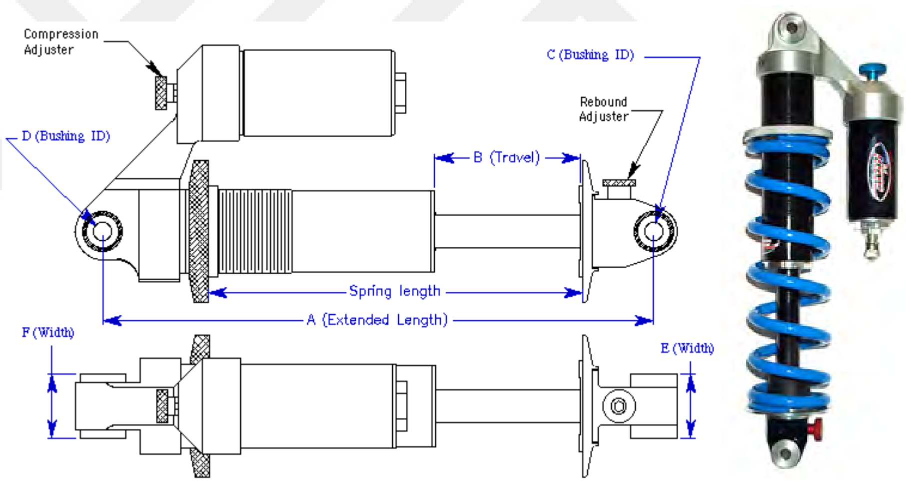

Figure 6.6 The Jupiter-5® damper and the spring used in the car 201 [63].

6.3. Front anti-roll bar

The function of the anti-roll bars is to reduce the body roll inclination during cornering and to influence the cornering behaviour in terms of under or oversteering [61]. A stiffer front axle mounted anti-roll bar promotes the tendency to understeer and improves stability when changing lanes. A rear axle mounted anti-roll bar promotes oversteer. An anti roll bar increases the load on the outside wheel by lifting the inside wheel. However, the load transfer provided by the anti roll bar is not reversible during the manoeuvres. That means the transferred load to the outside front wheel cannot be released back as long as the cornering manoeuvre continues even though the vehicle reaches a steady condition.

Figure 6.7 CAD design of the front suspension's damper and anti roll bar placement

While the balanced understeering effect gives an ordinary driver a more secure handling impression than an oversteering vehicle can give, some oversteer may be helpful to an experienced driver to cope with severe manoeuvres. However, the anti-roll bar also has disadvantages. The higher the anti-roll bar rate , the less the total springing responds when the vehicle is moving over a bumpy road, leaving the engine to 'copy' the road. An understeering vehicle tends to go wide at a turn, which is especially undesirable for a race car. The rear suspension load transfer mechanism was therefore developed to overcome this disadvantage.

6.4. Rear Load Transfer Mechanism

In this system, two damper units mounted diagonally across the rockers are used to transfer the load. Because the damping stiffness is proportional to the roll velocity of the vehicle, when the roll velocity becomes zero, the load transfer to the outer wheel provided by these auxiliary dampers is removed. Therefore, in the first stages of a cornering manoeuvre, as the roll velocity increases, the load transfer on the rear axle increases slightly and the vehicle develops oversteer characteristic, while for the rest of the manoeuvre, as a steady roll condition is reached and the additional load transfer is removed, its handling behaviour is dominated by understeering effect. An open view of the load transfer mechanism mounted on the top edges of the differential box is shown in Figure 6.8, below.

Figure 6.8 Rear suspension system diagonal damper-load transfer mechanism (Car-201)

6.5. Suspension System Analysis

The CAD images of both front and rear suspension geometry are shown in Figure 6.9. As shown in Figure 6.10, the spring and damper unit of the front suspension is actuated by a push rod connected to a rocker which moves the damper and spring unit mounted on the bottom plate of the vehicle.

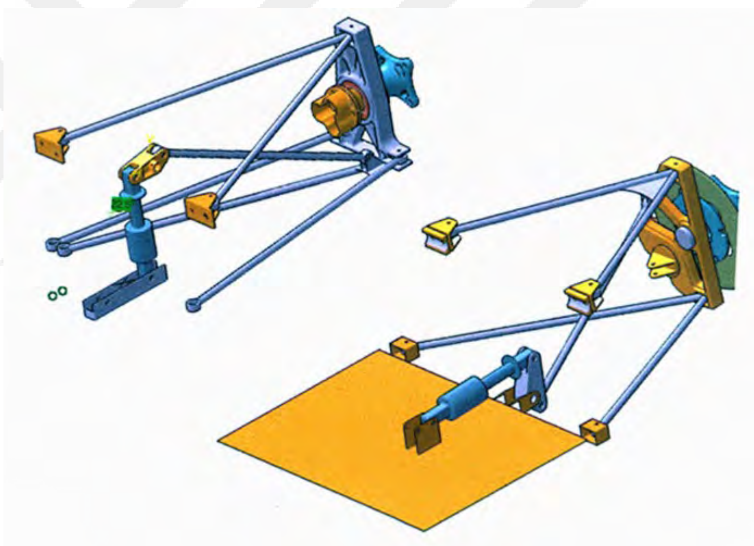

Figure 6.9 Rear and front suspension design [60]

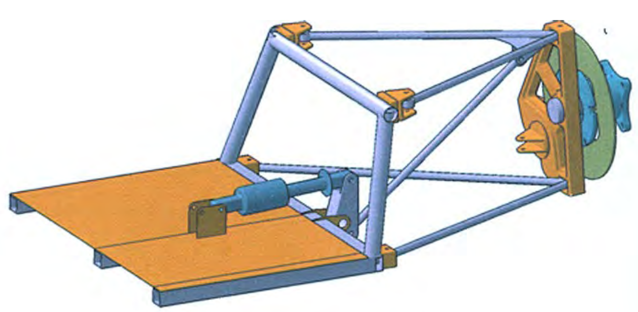

Figure 6.10 Front suspension design without anti roll bar [60].

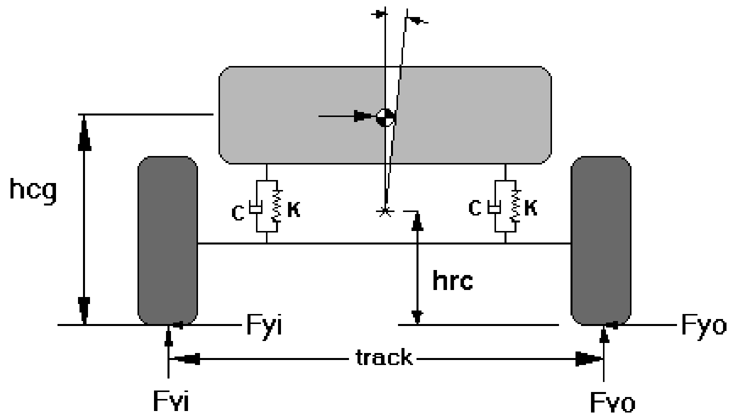

Figure 6.11 Force analysis of a vehicle during roll motion

Figure 6.11 shows the forces acting on a vehicle during roll motion. The force distribution at each wheel is derived from Figure 6.11 and they are shown in the Equations (6.1) to (6.4).

$$F_{vof} = \left(0.5 \cdot m_f \cdot g\right) + \left(\frac{1}{trackf}\right) \cdot \left(m_{uf} \cdot \left(\dot{V} + r \cdot U\right) \cdot h_u + \left(K_{\phi f} + K_{\phi Aroll}\right) \cdot \phi + C_\phi \cdot \dot{\phi}\right) \quad (6.1)$$

$$F_{vif} = \left(0.5 \cdot m_f \cdot g\right) - \left(\frac{1}{trackf}\right) \cdot \left(m_{uf} \cdot \left(\dot{V} + r \cdot U\right) \cdot h_u + \left(K_{\phi f} + K_{\phi Aroll}\right) \cdot \phi + C_\phi \cdot \dot{\phi}\right) \quad (6.2)$$

$$F_{vor} = \left(0.5 \cdot m_r \cdot g\right) + \left(\frac{1}{trackr}\right) \cdot \left(m_{ur} \cdot \left(\dot{V} + r \cdot U\right) \cdot h_u + K_{\phi r} \cdot \phi + \left(C_\phi + C_{\phi Aux}\right) \cdot \dot{\phi}\right) \quad (6.3)$$

$$F_{vir} = \left(0.5 \cdot m_r \cdot g\right) - \left(\frac{1}{trackr}\right) \cdot \left(m_{ur} \cdot \left(\dot{V} + r \cdot U\right) \cdot h_u + K_{\phi r} \cdot \phi + \left(C_\phi + C_{\phi Aux}\right) \cdot \dot{\phi}\right) \quad (6.4)$$

where, *f* and *r* are the suffixes used for ‘front’ and ‘rear’

m = vehicle mass (kg)

g = gravitational acceleration (9.81 m/s^2)

h_u =height of unsprung mass (m)

K_ϕ , C_ϕ = Roll Stiffness, damping

$\phi, \dot{\phi}$ = Roll angle, velocity

Velocity diagram approach is used to analyse the kinematics of both front and rear suspension systems. The drawings of the suspension systems were made available and velocity diagram of the wheel and the strut was derived using the CAD design software Solidworks 2003. In the classical double wishbone suspension system, the spring-damper system is assumed to be in the same vertical axis as the tyres for simplicity. All suspensions are functionally equivalent to two springs. The lateral separation of the springs causes them to develop a roll resisting moment proportional to the difference in roll angle between the body and axle. The stiffness is given by:

$$K_\phi = \frac{1}{2} \cdot K_s \cdot s^2 \tag{6.5}$$

where:

K_ϕ = Roll stiffness of the suspension

K_s = Vertical rate of each of the left and right springs

s = Lateral separation of the springs

A method of graphical analysis of the suspension behaviour [64], [65] is presented in which the roll characteristics are determined about an arbitrary point, which does not move as the body rotates. In the Figure 6.12, O is at the intersection of the vehicle centre line with the ground plane. The inboard points of attachment of the links are A and B. The wheel contact point is O'. The position of the roll centre is determined by extending an imaginary axis from the suspension links until a point of intersection is obtained.

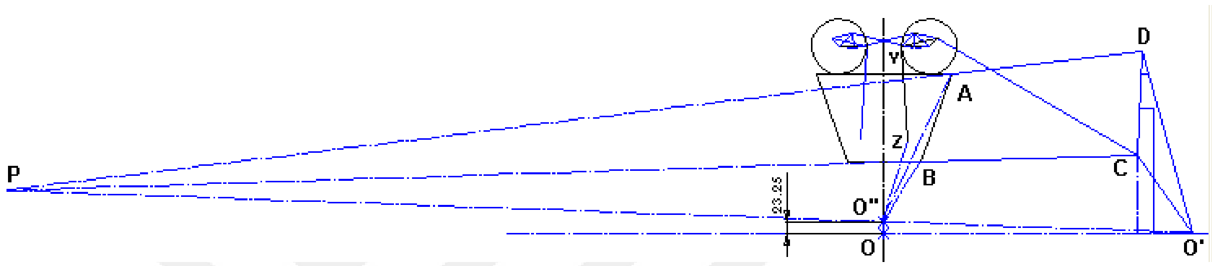

Figure 6.12 Determination of rear roll centre of the vehicle (Car-201)

If this intersection point is named P, a line from P through the point O' cuts the centre line of the body at O'' (Figure 6.12 and 6.13). The formation of the velocity diagram starts from O'' with vectors *o''b*, *o''a* perpendicular to O''B and O''A respectively and also equal in length to these distances by the assumption of rotational velocity of 1 radian per second (see Figure 6.14). Similarly, *ad* is perpendicular to AD and *o''d* perpendicular to O'D. In the Figure 6.14, only the significant vectors are shown for the analysis. In fact, the arbitrary point analysis is the first step to obtain the initially unknown vector measures [64]. By using the measures from the Figure 6.14, then, Figure 6.15 can be obtained to give the ratio between the spring and wheel motions.

Considering the suspension of Figure 6.13, an arbitrary angular velocity is applied to the link BC, the remaining stationary. *bc* is perpendicular to BC and *ad* is perpendicular to AD. Both *a* and *b* are points of zero velocity and therefore coincident with *o*. Since the length *bc* in Figure

6.14 is known from the application of the arbitrary angular velocity to BC in Figure 6.13, similarly, *d* is located since *cd* is perpendicular to CD; *o'* is located since *o'c* is perpendicular to O'C and *o'd* is perpendicular to O'D.

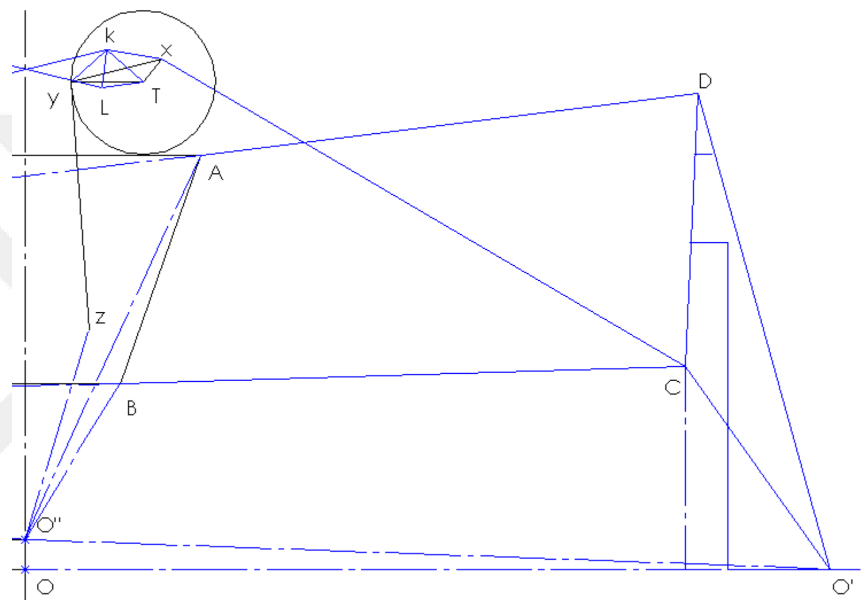

Figure 6.13 Rear suspension links and spring-damper placement (Car-201)

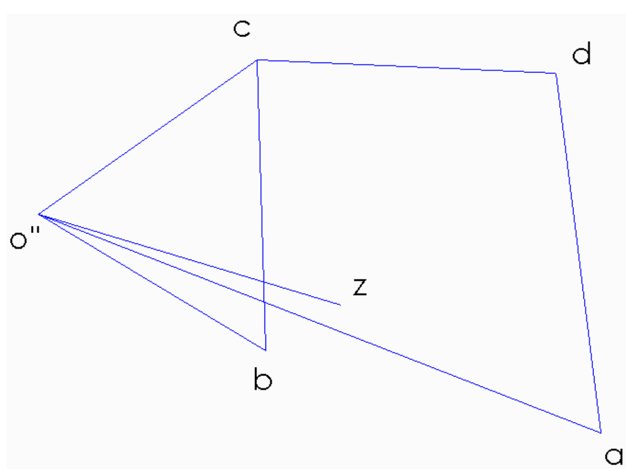

Figure 6.14 Velocity Diagram (Car 201)

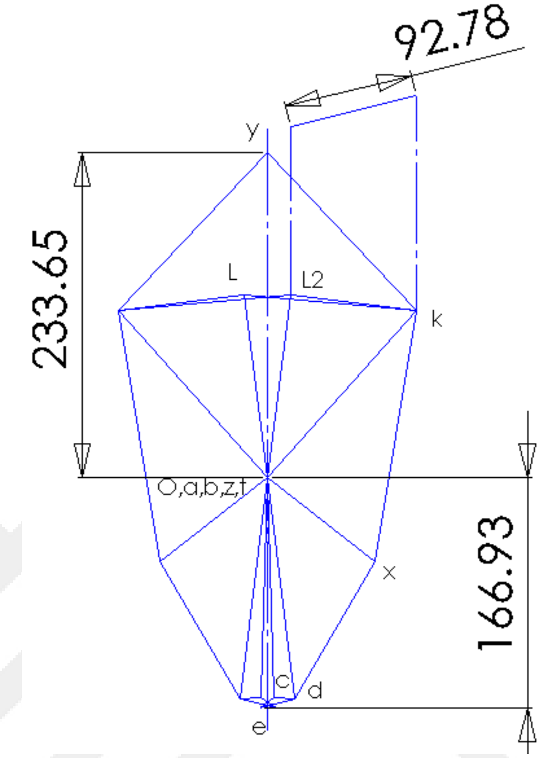

Figure 6.15 Complete velocity diagram of the rear suspension system (Car 201)

By considering Figures 6.13 and 6.15, let [64]

$$oy\,/\,o''o' = n \tag{6.6}$$

Therefore, vertical force F_v can be shown to be proportional to spring force F_s in Equation (6.7).

$$F_v = -F_s \cdot n \tag{6.7}$$

and

$$\partial F_v / \partial v = -F_s \cdot \partial n / \partial v - n \cdot \partial F_s / dv \tag{6.8}$$

thus

$$K_v = \partial F_v / \partial v = -\left(F_s \cdot \partial n / \partial v + K \cdot n^2\right) \tag{6.9}$$

When the body rolls then no vertical displacement of the wheels occurs since this has been reduced by the rotation of the body about O''. Since both suspension springs are involved the suffices *l* and *r* are used and M is the moment about the centre of O [64],

$$M\left(Oe \;\; / O''O'\right) = F_{sl}\left(-Oy\right) + F_{sr}\left(+Oy\right) \tag{6.10}$$

$$n_\phi = Oy / \left(Oe / O''O'\right) \tag{6.11}$$

$$M = F_{sl} \cdot \left(-n_\phi\right) + F_{sr} \cdot \left(+n_\phi\right) \tag{6.12}$$

Differentiating with respect to ϕ, the roll angle,

$$\partial M / \partial \phi = F_{sl} \partial\left(-n_\phi\right) / \partial \phi + F_{sr} \partial\left(+n_\phi\right) / \partial \phi + \left(-n_\phi\right) \partial F_{sl} / \partial \phi + \left(+n_\phi\right) \partial F_{sr} / \partial \phi \tag{6.13}$$

If it is assumed that positive and negative suspension movements are symmetrical, then the expression may be simplified [65]:

$$\partial M / \partial \phi = 2 \cdot K \cdot n_\phi^2 \tag{6.14}$$

Since the springs and dampers are mounted concentrically and they travel the same distance, the same coefficients are valid for the effective damping stiffness, which is given in Equation (6.15).

$$\partial M / \partial \phi' = 2 \cdot C \cdot n_{\phi}^{2} \tag{6.15}$$

Figure 16 shows the front suspension geometry and the velocity diagrams, obtained using the same approach explained before. From the scaled Figures 6.13 to 6.16, if the numerical values are applied to the equations 6.14 and 6.15, the resulting effective roll stiffness K_{ϕ} and roll damping C_{ϕ} for both rear and front suspensions are presented in Table 6.1. n_{ϕ} is a constructive constant that is determined in the initial design studies. Spring and Damper rates are the variable design parameters which can be modified after the initial design.

Table 6.1 Stiffness and damping values obtained by the velocity diagram approach

	Roll Stiffness	**Auxiliary Stiffness**	**Roll Damping**	**Auxiliary damping**
Front Suspension	0.991*Kf	3000	0.991*Cf	-
Rear Suspension	1.587*Kr	-	1.587*Cr	0.2503*Cra

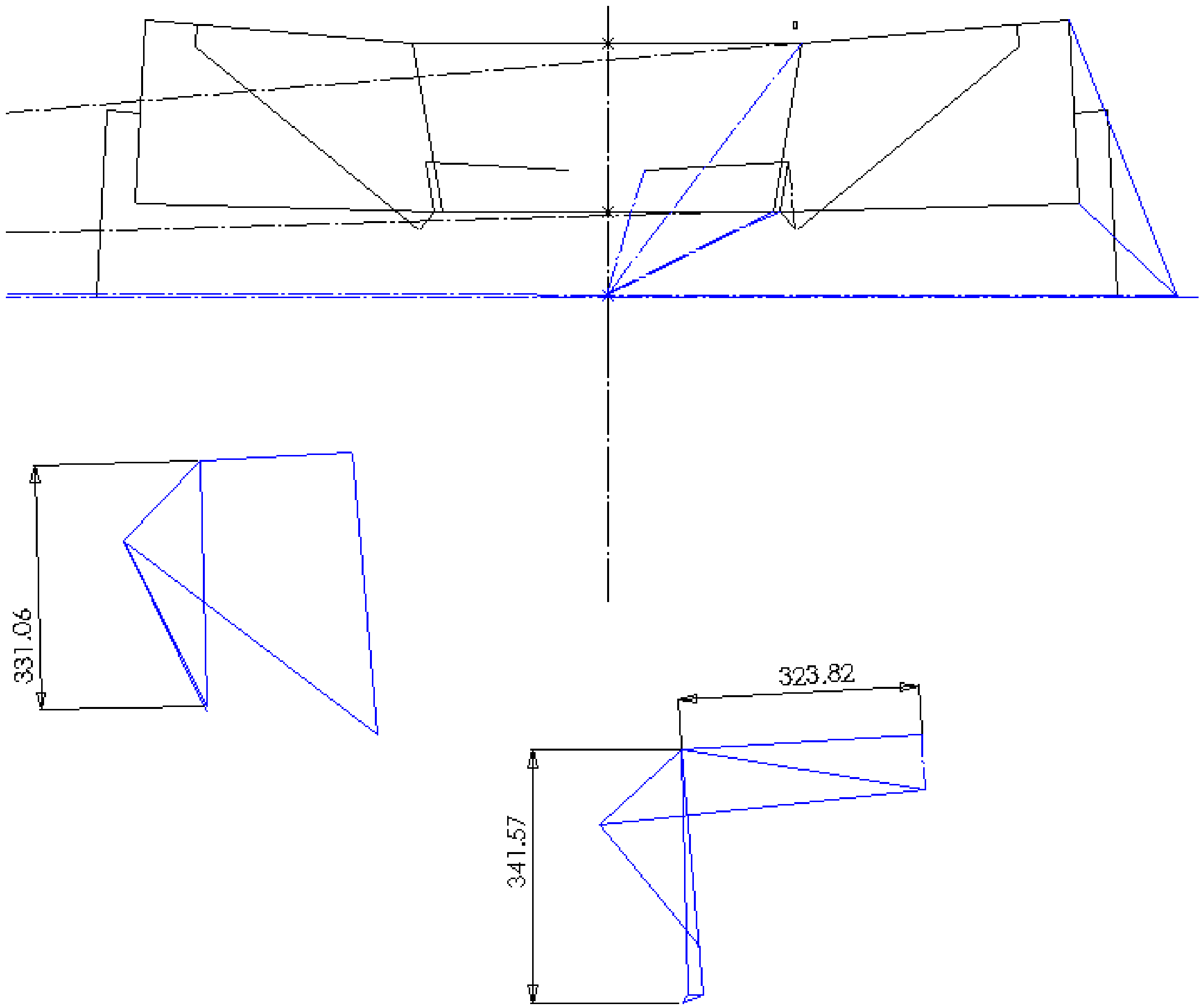

Figure 6.16 Front suspension links and velocity diagrams (Car-201)

The simulation results which are presented in the following sections represent the response of the initial design of the Car-201, which uses the suspension system with the load transfer mechanism.

6.6. Simulation Results and Discussion

Simulation of vehicle response was carried out using the HANDSIM simulation tool. The simulation was carried out at a vehicle speed close to the maximum speed at which the vehicle can traverse the given path without loss of control. Vehicle speed is kept constant during the manoeuvre by a fuzzy logic controller which was also discussed in the previous chapter.

6.6.1. Formula SAE Car-201:

Figures 6.17 to 6.24 show the vehicle responses for the Car-201 with and without the rear suspension auxiliary damper load transfer mechanism. A minimum vehicle speed, which is thought to be enough to observe the effects of the suspension system on vehicle handling, especially, in terms of the rear load transfer mechanism, is chosen. Car-201 has a front biased weight distribution of 55% front – 45% rear.

6.6.1.1. Simulation results with the original design parameters:

The parameters used in the vehicle simulation are given in the Table 6.2. The method is to run the simulation both with and without the rear load transfer mechanism. Auxiliary damper rate is set to various values to observe the handling response of the car with the mechanism. The vehicle has intrinsic understeer characteristic due to the weight distribution, which is 55% front and 45% rear. However, the longitudinal velocity of the vehicle and lateral load transfer and also the resultant tyre slip angles determines the actual characteristics.

Table 6.2 Vehicle control and simulation parameters

Vehicle Speed (constant)	(kph)	40
Steer Angle for Constant Steer Test **Path Coordinates**	(degree) (m)	3º X(0, 30, 60, 90, 120, 105, 70, 40) Y(0, 8, 0, 12, 25, 70, 50, 80)
Wheelbase[front, rear]	(m)	0.742, 0.908
Track [front, rear]	(m)	1.342, 1.28
Mass of vehicle (Including driver)	(kg)	300
Roll, Yaw inertias	(kgm^2)	20, 200
Damper Rate [front, rear]	(Ns/m)	750, 750
Auxiliary Damper Rate	(Ns/m)	variable (see Figure and Table 6.4)
Spring Rate [front, rear]	(N/m)	22000, 22000
Anti Roll Bar Rate	(Nm/rad)	3000
Height of C.G	(m)	0.285
Roll Centre [front, rear]	(m)	0.0093, 0.02325

6.6.1.1.1. Vehicle handling simulation at constant speed and steer angle

Figure 6.17 shows the resulting paths without the rear load transfer mechanism and with it using various damping rates. A path improvement of up to 7 cm with 10000 Ns/m auxiliary damper rate can be seen in the figure. Figure 6.18 shows the lateral load transfer and resultant load distribution at each tyre both for the vehicle with and without auxiliary dampers. The results from the vehicle without the auxiliary dampers are shown all in grey colour to reduce the complexity of the figure. This figure shows a slight decrease in the front load transfer with a corresponding increase in the rear load transfer, thus providing a slight oversteering tendency during the first 0.1 seconds of the manoeuvre. Roll rate, roll angle and yaw rate responses of the vehicle is shown in Figures 6.19, 6.20 and 6.21, respectively.

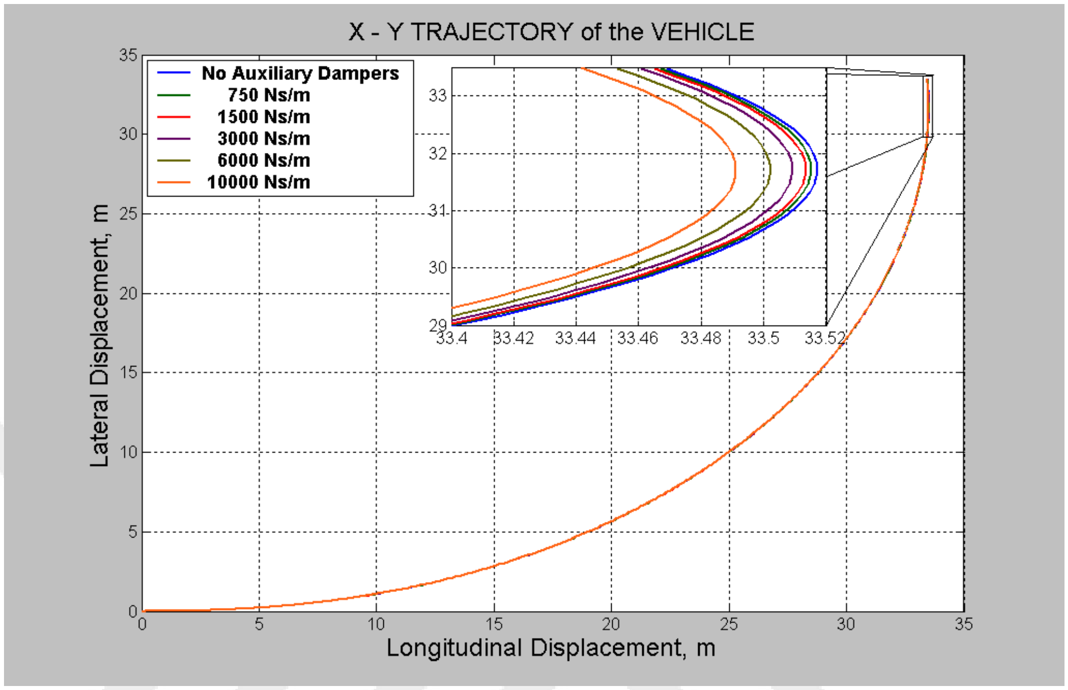

Figure 6.17 Resultant vehicle trajectory for Car-201 at 43 Kph.

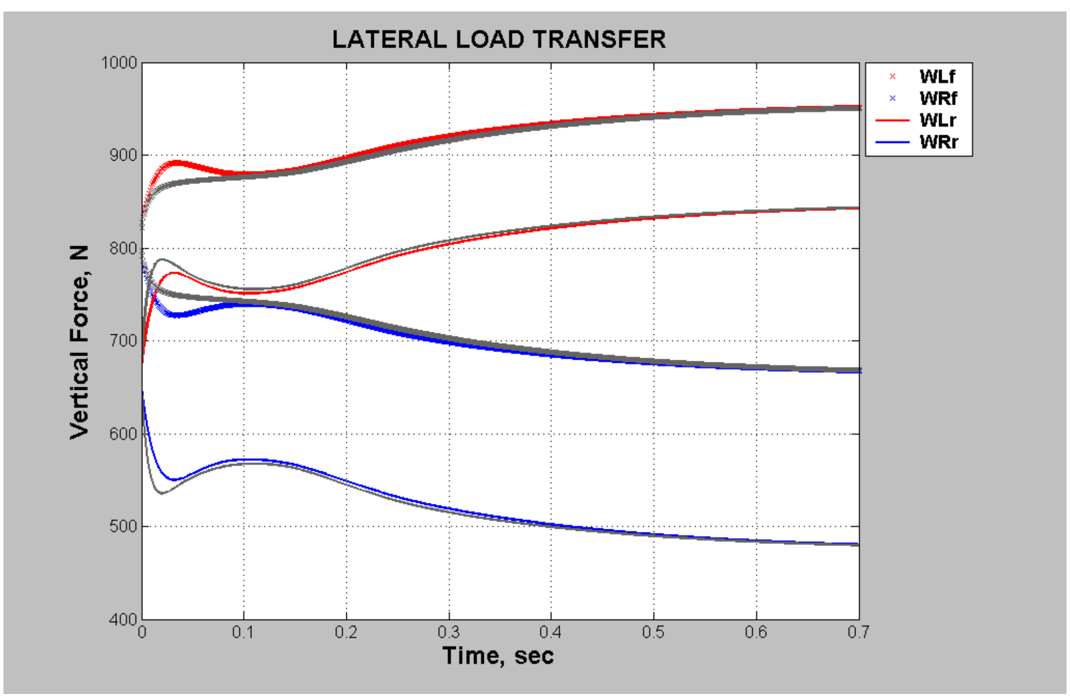

Figure 6.18 Lateral load transfer of Car-201 at 43 Kph- (2250 Ns/m auxiliary damper rate).

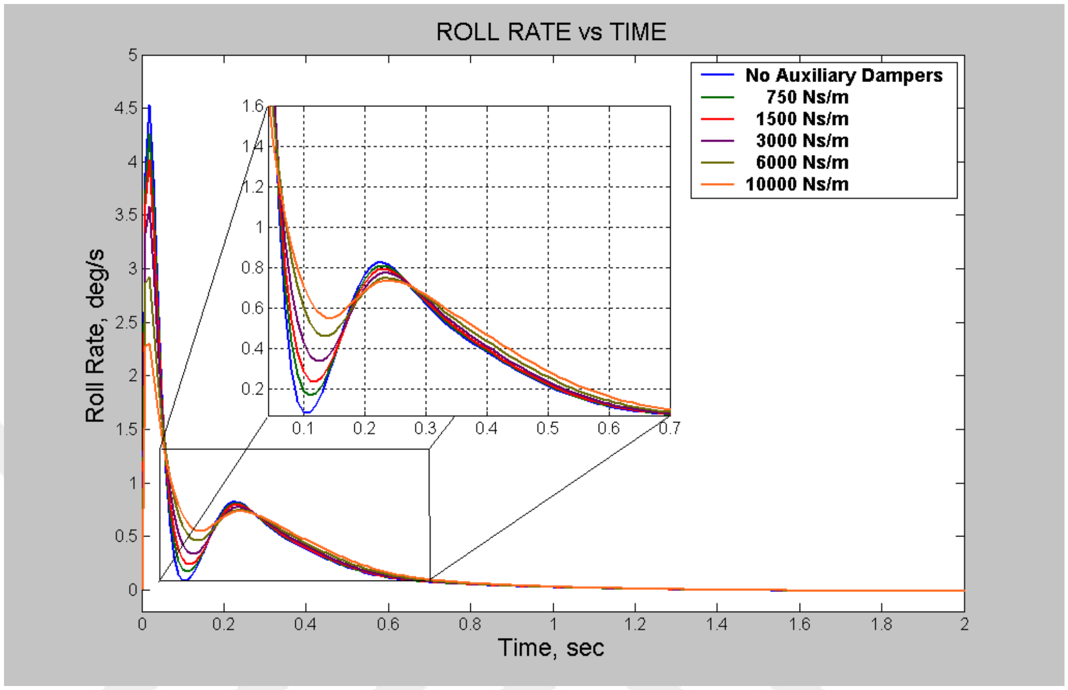

Figure 6.19 Roll rate response of Car-201 at 43 Kph.

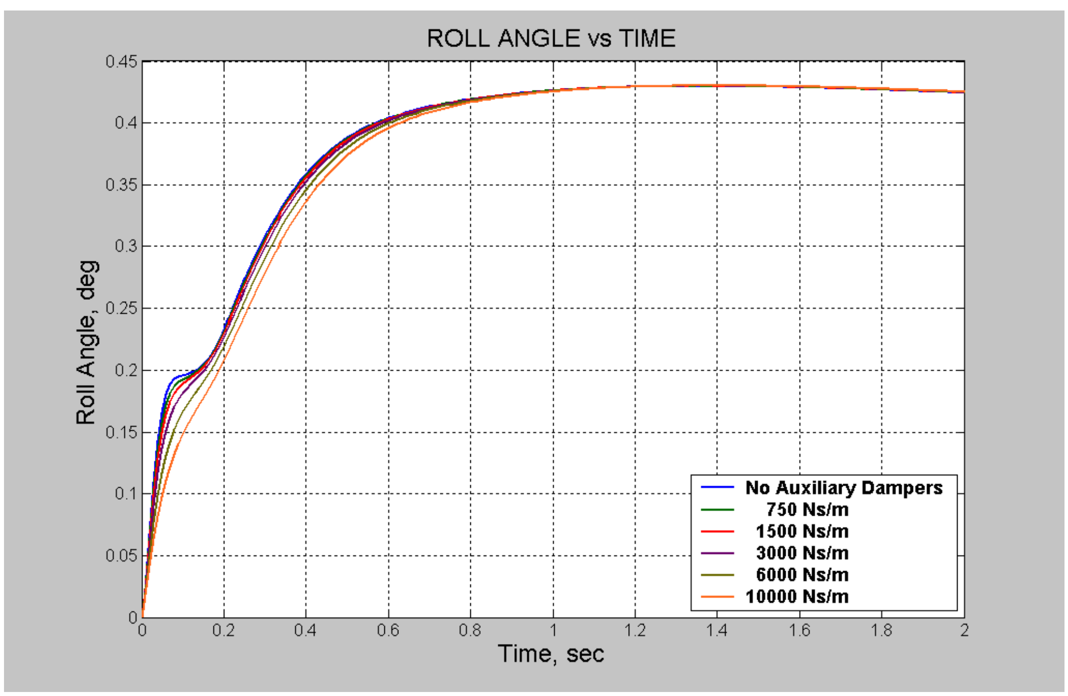

Figure 6.20 Roll angle response of Car-201 at 43 Kph.

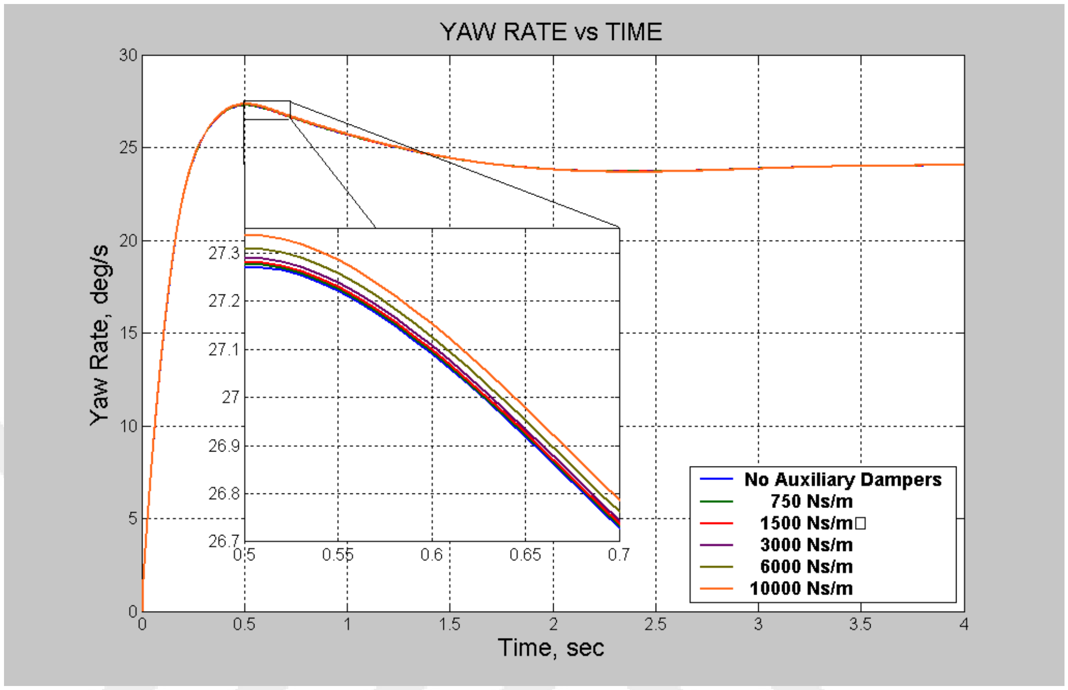

Figure 6.21 Yaw rate response of Car-201 at 43 Kph.

The simulation results provided by constant steer angle and constant vehicle speed reveals important information about Car-201. Firstly, even though the effects due to the rear auxiliary dampers are small, the theoretical basis which was explained in the first sections of this chapter is correct. Secondly, however, the positive effect of the system can only be obtained by using extremely high damper rates for Car-201 with its original design parameters. On the other hand, these extreme damper rates can be eliminated by modification of the motion ratio between the tyre and struts. For this reason, the rocker which is responsible for transferring the tyre motion to the struts and auxiliary dampers is re-designed to improve the motion ratio.

6.6.1.2. The effect of Rocker shape during load transfer:

The method of obtaining the velocity diagram and calculation of the equivalent roll stiffness and damping were discussed in Section 6.5. The ratio between the velocity vector of auxiliary damper and tyre is the key element for the amount of obtainable roll damping and stiffness on a vehicle (See Equations (6.11) and (6.14) & velocity diagram in Figure 6.15). The higher the ratio obtained, the higher the roll damping that can be provided by the load transfer mechanism. Higher roll damping leads to a higher load transfer at the rear and this can result in increased oversteer characteristic, and as a result, an improved path. A very simple design change on the rockers is suggested to obtain higher roll damping from the system which does not seem to be effective with the original design parameters. A rocker is supposed to transfer the vertical motion of the tyre to the struts which are expected to absorb the disturbing force caused by the tyre and road interaction and keep the tyre in contact with the road. By doing this a load transfer is also developed from inner tyre to the outer tyre of a vehicle in a cornering manoeuvre. Therefore, from the given geometry of car-201 suspension system, rockers are important in terms of providing the motion ratio between the tyre and struts. Figure 6.21 shows the original and proposed rocker geometry while Figure 6.22 presents the modified form of the velocity diagram which was originally presented in Figure 15. K' and X' show the new extended points of the rocker instead of K and X respectively (Figure 6.22). The new shape of the rocker (Rocker-A) is proposed as TLYK’X’ instead TLYKX.

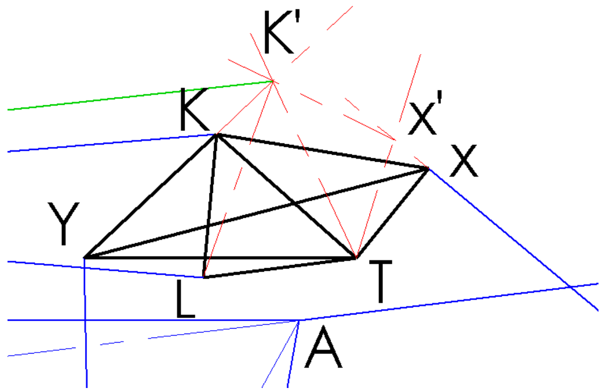

Figure 6.22 Original and the modified rocker of Car-201. (Rocker-A)

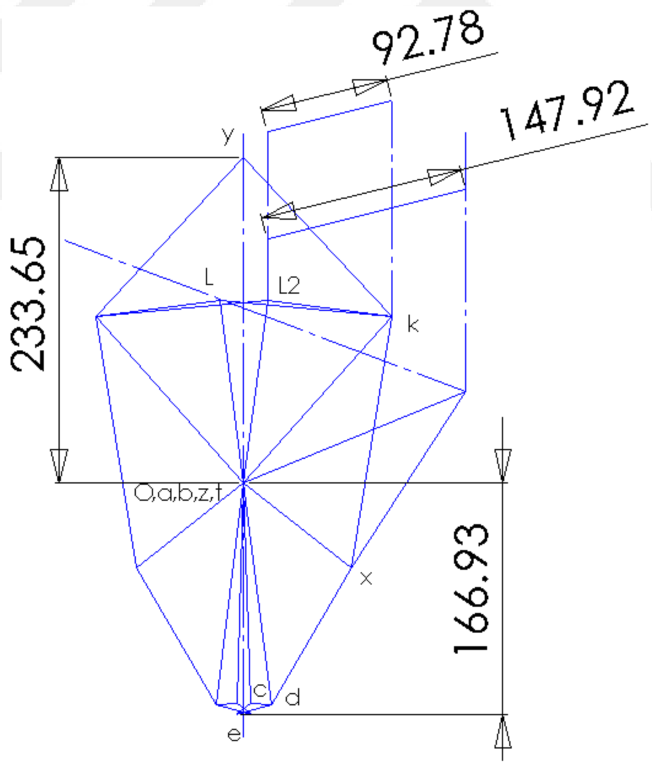

Figure 6.23 Velocity diagram of the rear suspension system (Original axle+Rocker-A)

In Figure 6.23, $n_{\phi} = 0.564$ from the Equation (6.11) in Section 6.5 with the modified rocker instead of $n_{\phi} = 0.3537$ provided by the original rocker design. This modification produces

2.54 times the roll damping provided by the auxiliary dampers calculated from the Equation (6.15). Therefore the auxiliary damper coefficients can be reduced by a factor of 2.54 with the new design while providing the same effect.

6.6.1.2.1. Simulation results with fuzzy path planning (Rocker-A Modification)

The constant steer angle test has proved the effect of the system even though the observable effect was so little. A more realistic path using fuzzy path planning is applied for the simulation in this section. Simulation is undertaken with the Rocker-A modification and the similar vehicle control parameters which were presented in Table 6.2. Some of the resulting responses from the simulation are shown from Figure 6.24 to 6.26. Auxiliary Damping rate is 2250 Ns/m which is equivalent of 5627 Ns/m damper rate with the original design. Figure 6.24 shows the roll rate response of the vehicle followed by the roll angle response in Figure 6.25. As the roll rate decreases in the first parts of the turn roll angle decreases and this response is followed by a little increase in the roll rate and increase in the roll angle. Therefore, resulting vehicle trajectory shows an improved, quicker turn of the vehicle. However, instead of providing a better trajectory, the results still shows the benefit of the system is not enough at the chosen vehicle longitudinal velocity and with the modified Rocker-A. As a result of this, a further modification to the system is proposed and the simulation is undertaken at higher speed in the section 6.6.1.3.1.

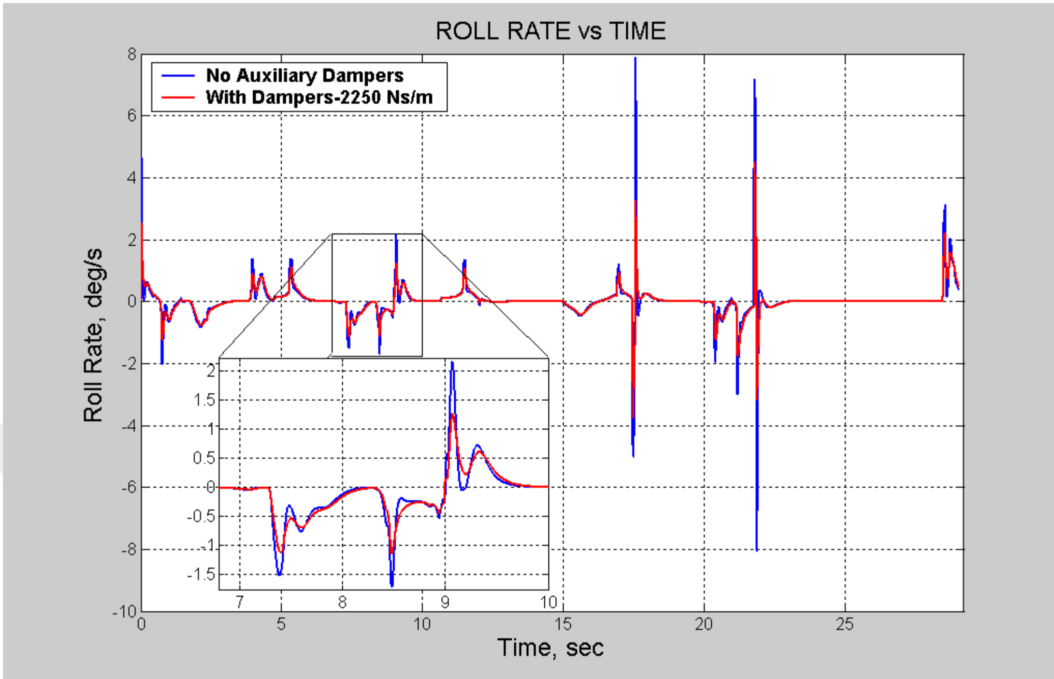

Figure 6.24 Roll rate response of Car-201 at 40 kph with 2250 Ns/m Damper rate

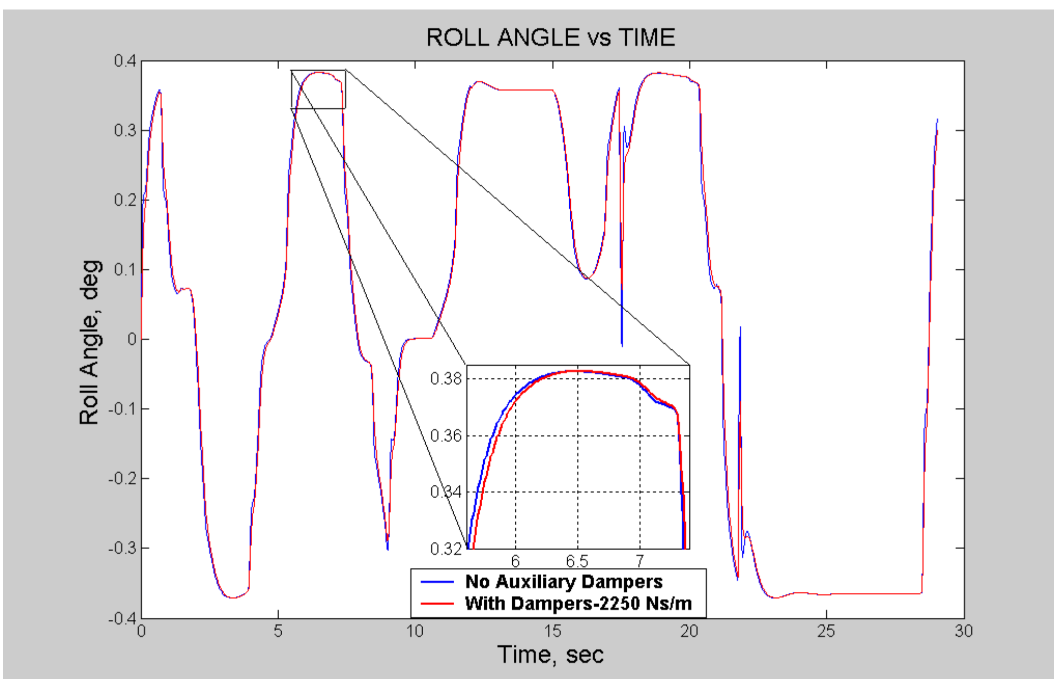

Figure 6.25 Roll angle response of Car-201 at 40 Kph with 2250 Ns/m damper rate

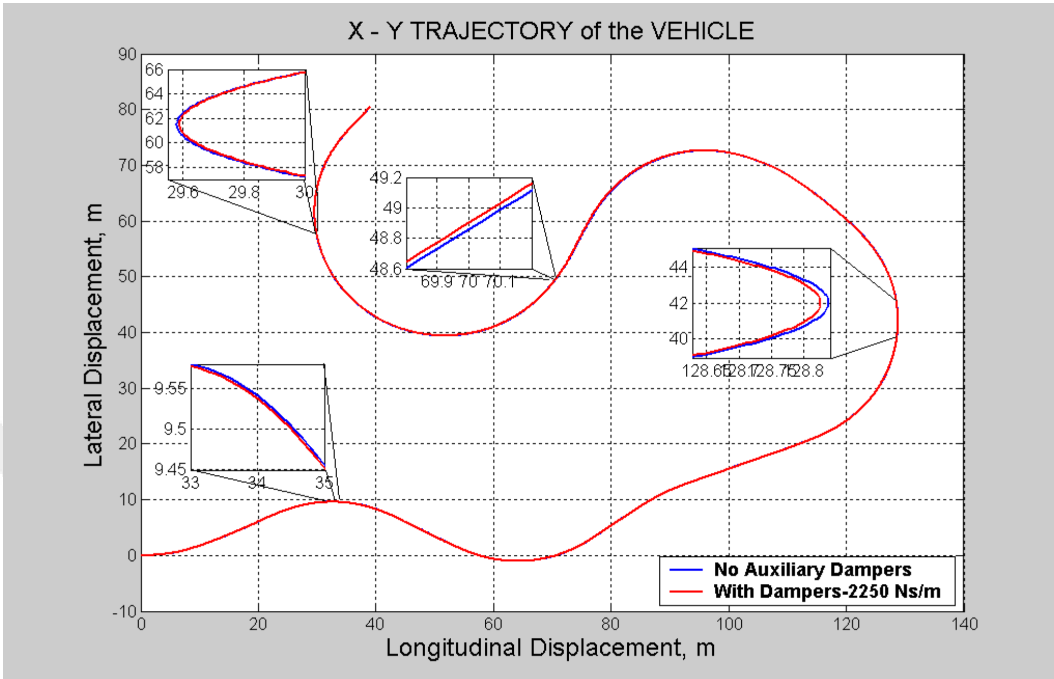

Figure 6.26 Resulting vehicle trajectory at 40 Kph with 2250 Ns/m damper rate.

6.6.1.3. A complete rear axle and a further rocker modification

Figure 6.27 shows a further modification to Rocker-A to improve the motion ratio between the tyre and struts. Therefore, K' is at the intersection of axis YK and vertical XK' and X' is moved forward to the intersection point that is provided by vertical TX' on YT plane. In fact the new Rocker-B is a part of the new rear axle design which is also shown in Figure 6.28. The main aim in the modification of the rear axle is to keep the main dampers' motion ratio the same as it was while increasing the auxiliary dampers' motion ratio.

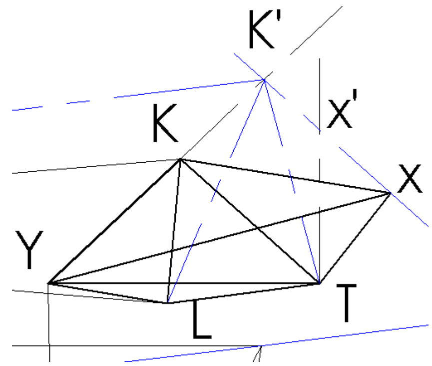

Figure 6.27 Final Modification for the rocker (Rocker-B)

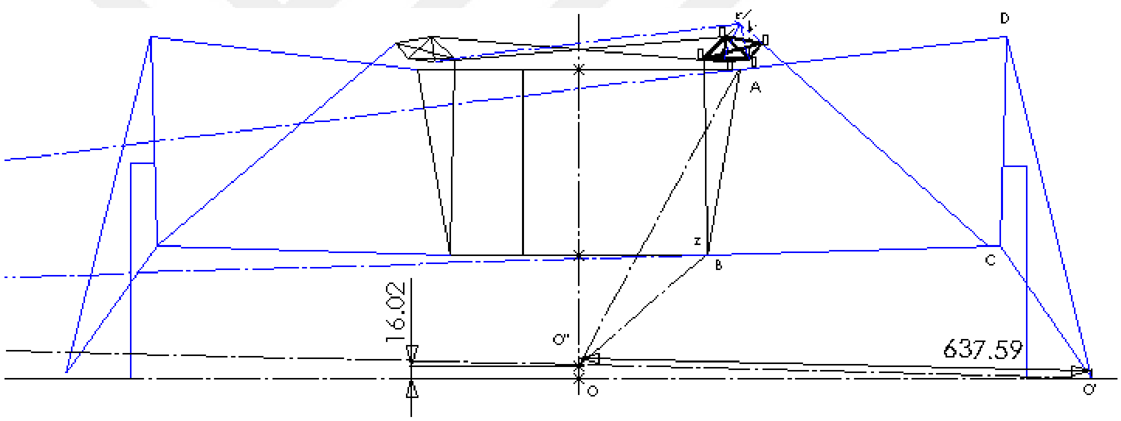

Figure 6.28 Modified rear axle design for Car-201

From the equation (6.11) and the velocity diagram given in Figure 6.29, the ratio $n_{\phi} = 0.716$. This ratio provides 4.096 times higher auxiliary damping stiffness than the original design. The new coefficients in calculation of roll stiffness and damping are presented in Table 6.3. From the new resulting coefficients, an equivalent damper rates table, which is Table 6.4, may be derived. This table suggests the new damper rates can be used instead the ones used in the original design. That means the same responses can be taken from the vehicle with the new and reduced damping rates.

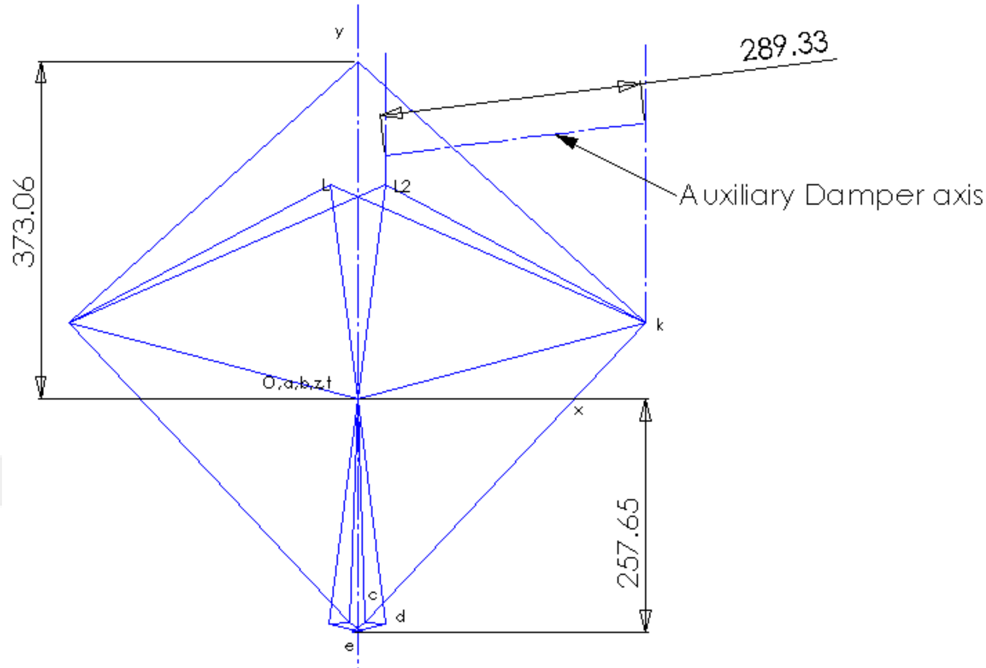

Figure 6.29 Resultant velocity diagram of the new rear suspension system.

Table 6.3 Stiffness and damping values resultant by the velocity diagram approach

	Roll Stiffness	Auxiliary Stiffness	Roll Damping	Auxiliary damping
Front Suspension	0.991*Kf	6000	0.991*Cf	-
Rear Suspension	1.704*Kr	-	1.704*Cr	1.0253*Cra

Table 6.4 Equivalent Damper Rates provided by the design modifications

Auxiliary Damper Rates (Original Design) (Ns/m)	Equivalent Damper Rates (With Rocker-A) (Ns/m)	Equivalent Damper Rates (Fully Modified Rear Axle & Rocker-B) (Ns/m)
750	295	183
1500	589	366
3000	1179	732
6000	2358	1464
10000	3930	2441

6.6.1.3.1. Simulation results with fuzzy path planning (Rocker-B & Axle Modification)

The same damper rate is used in the simulation as for the previous simulations. However, this same damper rate is equivalent to 9216.6 Ns/m of original design with the modified values. The results are shown from Figure 6.30 to Figure 6.34. The yaw rate response of the vehicle is presented in Figure 6.30. In the first 15 seconds of the travel a general yaw rate increase due to the auxiliary dampers can be observed. Beyond this period, the two vehicles possess virtually identical yaw rates but with the auxiliary dampers leading the standard vehicle. This is as a result of the higher yaw rate of the modified vehicle in the first 15 seconds resulting in completion of the defined path quicker and with a shorter path. Therefore, the simulation is completed earlier with the auxiliary dampers than without the auxiliary dampers. Figures 6.31 and 6.32 show roll rate and roll angle responses of the vehicle, respectively. However, it is also clear that at the given velocity, the fuzzy driver is struggling to keep the vehicle on the given path which is shown in Figure 6.33. The lateral load transfer history of the vehicle confirms the initial oversteer and then understeer tendency of the vehicle by the initially increased load transfer at the rear (decreased load transfer at the front) followed later by a reversal of the load transfer. The load transfers without the auxiliary dampers are shown in grey colour in Figure 6.34.

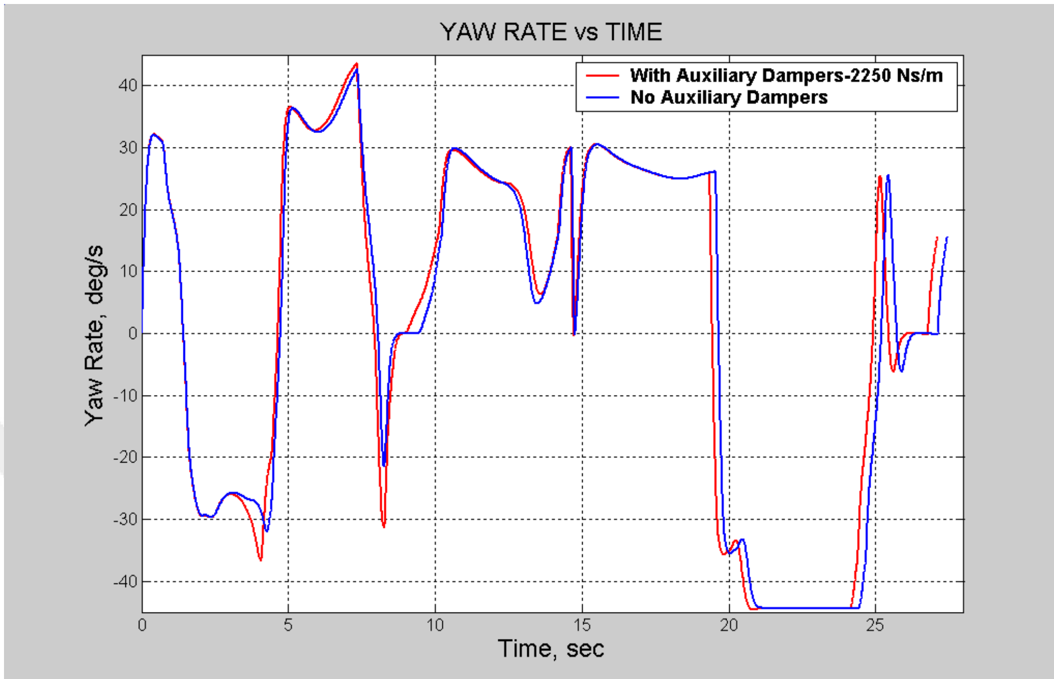

Figure 6.30 Yaw rate response of Car-201 at 48 kph and with 2250 Ns/m damper rate

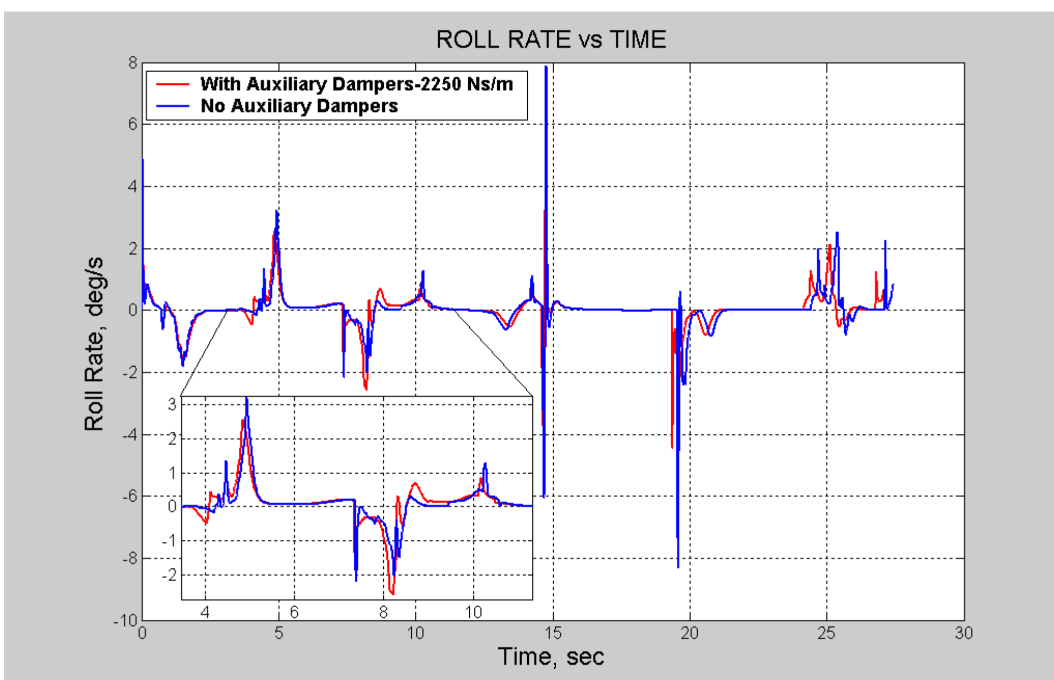

Figure 6.31 Roll rate response of Car-201 at 48 kph with 2250 Ns/m Damper rate

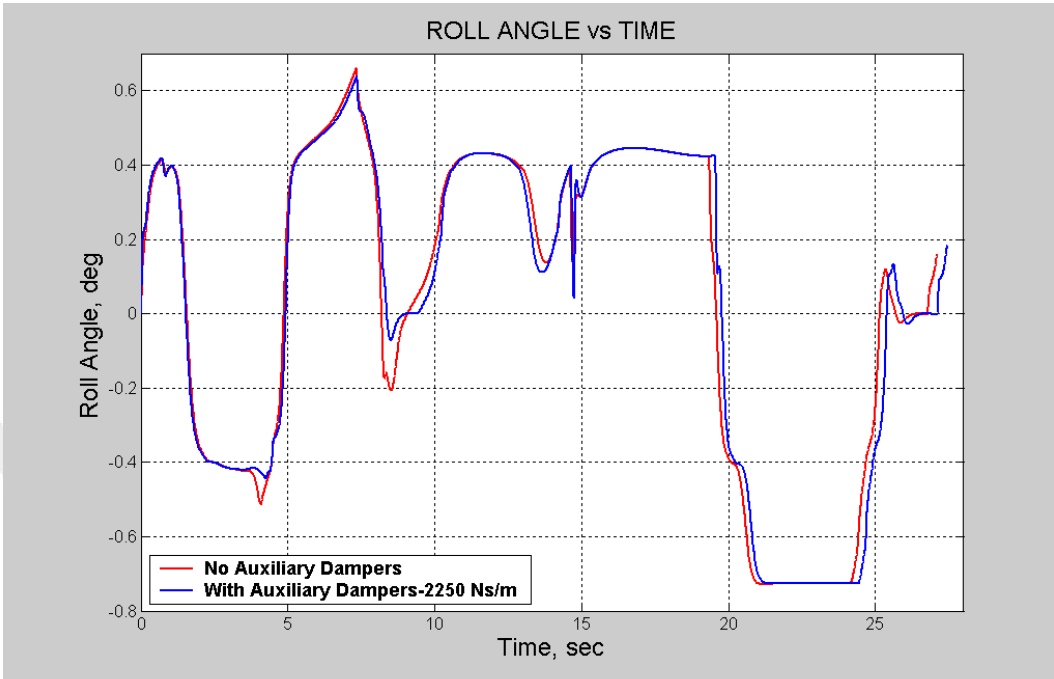

Figure 6.32 Roll angle response of Car-201 at 48 Kph with 2250 Ns/m damper rate

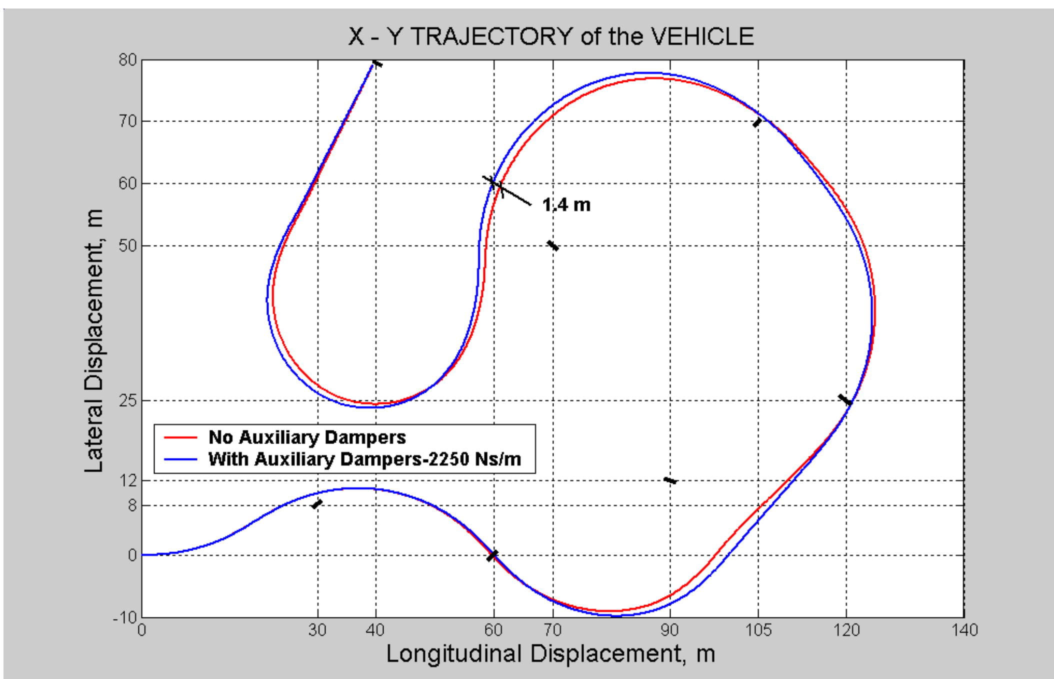

Figure 6.33 Resulting vehicle trajectory at 48 Kph with 2250 Ns/m damper rate.

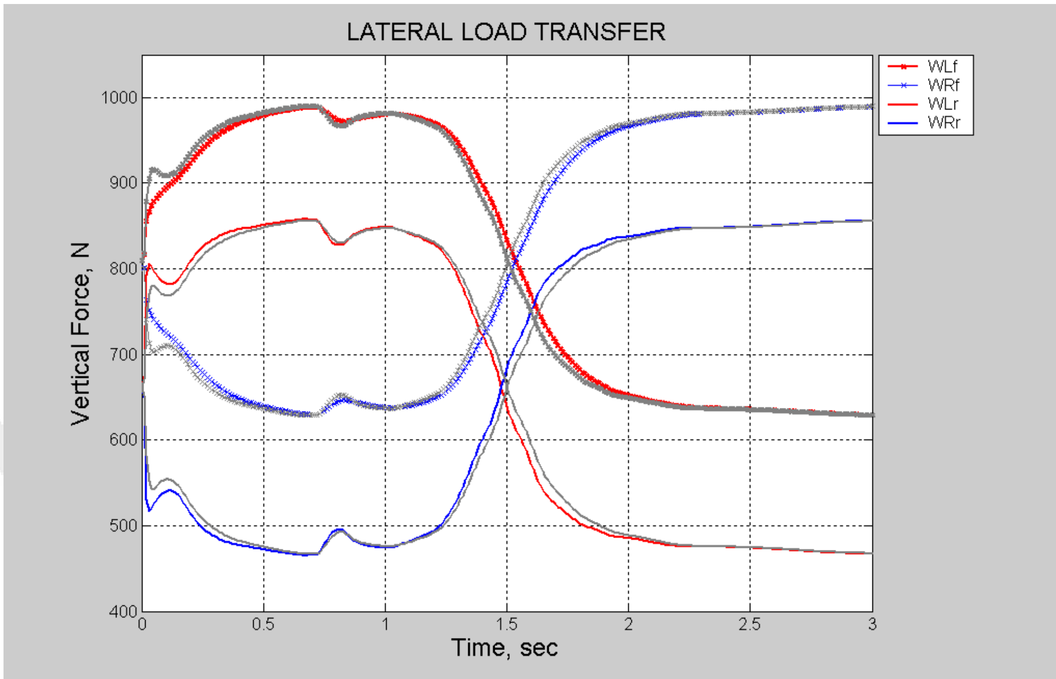

Figure 6.34 Lateral load transfer of the vehicle with and without the rear load transfer

6.7. Conclusions

The Car 201 was designed to get round the twisting Formula SAE/Student circuits as quickly as possible and safely. The load transfer mechanism was designed for the rear suspension system to help achieve this objective. The simulation results of the original Car-201 discussed above show that the original design of the vehicle is not suitable enough for this purpose. Car 201 is an understeering vehicle which is not ideal in a racing car. However, this car has been designed for the students who have little opportunity to experience driving the car on the road. Therefore, an understeering car which is easier to control at the limit of traction may be the best choice in the circumstances. The design of the suspension system very much affects the ride and handling properties of the vehicle. While a well designed rear load transfer mechanism can build an oversteering tendency on an understeering vehicle, the rear suspension geometry of Car-201 with its long suspension links and narrow differential box has been shown not to be a good base for the rear load transfer mechanism. However, while keeping most of the existing design, it has been possible to find a cost effective solution through the re-design of the load transfer rocker to provide a more suitable wheel to damper velocity ratio. It has been shown that the rocker geometry is very important in force transfer and the velocity diagram can be used to obtain a suitable design.

Although a design change can also be made for the front suspension geometry, possible changes may be limited due to the initially designed leg placement of the driver. Besides, this study was especially focused on the rear suspension system.

Under these conditions, the rear load transfer mechanism is analysed and by a proper modification of the rockers and axle the benefits of the system are shown. Nevertheless, it should be pointed out that although the vehicle speed has been kept constant during the simulations, longitudinal load transfer which would result from reciprocating motion of the struts during severe cornering is ignored. As a result, it is shown that the rear load transfer mechanism can be used in future models of the student cars and, indeed in road going cars, with a proper optimisation of the struts and anti-roll bar rates and the design of the links and rockers, to improve the handling performance.

CHAPTER 7

FUZZY LOGIC CONTROL OF VEHICLE YAW MOTION

7.1. Introduction

Vehicle yaw rate error is used as the control parameter in this study while the corrective braking and traction forces are applied on the wheels individually. The model is developed in the Matlab© programming environment using a Simulink© vehicle model under Fuzzy logic control intended both to mimic how a real driver would steer the vehicle to create a path through the specified points as discussed in Chapter 5, and to control the vehicle yaw rate at the same time. The simulation is carried out using the Handsim tool. Several different control methods have been used in the study of vehicle yaw control. In this chapter, the main purpose is to present the use of fuzzy control methodology in vehicle yaw rate control. Fuzzy yaw rate control is used in combination with speed control and vehicle path planning in the form of a fuzzy driver model. The Formula Student Car-201 parameters are used for the simulation.

7.2. Control Methodology

Vehicle yaw rate control using fuzzy logic theory is assessed in various given paths at constant vehicle speed. Providing constant vehicle speed during the simulation is also a part of the job of the fuzzy logic controller. The same 4-Degree of freedom (DOF) vehicle model is used to get the responses of the vehicle as used in Chapters 5 and 6 for the path planning and suspension modelling study. Yaw error feedback to the fuzzy controller is provided by the reference 2 DOF model for the same vehicle but with 50% front 50% rear weight distribution. Theoretically this vehicle has neutral steer characteristics, hence ideal yaw rate, which is the ideal handling characteristic for a vehicle. Tractive force is applied at the rear wheels to keep the velocity constant as the corrective braking forces are being applied at the inner or outer front wheels depending on the orientation of the car.

7.3. Fuzzy inference system (FIS) for vehicle yaw control:

The same fuzzy inference system presented in Chapter 5 is used with additional inputs and outputs for vehicle speed and yaw control. The complete FIS is shown in Figure 1 below. Suffixes *i*, *o*, *f* and *r* refer to *inner*, *outer*, *front* and *rear*, respectively. In this respect, while inputs *Error1*, *Error2*, *Distance* and output *SteerAngle* manage the action of path planning, in other words these inputs and output are parts of the fuzzy driver model, Inputs *YawError*, *SpeedError* and outputs P_{bif}, P_{bof}, P_{bir}, P_{bor}, which are the brake pressures at each wheel, and *Throttle* serve to keep the velocity constant and yaw rate to the reference yaw rate as close as possible.

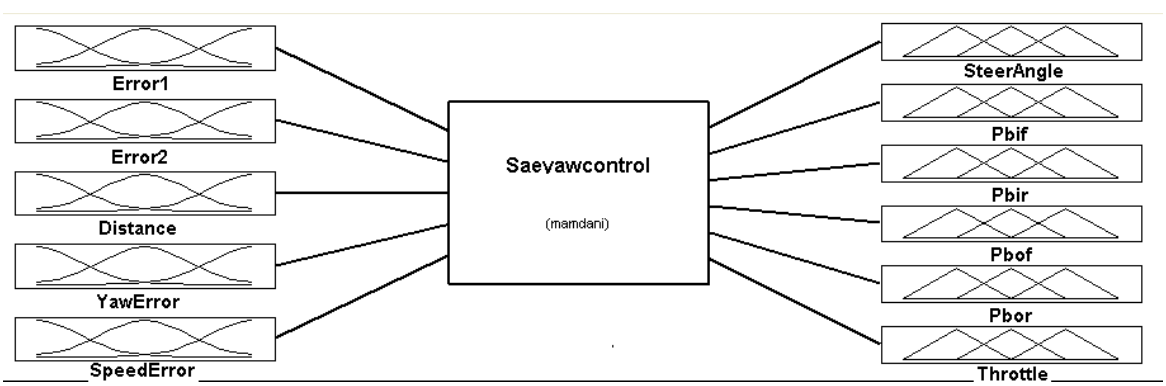

Figure 7.1 Complete fuzzy inference system (FIS)

7.3.1. Speed control:

Speed control depends on to read the vehicle speed changes between the initial speed of the vehicle and the final read speed during simulation. Figure 7.2 shows the membership functions for the speed error input. In all the figures M-, L-, L+ and M+ refer to Negative-Medium, Negative-Low, Positive-Low and Positive-Medium.

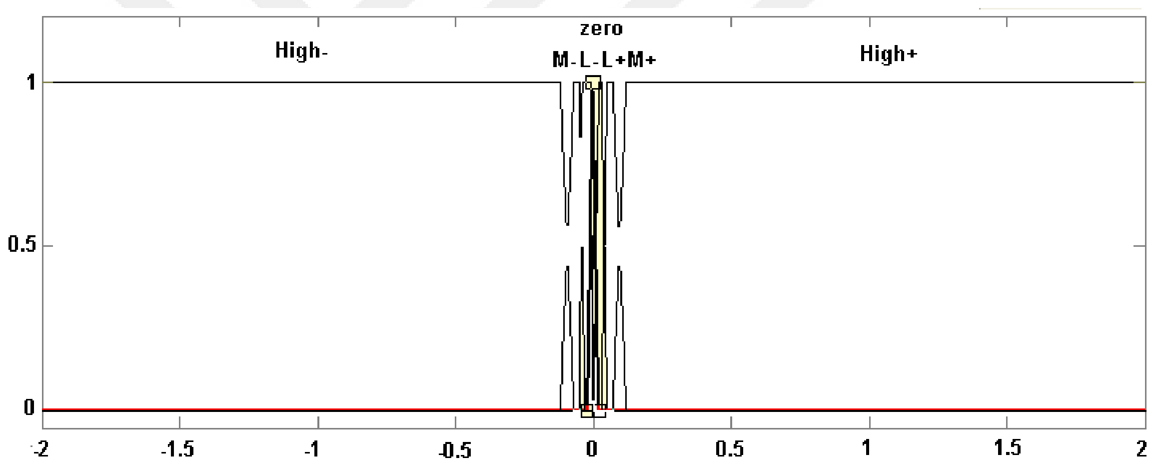

Figure 7.2 Membership functions for *SpeedError (kph)*

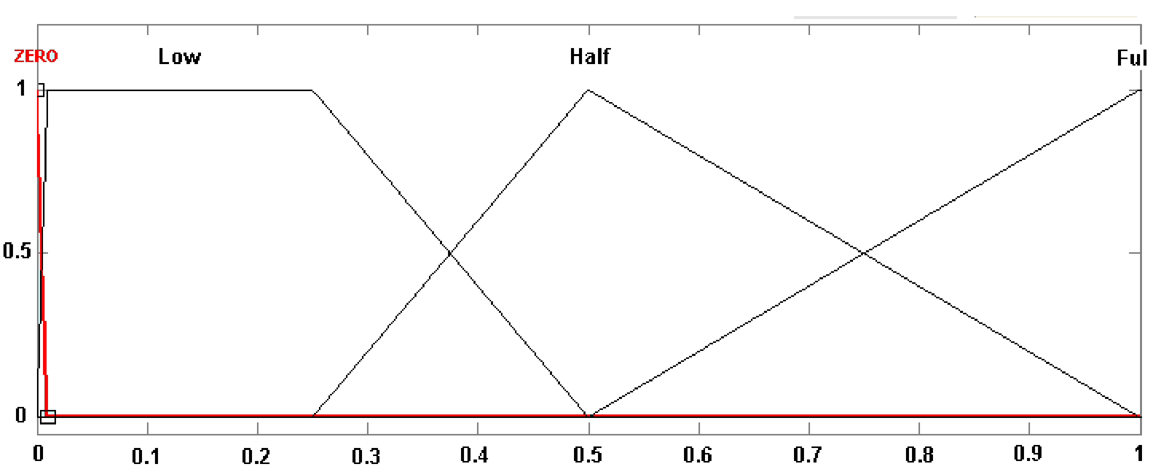

Figure 7.3 Membership functions for *Throttle* .

Membership functions of the output throttle are shown in Figure 3. When the speed is checked and the feedback signal is sent to the fuzzy controller, the quantity of the error is read and a decision is made by the fuzzy rules by sending a suitable throttle position to the vehicle model. Throttle position determines the necessary tractive force to keep the velocity constant from the equations given below.

Maximum Traction force for a rear-wheel drive vehicle [66]:

$$F_{\max} = \frac{\mu W\left(a - f_r h_{CG}\right)/L}{1 - \mu \cdot h_{CG}/L} \tag{7.1}$$

where, μ is road adhesion, W is the weight of the vehicle, and f_r is the coefficient of rolling resistance.

Instantaneous traction force:

$$F_x = throttle \cdot F_{\max} \tag{7.2}$$

Due to the fact that the vehicle travels on a flat surface and very small velocity changes are sensed and then fuzzy inference system reacts to this condition, resulting throttle position will always be kept Low. Therefore, the effect of the small traction forces developed at the rear wheels may be negligible in terms of the longitudinal load transfer.

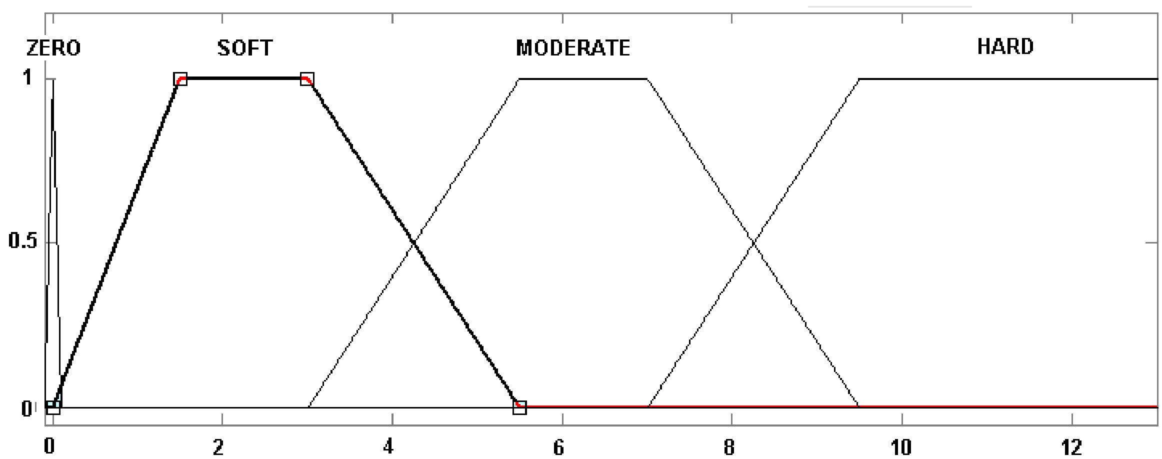

Figure 7.4 Membership functions for all Brake Pressure Outputs (P_b = MPa)

Although brakes are the main control tool of yaw rate control, possible excessive speed needs to be decreased quickly. In this case, Brake pressure outputs are also used to limit the top speed. Fuzzy membership functions of *brake pressures* are shown in Figure 7.4 and all the Fuzzy rules regarding to speed control are given below:

17. **If *SpeedError* is *Low-* then *throttle* is *Low***
18. **If *SpeedError* is *Low+* then *throttle* is *Zero***
19. **If *SpeedError* is *Medium-* then *throttle* is *half***
20. **If *SpeedError* is *Medium+* then *throttle* is *zero* and *Pbif, Pbof, Pbir, Pbor* are *Soft***
21. **If *SpeedError* is *High-* then *throttle* is *full***
22. **If *SpeedError* is *High+* then *throttle* is *zero* and *Pbif, Pbof, Pbir, Pbor* are *Medium***

Brake pressure is limited to 13 MPa in fuzzy inference system in Figure 7.4. Braking force produced on the system can be calculated by the equations (7.3) and (7.4), which were already discussed in Chapter 3.

$$T_b = bgain \cdot P_b \tag{7.3}$$

$$F_b = \frac{T_b}{r} \tag{7.4}$$

7.3.2. Yaw rate control:

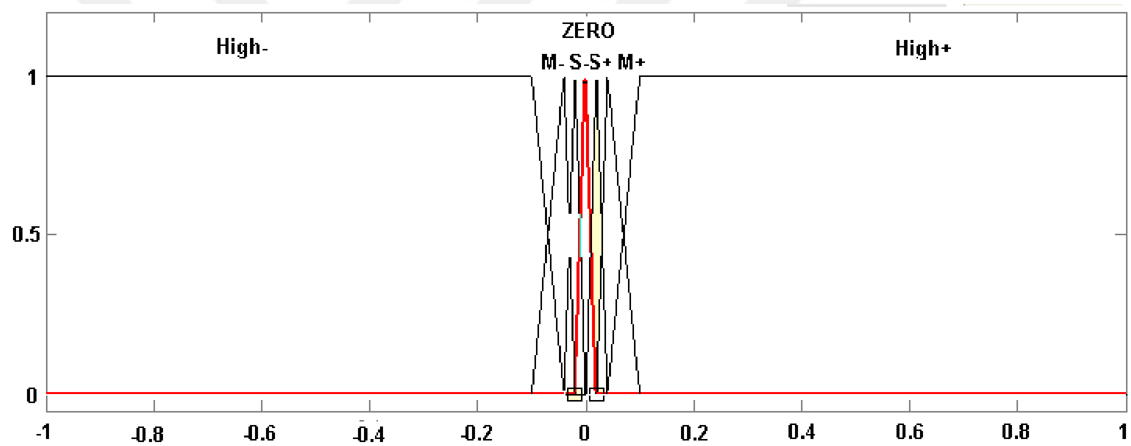

Figure 7.5 Membership functions for YawError (deg/s)

The membership functions of yaw rate input are shown in Figure 7.5 and the corresponding rules are given below:

23. **If *YawError* is *Zero* then *Pbif, Pbof, Pbir, Pbor* are *Zero***
24. **If *YawError* is *Small+* then *Pbif* is *Soft* and *Pbof, Pbir, Pbor* are *Zero***
25. **If *YawError* is *Small-* then *Pbof* is *Soft* and *Pbif, Pbir, Pbor* are *Zero***
26. **If *YawError* is *Medium+* then *Pbif* is *Medium* and *Pbof, Pbir, Pbor* are *Zero***
27. **If *YawError* is *Medium-* then *Pbof* is *Medium* and *Pbif, Pbir, Pbor* are *Zero***

28. If *YawError* is *High+* then *Pbif* is *Hard* and *Pbof, Pbir, Pbor* are *Zero*

29. If *YawError* is *High-* then *Pbof* is *Hard* and *Pbif, Pbir, Pbor* are *Zero*

The two degree of freedom vehicle model with equally distributed front and rear weight is used as a reference model to provide a reference yaw rate during the simulation. A general Simulink model of the vehicle yaw control is shown in Figure 7.6. The model equations used are based on the equations developed in Chapters 4, 5 and 6.

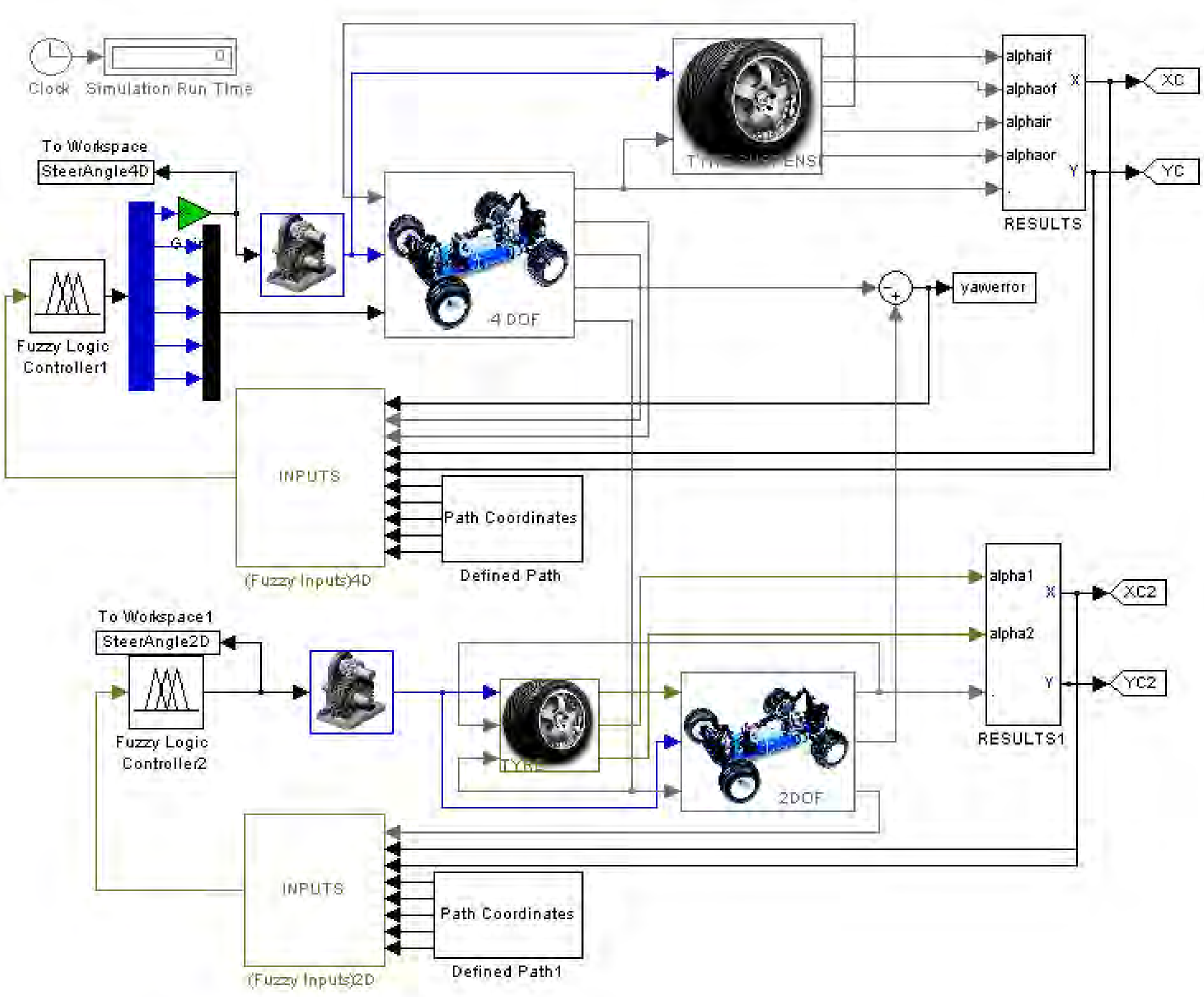

Figure 7.6 Simulink model of the vehicle yaw control

7.4. Simulation and Results

Simulation vehicle parameters are based on the modified Car-201 in Chapter 6. The Simulation has been carried out with a slalom type path at various vehicle velocities. The slalom type of path has been chosen because it is one of the most demanding paths to test the manoeuvrability of the vehicle.

Vehicle Path coordinates : X(0, 30, 60, 90, 120, 150) Y(0, 10, 3, 10, 3, 10)

Vehicle Speed : 30 Kph

The simulation results from Figures 7.7 to 7.10 show the response of the vehicle at 30 Kph. In the comparison figures, green lines refer to the reference vehicle's responses. Blue lines are for the realistic vehicle without yaw rate control and red lines refer to the vehicle with yaw rate control.

Figure 7.7 shows a slight improvement in vehicle path by use of the yaw rate control of the vehicle. Resulting yaw rate responses of the vehicle are shown in Figure 7.8. In this figure, slight decreases or increases in yaw rate can be seen following the same responses of the reference vehicle.

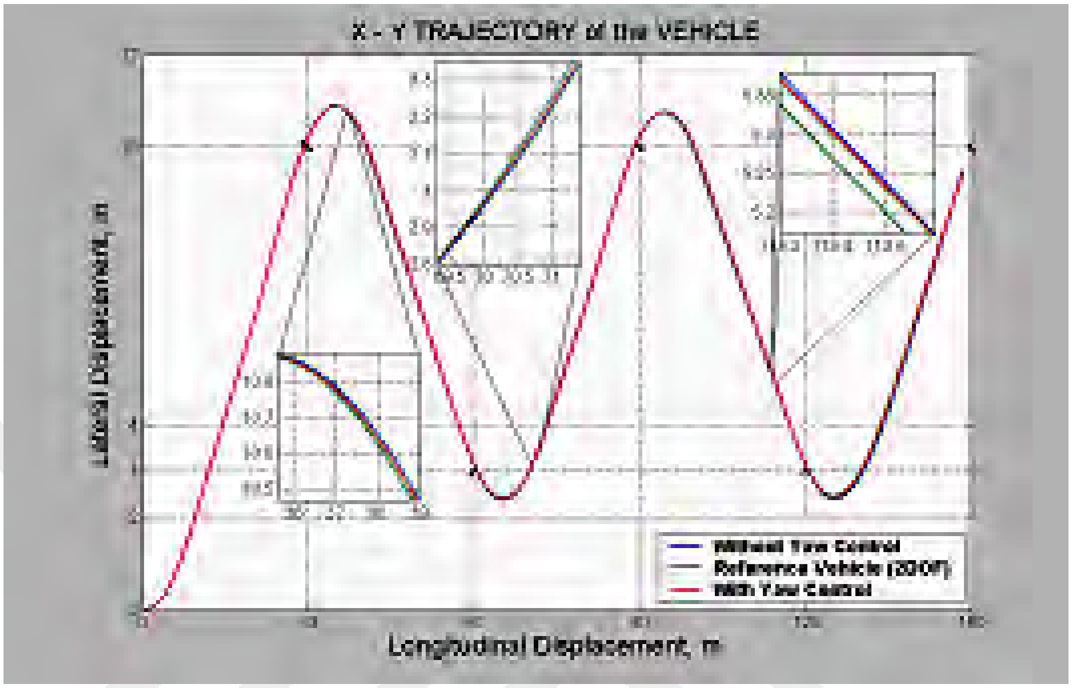

Figure 7.7 Resultant vehicle path at 30 Kph vehicle speed

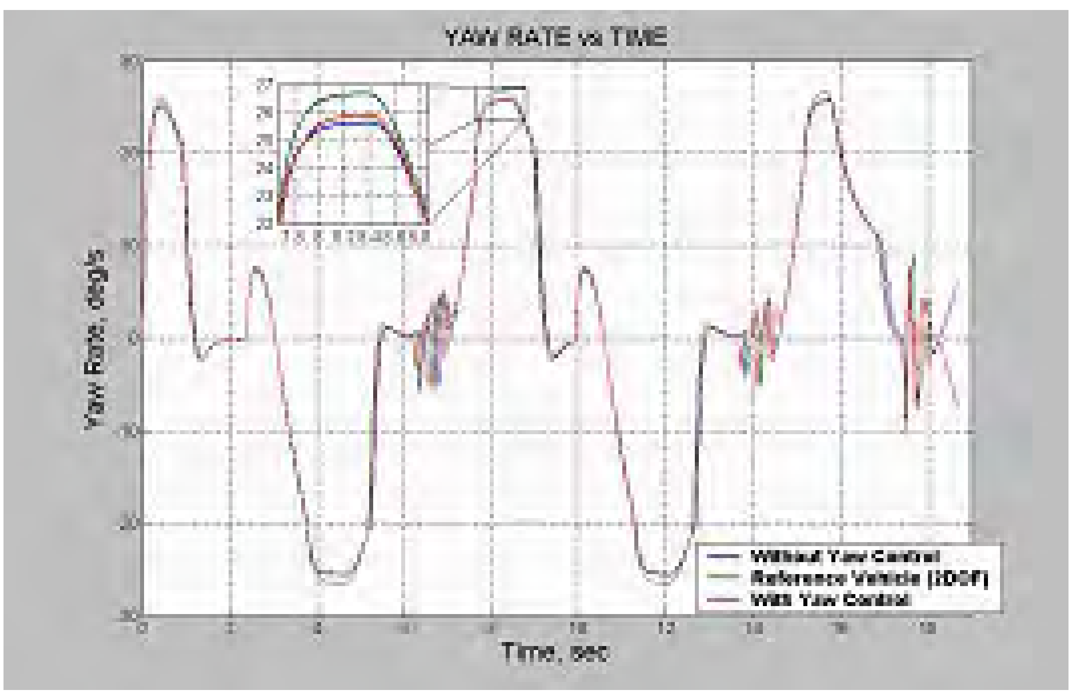

Figure 7.8 Vehicle yaw rate response at 30 Kph vehicle speed

The efficiency of the vehicle speed control can be seen in Figure 7.9 for the vehicle without yaw control and finally the braking force provided to control the vehicle yaw rate is presented in Figure 7.10. The level of braking force varies from about 1/40 to 1/10 of the maximum braking force applicable to the wheels.

.

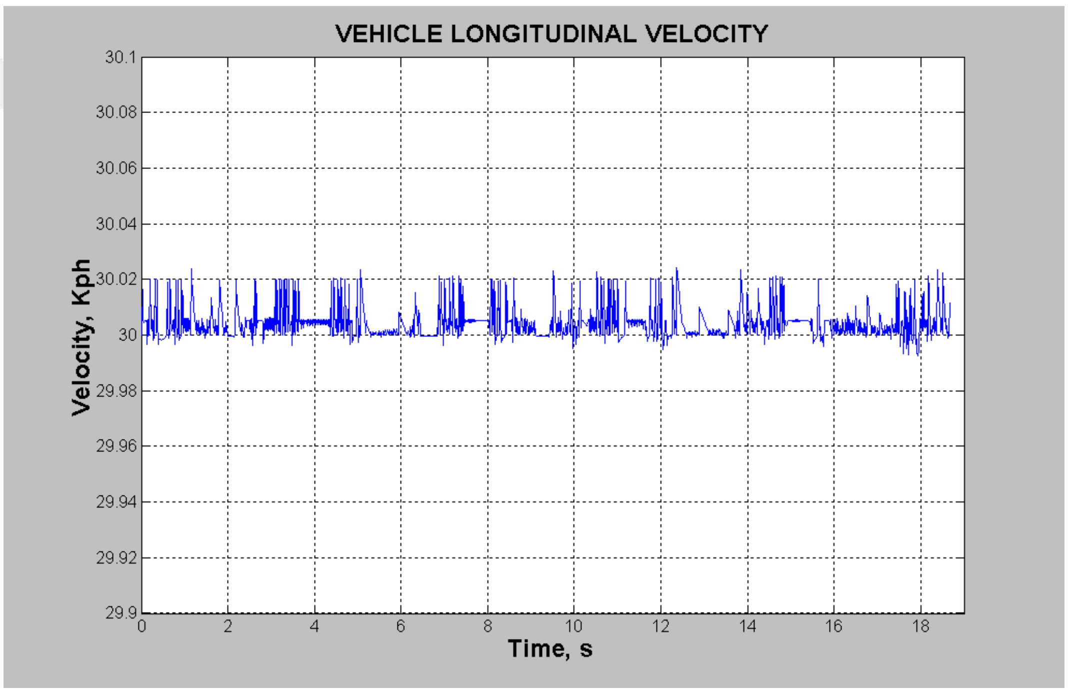

Figure 7.9 Vehicle speed control at 30 Kph.

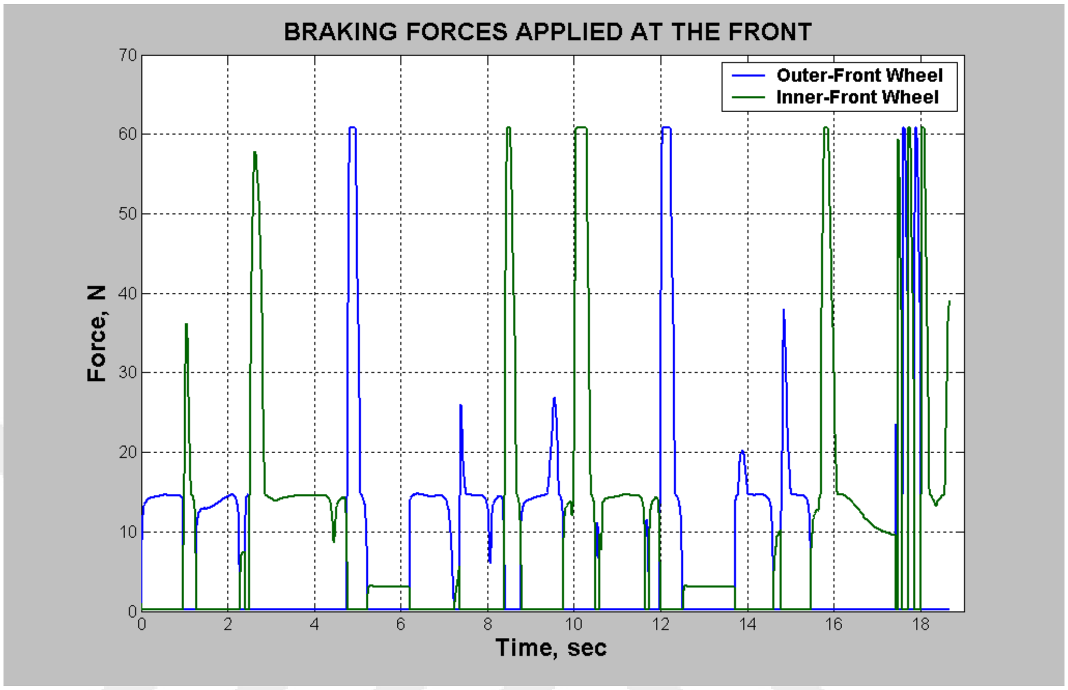

Figure 7.10 Braking forces distributed at the wheels to control yaw rate at 30 Kph.

Vehicle Speed: 40 Kph

The simulation results at 40 kph vehicle longitudinal speed are presented from Figures 7.11 to 7.14. The effect of the controller is more apparent at this higher speed. The vehicle is significantly stabilised after the 60th meter longitudinal displacement in Figure 7.11. Figure 7.12 shows slight differences in vehicle speed between the controlled and uncontrolled vehicle due to the additional braking forces applied to the controlled vehicle. However, because the decrease in velocity is very small, its effect on vehicle yaw rate (Figure 7.13) and vehicle path is negligible.

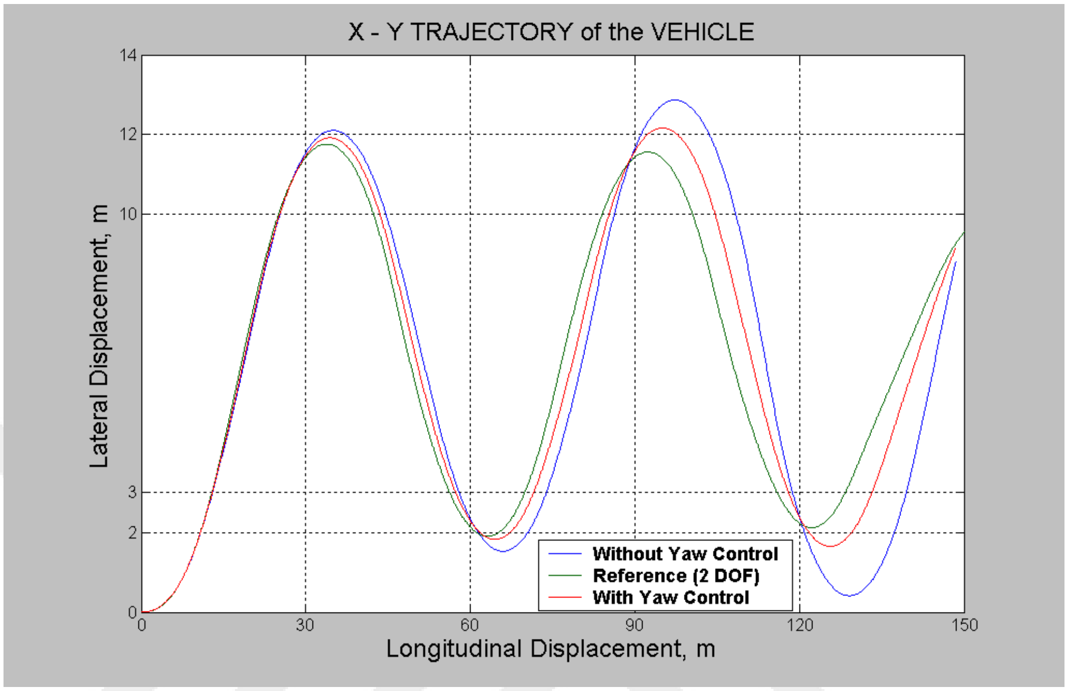

Figure 7.11 Resulting vehicle path at 40 Kph vehicle speed

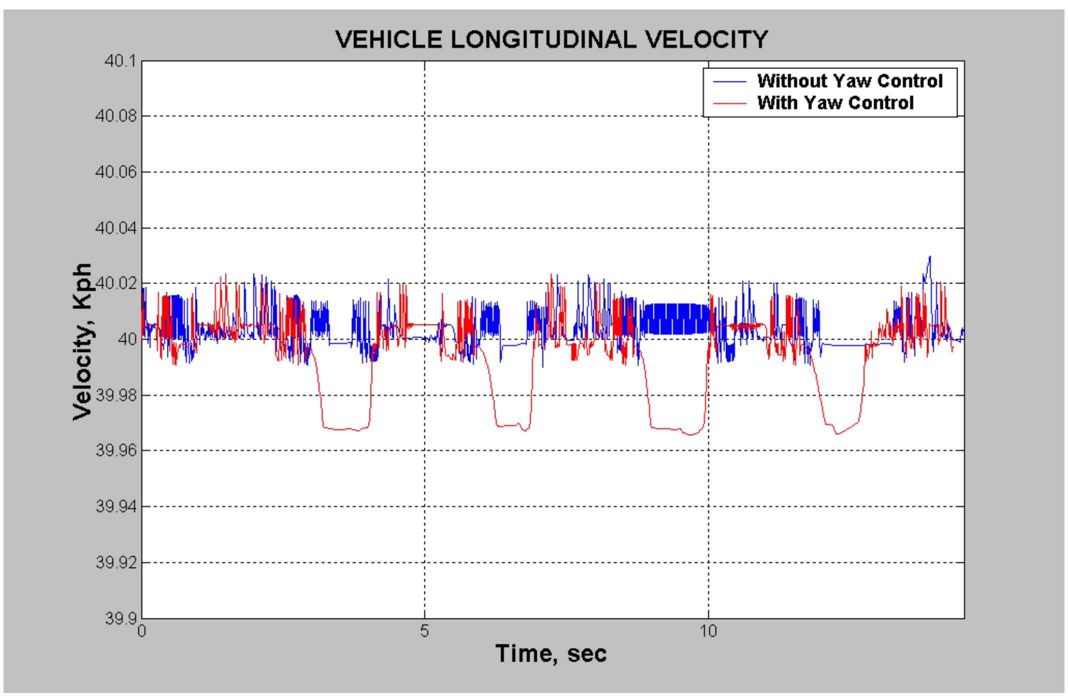

Figure 7.12 Vehicle speed control at 40 Kph.

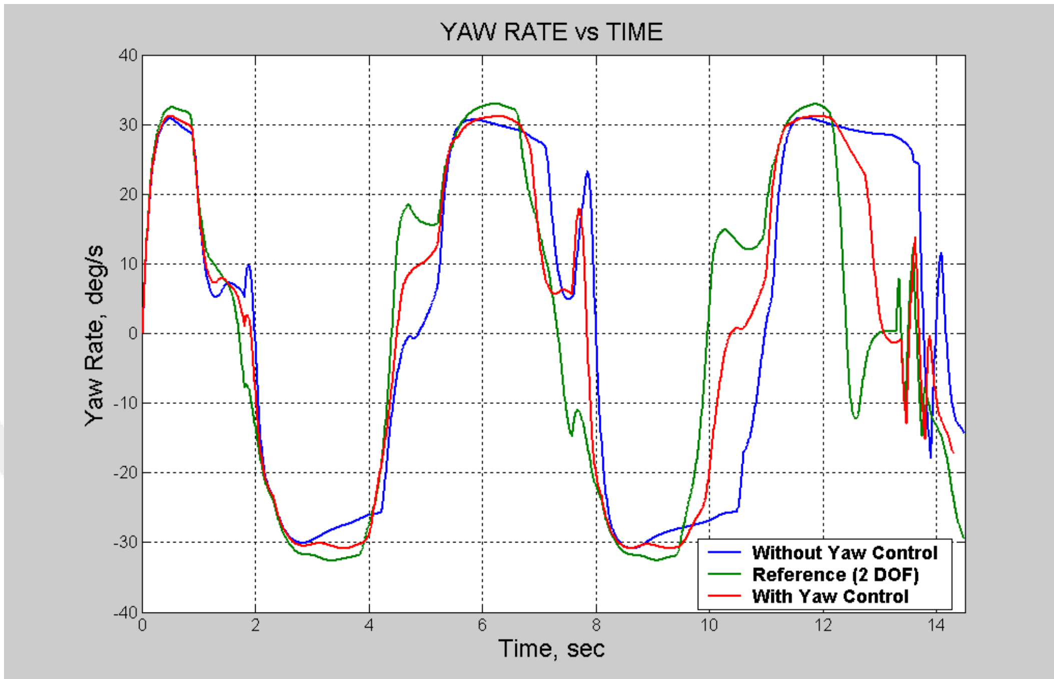

Figure 7.13 Vehicle yaw rate response at 30 Kph vehicle speed

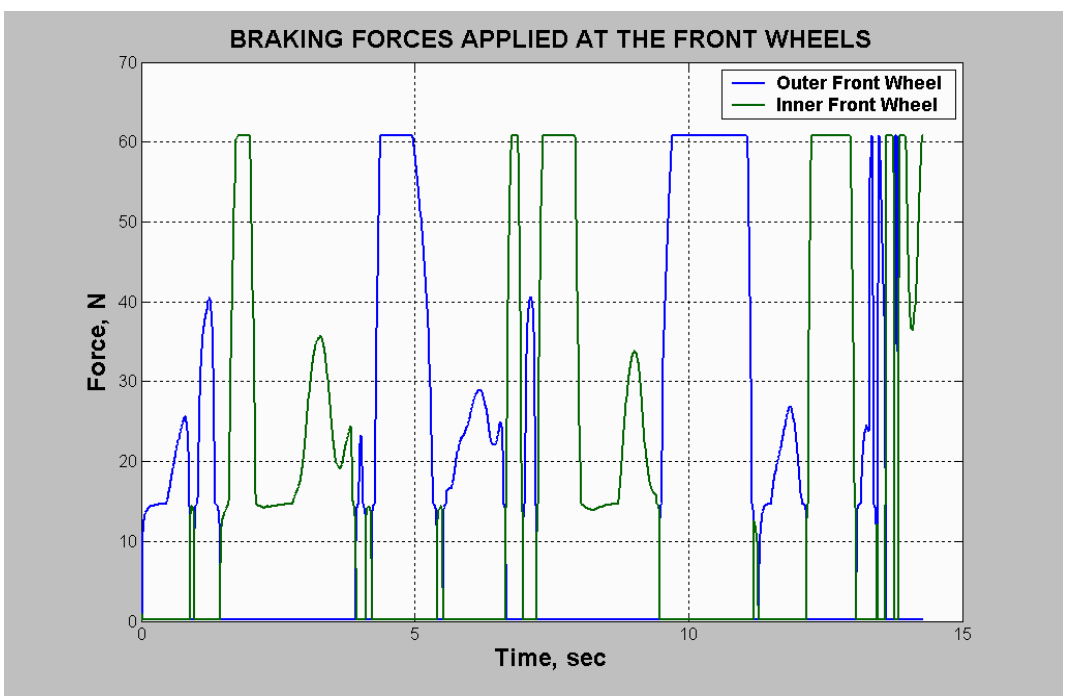

Figure 7.14 Braking forces distributed at the wheels to control yaw rate at 40 Kph.

Figure 7.14 shows the braking forces applied on both front wheels. The amount of the brake force is not very different from the brake force at the lower speed (30 Kph).

7.5 Conclusions

A combined vehicle fuzzy control scheme has been realised including fuzzy path planning, vehicle speed and yaw rate control. The results obtained from the simulations show that a reasonable improvement in handling performance can be obtained by the combined use of braking and tractive force inputs for yaw rate control. It is also shown that with a proper tuning of the fuzzy rules the efficiency of the controller and the handling dynamic properties of the vehicle can be improved..

CHAPTER 8

PROJECT CONCLUSIONS

1. A review of published work on tyre and vehicle handling modelling, and vehicle yaw control methods to improve the handling behaviour of the vehicle has established a need for a vehicle handling model which has ease of use.

2. Mathematical modelling of the vehicle has been studied. The model equations cover two and four degrees of freedom systems. The two-degree of freedom system simply includes lateral and yaw motions of the vehicle. The four degrees of freedom model adds longitudinal motion and roll motion to the simple two degrees of freedom model.

3. The vehicle handling simulation tool presented here has been developed in the MATLAB/SIMULINK environment. These tools provide the researcher with a flexible and easy program development environment. The knowledge of other high level computer programming language like FORTRAN or C++ is not necessary. Most commercial simulation tools or packages are general purpose tools and are often difficult to adapt for a research study so it has been a necessity to consider a special simulation tool for this study. Therefore, the HANDSIM has been tailored specifically to the needs of research in vehicle handling dynamics in an uncomplicated manner such that it can be modified or further developed in the future.

4. Vehicle handling response is often assessed by using simple manoeuvres such as sinusoidal steer, constant radius and constant speed turn tests. Although these tests, either physical or by computer simulation, can give a good understanding of the vehicle behaviour, real driving conditions and vehicle paths can be much more complicated. To assess vehicle response on real roads, researchers have developed sophisticated mathematical models which are generally based on high order polynomials for vehicle path tracking. However, in this study a generic vehicle path planning method which is in the form of a driver model is used for vehicle path definition. The driver model has been developed by using Fuzzy Logic Theory to imitate a human driver. The method used in this study is aimed at producing a driver model which can be used or easily modified for any vehicle. The fuzzy driver model includes four inputs which are two angle errors to the next two defined target points, distance to the first target, and vehicle speed. The output of the model, which is the controlled variable of the vehicle model, is steering wheel angle. This translates to the steer angle at the tyres determined by the choice of the steering system gear ratio. The fuzzy driver model sets the vehicle direction based on the next two target points in the vehicle path at each time step of the simulation. This is to take into account that a real driver will steer the vehicle not simply to reach the next target point but also to orient it in a suitable direction to approach the subsequent target point. The fuzzy driver can make a corrective manoeuvre to target the approaching second point in the last 15 metres before the first target. The results show that at low and moderate vehicle speeds the simulation vehicle seems to exhibit a good stability by hitting almost all the defined points. However, at higher speeds the fuzzy driver has difficulty in following the desired path especially where the path is defined with closely spaced points and sharp angles.

5. The implementation of the fuzzy driver into the HANDSIM has enhanced the capabilities of the tool and it has been applied in studying the effect of suspension design on vehicle handling performance. A novel rear suspension system, implemented in a University of Birmingham Racing (UBR) Formula Student car (Car 201), is modelled using the developed simulation tool, HANDSIM, and the effect of the system on the vehicle's handling performance is discussed by considering the results obtained from the simulation. The Car-201 was designed to get round the twisting Formula SAE/Student circuits as quickly as possible and safely. A load transfer mechanism was designed for the rear suspension system to help achieve this objective. The velocity diagram approach has been used in analysing the kinematics of the suspension system. It has been shown that the rocker geometry is very important in force transfer and the velocity diagram can be used to obtain a suitable design. Therefore, the shortcomings of the existing design, namely the like low motion transfer ratio from the wheels to the main struts and the auxiliary dampers of the rear load transfer mechanism have been exposed and a cost effective solution has been suggested based on modifications to the rocker and the whole axle to produce a more efficient load transfer system using the same approach. As a result, it is shown that the rear load transfer mechanism can be used in future models of the student cars and, indeed in road going cars, with a proper optimisation of the struts and anti-roll bar rates and the design of the links and rockers, to improve the handling performance.

6. The suspension system with the rear load transfer mechanism can be referred to as a passive control system aiming to increase the load transfer to the outer-rear tyre and, hence, the vehicle yaw rate at the beginning of a turn. A combination of fuzzy path planning, vehicle

speed control and yaw rate control using fuzzy logic has been implemented for similar purposes. A reference neutral steer vehicle, which has two degrees of freedom and provides the ideal yaw rate for the given conditions, is used to provide the yaw rate error feedback to the fuzzy controller. Corrective braking and tractive forces are applied to build up the demanded yaw rate. By considering that the tractive and braking forces applied as corrective control inputs for the yaw control of the vehicle are small, the pitching effect of these forces are negligible, and as a result the pitch degree of freedom is simply ignored. This avoids unnecessary modelling complexity and extra computational costs. The results obtained from the simulations show that a reasonable improvement in handling performance can be obtained by the combined use of braking and tractive force inputs for yaw rate control. It is also shown that with a proper tuning of the fuzzy rules the efficiency of the controller and the handling dynamic properties of the vehicle can be improved.

CHAPTER 9

FUTURE WORK

A general vehicle handling dynamics simulation tool HANDSIM has been developed. Even though the initial idea was to provide a simulation tool, which has ease of use and accuracy, the tool has been well improved covering some capabilities like vehicle path planning, a feature that can not be found in any ordinary vehicle dynamics simulation tool. HANDSIM has been validated against one of the well known vehicle dynamics simulation tools CarSimEd©. The accuracy of the tool can also be assessed by real road tests of a vehicle. HANDSIM's tyre model depends on creating an interpolation tyre data library. The best simulation results can be obtained by the experimentally obtained smoothed data for a tyre, which is specifically used on the test vehicle.

The fuzzy driver model is tuned to maintain the vehicle velocity constant. The main reason in the selection of Fuzzy Logic as a vehicle controller was its nature of using human reasoning. Therefore, it is thought to be one of the best choices to imitate a human driver. However, a real driver would also use the brakes and gas pedal to accelerate the vehicle in corners when the driver feels the necessity to do so. From this point of view, the existing fuzzy driver can partly imitate a real driver. A future study should be aimed at developing a more intelligent driver model. Additionally, there will be a need for a more complex (at least five or six degrees of freedom) vehicle model including the pitch motion. This will enable longitudinal load transfer of the vehicle to be taken into account, presenting a more accurate simulation both in terms of the driver's actions and, even though the effect is small, the effects of the corrective braking and tractive forces of the vehicle yaw control on the vehicle.

The existing fuzzy controller has static membership functions. As a result of this, braking and driveline gains have been introduced to generalise the controller for any type of vehicle in HANDSIM. Instead of using gain factors, a new study can be focussed on to Neuro-Fuzzy inference systems, which have membership functions with variable parameters during a learning process from the given data. Also, a limitation study defining the width of a real road can be added to the same study.

The use of fuzzy logic is in an increasing trend in intelligent control theories. This thesis has presented an important coverage of fuzzy logic in vehicle dynamics.

REFERENCES

1. Sayers, M.W., *Vehicle models for real time simulation applications*.
2. Guo, K., L. Ren, and Y. Hou. *A non-steady tire model for vehicle dynamic simulation and control*. in *AVEC'98*. 1998.
3. Zegelaar, W.A., *The dynamic tyre response to brake torque variations and road unevenness*. 1998, Delft University-Holland: Delft. p. Mechanical Engineering.
4. Alter, D.M., *Transient and steady-state performance comparison of two-wheel-steer and four-wheel-steer vehicle models.* 1989, University of Illinois at Urbana Champaign.
5. Huston, J.C. and D.B. Johnson, *Effect of the normal force dependence of cornering stiffness on the lateral stability of recreational vehicles.* SAE Transcations, 1980. **89**(SAE 800161).
6. Pacejka, H.B. and I.J.M. Besselink, *Magic formula tyre model with transient properties.* Vehicle System Dynamics Supplement, 1997. **27**: p. 234-249.
7. Pacejka, H.B. and E. Bakker, *"The Magic Formula Tyre Model.* Vehicle System Dynamics Supplement, 1991. **21**: p. 1-18.
8. Mizuno, M., T. Takahashi, and M. Hada. *Magic formula tire model using the measured data of a vehicle running on actual roads*. in *AVEC'98*. 1998.
9. Bakker, E., L. Nyborg, and H.B. Pacejka, *Tyre modelling for use in vehicle dynamics studies.* SAE Transactions, 1987. **SAE 870421**.

10. Jang, B. and D. Karnopp, *Simulation of Vehicle and power steering dynamics using tyre model parameters matched to whole vehicle experimental results.* Vehicle System Dynamics, 2000. **33**: p. 121-133.

11. Kusaka, K., et al., *Transient Tire Model for Handling Analysis and Prediction.* 1995.

12. Lee, A.Y., *Emulating the Lateral Dynamics of a Range of Vehicles Using A Four-Wheel-Steering Vehicle*. 1994, Jet Propulsion Laboratory.

13. Best, M.C. and T.J. Gordon. *Real time state estimation of vehicle handling dynamics using an adaptive Kalman filter 9836590*. in *AVEC'98*. 1998.

14. Kim, S.H. and G. Gim, *"Semi physical tyre model for cornering simulations of vehicles.*, Hancook Tire Co.Ltd-Vehicle Dynamics Research Team.

15. Maurice, J.P. and H.B. Pacejka, *Relaxation length behaviour of tyres.* Vehicle System Dynamics Supplement, 1997. **27**: p. 339-342.

16. Wang, Y.Q., R. Gnadler, and R. Schieschke, *Vertical load-deflection behaviour of a pneumatic tire subjected to slip and camber angles.* Vehicle System Dynamics Supplement, 1996. **25**: p. 137-146.

17. Dixon, J. C., *Tires Suspension and Handling,* SAE, 1996, ISBN: 1-56091-831-4

18. Wong, J.Y., *Characterization of Cornering behavior of tires*, in *Theory of Ground Vehicles*. 2001. p. 44.

19. Oertel, C., *On modelling contact and friction-Calculation of tyre response on uneven roads.* Vehicle System Dynamics Supplement, 1997. **27**: p. 289-302.

20. Kuppers, T., C. Schroder, and K.U. Kohne. *Heavy truck modelling and validation concerning handling*. in *AVEC'96*. 1996. Aachen, Germany.

21. Maurice, J.P., M. Berzeri, and H.B. Pacejka, *Pragmatic tyre model for short wavelength side slip variations.* Vehicle System Dynamics, 1999. **31**: p. 65-94.

22. ADAMS/Tire. “http://engineering.software-directory.com/cdprod1/swhrec/...”

23. Gim, G., *Transient Tire Model for Cornering Simulations of Vehicles.* 1995.

24. Cambiaghi, D. and M. Gadola, *Tyre modelling with the use of neural nets for vehicle dynamics studies.* ATA Journal- Ingegneria Automotoristica, 1996. **3**.

25. Blundell, M., *The Influence of Suspension and Tyre Modelling on Vehicle Handling Simulation*, PhD Dissertation, 1997, Coventry University.

26. Olatunbosun. Automotive Engineering Lecture Notes.

27. Rahnejat, H., *Multibody dynamics: Historical evolution and application.* Proc Instn Mech Engrs, 2000. **214**(C): p. 149-173.

28. McHenry, R.R., *An analysis of the dynamics of automobiles during simultaneous cornering and ride motions, in handling of vehicles under emergency conditions 28-48.* Proc. Instn Mech. Engrs, 1968. **13**: p. 24-48.

29. You, S.S. and S.K. Jeong, *Vehicle dynamics and control synthesis for four wheel steering passenger cars.* Proc Instn Mech Engrs, 1998. **212**(D).

30. Russo, M., R. Russo, and A. Volpe, *Car parameters identification by handling manoeuvres.* Vehicle System dynamics.

31. Kim, C., P. Ro, and H. Kim, *Effect of the suspension structure on equivalent suspension parameters.* Proc Instn Mech Engrs, 1999. **213**(D): p. 457-469.

32. Horiuchi, S., K. Okada, and S. Nohtomi, *Improvement of vehicle handling by nonlinear integrated control of wheel steering and four wheel torque.* JSAE Review, 1999. **20**: p. 459-464.

33. Wallentowitz, H. and P. Holdmann, *Hardware and software demands on adjustable shock absorbers for trucks and passenger cars*. 1995, IKA.

34. Ellis, J., R., *Vehicle dynamics*. First ed. 1969: London Business Books Limited.

35. Heydinger, J. and A. Ronald, *Effects of loading on vehicle handling.* SAE Transactions, 1998. **980228**: p. 407-415.

36. Abe, M., N. Ohkubo, and Y. Kano, *A direct yaw moment control for improving limit performance of vehicle handling-comparison and cooperation with 4WS.* Vehicle System Dynamics Supplement, 1996. **25**.

37. Furukawa, Y. and M. Abe, *Advanced chassis control systems for vehicle handling and active safety.* Vehicle System Dynamics, 1997. **28**: p. 59-86.

38. Nagai, M., U. Etsuhiro, and M. Antonio, *Integration of Linear Systems and Neural Networks for the Design of Nonlinear Four-Wheel-Steering Systems.* JSAE Review, 1995. **16**(2): p. 213-214.

39. Harada, M., K. Tobimatsu, and H. Harada. *Improvement of stability in cornering on uneven roads*. in *AVEC '98*. 1998.

40. Nagai, M., Ueda, E., Moran, A., *Integration of Linear Systems and Neural Networks for the Design of Nonlinear Four-Wheel-Steering Systems***,** *JSAE Review*, Volume 16, Issue 2, April 1995, Pages 213-214

41. Fukada, Y., “Slip-angle estimation for vehicle stability control”, Vehicle System Dynamics, vol. 32, pp.375-388, 1999.

42. Lauffenburger, J. Ph., Basset, M., Coffin, F., Gissinger, G. L., (2002). Driver-aid system using path planning for lateral vehicle control. Control Engineering Practice 0, pp. 1-15.

43. Mouri, H., Furusho, H., Investigation of automatic path tracking comparing the performance of LQ control with that of PD control, Trans. JSAE, Vol. 30, No. 1, pp. 121-126 (1999).

44. Furusho, H., Mouri, H., Research on automated lane tracking using linear quadratic control procedure for curved path, JSAE Review, vol. 20, No. 3, pp. 325-329 (1999).

45. Marumo, Y., Mouri, H., Wang, Y., Kamada, T., Nagai, M., (2000). Study on automatic path tracking using virtual point regulator. JSAE Review 21, pp. 523-528.

46. Piancastelli, L., Sarubbi, G., An EESP Fuzzy control system for the recovery of the initial direction after an initial spin. XII ADM Conference Proceedings, Rimini-Italy, pp. 134-143. (2001).

47. Nwagboso, C. O., *Automotive Sensory Systems,* Kluwer Academic Publishers; ISBN: 0412458802

48. Ellis, J. R., *Vehicle Handling Dynamics*, Professional Engineering Publishing, 1994, ISBN: 0852988850.

49. Goodyear Tires, *Formula SAE Tyre Data: 20.0x6.5-13,* http://www.goodyear.com

50. Matlab Help

51. Dixon, J. C., *Tires Suspension and Handling*, SAE, 1996, ISBN: 1-56091-831-4

52. Genta, G., *Motor Vehicle Dynamics: Modelling and Simulation*, World Scientific Pub Co., 1998, ISBN: 9810229119.

53. ACSL (Advanced Computer Systems Limited) Simulation tool, 1998, http://www.acsl.com

54. ADAMS/Car, Mechanical Dynamics Inc, http://www.adams.com/mdi/product/modules.htm

55. CarSimEd Manual, Version 4.5, http://www.trucksim.com

56. Gillespie, T. D., *Fundamentals of Vehicle Dynamics,* SAE Inc, 1992, ISBN: 1-56091-199-9.

57. Tan, H.S., *Lane changing with look-down reference systems on automated highways*, Control Engineering Practise, 8 (200), 2000, pp.1033-1043.

58. Aracil, J., Heredia, G., Ollero, A., *Global stability of fuzzy path tracking sing frequency response*, Engineering Applications of Artificial Intelligence, vol. 13, 2000, pp. 109-119.

59. Verbrugge, H. B., *Fuzzy Logic Control: Advances in Applications*, World Scientific, 1999. ISBN: 9810238258.

60. Odling, S., *Formula SAE 2001 Suspension System,* Final Year Project, 2001, Department of Mechanical & Manufacturing Engineering, University of Birmingham.

61. Fenton, J., *Handbook of Automotive Powertrains and Chassis Design,* Professional Engineering Publishing, 1998, ISBN: 1 86058 075 0.

62. Clements, B., *Formula SAE 2001-Shock Absorbers Design*, Final Year Project, 2001, Department of Mechanical & Manufacturing Engineering, University of Birmingham.

63. Risse Racing Technologies, *Technical drawing of Jupiter-5*, http://www.risseracing.com

64. Fenton, J., *Handbook of Automotive Design Analysis,* Butterworth Co, 1976, ISBN: 0 408 00241 7.

65. Ellis, J. R., *Vehicle Dynamics*, London Business Books Limited, 1969, ISBN: 220 99202 9.

66. Wong, J.Y., *Theory of Ground Vehicles*, John Wiley & Sons,Inc., 3rd Edition, 2001, ISBN: 00-043853.

APPENDIX A

INTERPOLATION TYRE DATA

A1. DUNLOP D8 195/65 R15 [25]

LATERAL FORCE (N) WITH SLIP ANGLE (DEG) AND VERTICAL LOAD (KG) SPLINE/100
α = -10,-8,-6,-4,-2,0,2,4,6,8,10
Y = 2002148,2050,1806,1427,867,16,-912,-1508,-1881,-2067,-2151
Y=400,3967,3760,3409,2727,1620,75,-1587,-2776,-3482,-3759,-3918
Y=600,5447,5099,4436,3385,1962,94,-1893,-3397,-4557,-5049,-5269
Y=800,6738,5969,4859,3533,2030,66,-1971,-3662,-5122,-6041,-6500
ALIGNING MOMENT (NM) WITH SLIP ANGLE (DEG) AND LOAD (KG) SPLINE/200
X=-10,-8,-6,-4,-2,0,2,4,6,8,10
Y=200,4.6,-0.1,-6,-11.1,-10.9,-1.3,10.6,11.2,7.9,3.2,-0.3
Y=400,-4.8,-19.6,-39,-52.1,-41.9,-6.7,35.8,49.1,38.6,23.4,10.1
Y=600,-36.5,-73.1,-102.6,-107.9,-78.7,-14.2,60.6,96.2,93.4,65.8,40.7
Y=800,-105.1,-181.1,-206.1,-172.4,-116.0,-23.6,79.9,143.3,172.2,141.5,98.5

A2. GOODYEAR Formula SAE 20.0x6.5-13 [ ]

Vertical Force:
F_z = [445.78 1114.45 1783 2541.8] [N]
Slip Angle:
alpha = [-8,-7,-6,-5,-4,-3,-2,-1,0,1,2,3,4,5,6,7,8] [degree]
Lateral Force:
F_y = [-306 -298 -290 -280 -264 -224 -168 -84 -8 112 184 224 248 266 272 280 278;
-664 -648 -624 -588 -532 -428 -296 -124 -24 207 356 460 536 580 592 628 632;
-868 -828 -772 -700 -576 -418 -320 -136 -44 220 392 532 628 728 780 828 864;
-924 -864 -792 -688 -568 -436 -284 -124 -36 204 364 508 646 734 816 880 936]

A3. AVON 20.0x6.0-13 (Experimental Data Provided in The University of Birmingham)

F_v = [294.2 392.3 490.35 588.4 686.5 784.6 882.63 980.7]'; [N]

alpha = [-10 -9 -8 -7 -6 -5 -4 -3 -2 -1 0 1 2 3 4 5 6 7 8 9 10]'; [degree]

C_α = [30.7 34.46 40.2 46.52 58.89 67.6 86.9 111.28 157.94 270.13 320 270.13 157.94 111.28 86.9 67.6 58.89 46.52 40.2 34.46 30.7;
42.87 48.75 55.7 65.52 76.1 91.95 116.17 161.27 234.48 367.42 470 367.42 234.48 161.27 116.17 91.95 76.1 65.52 55.7 48.75 42.87;
50.6 57.64 66.56 77.25 91.98 111.85 141.42 188.12 268.36 411.37 566.32 411.37 268.36 188.12 141.42 111.85 91.98 77.25 66.56 57.64 50.6;
65.6 74.71 75.46 99.3 116.8 142.8 179.8 237.2 339.16 526.82 670 526.82 339.16 237.2 179.8 142.8 116.8 99.3 75.46 74.71 65.6;
72 81.4 90.57 106 124.7 152.47 189.9 245.84 344.86 575.55 720 575.55 344.86 245.84 189.9 152.47 124.7 106 90.57 81.4 72;
90.5 100.77 114.39 132.44 156.12 181.6 227.65 299.3 424.8 705 900 705 424.8 299.3 227.65 181.6 156.12 132.44 114.39 100.77 90.5;
109.1 123.4 136.7 160.84 191.9 232.3 292 381.96 525.1 760.8 950 760.8 525.1 381.96 292 232.3 191.9 160.84 136.73 123.39 109.1;
123.46 138.33 156.62 182.24 215.66 262.51 325.36 414.15 569.25 866.46 1100 866.46 569.25 414.15 325.36 262.51 215.66 182.24 156.62 138.33 123.46];

APPENDIX B

PUBLICATIONS

This appendix contains three research papers which have been presented throughout the course of this work.

B1 A Generic Fuzzy Pilot and Path Planning for Vehicle Handling Dynamics Simulation Studies

SAE Conferences: Future Transportation Technologies, Costa Mesa, California, USA, 23rd June, 2003

B2 A Fuzzy Logic Application on Vehicle Path Planning and Yaw Control

Proceedings of the 9th Annual Research Symposium of Postgraduate Research University of Birmingham, 7th May, 2003, pp. 50-54. ISBN 07044 24150

B3 A new vehicle handling dynamics simulation tool: Handsim

Proceedings of the 7th Annual Research Symposium of Postgraduate Research University of Birmingham, 5th May, 2001, pp. 26-30, ISBN 07044 23057

03FTT-39

A Generic Fuzzy Pilot and Path Planning for Vehicle Handling Dynamics Simulation Studies

Erdem Uzunsoy & Oluremi A. Olatunbosun

Vehicle Technology Research Centre-University of Birmingham

ABSTRACT

Computer simulation has been used in vehicle dynamics studies for decades. Advances in the science of vehicle dynamics and far more improved computer technology now enable automobile manufacturers to get closer to zero-prototype production than ever before. From the computer simulation point of view, having a general path generator can present the researchers with great flexibility in defining vehicle handling dynamics tests. The process used for generating the vehicle's path in this study is referred to as 'path planning' because of some distinctive approaches used. A vehicle model is used in conjunction with the fuzzy pilot model to generate the vehicle's path through a number of specified points through which the vehicle must pass. The simulation is carried out in the Matlab© programming environment using a Simulink© vehicle model under Fuzzy logic control intended to imitate how a real driver would steer the vehicle to create a path through the specified points. The complexity of the path is defined by the specified points and their spacing, which can be used to describe road features such as corners, chicanes etc. The ability of a vehicle to negotiate the defined road features can therefore be simulated by testing how accurately the vehicle model/fuzzy pilot combination can create a path through the specified points.

INTRODUCTION

The three types of generalised tests normally used for vehicle handling dynamics are lane change, constant radius steer and constant steer. These are idealised tests, which have little bearing on normal driving. From the computer simulation point of view, having a general path generator can present the researcher with great flexibility in defining vehicle handling dynamics tests. For example, in the simulation studies, a lane change manoeuvre can simply be represented by sinusoidal steer, with the frequency and amplitude of the sine function being used to define the vehicle position. However, the steering input required for a lane change manoeuvre by a driver driving a real vehicle is not sinusoidal and the vehicle path cannot be represented by a simple mathematical function. Therefore, complex mathematical functions, especially higher order polynomials are generally used to define the vehicle path.

Lauffenburger et al. [1] applied polar polynomial curves to represent the desired path of a vehicle and fuzzy logic control was used to determine the constraints of the maximum points of the polynomial, with the driver's profile, in terms of experience, being used as an additional parameter. An inexperienced driver negotiating a bend increases the steering angle smoothly during the first half of the turn and decreases it during the second half. This technique is guided by maximum comfort and safety. The trajectory in the same turn is completely different for an experienced driver whose objective is to minimise the time taken to traverse the turn. A number of vehicle path tracking researches [2, 3] are mainly aimed at the future automated highway systems and a number of different approaches have been used in these studies. Mouri and Furusho [4, 5] proposed a path tracking system to regulate the lateral position at the centre of gravity of the vehicle by minimising a cost function based on the lateral displacement at the centre of gravity and the front wheel steering angle. A virtual point regulator, which also takes the yaw angle into consideration in addition to this basic approach, has been proposed by Marumo et al. [6]. The virtual point is at a point on the driver's line of sight and is a function of the vehicle yaw angle, the lateral displacement at the vehicle centre of gravity and the distance between the virtual point and the centre of gravity. The cost function is, therefore, now based on the lateral displacement at the virtual point and the front wheel steering angle. This increases the robustness and the performance of the control system. Due to the nature of processes like using a virtual point to represent, simply, the human driver's line of sight, intelligent control system models which can mimic the driver's experience, such as fuzzy logic control or neural networks, are the most preferable control schemes in these studies. These control models are intended basically to command the steer angle. Additionally, yaw angle error and yaw rate may also be used as inputs to the intelligent control system. This kind of process, based on fuzzy logic, was referred to as 'fuzzy pilot' by Piancastelli & Sarubbi [7].

In the current study, a vehicle model is used in conjunction with a fuzzy pilot model to generate the vehicle's path through a number of specified points, through which the vehicle must pass. The simulation is carried out in the Matlab© programming environment using a Simulink© vehicle model under Fuzzy logic control intended to mimic how a real driver would steer the vehicle to create a path through the specified points. The complexity of the path is defined by the specified points and their spacing, which can be used to describe road features such as corners, chicanes etc. The ability of a vehicle to negotiate the defined road features can therefore be simulated by testing how accurately the vehicle model/fuzzy pilot combination can create a path through the specified points. The fuzzy pilot model can be used in conjunction with a vehicle model of any complexity provided it is available as a Simulink© model.

The simulation model is implemented for a generalised vehicle model and although the specific vehicle models used in this study are fairly simple, vehicle models of any complexity can be used. The vehicle model is simply included as a Simulink block in the overall simulation model.

VEHICLE DYNAMICS MODEL

The vehicle models used in this study are based on the well known '2-wheel' model in the form of two degrees of freedom (2 DOF) and three-degrees of freedom (3 DOF) 'Equations of Motion'.

AXIS SYSTEM

The vehicle body-fixed axis (moving coordinates) system is employed in the derivation of the equations of motion. However, the overall trajectory of the vehicle is represented in the earth-fixed coordinate system. The ISO moving coordinates system is illustrated below in Figure 1, where, U, V, W are the velocities of the vehicle in the longitudinal, lateral and horizontal axes and p, q and r are the roll, pitch and yaw inertias of the vehicle, respectively.

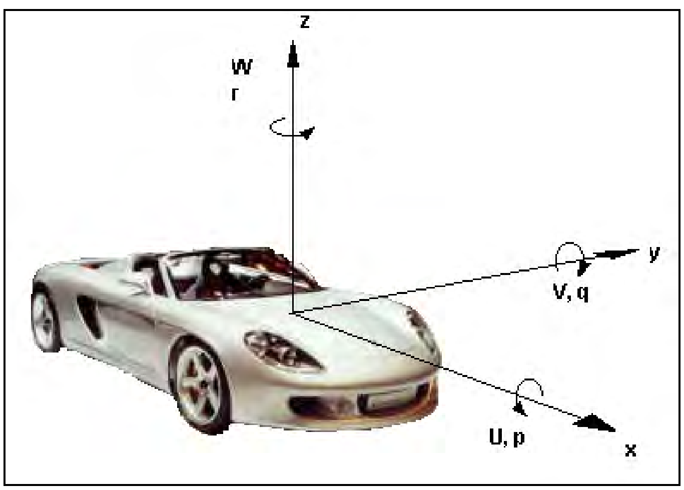

Figure 1. Moving coordinate system

TWO-DEGREE OF FREEDOM (2DOF) VEHICLE MODEL

The 2 DOF model simply considers the lateral and the yaw motion of the vehicle as in the equations [Eq.1] and [Eq.2], respectively [6].

Σ F_y = $m(\dot{V}+rU)$ [Eq.1]

Σ M_z = $I_{zz}\dot{r}$ [Eq.2]

where, Fy is lateral force, m is the mass of vehicle, V is lateral velocity, r is yaw velocity, U is Forward velocity, M_z is aligning moment and I_{zz} is yaw inertia with respect to the z-axis.

THREE DEGREE OF FREEDOM (3 DOF) VEHICLE MODEL

The 3 DOF model simply adds the roll motion and, as a result, lateral load transfer of the vehicle. The equations of motion [8] are as follows:

Σ F_y = $m(\dot{V}+rU)$ [Eq.3]

Σ M_z = $I_{zz}\dot{r}$ [Eq.4]

Σ M_x = $I_{xx}\dot{p}$ [Eq.5]

where, Mx is the moment around the x-axis, I_{xx} is roll inertia and p is roll velocity.

VEHICLE SIMULINK MODEL & FUZZY PATH PLANNING

A general vehicle system Simulink© model is shown in Figure 2. The main blocks of the model are the vehicle model, the tyre model and the fuzzy pilot. The other blocks are required to enable the simulation to run correctly and include input and calculation blocks. The results provided by the Vehicle Model, Tyre dynamics and Defined Path sub blocks are processed in the Fuzzy Inputs sub-block and then sent to the fuzzy logic controller block which is called 'fuzzy pilot'. As mentioned in a previous section, the vehicle model block is replaceable by any vehicle model regardless of its complexity. The tyre model implemented in this study is based on interpolation of empirical data but, again, any suitable tyre model may be used. The direction of the vehicle is determined in the Angles block of the vehicle Simulink model.

Figure 3 shows the target points which the vehicle must pass through in relation to its instantaneous position. The point O(x_0,y_0) represents the instantaneous position of the vehicle, with OX' and OY' representing the instantaneous forward and lateral moving axes respectively. Points A(x_1,y_1) and B(x_2,y_2) represent the first and second target points which the vehicle must pass through respectively. The angle between the current heading direction of the vehicle (OX') and the direction of the first target point (OA) provides the input 'Error1' for the fuzzy pilot (i.e. the angle AOX'). The fuzzy pilot also uses Beta (the angle between the direction of the first target point (OA} and the direction AB from the first target point to the second target point) as the second input to the inference system.

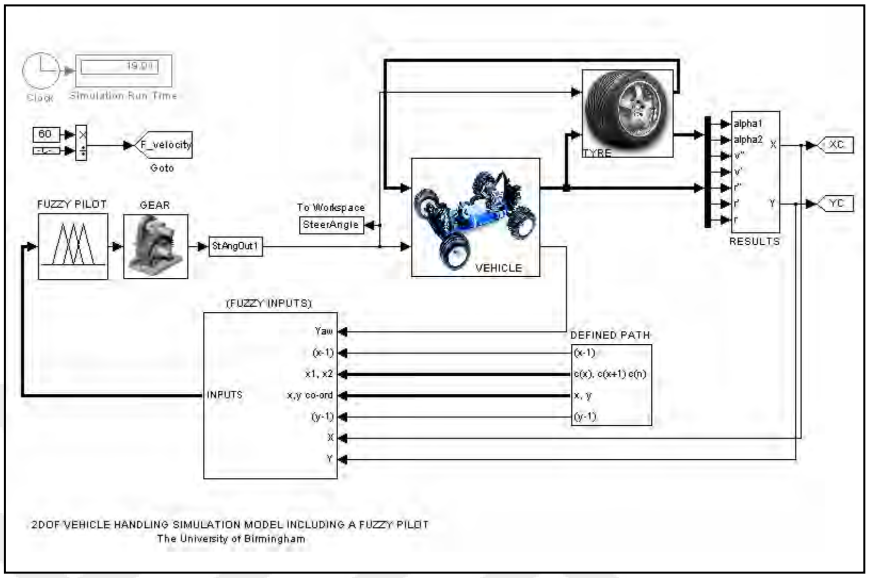

Figure 2. Simulink vehicle model including the fuzzy pilot

The Fuzzy pilot is intended to react as a real driver, so it determines the direction in which to turn the steering wheel, and by how much, by considering the membership functions of the relevant inputs. A basic representation of the fuzzy inference system is shown in Figure 4. Inputs are simply weighted by the membership functions by considering certain situations defined by the fuzzy rules and the output is obtained as a change in steering wheel angle. A limit can be placed on the steering wheel angle to prevent extreme manoeuvres. In this study the steering wheel angle has been limited to ± 80º. This represents a maximum of ±5º steer angle at the road wheel with a steering gear ratio of 16. The gear is placed just after the fuzzy controller to represent the real gear ratio concept of the vehicle steering wheel system. Therefore, various maximum values of the road wheel steer angle can be provided for different steering systems.

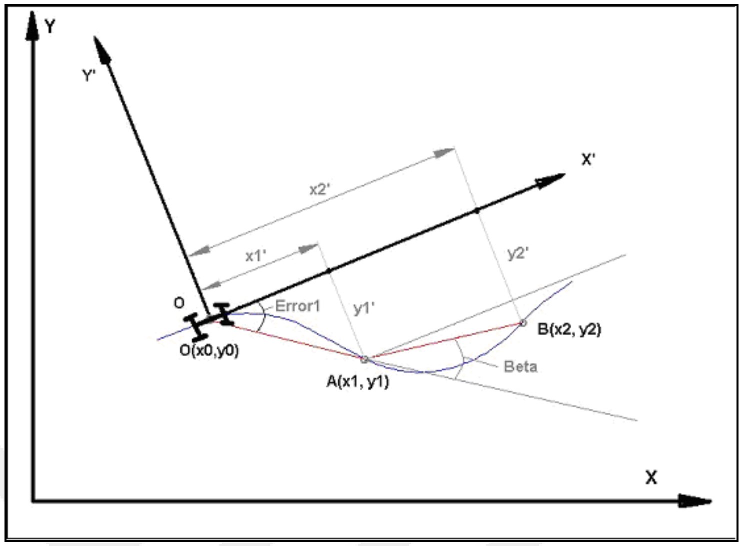

Figure 3. Moving axis system and the error formation.

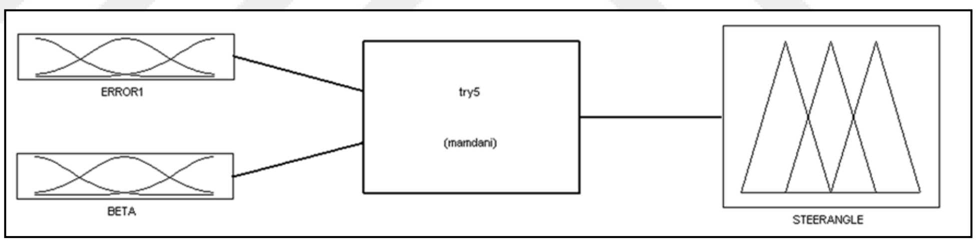

Figure 4. The inputs and outputs of the fuzzy inference systems

INPUT MEMBERSHIP FUNCTIONS

A membership function defines how each point in the input space is mapped to a degree of membership from 0 (non-member) to 1 (full membership). The inputs to the fuzzy inference system used in this study are Error1 and Beta which have been previously defined. Figure 5 shows the membership functions defined for Error1.

- There are seven membership functions namely [-]C, [-]B, [-]A, ZERO, [+]A, [+]B and [+]C which are used as inputs to the fuzzy inference system in terms of Error1. Each function possesses a degree of membership to which a weighting factor can then be applied depending on the vehicle’s position in relation to the target point, along with the combined rules:

‘A’ represents small values of the angle Error1 either in positive or negative direction.

‘B’ represents medium values of the angle Error1.

‘C’ represents high values of the angle Error1.

- X-axis of the membership function refers to the current value of Error1 i.e. the angle between the current heading direction and the direction of the first target point. The angle range shown in Figure 3.4 is kept at ±20º to show the narrow ranged membership functions ZERO, A and B. However the actual range of C extends through ±180º to represent higher values of the angle Error1.

- Y-axis of the membership function refers to a logical degree of membership between 0 (false) and 1 (true).

Similarly, Beta also has seven membership functions.

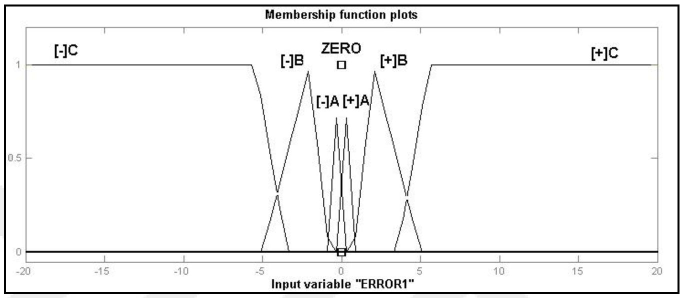

Figure 5. Membership functions of the fuzzy input Error 1

OUTPUT MEMBERSHIP FUNCTIONS

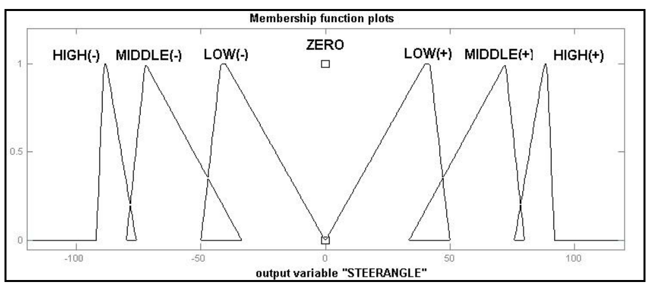

Figure 6. Membership functions of the fuzzy output Steer angle

The membership functions of the output of the fuzzy inference system as a function of the output steer angle are shown in Figure 6.

Seven membership functions are defined for the output data:

- High(+) for (+) positive high steering angles

- Middle(+) for moderate positive steering angles

- Low(+) for (+) low positive steering angles

- Zero for zero steering angle

- High(-) for (-) negative high steering angles
- Middle(-) for moderate negative steering angles
- Low(-) for (-) low negative steering angles

The output in terms of change in steering angle depends not only on the membership functions but also on the defuzzification method. A number of defuzzification methods are available e.g.: 'largest of maximum (lom)', 'mean of maximum (mom)', 'smallest of maximum (som)' and 'centroid' [9]. For instance, if the defuzzification method is chosen as '**centroid**' then the angle returns the centroid of the area under the membership function. The proposed model is thought to be best represented by the centroid type of method because of consistency at the angle changes. The methods like 'lom' and 'som' can cause sharp increases and decreases in steering angle, which a human driver cannot achieve in terms of steering wheel angle.

PROCESSING THE RULES

The following are some examples of the processing rules used by the fuzzy inference system:

1. If **Error1** is (+A) then **SteerAngle** is LOW(+) [1]

2. If **Error1** is (-C) then **SteerAngle** is HIGH(-) [1]

3. If **Error1** is (-A) and **Beta** is C(-) then **SteerAngle** is MIDDLE(-) [1]

The terms in the rules have been explained in the previous sections. The number in bracket after the rule represents the weighting factor for that particular rule. This ranges from 0 to 1. A positive value of Error1 indicates that the defined point is in the positive area of the coordinates with respect to the current vehicle position. The fuzzy driver can interpret this as a requirement to turn to the left, which is taken positive. Because the angle is low (+A), the fuzzy pilot reacts softly making a slight change, which is Low(+) in steer angle. However, a high negative value of the error, (-C) as in the rule number 2 means that the target point makes a large angle with the instantaneous direction of the vehicle. Therefore, the fuzzy pilot interprets this as a requirement to turn right, i.e. opposite action to that required by rule 1. Moreover a large change in steering angle is required, hence High(-). The third rule is more complex than the first two. Error1 is a low negative angle, therefore, the steer angle should decrease slowly; however, a negative value of the angle Beta makes different demands. Because Beta is an angle difference between the instantaneous direction of the first target point and the direction from the first to the second target point, (Eq.6), any negative Beta indicates that the second target point is to the left of the first one. Since this negative angle has a large value a sharp turn the left is required to reach the second target from the first.

$$Beta = -Error1 - \tan^{-1}\left(\frac{y_2' - y_1'}{x_2' - x_1'}\right) \qquad \text{[Eq.6]}$$

The main objective of the pilot is to pass through the first defined target while heading towards the second target at an angle, which is as narrow as possible. To achieve this objective, even if a low steer angle decrement is enough to reach the first target (LOW[-]), a sharper turn is preferred to get the vehicle into position to make the approach to the second target easier. Therefore, the output membership function MIDDLE(-) is chosen to satisfy this objective.

The other rules are based on similar logic and are applied to cover every possible operational situation. Further examples and discussions on processing the rules are included in the Simulation results section.

SIMULATION & RESULTS

Some sample simulation results obtained from the developed Simulink model are considered in this section. Basic vehicle parameters used for the simulations are shown in Table 1.

Table 1. Vehicle parameters used for the simulation

VEHICLE PARAMETERS	VALUE
Roll Inertia Ixx (kgm^2)	507
Yaw Inertia Izz (kgm^2)	1728
Height of C.G. (m)	0.6
Wheelbase (m)	2.3
Vehicle Mass (Front) (kg)	626.087
Vehicle Mass (Front) (kg)	573.917
Total Vehicle Mass (kg)	1200
Height of C.G. Unsprung Mass	0.3
Track Width (m)	1.3

DEFINED VEHICLE TRAVEL COORDINATES:

X (0, 30, 60, 90, 120, 105, 70, 40);

Y (0, 8, 0, 8, 25, 100, 150, 175);

The results in figures 7 to 10 are for simulations carried out at a number of vehicle forward velocities for 2DOF and 3DOF models traversing the defined coordinates. The results are compared both in terms of velocities and 2DOF and 3DOF system vehicle models. The defined (X, Y) coordinates define a path through a chicane followed by a sharp turn through an obtuse angle. The proposed straight-line paths through the defined points are shown by using the arrows in black starting in figure 7 and figure 8. The actual trajectories described by the 2DOF vehicle model at different speeds are shown in figure 7 while those for the 3DOF model are shown in fig 8. The Fuzzy Logic control rules used in the simulation have been kept at a minimum for these first set of simulations. The basic approach in the fuzzy control is to realise the defined path using the angle error to the first target point as an input to the controller while taking into consideration the required angle of approach to the first target for its subsequent heading towards the second target. Once the first target point is reached, the second point becomes the primary target and the third point the secondary target etc.

The results show that at low speed the 2DOF vehicle model can traverse the points quite accurately, but as the speed increases beyond 50 km/hr the vehicle is unable to generate enough cornering power to traverse the points accurately. The 3DOF model is less accurate than the 2DOF model in traversing the points at speeds beyond 20 km/hr. This is due to the loss of cornering power resulting from weight transfer across the vehicle due to rolling. Figures 9 and 10 show the comparative accuracy of the 2 models at speeds of 60 km/hr and 20 km/hr

Table 2. Time to complete the defined path

Vehicle Speed (kph)	Time (sec) 2 DOF	Path length (m) 2 DOF	Time / 3 DOF (sec)	Path length (m) 3 DOF
10	113.8	316.11	114.2	317.22
20	57.27	318.17	57.5	319.44
50	23.07	320.42	23.62	328.05
60	19.91	331.83	22.17	369.5

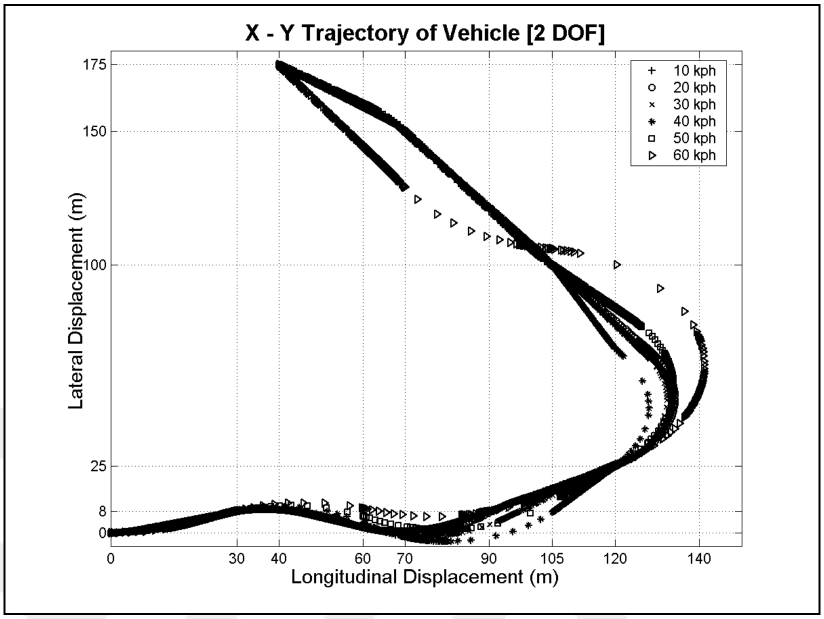

Figure 7. X-Y trajectory of the vehicle at various forward speeds for 2 and 3 DOF model

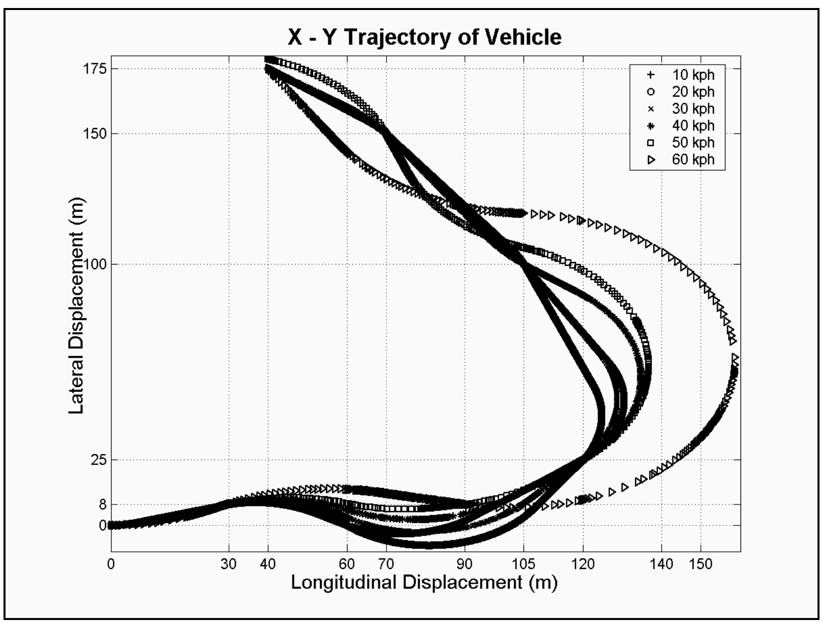

Figure 8. X-Y trajectory of the vehicle at various forward speeds for 3 DOF model

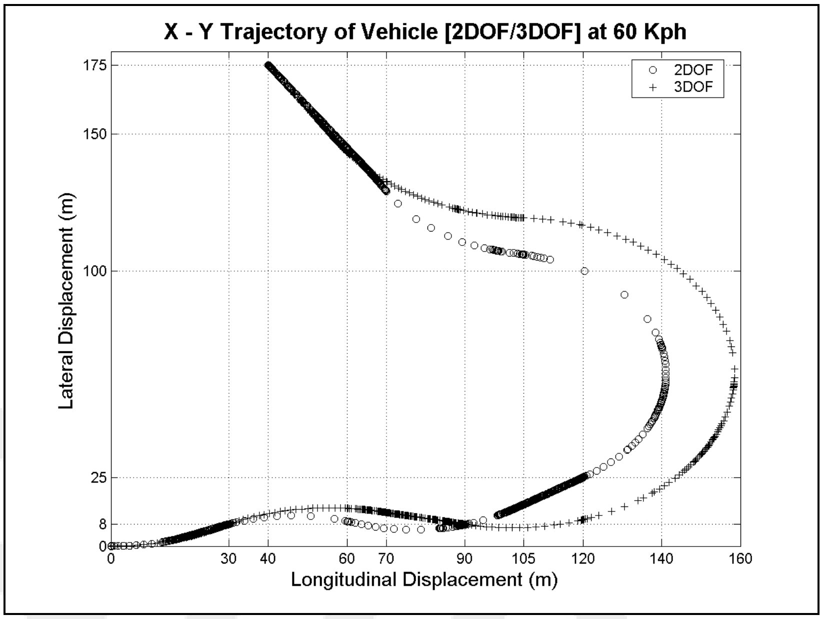

Figure 9. X-Y trajectory of the vehicle at 60 Kph forward speed.

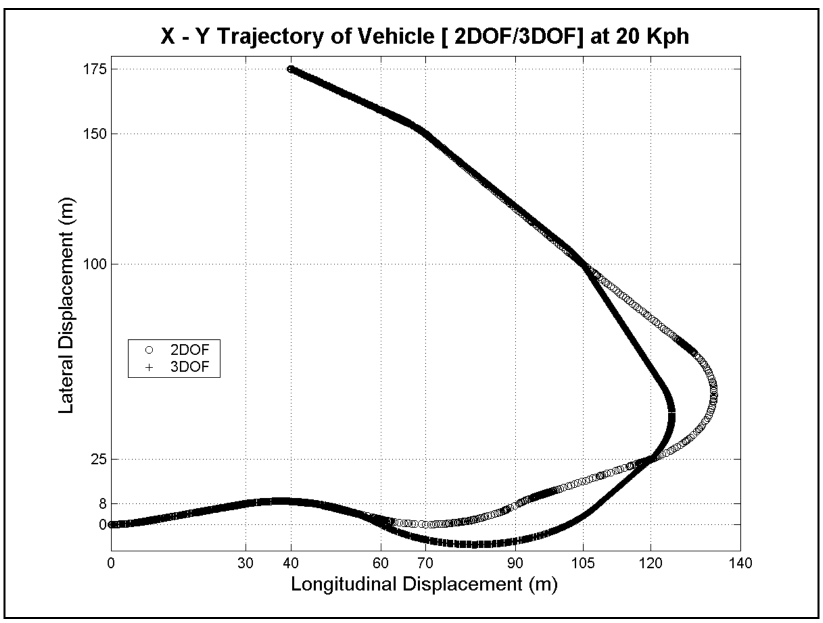

Figure 10. X-Y trajectory of the vehicle at 20 Kph forward speed

CONCLUSIONS

A fuzzy path-planning model has been developed. The model is intended to mimic a real driver by using fuzzy logic control algorithms. This enables realistic paths, which can be used for vehicle dynamics handling tests to be generated without the use of complicated mathematical functions. The preliminary results shown indicate that a fuzzy pilot is able to mimic a real driver. At low vehicle speeds a path through the specified points can be traced with good accuracy. At higher speeds there is some loss of accuracy, partly due to limitations in the handling dynamics of the vehicle. This is evident from the comparison of the paths generated by the 2DOF and 3DOF vehicle models where the loss of cornering power of the 3DOF models due to lateral weight transfer results in loss of accuracy. There is a need to improve the fuzzy inference system to mimic a real driver more accurately. Certainly, the achievable path through any set of points is limited by dynamics limits of the vehicle and the interconnection between the vehicle and driver. Further improvements may be achieved with the implementation of automatic control systems such as vehicle yaw rate control.

REFERENCES

1. Lauffenburger, J. Ph., Basset, M., Coffin, F., Gissinger, G. L., (2002). Driver-aid system using path planning for lateral vehicle control. Control Engineering Practice 0, pp. 1-15.

2. Tan, H.S., Lane changing with look-down reference systems on automated highways. Control Engineering Practice, 8 (200), pp.1033-1043, (2000).

3. Aracil, J., Heredia, G., Ollero, A., Global stability of fuzzy path tracking using frequency response. Engineering Applications of Artificial Intelligence, vol. 13, pp. 109-119, (2000).

4. Mouri, H., Furusho, H., Investigation of automatic path tracking comparing the performance of LQ control with that of PD control, Trans. JSAE, Vol. 30, No. 1, pp. 121-126 (1999).

5. Furusho, H., Mouri, H., Research on automated lane tracking using linear quadratic control procedure for curved path, JSAE Review, vol. 20, No. 3, pp. 325-329 (1999).

6. Marumo, Y., Mouri, H., Wang, Y., Kamada, T., Nagai, M., (2000). Study on automatic path tracking using virtual point regulator. JSAE Review 21, pp. 523-528.

7. Piancastelli, L., Sarubbi, G., An EESP Fuzzy control system for the recovery of the initial direction after an initial spin. XII ADM Conference Proceedings, Rimini-Italy, pp. 134-143. (2001).

8. Best, M. C., Gordon, T., J., Real time state estimation of vehicle handling dynamics using an adaptive kalman filter. AVEC ’98, Proc., 9836590, pp. 183-188, (1998).

9. Fuzzy logic toolbox tutorial, The Mathworks Inc., (2002).

A FUZZY LOGIC APPLICATION ON VEHICLE PATH PLANNING AND YAW CONTROL

E. Uzunsoy & O. A. Olatunbosun

Vehicle Dynamics Group
School of Engineering
Mechanical and Manufacturing Engineering
University of Birmingham
Edgbaston
Birmingham B15 2TT

In this paper, fuzzy vehicle path planning and the preliminary results of the vehicle yaw control are discussed. In the last decade, intelligent control schemes have been increasingly applied in various fields. However, there is still a lack of experience in the intelligent control schemes such as fuzzy logic and neural networks in the automotive applications. A vehicle model is used in conjunction with the fuzzy driver model to generate the vehicle's path through a number of specified points through which the vehicle must pass. The simulation is carried out in the Matlab© programming environment using a Simulink© vehicle model under Fuzzy logic control intended to imitate how a real driver would steer the vehicle to create a path through the specified points. While the response of the vehicle is assumed as a real driver's actions, the same fuzzy logic controller is used to control the yaw motion of the vehicle by applied braking and tractive forces at each wheel, independently.

Introduction

Computer simulations have been a greater importance in revealing the vehicle responses in the design process than ever before. The vehicle manufacturers have been focused on the zero-prototype vehicle production by the new developments in the computer technology. From the computer simulation point of view, having a general path planner can present the researcher with great flexibility in defining vehicle handling dynamics tests. Vehicle handling dynamics tests can be classified as constant radius turn, constant steer angle turn, lane change and sinusoidal manoeuvres. In the simulation studies, constant steer angle turn type tests can simply be managed by the basic vehicle modelling taking the steer angle as a controller input. A lane change manoeuvre can simply be represented by sinusoidal steer, with the frequency and amplitude of the sine function being used to define the vehicle position. However, the steering input required for a lane change manoeuvre by a driver driving a real vehicle is not sinusoidal and the vehicle path cannot be represented by a simple mathematical function. As a result, complex mathematical functions like polynomials are used to define the vehicle path in this respect.

Polar polynomial curves to represent the vehicle path were applied by Lauffenburger et al. Fuzzy logic control is used to define the maximum and minimum points of the polynomial in terms of experience. A number of vehicle path tracking researches (Tan, 2000 – Aracil *et al*, 2000) are mainly aimed at the future automated highway systems and a number of different approaches have been used in these studies. A path tracking system was proposed to regulate the lateral position at the centre of gravity of the vehicle by minimising a cost function based on the lateral displacement at the centre of gravity and the front wheel steering angle (Mouri and Furusho, 1999). A virtual point regulator, which also takes the yaw angle into consideration in addition to this basic approach, has been proposed (Marumo *et al*, 2000).

Meanwhile, intelligent control systems like fuzzy logic and neural networks in the vehicle dynamic tests can be used to represent the driver's sight and possible reactions while additional mathematical modelling is avoided. From this point of view, a fuzzy driver model which can be used in conjunction with a vehicle model of any complexity provided it is available as a Simulink© model for any vehicle manoeuvre is introduced (Uzunsoy and Olatunbosun, 2003)

A provided vehicle path by the fuzzy driver model is used to analyse the vehicle responses for the purpose of controlling the vehicle yaw. If the traction force and braking force are properly distributed to the right and left wheels, a yaw moment will be obtained in accordance with the forces distributed and thus the vehicle lateral motion can be accurately controlled. A yaw control system controls the vehicle motions by a yaw moment, which is actively generated by the intentional distribution of the tyre longitudinal forces. One of the important advantages of this method is that the tyre longitudinal force has no feed back from the vehicle motion as long as it is within the limit of the tyre capacity due to the vertical load. These systems using tractive / braking forces have been researched and developed to improve handling and stability. One such system uses active traction control system of each wheel through the feedback of state variables, such as yaw rate and/or vehicle body slip angle. These active control systems can generate yaw moment directly to compensate for vehicle yaw motion not only in linear ranges but also in non-linear ranges. Therefore, the direct yaw moment control systems are expected to suppress the deterioration of the steering control effects in non-linear or large lateral acceleration ranges (Furukawa, Y., Abe, M., 1997). Vehicle yaw rate error is used as the control parameter in this study while the corrective braking and traction forces are applied on the wheels individually. The model is developed in the Matlab© programming environment using a Simulink© vehicle model under Fuzzy logic control intended both to mimic how a real driver would steer the vehicle to create a path through the specified points and to control the vehicle yaw rate at the same time and the simulation is carried out in the Handsim, which is a vehicle handling dynamics simulation tool (Uzunsoy and Olatunbosun, 2001). The complexity of the path is defined by the specified points and their spacing, which can be used to describe road features such as corners, chicanes etc.

Vehicle Dynamics Model

The vehicle dynamics models applied in this study are well known two-degree of freedom (2 DOF), bicycle model (Equations 1 and 2), which is to provide the reference yaw rate for the planned vehicle path and four-degree of freedom model (4 DOF). The 4 DOF model adds the longitudinal and roll dynamics of the vehicle into the model (Equations 3 and 4). However, because the braking and traction forces applied are assumed as corrective small forces, longitudinal load transfer is ignored.

2 DOF Model Equations

$$\sum F_y = m(\dot{V} + rU) \quad \text{[Eq.1]}$$

$$\sum M_z = I_{zz} \cdot \dot{r} \quad \text{[Eq.2]}$$

4 DOF Model Equations

$$\sum F_x = m(\dot{U} + rV) \quad \text{[Eq.3]}$$

$$\sum F_y = m(\dot{V} + rU) \quad \text{[Eq.4]}$$

$$\sum M_x = I_{xx} \cdot \dot{p} \quad \text{[Eq.5]}$$

$$\sum M_z = I_{zz} \cdot \dot{r} \quad \text{[Eq.6]}$$

Braking and Traction Forces

The derivation of the braking and traction forces is shown from the Equation 7 to 10, below. The brake gain depends on the type of the brake, which is for disc brake presented in this study. The notations used for the equations are defined in the Table 1.

$$T_b = bgain \cdot P_b \quad \text{[Eq.7]}$$

$$F_b = T_b / rt \quad \text{[Eq.8]}$$

$$T_d = dgain \cdot thr \quad \text{[Eq.9]}$$

$$F_x = T_d / rt \quad \text{[Eq.10]}$$

Table 1. Notations used in the model equations

$F_{x,y}$	Longitudinal and lateral forces [N]	**F_b**	Braking force
$M_{x,z}$	Moments on the x and z directions [Nm]	**T_b,T_d**	Braking and driveline torque
m	mass of the vehicle [kg]	**rt**	Effective tyre radius
V	Vehicle lateral velocity, acceleration	**bgain**	braking gain
r	vehicle yaw rate	**dgain**	Driveline gain
U	Vehicle forward velocity	**thr**	Throttle position in percentage
I_{xx},I_{zz}	Inertias on the x and z directions	**P_b**	Brake pressure
p	vehicle roll rate		

Fuzzy Path Planning & Yaw Rate Control

Simulink model of vehicle is shown in the Figure 1. The steer angle input provided by the fuzzy logic controller is processed in both 2-DOF and 4-DOF vehicle models. The whole simulation is run by the 4-DOF vehicle model. However, the 2-DOF model which is run by the same driver's actions presents the idealised or maximum achievable manoeuvre option for any time step. Yaw rate error is obtained by the difference between the reference yaw rate from the 2-DOF and the yaw rate from the 4-DOF model. Control logic is based on a four wheel drive vehicle which the traction force can be distributed either to the front or rear axle at any particular time. Also it is assumed that each wheel brakes include independent actuators for the small braking inputs. For instance in a left turn manoeuvre, if the yaw error is greater than 'zero', the vehicle tends to travel to the right side of the path achievable by the ideal vehicle. Then, a small brake pressure is applied on the left-front wheel. This action aims to make up the yaw rate loss of the vehicle. However, both the corrective braking inputs and the lateral forces on the steered front wheels cause the vehicle to loose its speed. The aim is, as an ordinary driver would do, to keep the vehicle at almost constant speed. Therefore, if the braking force is on the front wheels a traction force is applied to the rear axle or vice-versa.

Simulink Model & Fuzzy Logic Controller

Fuzzy inference system for path planning and vehicle yaw rate control is shown in the Figure 2. The controller has three inputs for the path planning, which are the angles to the first and second defined points and the distance between the target point and the current point of the vehicle (Error1-Error2). The fourth input is the yaw rate error for the yaw control.

There are nine outputs in the inference system. These are steer angle, braking pressure P_b and the driveline torque T_d for each wheel. Because the vehicle path planning was subject to another study (Uzunsoy & Olatunbosun, 2003). Therefore, only the yaw rate control results are being focused in this study.

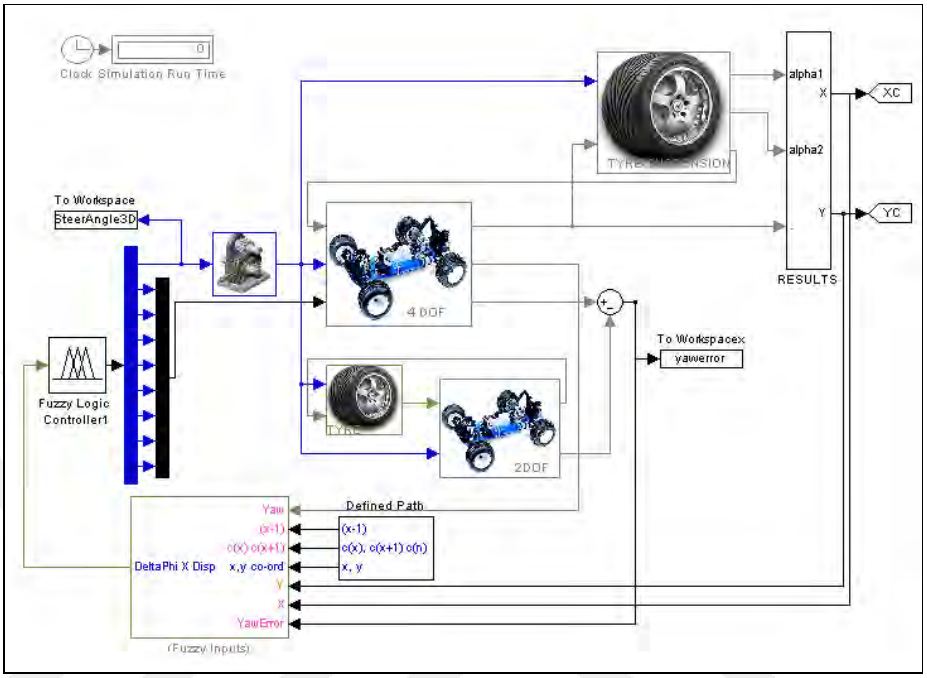

Figure 1. Vehicle Simulink model.

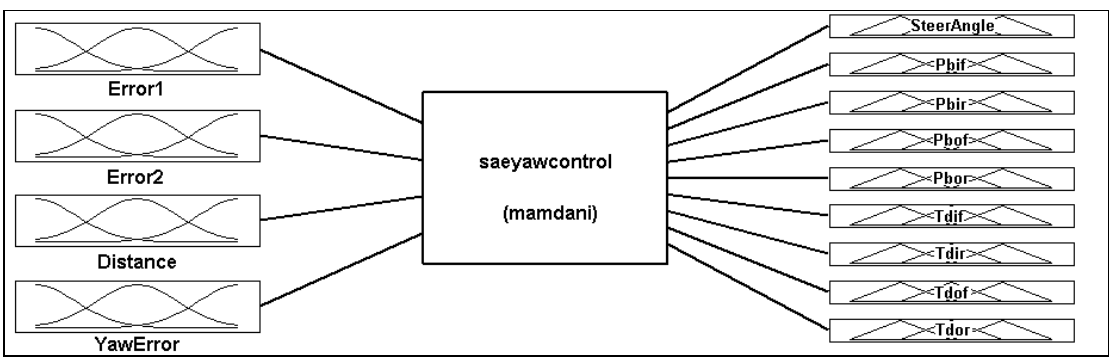

Figure 2. Fuzzy inference system (FIS) for path planning and yaw rate control

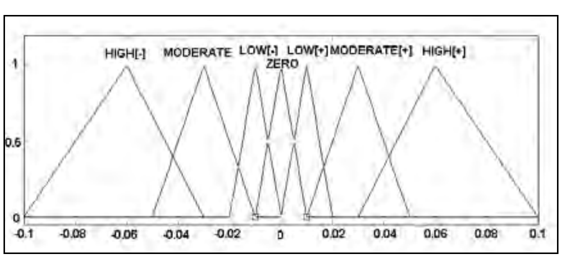

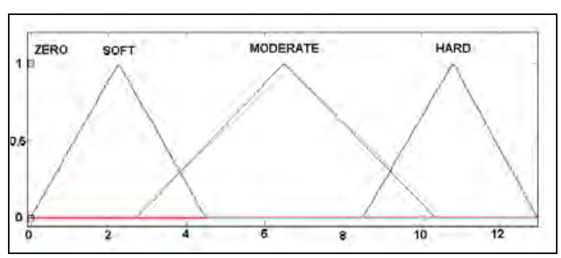

Figure 3. MFs for YawError **Figure 4. MFs for Brake pressure**

Fuzzy Logic Rules

Some of the basic rules applied in the fuzzy logic controller to take the vehicle yaw and forward velocity under control are shown in the Table 2. In the table, while 'I' and 'O' refer to 'inner' and 'outer', 'F' and 'R' refer to 'front' and 'rear', respectively.

Table 2. Basic Fuzzy Rules for the Yaw Rate Control

INPUT	**OUTPUTS**							
	Braking Pressures (Pb)				**Driveline Torques (Td)**			
YawError	**IF**	**OF**	**IR**	**OR**	**IF**	**OF**	**IR**	**OR**
ZERO	ZERO	ZERO	ZERO	ZERO	-	-	-	-
LOW[+]	-	-	-	LOW	LOW	LOW	-	-
LOW[-]	LOW	-	-	-	-	-	LOW	LOW
MODERATE[+]				MOD.	MOD.	MOD.	-	-
MODERATE[-]	MOD	-	-	-	-	-	MOD	MOD
HIGH[+]				HIGH	HIGH	HIGH	-	-
HIGH[-]	HIGH	-	-	-	-	-	HIGH	HIGH

Simulation and Results

Simulation is carried out using the parameters for a racing car which was produced in the University of Birmingham, for the purpose of Formula SAE student racings. Some sample simulation results obtained by the developed model are considered in this section. The simulation is run at 20 kph with the defined points X(0, 30, 60, 90, 120, 105, 70, 40) and Y(0, 15, 0, 8, 25, 120, 150, 120).

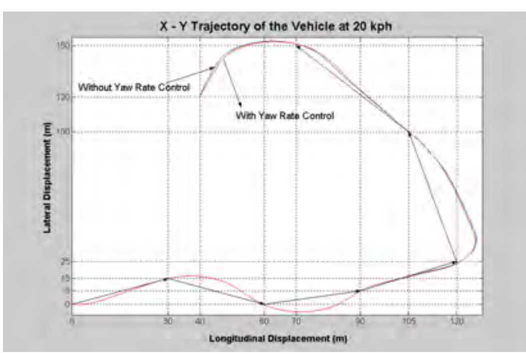

Figure 5. X-Y Trajectory with and without yaw rate control

Figure 6. Vehicle forward velocity with and without control

Conclusions

Fuzzy path planning and yaw rate control are applied on a Formula SAE Student racing car. A racing car is supposed to has better handling characteristics than an ordinary passenger car due to its design properties. Therefore it is expected that the refinement obtained by the yaw rate control can be less than a passenger car. However, the preliminary results show that a reasonable compromise obtained by the combined braking and tractive force inputs and it is shown that with a proper tuning of the fuzzy rules the efficiency of the controller and the handling dynamic properties of the vehicle can be improved.

References

Aracil, J., Heredia, G., Ollero, A., 2000, Global stability of fuzzy path tracking using frequency response. *Engineering Applications of Artificial Intelligence*, **13**, pp. 109-119.

Furukawa, Y., Abe, M., 1997, Advanced chassis control systems for vehicle handling and active safety", *Vehicle System Dynamics*, **28**, pp. 59-86.

Lauffenburger, J. Ph., Basset, M., Coffin, F., Gissinger, G. L., 2002. Driver-aid system using path planning for lateral vehicle control. *Control Engineering Practice 0*, pp. 1-15

Mouri, H., Furusho, H., 1999, Investigation of automatic path tracking comparing the performance of LQ control with that of PD control, *Trans. JSAE*, **30**, No. 1, pp. 121-126.

Tan, H.S., 2000, Lane changing with look-down reference systems on automated highways. *Control Engineering Practice*, 8 (**200**), pp.1033-1043.

Uzunsoy, E., Olatunbosun, O. A., 2001, A new vehicle handling dynamics simulation tool: Handsim, *7th Proceedings of Annual Research Symposium of Postgraduate Research-Birmingham University*, pp. 26-30.

Uzunsoy, E., Olatunbosun, O. A., 2003, A generic fuzzy pilot and path planning for vehicle handling dynamics studies, SAE Conferences-Future Transportation Technologies, 3 FTT

A NEW VEHICLE HANDLING DYNAMICS SIMULATION TOOL: HANDSIM

E. Uzunsoy & O. A. Olatunbosun

Automotive Research Group
School of Manufacturing and Mechanical Engineering
University of Birmingham
Edgbaston
Birmingham B15 2TT

This paper presents a new vehicle handling dynamics simulation tool, HANDSIM, which is being developed for advanced handling dynamics studies. The simulation is carried out using MATLAB®, which is a matrix based computation environment. The Mathematical model is adapted into the Graphical User Interface (GUI) for ease of use. The goal of this work is to produce a tool for the handling dynamics of vehicles using state of the art simulation techniques. The preliminary results will be validated by comparing them with results obtained from CarSimEd®, a well-known vehicle dynamics simulation tool.

Introduction

Computer models for simulating automotive vehicle braking and handling dynamics have been in use for decades. The main reason for this is financial. It costs much less to try an idea on a computer than out on a test track. It is cheaper and much faster to digitally prototype. There are also a number of situations, which are very difficult and costly to test experimentally like roll over limits of trucks. However, very complicated mathematical models are needed to represent real vehicle handling situations correctly but consideration of cost and accuracy limit the ability of most models to reproduce real life behaviour. Some of the early simulations used special hardware and were capable of real time simulation. Whether the simulations were performed with analogue, digital, or hybrid computers, model equations were formulated as a set of non-linear ordinary differential equations (ODEs). Although vehicle simulation was shown to be technically feasible, the software was so difficult to use that simulation remained an exotic technology, limited to researchers and few specialists. However, in the mid-1980's two new types of software became available that helped make simulation a more popular engineering tool. One is the interactive graphical simulation environment, such as Simulink/MATLAB®. The other is the mechanical multibody simulation program such as ADAMS® (Sayers, 1998).

The creation of HANDSIM was motivated by the need to provide simple and accurate design and development of a controller for stabilisation of a vehicle during cornering manoeuvres, which will be carried out in the next phase of this study. Accuracy of vehicle handling simulation is highly dependent on the fidelity of the tyre model, which generally requires very complex analytical representation, as discussed in a later section. For this reason, measured tyre data is implemented directly as a tyre model by using interpolation methods. Therefore, determination of a large number of coefficients for a complex mathematical representation is avoided. Furthermore, an opportunity is been given to include non-linearities inherent in tyre data obtained under realistic test conditions. As a result, an easy to use handling model, which can be regarded as a semi-linear handling model, has been obtained. The model provides for a library of tyre data to be implemented from which the appropriate tyre data set can be selected for use in vehicle handling simulation. The validation is done by using the CarSimEd® which is a popular vehicle handling simulation and analysis software.

Tyre Model

The pneumatic tyre represents the interaction points between the vehicle and the road surface and therefore its dynamic behaviour is of vital importance in vehicle handling studies. According to Rahnejat (2000), tyre models for vehicle-handling dynamics studies may be classified in two main categories: those employing basic physical equations to create a model by considering tyre structure and material properties, referred to as physical tyre model, or those using measured data in a graphical or tabulated format or using empirically obtained formulae that is called as empirical tyre models. The pneumatic tyre is made up of a multi-layered, non-uniform, anisotropic, cord-rubber composite (Dixon, 1996). Therefore, a physical model, which takes into account the detailed construction, can only be achieved by techniques such as finite element analysis. Therefore, tyre modelling constitutes an entire subject area by itself. Some simplification is thus required in representing tyre behaviour for use in vehicle handling studies. As a result, It is better to build a model on the basis of measured tyre data. For that reason, interpolated tyre data are used in this study to implement a model into the vehicle-handling model. Figure 1 shows the tyre handling characteristics surface developed from measured data for a DUNLOP 195/65 R15 tyre using interpolation techniques (Blundell, 1997).

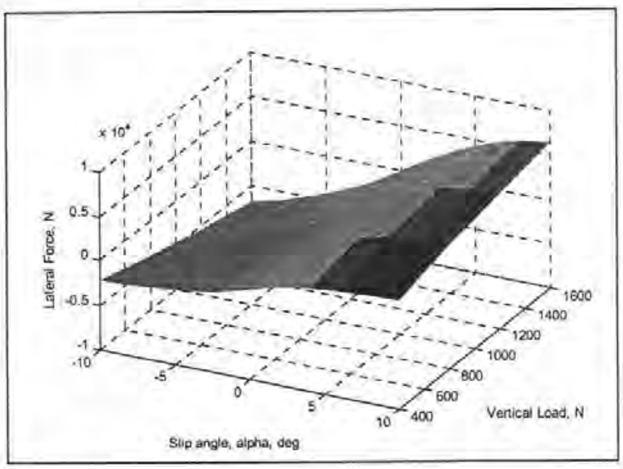

Figure 1. Interpolation tyre data for DUNLOP 195/65 R15

Vehicle Handling Modelling

This model is implemented in the form of relatively simple two-degree and three-degree of freedom handling dynamics models. The vehicle is assumed to be travelling on a smooth road surface, however, lateral load transfer is included to allow roll movement of the vehicle (3DOF Model) during lane change or cornering manoeuvres. Using the notation and data defined in Table 1, the dynamic equations of motion are derived based on the ISO axis system (Fig. 2) as follows:

Table 1. Model derivation parameters.

Symbol	Definition	Unit	Symbol	Definition	Unit
m	Total vehicle mass	kg	r, $\dot{r}$	Yaw velocity, acceleration	deg/s deg/s^2
U	Longitudinal velocity	m/s	Y	Vehicle side force	N
V, $\dot{V}$	Lateral velocity. acceleration	m/s m/s^2	N	Vehicle yaw moment	kgm^2/s
W	Vertical velocity	m/s	L	Vehicle roll moment	kgm^2/s
p, $\dot{p}$	Roll velocity, acceleration	deg/s deg/s^2	I	Inertia moment	kgm^2
q, $\dot{q}$	Pitch velocity, acceleration	deg/s deg/s^2		Roll angle	deg

The model equations are derived using Newton Laws and simply reduced into the form given in equations (1), (2), (3), (4), and (5). In the classical vehicle handling analysis, for the constant longitudinal velocity, the longitudinal motion of the vehicle in the x-axis can be ignored for both 2DOF and 3DOF model.

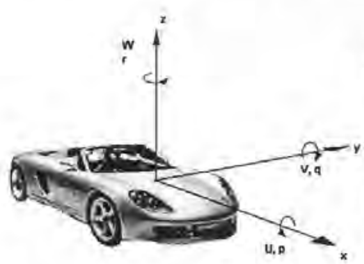

Figure 2. ISO axis System

2 degree of freedom model:

$$m(\dot{V} + rU) = Y \quad - Y_v V - Y_r r \tag{1}$$

$$I_{zz}\dot{r} = N_s s - N_v V - N_r r = [illegible] M_z \tag{2}$$

3 degree of freedom model:

$$m(\dot{V} + rU) = Y \quad - Y_v V - Y_r r - Y_p p + Y \tag{3}$$

$$I_{zz}\dot{r} = N_s s - N_v V - N_r r - N_p p + N \tag{4}$$

The notation of the Y, N, and L indexed with the variables V, r, and s are called stability derivatives, which denote the rate of change of lateral force, yaw moment and roll moment with respect to these variables.

The MATLAB environment provides standard solutions for ordinary differential equations (ODEs). The MATLAB ode45 algorithm is used as a solver for the equations of motion. It is based on an explicit Runge-Kutta (4, 5) formula, the Dormand-Prince pair. In general, ode45 is the best method for the 'first try' for the most problems. (Mathworks). Equations of motions have been transformed to m. files, which can be run in MATLAB environment.

Simulation, Results & Validation

HANDSIM has been implemented with a graphical user interface, created in MATLAB® for ease of use. Results obtained from HANDSIM have been validated using CarSimEd®. For the comparison of the simulation results the parameters have been partly chosen from CarSimEd®'s ready to use data files. The rest of the parameters have been equalised by considering different input parameters required for HANDSIM and CarSimEd®. Simulation control parameters and some of the vehicle parameters used for both tools are presented below in tables 2 and 3. The comparison shown here is based on HANDSIM's 3DOF vehicle handling model with understeer vehicle characteristics. Simulation run time also has an important place in analysis. However, it also depends on the computer speed. The CarSimEd® model has much more complexity than the current HANDSIM model implementation, hence it is hardly surprising that HANDSIM's run time is less than half of that of CarSimEd® for an equivalent model.

Table 2. Control parameters of

CONTROL PARAMETERS	VALUE
Longitudinal Velocity	50 kph
Steering Angle	3°
Simulation Time	10 sec

Table 3. Some of the vehicle parameters used in comparison

VEHICLE PARAMETERS	VALUE
Roll Inertia Ixx (kgm^2)	507
Yaw Inertia Izz (kgm^2)	1728
Height of C.G. (m)	0.6
Wheelbase (m)	2.3
Vehicle Mass (Front) (kg)	626.087
Vehicle Mass (Front) (kg)	573.917
Total Vehicle Mass (kg)	1200
Height of C.G. Unsprung Mass	0.3
Track Width (m)	1.3

The resultant graphs of both simulation tools are depicted in the figures 3 to 8 below. All figures except Figure 7 and 8 show both the CarSimEd® and HANDSIM results together. In general there is close agreement between the results obtained form the two different simulation tools. As it can be seen from the Figure 3, X-Y trajectory of the vehicle during the given simulation time period, almost the same as in each simulation tools. In like manner, the results

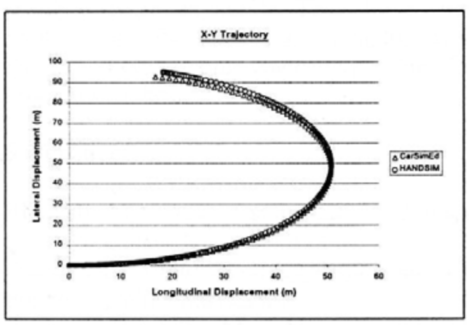

Figure 3. X-Y Trajectory of the vehicle

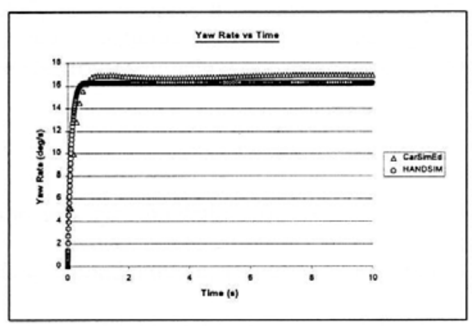

Figure 4. Vehicle yaw rate vs time

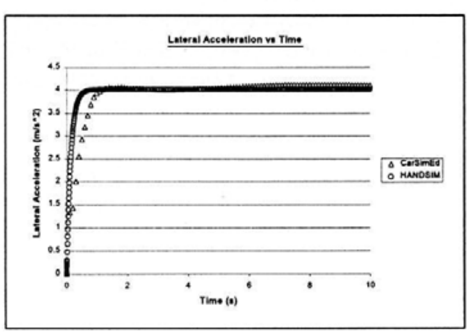

Figure 5. Vehicle lateral acceleration vs time

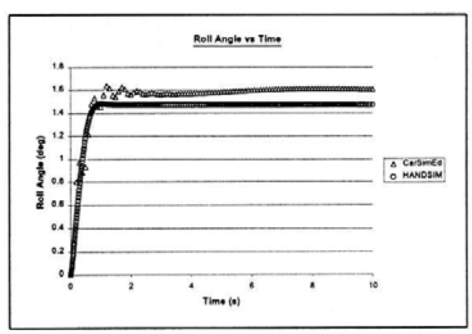

Figure 6. Vehicle roll angle vs time

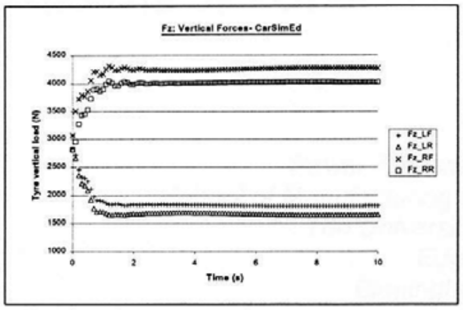

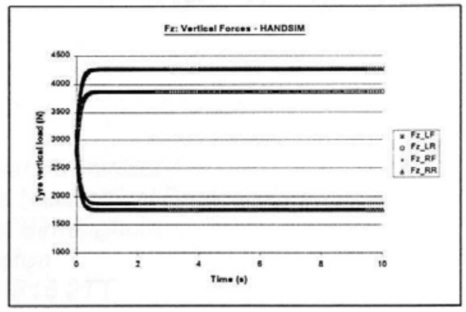

Figure 7. Lateral load transfer: CarSimEd

Figure 8. Lateral load transfer: HANDSIM

of acceleration, velocity and load transfer show close agreement. However, it is also clear that the transient response in the CarSimEd® takes a bit more time to reach steady conditions than the HANDSIM. The difference is particularly apparent in the figures 6, 7 and 8, which are mainly affected by the suspension characteristics of the vehicle. Since CarsimEd® includes more complex suspension characteristics in detail, this is not unexpected. In addition, it includes the relaxation dynamics of the tyre, road friction, suspension models with non-linear springs and dampers, etc.

Conclusions

The current study shows that for certain model parameters, the HANDSIM and the CarSimEd® represent the reasonably similar results. The goals of simplicity and accuracy have been successfully achieved during the first phase of the study. Therefore, it is shown that the HANDSIM can be developed for further studies so that it can be used in advanced vehicle handling dynamics studies. Thus, the ongoing study is to increase the model complexity by implementing the braking and longitudinal acceleration features. However, the main goal is directed to create some control algorithms for the stability of vehicle using different steer and drive approaches.

References

Blundell, M., 1997, The influence of suspension and tyre modelling on vehicle handling simulation, *PhD thesis*, 135-144

Dixon, J.C., 1996, *Tires Suspension and Handling* Second Edition, (Society of Automotive Engineers, Warrandale, Pa.)

Rahnejat, H., 2000, Multi-body dynamics: historical evolution and application, *Proc. Instn. Mech. Engrs*, **214**, Part C, 149-172

Sayers, M.W., 1998, Vehicle models for real time simulation applications, *International Symposium on Advanced Vehicle Control, AVEC'98*, Nagoya, Japan.

The MathWorks, 1999, *Using MATLAB* Version 5, (The Mathworks Inc., Natic MA), http://www.mathworks.com.

APPENDIX C

SELECTED MATLAB PROGRAMMING ROUTINE

C1. The Matlab m.file responsible for the main control of the simulation

This m. file is written for running the simulation with the suitable vehicle parameters selections.

```
% MAINFRAME  The main 'coordinator' of simulator.
tic;

if exist('outfile')
   s = 10;
   keep outpath outfile
else
   clear
end

goofy = 0;

page1 = findobj(0,'tag','page1');                    %The page which is written 'Handling Simulation'
page1b = findobj(0,'tag','page1b');                  %"Data Entry"
pagetyre = findobj(0,'tag','pagetyre');
list2 = findobj(page1,'tag','list2');                %list2=By data list
list2_value = get(list2,'value');
manual2 = findobj(page1,'tag','manual2');            %Manual input
dataless = findobj(page1b,'tag','dataless');

if list2_value == 1
   if exist('outfile') & exist('outpath') & ischar(outfile) & ischar(outpath)
      loader1;
      goofy = manual_read(dat);
   else
      [outpath outfile] = loader;
      if outfile == 0
         goofy = 2;
      else
         loader1;
         goofy = manual_read(dat);
      end
   end
else
%%%%%%%%%%%%%%%%%%%%%%%%%%%%%%%%%%%%%%%%%%%%%%%%%%%%%%%%%%%%%%%%%%%%%%%%%%%%%%%%%%%%%%%%%%%%%%%%%%%%%%%%%%%%%%%%%%%%%%
%% %%%%%%%==>[ RETRIEVING PRE-SIMULATION PARAMETERS FROM PAGE1b ]<==%%%%%%%%
   loadedfile = findobj(page1,'tag','loadedfile');
   set(loadedfile,'string','C:\*.*');
end
%%%%%%===>[ RETRIEVING SIMULATION PARAMETERS ]<===%%%%%%%%%%%%%%%%%%%%%%

modelin = findobj(page1,'tag','in_model');           %get tag
modeluse = get(modelin,'value');                     %determine model to use

option = findobj(page1,'tag','opt_speed');
opt = get(option,'value');

steerin = findobj(page1,'tag','in_steer');
steeruse = get(steerin,'value');                     %Will return 'empty' matirx

simdata;
```

```
switch steeruse
   case 3                                                             %Generated path
      period = 0;
      notsine=1;
   case 2                                                             %sine steer
      Sineperiod = findobj(page1,'Tag','in_period');
      period = eval(get(Sineperiod,'string'));
      notsine = 0;
   case 1                                                             %constant radius
      period = 0;
      notsine = 1;
end

tita1 = read(page1,'in_tita');
if isempty(vel_Ukmh)|isempty(tita1)|isempty(time)
   goofy = 1;                                                        %checks integrity of parameters
end


%_____________________________________%
%WILL BAIL WHEN Goofy = 1 .

if goofy ~=0
   if goofy == 1
      errordlg('Null or invalid entry detected. Please check all parameters.',...
         'Vehicle Handling','replace');
   end
   break;
else

%%%%%%%%%%%%%%%%%%%%%%%%%%%%%%%%%%%%%%%%%%%%%%%%%%%%%%%%%%%%%%%%%%%%%%%%%%%%%%%%%%%%%%%%%%%%%%%%%%%%%%%%%%%%%%%%%%%%%%%%%%%%%%%%%%%%%%%%%%%%%%%%%%%
%%%%%%%%%%%%%%%%%%%%%%%%%%%%%%%% [ Error Situation for Tyre Data ] %%%%%%%%%%%%%%%%%%%%%%%%%%%%%%%%%%%%
%%% %=================================================================%

   withouttyredata = findobj(page1b,'tag','dataless');
   wthouttyre=get(withouttyredata,'value');
   s = findobj(page1b,'tag','loaddefault');
   s1 = findobj(0,'tag','pagetyre');
   s2 = findobj(pagetyre,'tag','dat24');
   ll = get(s2,'value');
   l=get(s,'value');
   z1 = findobj(pagetyre,'tag','active');
   z2 = get(z1,'value');

   if l == 0
      if wthouttyre == 0
         if z2 == 0
            warndlg('Tyre data error! Please choose a tyre data option to continue','Warning!...');
            break;
         end
      end
   end

   k = findobj(page1b,'tag','dataless');
   z = findobj(page1b,'tag','loaddefault');

   h = get(k,'value');
   h1 = get(z,'value');
   stx=findobj(page1,'tag','st');
   st = eval(get(stx,'string'));

   switch modeluse                %It selects the degree of freedom
      case 1
         if st > 0
            dof2;
         elseif steeruse ==3;
            data1;
            if mass > 800
```

```
            sim('tezicinps');%('saeyawcontrol');%[t,x,y]=
        else
            simdata2d;
            sim('saeyawcontrol2D');
        end
    end
  case 2
    if st > 0
        tridof;data1;
    elseif steeruse ==3;
        data1;
        if mass > 800
            sim('tezicinps');
        else
            simdata;
            sim('tezicin');
        end

    else
        tridof;data1;
    end

end
if modeluse == 1
  main2;           %Tyre Data
else
  data1;

end
a = fwheelbase*cor_stiff;
b = rwheelbase*cor_stifr;
k = (a - b);

vel_char = findobj(page1,'tag','vel_char');
str_char = findobj(page1,'tag','steer_text');
text_char_speed = findobj(page1,'tag','text_char_speed');
runtime = findobj(page1,'tag','runtime');
bat = 1;
switch bat
  case (k == 0)
    char_steer = 'Neutral Steer';
    disp('Neutral Steer');
  case (k < 0)
    char_steer = 'Under Steer';
    disp('Under steer');
    set(text_char_speed,'string','Characteristic Speed:');
    char_vel = (rwheelbase+fwheelbase)*(-(cor_stiff*cor_stifr)/ ...
        (mass*((fwheelbase*cor_stiff)-(rwheelbase*cor_stifr))))^0.5; % mass has multiplied by 9.807
  case ( k > 0)
    char_steer = 'Over Steer';
    disp('Over Steer');
    set(text_char_speed,'string','Critical Speed:');
    char_vel = (rwheelbase+fwheelbase)*((cor_stiff*cor_stifr)/ ...
        (mass*((fwheelbase*cor_stiff)-(rwheelbase*cor_stifr))))^0.5
end
if steeruse == 3
  finish = toc;
  set(runtime,'string',finish);
  toc;
else

  finish = toc;
  set(runtime,'string',finish);
  stat1 = findobj(page1,'tag','stat1');set(stat1,'string',nsteps);
  stat2 = findobj(page1,'tag','stat2');set(stat2,'string',nfailed);
  stat3 = findobj(page1,'tag','stat3');set(stat3,'string',nfevals);
  stat4 = findobj(page1,'tag','stat4');set(stat4,'string',npds);
  stat6 = findobj(page1,'tag','stat6');set(stat6,'string',nsolves);
  clear stat1 stat2 stat3 stat4 stat6
```

```
    toc;
  end
end
```

C2. Function file for alternating the radio buttons in the main interface

```
function pre_sim1(tag);

% alternating the radio buttons in Pre simulation box

h = get(gco,'value');

switch tag

case 'manual2'
  k = findobj(gcf,'tag','list2');

  if h == 1                      % and if h is exist,
     checked('list1',1);
     checked('preview',1);
     checked('current',1);
     checked('manual1');
     set(k,'value',0);              % then, set k (By data List) zero.The process will continue by manual input
  else
     set(gco,'value',1);
  end

case 'list2'                     % By data list
  k = findobj(gcf,'tag','manual2'); % Manual Input radiobutton: Cancels the manual data input with "set(k,'value',0)!!

  if h == 1
     set(k,'value',0);
     checked('manual1',1);
     checked('list1');
     checked('preview');
     checked('current');
  else
     set(gco,'value',1);
  end

case 'loaddefault'

  k = findobj(gcf,'tag','tyre');    % tyre is the tag of "Load New Tyre Data" pushbutton..
  k1= findobj(gcf,'tag','dataless');

  if h == 1
     checked('tyre',1);
     checked('dat1',1);
     checked('dat2',1);
     checked('corfront',1);
     checked('correar',1);
     checked('dataless',1);
     set(k,'value',0);
     set(k1,'value',0);
  else
     %set(gco,'value',0);
     checked('tyre',1);
     checked('dat1',1);
     checked('dat2',1);
     checked('corfront',1);
     checked('correar',1);
     checked('dataless',1);
     set(k,'value',1);

  end
```

```
case 'dataless'                    % Without Tyre Data pushbutton
  k = findobj(gcf,'tag','tyre');
  k1= findobj(gcf,'tag','loaddefault');

  if h == 1
     checked('dat1',0);
     checked('dat2',0);
     checked('corfront',0);
     checked('correar',0);
     checked('tyre',1);
     checked('loaddefault',1);
     set(k,'value',0);
     set(k1,'value',0);
  else
     checked('dat1',0);
     checked('dat2',0);
     checked('corfront',0);
     checked('correar',0);
     checked('tyre',1);
     checked('loaddefault',1);
     set(k,'value',1);

  end

%case 'brakethrotle'
%   k=findobj(gcf,'tag','of');


case 'opt_speed'
  k = findobj(gcf,'tag','opt_accu');

  if h == 1
     set(k,'value',0);
  else
     set(gco,'value',1);
  end

case 'opt_accu'
  k = findobj(gcf,'tag','opt_speed');

  if h == 1
     set(k,'value',0);

  else
     set(gco,'value',1);
  end
end
```

C3. Function file for alternating the interfaces for the new data entry

```
function pre_sim2(tag);

% to bring forth or create page with 'tag' when link 'Enter
% parameters' or '<< back' is pressed.
% This function controls the switching logic
% between inter1 and inter1b.

h = get(gco,'value');

switch tag
case 'page1b'                    % to switch from page1 to page1b
  x = findobj(0,'tag','page1b');
  if isempty(x)
```

```
    open ('inter1b.fig');
  else
    figure(x);
  end

case 'pagetyre'                 % to switch from page1b, to pagetyre (New Tyre data Entry window)
  x = findobj(0,'tag','pagetyre');
  if isempty(x)
    open ('tyredata.fig');

  else
    figure(x);
  end


case 'page1'                    % to switch from 'page1b' or 'pagetyre', to page 1
  x = findobj(0,'tag','page1');
  figure(x);

case 'page0b'                   %
  x = findobj(0,'tag','page0b');
  if isempty(x)
    open ('fig3.fig');
  else
    figure(x);
  end

end
```

C4. Function file for Two Degree of Freedom Vehicle Model

```
function [udot,alpha1,alpha2,Fyf,Fyr] = equation2DOF(t,u,init,mail);


%% TWO DEGREE OF FREEDOM EQUATIONS %%
%%%%%%%%%%%%%%%%%%%%%%%%%%%%%%%%%%%%%%%%%%%%%%%%%%%%%%%%%%%%%%%%%%
tita = mail(1);mass = mail(2);vel_U = mail(3);Iz = mail(4);Ix = mail(5);cor_stiff = mail(6);cor_stifr = mail(7);
algnmof = mail(8);algnmor=mail(9);fwheelbase = mail(10);rwheelbase = mail(11);notsine=mail(12);period=mail(13);
%%%%%%%%%%%%%%%%%%%%%%%%%%%%%%%%%%%%%%%%%%%%%%%%%%%%%%%%%%%%%%%%%%%%

switch notsine                                          % Switch for Sine steer
   case 0
      if t <= period
         tita1 = tita*sin(2*pi*period^-1*t);
      else
         tita1 = 0;
      end
   case 1
      tita1 =tita;
end

alpha1 = -(((u(1) + fwheelbase*u(2))/ (vel_U) ) - (tita));       % Front axle Slip angle (rad)

alpha2 = -(((u(1) - rwheelbase*u(2))/ (vel_U)) );                % Rear axle slip angle (rad)

Fyf = cor_stiff*alpha1;
Fyr = cor_stifr*alpha2;

v1 = ( ((  (Fyf*cos(tita)) + Fyr)/mass) - (u(2)*vel_U) );        % Lateral velocity

r1 = ( ((fwheelbase*Fyf)*cos(tita)) - (rwheelbase*Fyr) ) /Iz;    % Yaw velocity-algnmof

v2 = u(1);                                                       % Lateral displacement

r2 = u(2);                                                       % Yaw angle
```

```
X  = ((vel_U)*cos(u(4)) - u(1)*sin(u(4)));                    % Longitudinal displacement in Earth fixed Coord.
Y  = ((vel_U)*sin(u(4)) + u(1)*cos(u(4)));                    % Lateral displacement in Earth fixed Coord.

udot = [v1;r1;v2;r2;X;Y];
```

C5. Function file for Four Degree of Freedom Vehicle Model

```
function u = equation4DOF(t,u,init,mail,alpha,Fv1,co_stif,algnmo);


%DEFINITIONS OF THE TERMS TO THE FUNCTION FILE:
%===========================================

tita=mail(1);mass=mail(2);vel_U=mail(3);Iz=mail(4);Ix=mail(5);period=mail(6);sine=mail(7);d=mail(8);g=mail(9);ms=mail(10);
fwheelbase=mail(11);rwheelbase=mail(12);mf=mail(13);mr=mail(14);Hcg=mail(15);horcf=mail(16);Hu=mail(17);Hs=mail(18);trackf=mail(
19);Ix=mail(20);msf=mail(21);muf=mail(22);horcr=mail(23);Ix=mail(24);msr=mail(25);mur=mail(26);algnmor=mail(27);tita1=mail(28);Ksf
=mail(29);Ksr=mail(30);cf=mail(31);cr=mail(32);algnmof=mail(33);crd=mail(34);trackr=mail(35);krd=mail(36);Fxf=mail(37);Fxr=mail(38);
Fxor=mail(39);Fxof=mail(40);Fxir=mail(41);Fxif=mail(42);Fbof=mail(43);Fbor=mail(44);Fbif=mail(45);Fbir=mail(46);steptime=mail(47);w
thouttyre=mail(48);page1b=mail(49);ssep=mail(50);spd=mail(51);

%STEER ANGLE SELECTION for 'SINE STEER' or CONSTANT RADIUS:
%======================================================

switch sine
   case 0
      if t <= period
         tita2 = tita*sin(2*pi*(period^-1)*t);
      elseif period < t <= 1.5*period
         tita2 = 0;end
      if t > 1.5*period
         tita2 = tita*sin(2*pi*(period^-1)*t);
         % Single lane change because of zero steer angle.
      end
   case 1
      tita2 =tita;
end

%>[ SUSPENSION STIFFNESS & DAMPING PARAMETERS & LATERAL LOAD TRANSFER ]<
%=================================================================
Cfif = (cf*trackf^2/2);                          % Roll Damping-front
Cfir = (cr*trackr^2/2);                          % Roll Damping-rear
Kfif = (Ksf*trackf^2/2);                         % Roll Stiffness-front
Kfir = (Ksr*trackf^2/2);                         % Roll Stiffness-rear


alpha1 = -(((u(2) + fwheelbase*u(3))/ (u(1)) ) - (tita2));         % Front axle Slip angle (rad)
alpha2 = -(((u(2) - rwheelbase*u(3))/ (u(1))) );                    % Rear axle Slip angle (rad)



Fvof = (0.5*mf*9.807) +  (1/trackf) * ( (msf*(u(2)+u(3)*(u(1))) * d + muf*0.145*(u(2)+u(3)*(u(1))) + Kfif*u(5) + Cfif*u(4)) ); % LT-outer
front
Fvif = (0.5*mf*9.807) -  (1/trackf) * ( (msf*(u(2)+u(3)*(u(1))) * d + muf*0.145*(u(2)+u(3)*(u(1))) + Kfif*u(5) + Cfif*u(4)) ); % LT - inner
front
Fvor = (0.5*mr*9.807) +  (1/trackr) * ( (msr*(u(2)+u(3)*(u(1))) * d + mur*0.145*(u(2)+u(3)*(u(1))) + Kfir*u(5) + Cfir*u(4)) ); % LT - outer
rear
Fvir = (0.5*mr*9.807) -  (1/trackr) * ( (msr*(u(2)+u(3)*(u(1))) * d + mur*0.145*(u(2)+u(3)*(u(1))) + Kfir*u(5) + Cfir*u(4)) ); % LT - inner
rear

%> [ IF Condition for TYRE DATA Selection % Corn.Stiffness/Lateral Force Calc. ] <
%========================================================================

if wthouttyre == 1
   corstiff = findobj(page1b,'tag','dat1');
   corr_stiff = get(corstiff,'string');
```

```
    corstifr = findobj(page1b,'tag','dat2');
    corr_stifr = get(corstifr,'string');
    cof = eval(corr_stiff);
    cor = eval(corr_stifr);


    cor_stiff = cof;
    cor_stifr = cor;
    cor_stifof = cof/2;
    cor_stifor = cor/2;
    cor_stifif = cof/2;
    cor_stifir = cor/2;
else

    cor_stifof = interp2(alpha,Fv1,co_stif,alpha1,Fvof);                % (N/rad)
    cor_stifor = interp2(alpha,Fv1,co_stif,alpha2,Fvor);                % (N/rad)
    cor_stifif = interp2(alpha,Fv1,co_stif,alpha1,Fvif);                % (N/rad)
    cor_stifir = interp2(alpha,Fv1,co_stif,alpha2,Fvir);                % (N/rad)


    cor_stiff  = (cor_stifof + cor_stifif);                             % [N/rad]
    cor_stifr  = (cor_stifor + cor_stifir);

    %%% Aligning Moments %%%%
    algnmofo = interp2(alpha,Fv1,algnmo,alpha1,Fvof);
    algnmofi = interp2(alpha,Fv1,algnmo,alpha1,Fvif);
    algnmoro = interp2(alpha,Fv1,algnmo,alpha2,Fvor);
    algnmori = interp2(alpha,Fv1,algnmo,alpha2,Fvir);
    algnmof = (algnmofo + algnmofi);
    algnmor = (algnmoro + algnmori);
end

Fyof = cor_stifof.*alpha1;
Fyor = cor_stifor.*alpha2;
Fyif = cor_stifif.*alpha1;
Fyir = cor_stifir.*alpha2;

Fyf = (Fyof + Fyif);
Fyr = (Fyir + Fyor);

if u(3,1)-u(1,1) < -0.1        %Tractive force applied for the Constant Speed Vehicle test!!!!!
    Fxor=0;
    Fxir=0;
end

%>[ GENERAL EQUATIONS OF MOTION ]<
%========================================

u2 = (((Fxif+Fxof-Fbof-Fbif)*cos(tita2) + Fxir + Fxor - Fbir - Fbor -(Fyif+Fyof)*sin(tita2) )/ mass) + (u(3)*u(2));

v2 = ( (( ((Fyif+Fyof)*cos(tita2)) + ((Fxif+Fxof-Fbif-Fbof)*sin(tita2)) + (Fyir+Fyor))/mass) - (u(3)*(u(1))) );

r2 = ( (fwheelbase*(Fyif+Fyof)*cos(tita2)) + ((trackf/2)*(Fyif-Fyof)*sin(tita2)) + (fwheelbase*(Fxif-Fbif+Fxof-Fbof)*sin(tita2))+...
      ((trackf/2)*(Fxof-Fbof-Fxif+Fbif)*cos(tita2)) - (rwheelbase*(Fyir+Fyor)) - ((trackr/2)*(Fxir-Fbir-Fxor+Fbor))-algnmof)/Iz;

p2 = ( ms*(v2+u(3)*(u(1)))*d + ms*g*d*u(5) - (Cfif + Cfir)*u(4) - (Kfif + Kfir)*u(5) )/Ix;

fi = u(4);

v1 = u(2);                                    %=> result(i,5)lateral displacement

r1 = u(3);                                    % Yaw Angle

X  = ((u(1))*cos(u(7)) - u(2)*sin(u(7)));     %=> Longitudinal DISPLACEMENT Earth fixed

Y  = ((u(1))*sin(u(7)) + u(2)*cos(u(7)));     %=> Lateral DISPLACEMENT


u = [u2;v2;r2;p2;fi;v1;r1;X;Y];
```

APPENDIX D

FUZZY LOGIC CONTROL ROUTINES

D1. Two Degree of Freedom Model Path planning

```
[System]
Name='2DOFModel'
Type='mamdani'
Version=2.0
NumInputs=3
NumOutputs=1
NumRules=105
AndMethod='prod'
OrMethod='probor'
ImpMethod='prod'
AggMethod='max'
DefuzzMethod='centroid'

[Input1]
Name='Error1'
Range=[-360 360]
NumMFs=7
MF1='high-':'trapmf',[-427.5 -382.5 -18 -14]
MF2='zero':'trimf',[-2 0 2]
MF3='High+':'trapmf',[14 18 367.5 411.1]
MF4='MEDI+':'trimf',[2 14 18]
MF5='Low+':'trimf',[0 2 14]
MF6='MEDI-':'trimf',[-18 -14 -2]
MF7='Low-':'trimf',[-14 -2 0]

[Input2]
Name='Error2'
Range=[-360 360]
NumMFs=7
MF1='High-':'trapmf',[-380 -360 -18 -14]
MF2='zero':'trimf',[-2 0 2]
MF3='High+':'trapmf',[14 18 360 380]
MF4='Med+':'trimf',[2 14 18]
MF5='Low+':'trimf',[0 2 14]
MF6='Low-':'trimf',[-14 -2 0]
MF7='Med-':'trimf',[-18 -14 -2]

[Input3]
Name='Distance'
Range=[0 12]
NumMFs=3
MF1='LOW':'trimf',[0 12 12]
MF2='VL[SPEEDY]':'trimf',[0 0 12]
```

```
MF3='all':'trapmf',[0 0 12 12]
[Output1]
Name='SteerAngle'
Range=[-90 90]
NumMFs=7
MF1='Right/fast':'trapmf',[-90 -90 -80 -60]
MF2='Right/slow':'trimf',[-60 -40 0]
MF3='NoChange':'trimf',[-40 0 40]
MF4='Left/slow':'trimf',[0 40 60]
MF5='Left/fast':'trapmf',[60 80 90 90]
MF6='Right/Medi':'trimf',[-80 -60 -40]
MF7='Left/Medi':'trimf',[40 60 80]

[Rules]
5 5 -3, 4 (1) : 1
5 4 -3, 4 (1) : 1
5 3 -3, 4 (1) : 1
5 6 -3, 4 (1) : 1
5 7 -3, 4 (1) : 1
5 1 -3, 7 (1) : 1
7 6 -3, 2 (1) : 1
7 7 -3, 2 (1) : 1
7 1 -3, 2 (1) : 1
7 5 -3, 2 (1) : 1
7 4 -3, 2 (1) : 1
7 3 -3, 6 (1) : 1
4 5 -3, 7 (1) : 1
4 4 -3, 7 (1) : 1
4 3 -3, 7 (1) : 1
4 6 -3, 7 (1) : 1
4 7 -3, 7 (1) : 1
4 1 -3, 5 (1) : 1
6 6 -3, 6 (1) : 1
6 7 -3, 6 (1) : 1
6 1 -3, 6 (1) : 1
6 5 -3, 6 (1) : 1
6 4 -3, 6 (1) : 1
6 3 -3, 1 (1) : 1
3 5 -3, 5 (1) : 1
3 4 -3, 5 (1) : 1
3 3 -3, 7 (1) : 1
3 6 -3, 5 (1) : 1
3 7 -3, 5 (1) : 1
3 1 -3, 5 (1) : 1
1 6 -3, 1 (1) : 1
1 7 -3, 1 (1) : 1
1 1 -3, 6 (1) : 1
1 5 -3, 1 (1) : 1
1 4 -3, 1 (1) : 1
1 3 -3, 1 (1) : 1
2 2 -3, 3 (1) : 1
2 6 -3, 3 (1) : 1
2 5 -3, 3 (1) : 1
2 7 -3, 3 (1) : 1
2 4 -3, 3 (1) : 1
```

2 1 -3, 3 (1) : 1
2 3 -3, 3 (1) : 1
5 2 -3, 4 (1) : 1
7 2 -3, 2 (1) : 1
4 2 -3, 7 (1) : 1
6 2 -3, 6 (1) : 1
3 2 -3, 5 (1) : 1
1 2 -3, 1 (1) : 1
6 1 2, 1 (1) : 1
4 3 2, 5 (1) : 1
4 3 1, 4 (1) : 1
6 1 1, 4 (1) : 1
7 3 1, 1 (1) : 1
7 3 2, 7 (1) : 1
5 3 1, 3 (1) : 1
5 3 2, 5 (1) : 1
6 3 1, 1 (1) : 1
6 3 2, 7 (1) : 1
7 4 1, 6 (1) : 1
7 4 2, 4 (1) : 1
5 4 1, 2 (1) : 1
5 4 2, 7 (1) : 1
7 7 1, 4 (1) : 1
7 7 2, 6 (1) : 1
1 3 1, 1 (1) : 1
1 3 2, 7 (1) : 1
1 4 1, 1 (1) : 1
1 4 2, 7 (1) : 1
7 1 1, 4 (1) : 1
7 1 2, 6 (1) : 1
5 7 1, 7 (1) : 1
5 7 2, 2 (1) : 1
5 1 1, 7 (1) : 1
5 1 2, 6 (1) : 1
6 7 1, 2 (1) : 1
6 7 2, 6 (1) : 1
3 1 1, 5 (1) : 1
3 1 2, 2 (1) : 1
3 7 1, 5 (1) : 1
3 7 2, 2 (1) : 1
4 1 2, 6 (1) : 1
4 1 1, 5 (1) : 1
4 7 2, 2 (1) : 1
4 7 1, 5 (1) : 1
6 4 2, 4 (1) : 1
6 4 1, 1 (1) : 1
3 3 1, 7 (1) : 1
3 3 2, 5 (1) : 1
1 1 1, 6 (1) : 1
1 1 2, 1 (1) : 1
4 4 2, 7 (1) : 1
4 4 1, 4 (1) : 1
7 5 1, 6 (1) : 1
7 5 2, 4 (1) : 1
5 6 1, 7 (1) : 1

5 6 2, 2 (1) : 1
7 6 1, 3 (1) : 1
7 6 2, 2 (1) : 1
5 5 1, 3 (1) : 1
5 5 2, 4 (1) : 1
4 6 2, 2 (1) : 1
4 6 1, 5 (1) : 1
6 5 1, 1 (1) : 1
6 5 2, 4 (1) : 1

D2. Four Degree of Freedom Model Path planning & Yaw Control

Name=YawControl'
Type='mamdani'
Version=2.0
NumInputs=6
NumOutputs=6
NumRules=126
AndMethod='prod'
OrMethod='probor'
ImpMethod='prod'
AggMethod='max'
DefuzzMethod='centroid'

[Input1]
Name='Error1'
Range=[-360 360]
NumMFs=7
MF1='high-':'trapmf',[-427.5 -382.5 -18 -14]
MF2='zero':'trimf',[-1.5 0 1.5]
MF3='High+':'trapmf',[14 18 367.5 411.1]
MF4='MEDI+':'trimf',[-0.5 14 18]
MF5='Low+':'trimf',[0 0.5 14]
MF6='MEDI-':'trimf',[-18 -14 -0.5]
MF7='Low-':'trimf',[-14 -0.5 0]

[Input2]
Name='Error2'
Range=[-360 360]
NumMFs=7
MF1='High-':'trapmf',[-380 -360 -18 -14]
MF2='zero':'trimf',[-1.5 0 1.5]
MF3='High+':'trapmf',[14 18 360 380]
MF4='Med+':'trimf',[0.5 14 18]
MF5='Low+':'trimf',[0 0.5 14]
MF6='Low-':'trimf',[-14 -0.5 0]
MF7='Med-':'trimf',[-18 -14 -0.5]

[Input3]
Name='Distance'
Range=[0 12]

```
NumMFs=3
MF1='LOW':'trimf',[0 12 12]
MF2='VL[SPEEDY]':'trimf',[0 0 12]
MF3='all':'trapmf',[0 0 12 12]

[Input4]
Name='YawError'
Range=[-1 1]
NumMFs=7
MF1='LOW[-]':'trimf',[-0.04 -0.02 0]
MF2='ZERO':'trimf',[-0.02 0 0.02]
MF3='LOW[+]':'trimf',[0 0.02 0.04]
MF4='MODERATE[+]':'trimf',[0.02 0.04 0.1]
MF5='HIGH[+]':'trapmf',[0.04 0.1 1 1]
MF6='MODERATE[-]':'trimf',[-0.1 -0.04 -0.02]
MF7='HIGH[-]':'trapmf',[-1 -1 -0.1 -0.04]

[Input5]
Name='SpeedError'
Range=[-2 2]
NumMFs=7
MF1='low-':'trapmf',[-0.05 -0.04 -0.01 0]
MF2='low+':'trapmf',[0 0.02 0.03 0.05]
MF3='zero':'trimf',[-0.02 0 0.02]
MF4='M-':'trapmf',[-0.12 -0.07 -0.05 -0.03]
MF5='High-':'trapmf',[-2 -2 -0.12 -0.07]
MF6='M+':'trapmf',[0.03 0.05 0.07 0.12]
MF7='High+':'trapmf',[0.07 0.12 2 2]

[Input6]
Name='Speed'
Range=[0 80]
NumMFs=1
MF1='mf1':'trimf',[0 0 80]

[Output1]
Name='SteerAngle'
Range=[-90 90]
NumMFs=7
MF1='Right/fast':'trapmf',[-90 -90 -80 -60]
MF2='Right/slow':'trimf',[-60 -40 0]
MF3='NoChange':'trimf',[-40 0 40]
MF4='Left/slow':'trimf',[0 40 60]
MF5='Left/fast':'trapmf',[60 80 90 90]
MF6='Right/Medi':'trimf',[-80 -60 -40]
MF7='Left/Medi':'trimf',[40 60 80]

[Output2]
Name='Pbif'
Range=[-0.1 13]
NumMFs=4
MF1='SOFT':'trapmf',[0 1.5 3 5.5]
MF2='MODERATE':'trapmf',[3 5.5 7 9.5]
MF3='HARD':'trapmf',[7 9.5 13 13]
MF4='ZERO':'trimf',[-0.1 0 0.1]
```

```
[Output3]
Name='Pbir'
Range=[-0.1 13]
NumMFs=4
MF1='SOFT':'trapmf',[0 1.5 3 5.5]
MF2='MODERATE':'trapmf',[3 5.5 7 9.5]
MF3='HARD':'trapmf',[7 9.5 13 13]
MF4='ZERO':'trimf',[-0.1 0 0.1]

[Output4]
Name='Pbof'
Range=[-0.1 13]
NumMFs=4
MF1='SOFT':'trapmf',[0 1.5 3 5.5]
MF2='MODERATE':'trapmf',[3 5.5 7 9.5]
MF3='HARD':'trapmf',[7 9.5 13 13]
MF4='ZERO':'trimf',[-0.1 0 0.1]

[Output5]
Name='Pbor'
Range=[-0.1 13]
NumMFs=4
MF1='SOFT':'trapmf',[0 1.5 3 5.5]
MF2='MODERATE':'trapmf',[3 5.5 7 9.5]
MF3='HARD':'trapmf',[7 9.5 13 13]
MF4='ZERO':'trimf',[-0.1 0 0.1]

[Output6]
Name='Throttle'
Range=[0 1]
NumMFs=4
MF1='ZERO':'trimf',[-0.01 0 0.01]
MF2='low':'trapmf',[0 0.01 0.25 0.5]
MF3='half':'trimf',[0.25 0.5 1]
MF4='full':'trapmf',[0.5 1 1.01 1.01]

[Rules]
5 5 -3 0 0 0, 4 0 0 0 0 0 (1) : 1
5 4 -3 0 0 0, 4 0 0 0 0 0 (1) : 1
5 3 -3 0 0 0, 4 0 0 0 0 0 (1) : 1
5 6 -3 0 0 0, 4 0 0 0 0 0 (1) : 1
5 7 -3 0 0 0, 4 0 0 0 0 0 (1) : 1
5 1 -3 0 0 0, 7 0 0 0 0 0 (1) : 1
7 6 -3 0 0 0, 2 0 0 0 0 0 (1) : 1
7 7 -3 0 0 0, 2 0 0 0 0 0 (1) : 1
7 1 -3 0 0 0, 2 0 0 0 0 0 (1) : 1
7 5 -3 0 0 0, 2 0 0 0 0 0 (1) : 1
7 4 -3 0 0 0, 2 0 0 0 0 0 (1) : 1
7 3 -3 0 0 0, 6 0 0 0 0 0 (1) : 1
4 5 -3 0 0 0, 7 0 0 0 0 0 (1) : 1
4 4 -3 0 0 0, 7 0 0 0 0 0 (1) : 1
4 3 -3 0 0 0, 7 0 0 0 0 0 (1) : 1
4 6 -3 0 0 0, 7 0 0 0 0 0 (1) : 1
4 7 -3 0 0 0, 7 0 0 0 0 0 (1) : 1
```

4 1 -3 0 0 0, 5 0 0 0 0 0 (1) : 1
6 6 -3 0 0 0, 6 0 0 0 0 0 (1) : 1
6 7 -3 0 0 0, 6 0 0 0 0 0 (1) : 1
6 1 -3 0 0 0, 6 0 0 0 0 0 (1) : 1
6 5 -3 0 0 0, 6 0 0 0 0 0 (1) : 1
6 4 -3 0 0 0, 6 0 0 0 0 0 (1) : 1
6 3 -3 0 0 0, 1 0 0 0 0 0 (1) : 1
3 5 -3 0 0 0, 5 0 0 0 0 0 (1) : 1
3 4 -3 0 0 0, 5 0 0 0 0 0 (1) : 1
3 3 -3 0 0 0, 7 0 0 0 0 0 (1) : 1
3 6 -3 0 0 0, 5 0 0 0 0 0 (1) : 1
3 7 -3 0 0 0, 5 0 0 0 0 0 (1) : 1
3 1 -3 0 0 0, 5 0 0 0 0 0 (1) : 1
1 6 -3 0 0 0, 1 0 0 0 0 0 (1) : 1
1 7 -3 0 0 0, 1 0 0 0 0 0 (1) : 1
1 1 -3 0 0 0, 6 0 0 0 0 0 (1) : 1
1 5 -3 0 0 0, 1 0 0 0 0 0 (1) : 1
1 4 -3 0 0 0, 1 0 0 0 0 0 (1) : 1
1 3 -3 0 0 0, 1 0 0 0 0 0 (1) : 1
2 2 -3 0 0 0, 3 0 0 0 0 0 (1) : 1
2 6 -3 0 0 0, 3 0 0 0 0 0 (1) : 1
2 5 -3 0 0 0, 3 0 0 0 0 0 (1) : 1
2 7 -3 0 0 0, 3 0 0 0 0 0 (1) : 1
2 4 -3 0 0 0, 3 0 0 0 0 0 (1) : 1
2 1 -3 0 0 0, 3 0 0 0 0 0 (1) : 1
2 3 -3 0 0 0, 3 0 0 0 0 0 (1) : 1
5 2 -3 0 0 0, 4 0 0 0 0 0 (1) : 1
7 2 -3 0 0 0, 2 0 0 0 0 0 (1) : 1
4 2 -3 0 0 0, 7 0 0 0 0 0 (1) : 1
6 2 -3 0 0 0, 6 0 0 0 0 0 (1) : 1
3 2 -3 0 0 0, 5 0 0 0 0 0 (1) : 1
1 2 -3 0 0 0, 1 0 0 0 0 0 (1) : 1
6 1 2 0 0 0, 1 0 0 0 0 0 (1) : 1
4 3 2 0 0 0, 5 0 0 0 0 0 (1) : 1
4 3 1 0 0 0, 4 0 0 0 0 0 (1) : 1
6 1 1 0 0 0, 4 0 0 0 0 0 (1) : 1
7 3 1 0 0 0, 1 0 0 0 0 0 (1) : 1
7 3 2 0 0 0, 7 0 0 0 0 0 (1) : 1
5 3 1 0 0 0, 3 0 0 0 0 0 (1) : 1
5 3 2 0 0 0, 5 0 0 0 0 0 (1) : 1
6 3 1 0 0 0, 1 0 0 0 0 0 (1) : 1
6 3 2 0 0 0, 7 0 0 0 0 0 (1) : 1
7 4 1 0 0 0, 6 0 0 0 0 0 (1) : 1
7 4 2 0 0 0, 4 0 0 0 0 0 (1) : 1
5 4 1 0 0 0, 2 0 0 0 0 0 (1) : 1
5 4 2 0 0 0, 7 0 0 0 0 0 (1) : 1
7 7 1 0 0 0, 4 0 0 0 0 0 (1) : 1
7 7 2 0 0 0, 6 0 0 0 0 0 (1) : 1
1 3 1 0 0 0, 1 0 0 0 0 0 (1) : 1
1 3 2 0 0 0, 7 0 0 0 0 0 (1) : 1
1 4 1 0 0 0, 1 0 0 0 0 0 (1) : 1
1 4 2 0 0 0, 7 0 0 0 0 0 (1) : 1
0 0 0 2 0 0, 0 4 4 4 4 0 (1) : 1
0 0 0 1 0 0, 0 4 4 1 4 0 (1) : 1
0 0 0 3 0 0, 0 1 4 4 4 0 (1) : 1

0 0 0 6 0 0, 0 4 4 2 4 0 (1) : 1
0 0 0 4 0 0, 0 2 4 4 4 0 (1) : 1
0 0 0 5 0 0, 0 3 4 4 4 0 (1) : 1
0 0 0 7 0 0, 0 4 4 3 4 0 (1) : 1
0 0 0 0 1 0, 0 0 0 0 0 2 (1) : 1
0 0 0 0 3 0, 0 0 0 0 0 1 (1) : 2
0 0 0 0 4 0, 0 0 0 0 0 3 (1) : 1
0 0 0 0 5 0, 0 0 0 0 0 4 (1) : 1
0 0 0 0 2 0, 0 0 0 0 0 1 (1) : 1
0 0 0 0 6 0, 0 4 1 4 1 1 (1) : 1
0 0 0 0 7 0, 0 2 2 2 2 1 (1) : 1
7 1 1 0 0 0, 4 0 0 0 0 0 (1) : 1
7 1 2 0 0 0, 6 0 0 0 0 0 (1) : 1
5 7 1 0 0 0, 7 0 0 0 0 0 (1) : 1
5 7 2 0 0 0, 2 0 0 0 0 0 (1) : 1
5 1 1 0 0 0, 7 0 0 0 0 0 (1) : 1
5 1 2 0 0 0, 6 0 0 0 0 0 (1) : 1
6 7 1 0 0 0, 2 0 0 0 0 0 (1) : 1
6 7 2 0 0 0, 6 0 0 0 0 0 (1) : 1
3 1 1 0 0 0, 5 0 0 0 0 0 (1) : 1
3 1 2 0 0 0, 2 0 0 0 0 0 (1) : 1
3 7 1 0 0 0, 5 0 0 0 0 0 (1) : 1
3 7 2 0 0 0, 2 0 0 0 0 0 (1) : 1
4 1 2 0 0 0, 6 0 0 0 0 0 (1) : 1
4 1 1 0 0 0, 5 0 0 0 0 0 (1) : 1
4 7 2 0 0 0, 2 0 0 0 0 0 (1) : 1
4 7 1 0 0 0, 5 0 0 0 0 0 (1) : 1
6 4 2 0 0 0, 4 0 0 0 0 0 (1) : 1
6 4 1 0 0 0, 1 0 0 0 0 0 (1) : 1
3 3 1 0 0 0, 7 0 0 0 0 0 (1) : 1
3 3 2 0 0 0, 5 0 0 0 0 0 (1) : 1
1 1 1 0 0 0, 6 0 0 0 0 0 (1) : 1
1 1 2 0 0 0, 1 0 0 0 0 0 (1) : 1
4 4 2 0 0 0, 7 0 0 0 0 0 (1) : 1
4 4 1 0 0 0, 4 0 0 0 0 0 (1) : 1
7 5 1 0 0 0, 6 0 0 0 0 0 (1) : 1
7 5 2 0 0 0, 4 0 0 0 0 0 (1) : 1
5 6 1 0 0 0, 7 0 0 0 0 0 (1) : 1
5 6 2 0 0 0, 2 0 0 0 0 0 (1) : 1
7 6 1 0 0 0, 3 0 0 0 0 0 (1) : 1
7 6 2 0 0 0, 2 0 0 0 0 0 (1) : 1
5 5 1 0 0 0, 3 0 0 0 0 0 (1) : 1
5 5 2 0 0 0, 4 0 0 0 0 0 (1) : 1
4 6 2 0 0 0, 2 0 0 0 0 0 (1) : 1
4 6 1 0 0 0, 5 0 0 0 0 0 (1) : 1
6 5 1 0 0 0, 1 0 0 0 0 0 (1) : 1
6 5 2 0 0 0, 4 0 0 0 0 0 (1) : 1
2 2 3 0 0 0, 3 0 0 0 0 0 (1) : 1
2 6 3 0 0 0, 3 0 0 0 0 0 (1) : 1
2 5 3 0 0 0, 3 0 0 0 0 0 (1) : 1
2 7 3 0 0 0, 3 0 0 0 0 0 (1) : 1
2 4 3 0 0 0, 3 0 0 0 0 0 (1) : 1
2 1 3 0 0 0, 3 0 0 0 0 0 (1) : 1
2 3 3 0 0 0, 3 0 0 0 0 0 (1) : 1